MATHEMATICAL MODELING OF THE IMPACT OF TEMPERATURE VARIABILITY ON MALARIA EPIDEMICS WITH OPTIMAL CONTROL

Temesgen Duressa Keno

A Dissertation Submitted to the Department of Applied Mathematics, School of Applied Natural Science

Presented in Partial Fulfillment of the Requirement for the Degree of Doctor of Philosophy in Applied mathematics

Office of Graduate Studies
Adama Science and Technology University

September, 2021
Adama, Ethiopia

MATHEMATICAL MODELING OF THE IMPACT OF TEMPERATURE VARIABILITY ON MALARIA EPIDEMICS WITH OPTIMAL CONTROL

Temesgen Duressa Keno

Supervisor

Prof. Oluwole Daniel Makinde

Co-supervisor

Dr. Legesse Lemecha Obsu

A Dissertation Submitted to the Department of Applied Mathematics, School of Applied Natural Science

Presented in Partial Fulfillment of the Requirement for the Degree of Doctor of Philosophy in Applied mathematics

Office of Graduate Studies

Adama Science and Technology University

September, 2021

Adama, Ethiopia

Declaration

I hereby declare that this dissertation entitled "**Mathematical Modeling of the Impact of Temperature Variability on Malaria Epidemics with Optimal Control**" is my original work. That is, it has not been submitted for the award of any academic degree, diploma or certificate in any other university. All sources of materials used for this dissertation have been duly acknowledged through appropriate citations.

Name of Student	Signature	Date

Recommendation

We, the supervisors of this dissertation, hereby certify that we have read and revised the dissertation entitled " **Mathematical Modeling of the Impact of Temperature Variability on Malaria Epidemics with Optimal Control**" prepared under our guidance by Temesgen Duressa Keno submitted in partial fulfillment of the requirements for the degree of Doctor of Philosophy in Applied Mathematics. Therefore, we recommend the submission of the dissertation to the department for further review and defense.

Supervisor	Signature	Date
Co-Supervisor	Signature	Date

Dedication

To everyone who supported me especially my brother Dereje Duressa for his love, understanding and support. Also to my mom and dad for their endless prayers for my success.

Approval Page

We hereby certify that the recommendations and suggestions made by the board of examiners are appropriately incorporated into the final version of the dissertation entitled "**Mathematical Modeling of the Impact of Temperature Variability on Malaria Epidemics with Optimal Control**" by Temesgen Duressa Keno.

Supervisor	Signature	Date
Co-Supervisor	Signature	Date

We, the undersigned, members of the Board of Examiners of the dissertation open defense by Temesgen Duressa Keno have read and evaluated the dissertation entitled "**Mathematical Modeling of the Impact of Temperature Variability on Malaria Epidemics with Optimal Control**" and examined the candidate during open defense. This is, therefore, to certify that the dissertation is accepted for partial fulfillment of the requirement of the degree of Doctor of Philosophy in Applied mathematics.

Chairperson	Signature	Date
Internal Examiner	Signature	Date
External Examiner 1	Signature	Date

External Examiner 2	Signature	Date

Finally, approval and acceptance of the dissertation is contingent upon submission of its final copy to the Office of Postgraduate Studies (OPGS) through the candidate's Department Graduate Council (DGC) and School Graduate Committee (SGC).

Department Head	Signature	Date
School Dean	Signature	Date
Office of Postgraduate Studies, Dean	Signature	Date

ACKNOWLEDGEMENTS

First of all, I would like to thank my supervisor Prof. Oluwole Daniel Makinde who helped me to do every activity in every time. My special and heart full gratitude and appreciation for his great assistance, contribution, useful suggestion and constructive idea on this excellence advising and limitless effort in encouraging me in my work, correcting and giving comments by devoting his time.

Next to that I acknowledge my co-supervisor Dr. Legesse Lemecha Obsu who gave me valuable suggestion and comments during the preparation of this dissertation. I greatly appreciate him not only for unlimited constructive advises in every aspect of my dissertation work, but also with his professional and personal ethic, that should be an icon for others.

Thirdly, I would like to thank my family those tired with me until now and supporting me by financial as well as encouraging me in every day to day and Adama Science and Technology University for the support that provided throughout this study.

Finally, I would like to thank my colleagues who helping me in all ways as well as who shared different ideas and supporting me by their own material needed to complete this dissertation.

Contents

Declaration i
Recommendation ii
Acknowledgements vi
List of Tables xi
List of Figures xiii
List of Acronyms xiv
List of Publications xv
Abstract xvi

1 INTRODUCTION **1**
1.1 Background of the Study 1
1.1.1 Cause of malaria 1
1.1.2 Modes of transmission 2
1.1.3 Symptoms of malaria 2
1.1.4 Control of malaria 2
1.1.5 Climatic variability and malaria 3
1.1.6 Global distribution of malaria 4
1.1.7 Role of mathematical modeling on malaria transmission 6
1.2 Statement of the problem 6
1.3 Objectives of the study 7
1.3.1 General objective 7
1.3.2 Specific objectives 7
1.4 Significance of the study 7
1.5 The scope of the study 8
1.6 Organization of the study 8

2 LITERATURE REVIEW **9**
2.1 Malaria transmission models 9

2.2 Malaria transmission models with optimal controls 12

3 RESEARCH METHODOLOGY 17

3.1 Study area 17

3.2 Data collection 17

3.3 Mathematical methods 17

4 MODELING SIRS MATHEMATICAL MODEL OF MALARIA DYNAMICS WITH TEMPERATURE VARIABILITY 19

4.1 Model description and formulation 19

4.2 Qualitative analysis of the model 22

4.2.1 Invariant region 22

4.2.2 Positivity of the solutions 23

4.2.3 Disease free equilibrium point 25

4.2.4 Basic reproduction number 25

4.2.5 Local stability of disease free equilibrium 27

4.2.6 Global stability of disease free equilibrium 28

4.2.7 Endemic equilibrium point 29

4.2.8 Local stability of endemic equilibrium 31

4.2.9 Global stability of endemic equilibrium 32

4.2.10 Bifurcation analysis 33

4.3 Local sensitivity analysis 38

4.3.1 Interpretation of sensitivity indices 41

4.4 Numerical simulations 41

5 MODELING SEIRS MATHEMATICAL MODEL OF MALARIA TRANSMISSION WITH TEMPERATURE VARIABILITY 49

5.1 Mathematical model formulation 49

5.2 Qualitative analysis of the model 52

5.2.1 Invariant region 52

5.2.2 Positivity of the solutions 54

5.2.3 Disease free equilibrium 56

5.2.4 Basic reproduction number 56

5.2.5 Local stability of disease free equilibrium 58

5.2.6 Global stability of disease free equilibrium 61

5.2.7 Endemic equilibrium point 61

5.2.8 Global stability of endemic equilibrium . . . 64
5.2.9 Bifurcation analysis . . . 66
5.3 Local sensitivity analysis . . . 72
5.3.1 Interpretation of the sensitivity indices . . . 74
5.4 Parameter estimation . . . 75
5.4.1 Data . . . 76
5.5 Numerical simulations . . . 77

6 OPTIMAL CONTROL AND COST EFFECTIVENESS ANALYSIS OF SIRS MALARIA DYNAMICS MODEL WITH TEMPERATURE VARIABILITY 84
6.1 Optimal control problem formulation . . . 84
6.2 Existence of the optimal controls . . . 85
6.3 Hamiltonian system . . . 88
6.4 Optimality system . . . 90
6.5 Numerical simulations . . . 91
6.6 Cost effectiveness analysis . . . 95

7 OPTIMAL CONTROL AND COST EFFECTIVENESS ANALYSIS OF SEIRS MALARIA TRANSMISSION MODEL IN THE PRESENCE OF TEMPERATURE VARIABILITY 99
7.1 Formulation of optimal control model . . . 99
7.2 Existence of the optimal controls . . . 101
7.3 Hamiltonian system . . . 102
7.4 Optimality system . . . 105
7.5 Numerical simulations . . . 106
7.6 Cost effectiveness analysis . . . 111

CONCLUSIONS AND RECOMMENDATIONS 114
Conclusions . . . 116
Future Research . . . 116
Recommendations . . . 117

REFERENCES 125

APPENDIX 126
APPENDIX A . . . 126
APPENDIX B . . . 135

APPENDIX C 137

List of Tables

4.1 Parameters description used for the model (4.1) 21
4.2 Sensitivity indices of parameters with respect to R_{01} 40
4.3 Sensitivity indices of parameters with respect to R_{02} 40
4.4 Parameters from literature value and assumed values used for model (4.1). . 42

5.1 Parameters description used for the model (5.1) 52
5.2 Sensitivity indices of parameters with respect to R_{0l} 73
5.3 Sensitivity indices of parameters with respect to R_{0m} 74
5.4 Procedures that used to estimate the model parameters 76
5.5 Total number of malaria infectious in East Shewa between 2010 and 2019. . 76
5.6 The estimated parameters used for the model (5.1) 77

6.1 Total amount of the infections saved and cost averted for all strategies . . . 97
6.2 Total amount of the infection averted and total cost with their ICER 97
6.3 Total infection averted and total cost of the strategies **C**, **A** and **D** 98
6.4 Total infection averted and total cost of the strategies **C** and **D** 98

7.1 Total amount of infection averted and total cost for all strategies 112
7.2 Increasing order of infections averted. 112
7.3 Comparison between interventions **B** and **A** 113
7.4 Comparison between interventions **A** and **D** 113

List of Figures

1.1 The image of (a) *An. gambiae*, (b) *An. arabiensis* and (c) *An. funestus* . . . 2
1.2 Life cycle of a mosquito. 4
1.3 The map shows the distribution of malaria worldwide. 4
1.4 The map shows the distribution of malaria in Africa. 5
1.5 The map shows distribution of malaria in Ethiopia 5

4.1 Flow diagram of malaria transmission model 20
4.2 Convergence of solutions for infected human to the equilibrium points . . . 42
4.3 Convergence of solutions for infected mosquitoes to the equilibrium points 43
4.4 Simulation results of susceptible and infected human with vary values of β_h 43
4.5 Simulation results of susceptible and infected mosquitoes with vary values of β_m 44
4.6 Simulation results of susceptible and recovered human for different value of ω_h 44
4.7 Simulation results of infected and recovered human with different values of μ_h 45
4.8 Simulation results of susceptible and infected mosquito with vary values of μ_m 45
4.9 Simulation results of infected and recovered of human with different value of γ_h 46
4.10 Simulation results of infected and recovered human with different values of δ 46
4.11 Sensitivity indices of basic reproduction number R_{01} and R_{02} respectively . 47
4.12 Human population and mosquitoes population with rise in temperature . . . 47
4.13 Bifurcation diagram of malaria transmission model with temperature variation 48

5.1 Flow diagram of malaria transmission with exposed compartment 51
5.2 Fitting of the model equation (5.1) to the real data in Table 5.5 78
5.3 Human population and mosquitoes population group when $\mathrm{R}_{0l} = 0.183$ . . 78
5.4 Human population and mosquitoes population group when $\mathrm{R}_{0m} = 13.758$. 79
5.5 Variation results of the exposed and infected humans for different value of α_h 79

5.6 Variation results of exposed and infected mosquitoes for a vary value of α_m 80
5.7 Variation of the infected and recovered humans with different values of μ_h . 80
5.8 Variation of the exposed and infected mosquitoes with different value of μ_m 81
5.9 Variation of infected and recovered humans with different value of γ_h 81
5.10 Variation of infected human and recovered human with varies values of δ . 82
5.11 Sensitivity indices of basic reproduction number R_{0l} and R_{0m} respectively . 82
5.12 Human and mosquitoes populations with rise in temperature respectively . . 83
5.13 Bifurcation diagram of the model when $\mathrm{T} = \mathrm{T}_0$ and $\mathrm{T} = \mathrm{T}_{\max}$ 83

6.1 Simulations use of treated bed net (u_1) and treatment of infected human (u_2) 93
6.2 Simulations use of treatment (u_1) and indoor spraying of insecticides (u_3) . 94
6.3 Simulations use of treatment (u_2) and spraying of insecticides (u_3) 95
6.4 Using the treated bed net (u_1), treatment (u_2) and indoor spraying (u_3) . . . 96
6.5 The total people averted with their respect total cost used for strategies . . . 98

7.1 Simulations result with strategy of treated bed net (u_1) and treatment (u_2) . 108
7.2 Simulations result with treated bed net (u_1) and indoor spraying (u_3) 109
7.3 Simulations result with treatment (u_2) and indoor spraying (u_3) 110
7.4 Simulations with treated (u_1), treatment (u_2) and indoor spraying (u_3) . . . 111
7.5 The total infections averted with their respect total cost expended of strategies 113

List of Acronyms

BRN	Basic Reproduction Number
DFE	Disease Free Equilibrium
EEP	Endemic Equilibrium Point
EPH	Ethiopian Public Health Institute
ICER	Incremental Cost Effectiveness Ratio
IVP	Initial Value Problem
ODE	Ordinary Differential Equation
OCP	Optimal Control Problem
PMP	Pontryagin Maximum Principle
RKM	Runge Kutta Method
SEI	Susceptible-Exposed-Infected
SEIRS	Susceptible-Exposed-Infected-Recovered-Susceptible
SI	Susceptible-Infected
SIRS	Susceptible-Infected-Recovered-Susceptible
WHO	World Health Organization

Contribution of the dissertation

Part of this dissertation has been published (under review) in the form of the following research papers on journals that are indexed in Scopus, Web of Science and PubMed.

1. Temesgen Duressa Keno, Oluwole Daniel Makinde and Legesse Lemecha Obsu. Modelling and Optimal Control Analysis of Malaria Epidemic in the Presence of Temperature Variability, *Asian-European Journal of Mathematics*, April 1(2021), https://doi.org/10.1142/S179355712250005X.

2. Temesgen Duressa Keno, Oluwole Daniel Makinde and Legesse Lemecha Obsu. Optimal Control and Cost Effectiveness Analysis of SIRS Malaria Disease Model with Temperature Variability Factor, *Journal of Mathematical and Fundamental Sciences,* **53**(1), 134-164, 2021.

3. Temesgen Duressa Keno, Oluwole Daniel Makinde and Legesse Lemecha Obsu. Impact of Temperature Variability on SIRS Malaria Disease Model, *Journal of Biological Systems*, **29**(3), 1-26, 2021.

4. Temesgen Duressa Keno, Oluwole Daniel Makinde and Legesse Lemecha Obsu (2021). Modeling the Malaria Transmission in the Presence of Temperature Variability, *Infectious Disease Modelling* (Under review).

Abstract

Malaria is an infectious disease that causes morbidity and mortality globally. In this study, we present two deterministic mathematical models of malaria transmission in the presence of temperature variability. The first is susceptible - infected - recovered - susceptible and susceptible - infected compartmental model. The model is both qualitatively and quantitatively analyzed. The local and global stability of the equilibrium points are shown using the Routh-Hurwitz criterion and Lyapunov function respectively. The sensitivity analysis of the model has described and the model exhibits forward and backward bifurcation. Moreover, we extended the model to the optimal control problem by incorporating three controls treated bed nets, treatment of infected and indoor insecticides spraying. The Pontraygin's minimum principle is applied to obtain the necessary condition for the optimal control problem. Based on the numerical simulation of the optimality system and cost effectiveness analysis, the combination of treatment and insecticide spraying is the most optimum and least cost strategy to minimize the disease. Secondly, we proposed and analyzed the susceptible - exposed - infected - recovered - susceptible and susceptible - exposed -infected compartmental model. The analysis of the model shows that the model is bounded and positive in certain domain. Applying the next-generation matrix method, the basic reproduction number with respect to the disease free equilibrium is computed. The local and global stability of the equilibrium points are obtained. The sensitivity analysis of the basic reproduction number with respect to all basic parameters was computed. The model has a forward and backward bifurcation. Using real data some parameters were estimated. Also the model is extended to optimal control problem. The Pontraygin's minimum principle is introduced to obtain the necessary condition for optimal control problem. Runge-Kutta forward-backward sweep method is used to solve the optimal control problem. Therefore, based on the numerical simulations of optimal control problem and cost-effectiveness analysis, the most optimal and least cost strategy to reduce the malaria is using treated bed nets and treatment.

Keywords: *Malaria epidemics; deterministic model; temperature variability; optimal control strategies; cost-effectiveness analysis.*

CHAPTER 1
INTRODUCTION

1.1 Background of the Study

Malaria is one of the oldest disease that causes mortality worldwide (Traoré et al., 2020). It is commonly associated with poverty and has a major negative effect on economic development especially in Africa (Koutou et al., 2018). The disease is widespread in the tropical and subtropical of the world. This includes much of Sub-Saharan Africa, Asia, and Latin America. In endemic regions of malaria, children under five, pregnant women and non-immune adults are most at risk of mortality due to the disease. Malaria infection can lead to serious complications affecting the brain, lungs, kidneys, and other organs. According to the latest world malaria report on December 2020, an estimated 229 million malaria cases were found and 409000 deaths due to malaria have occurred world wide and African region accounted for 94% of all cases in 2019 (WHO, 2020).

1.1.1 Cause of malaria

Malaria is a serious disease caused by a pathogen called protozoa. It is a vector-borne disease caused by a parasite known as *Plasmodium*. There are five Plasmodium parasite species that cause significant numbers of malaria infections in humans (Traoré et al., 2020). Those parasites are *Plasmodium falciparum, Plasmodium malariae, Plasmodium ovale, Plasmodium vivax* and *Plasmodium knowlesi*. *Plasmodium falciparum* is commonly found in Africa and the most common cause of infection in Africa and South East Asia. *Plasmodium falciparum* and *Plasmodium vivax* are the dominant species in the tropical areas and temperate regions, respectively (Yiga et al., 2020).

1.1.2 Modes of transmission

Malaria is transmitted to people through the infected female *Anopheles* mosquitoes while they bite humans for a blood meal for the development of their eggs. The parasite requires two hosts to complete its life cycle the vector female *Anopheles* mosquito and human. The bites of infected mosquitoes are the mode of transmission of the parasite between the human hosts (Mandal et al., 2011). And when an *Anopheles* mosquito bites a person infected with the malaria parasite, the mosquito becomes a carrier of the disease too. It can also be transmitted through blood transfusion and from mother to unborn child during the pregnancy period (Abiodun, 2017). The main vectors provided for the transmission of malaria in tropical Africa are *Anopheles gambiae, Anopheles arabiensis* and *Anopheles funestus* (Coetzee, 2004).

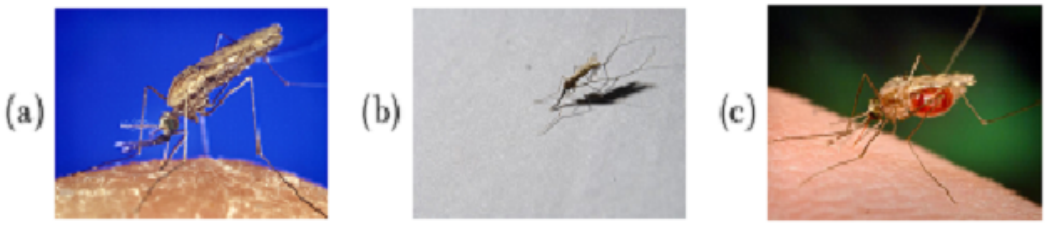

Figure 1.1: The image of (a) *An. gambiae*, (b) *An. arabiensis* and (c) *An. funestus* (Source: Centers for Disease Control and Prevention (CDC), 2016)

1.1.3 Symptoms of malaria

Malaria symptoms typically start within a few weeks after being bitten by an infected vector. But, some types of malaria parasites can lie dormant in the body for up to a year and cause relapses. Malaria starts with extreme cold, followed by high fever and severe sweating. These can be accompanied by vomiting, abdominal pain, rapid heart rate, fever, pain, chills and sweats may develop a few days (Agusto et al., 2012).

1.1.4 Control of malaria

Malaria is preventable if treatment and prevention measures are sought early. Currently, there is no vaccine for the malaria. Immunity is the balanced state of having adequate biological defenses to fight any disease. At birth, children are temporarily protected from infection due to the transfer of antibodies from mother (Abiodun, 2017). Numerous options have been

recommended to control of the malaria, among the best approach are in three categories. These are insecticide-treated bed net, treatment with anti-malarial drugs, and indoor residual spraying of insecticides (WHO, 2020). An insecticide-treated bed net is one of the strategy used to prevent mosquito-human contacts to reduce the number of bites per mosquito. This control strategy is the best effective control in reducing disease transmission (Agusto et al., 2013). Treatment with anti- malarial drug can also be used to prevent malaria. For instance, *Plasmodium falciparum* is treated by using chloroquine (EPHI, 2018). Indoor residual spraying strategy is also used to reduce mosquitoes that increase the mosquito death rate (Chu and White, 2021).

1.1.5 Climatic variability and malaria

Globally, the distribution of mosquitoes has been affected by different climatic factors such as temperature, rainfall and humidity. The impact of temperature and rainfall is therefore significant in the transmission dynamics of malaria. For instance, Alonso et al. (2011) found that the development of the parasite within the mosquito depends on temperature, taking about optimum at temperatures of 28^oC, but stops at temperatures below 16^oC. The authors revealed that temperature fluctuations below 16^oC and above 35^oC have a negative influence on development. Ngarakana-Gwasira et al. (2014) proposed assessing the role of climate change in malaria transmission in Africa. The authors have suggested that the parasite that causes the disease is sensitive to temperature and rainfall. Agusto et al. (2015) presented that the malaria transmission increases with the temperature range of 16^oC to 28^oC that create conditions that lead to mosquitoes breeding rates. Traoré et al. (2020) proposed a mathematical model of malaria transmission dynamics with temperature variations effect on mosquito. They have confirmed that climate factors have a great impact on the mosquito life cycle and parasite survival in mosquitoes.

Rainfall is one of the climate factor that indicates the probable survival of vector and the potential for malaria transmission (Jepson et al., 1947). It influences the abundance of aquatic habitats (eggs, larvae, and pupae) available for mosquitoes survival. Moist conditions in the tropics lead to a stable transmission of the malaria parasite. However, excessive rainfall can negatively influence mosquito breeding. Immoderate rainfall can lead to flushing of breeding sites and high losses of aquatic habitats (Paaijmans et al., 2007). Rainfall provides breeding sites for the mosquitoes that increasing the number of mosquito larval habitants (Yiga et al., 2020).

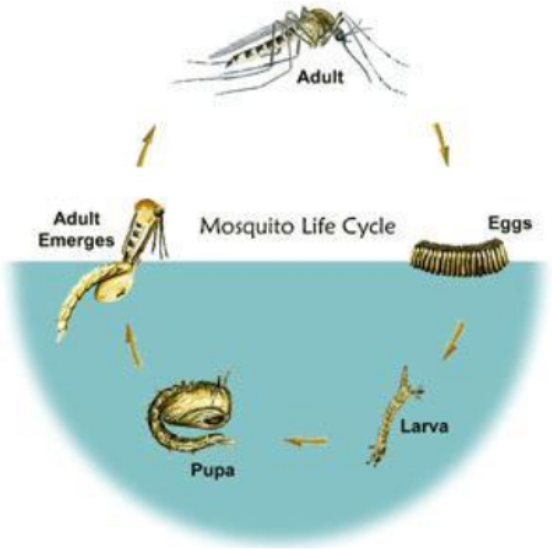

Figure 1.2: Life cycle of a mosquito.
(Source: www.mosquito.org/page/lifecycle)

1.1.6 Global distribution of malaria

The weather parameters such as temperature and rainfall can determine the disease epidemics and the distribution of malaria transmission worldwide (Thomson et al., 1997). The distribution of malaria transmit by mosquito and the impacts of climate change on malaria over world is depicted in Figure 1.3.

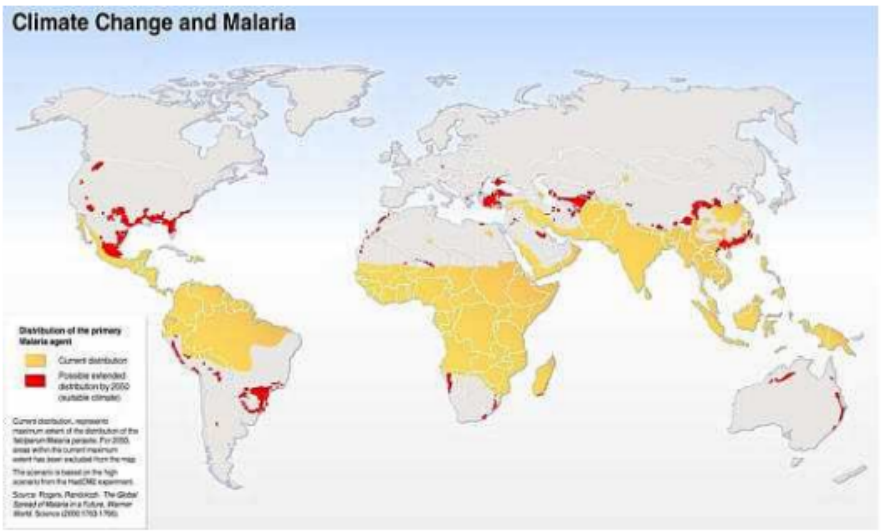

Figure 1.3: The map shows the distribution of malaria worldwide.
(Source: MARA, http://www.mara.org.za)

Malaria is an ancient disease having a huge social, economic, and health burden in Africa which is also been linked to poverty people suffering from malaria often struggle to earn their living. In 2019, most malaria cases were reported from African region is 94% (WHO, 2020).

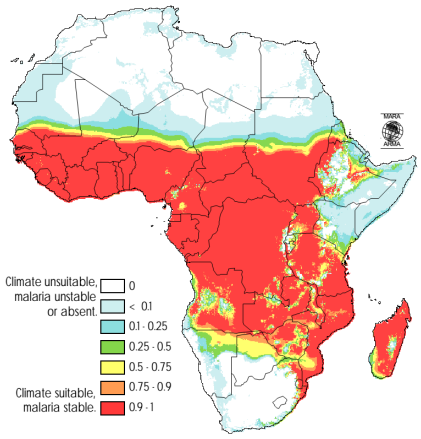

Figure 1.4: The map shows the distribution of malaria in Africa.
(Source: MARA, http://www.mara.org.za)

Malaria is one of the leading public health problems in Ethiopia. It is found in nearly 60% of the country are at risk of contracting malaria. In most of Ethiopia, peak malaria transmission occurs between September and December after the main rainy season from June to August. Certain areas with low malaria transmission period from April to June, following a short rainy season from February to March (EPHI, 2018).

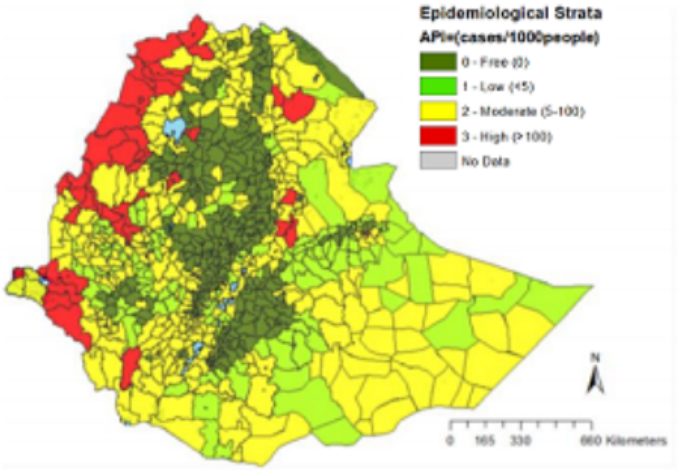

Figure 1.5: The map shows distribution of malaria in Ethiopia
(Source: Ethiopia National Malaria Indicator Survey, 2018)

1.1.7 Role of mathematical modeling on malaria transmission

Mathematical modelling is an important tool that has significant role in the study of infectious diseases. It has a major role in increasing our understanding of the dynamics of diseases and providing intervention strategies to mitigate the diseases. Mathematical model of malaria transmission has developed by Ronald Ross, who received the *Nobel Prize* in 1902 for his work on the life cycle of the malaria parasite (Ross, 1911). Ross developed a simple SIS for the human and SI for the vector model. From the Ross model, many mathematical models have been formulated considering the impact of temperature variability on malaria dynamics with optimal control strategies (Agusto, 2020; Traoré et al., 2020; Yiga et al., 2020; Herdicho et al., 2021). To best of our knowledge the impact of temperature variability on the transmission dynamics of malaria epidemics using a logistic growth of temperature variation with respect to the birth rate of mosquito and malaria infection with optimal control strategies and their cost-effectiveness is not studied. This is addressed in this dissertation by considering the logistic growth of temperature variation with respect to the birth rate of mosquito and malaria infection. Thus we proposed a mathematical model for the impact of temperature variability on the malaria epidemics by considering the logistic growth of temperature variation with respect to the birth rate of mosquito and malaria infection with optimal control and cost-effectiveness analysis.

1.2 Statement of the problem

Malaria remains one of the largest killer diseases in worldwide. Mathematicians have developed a significant and effective tool, namely mathematical models of malaria transmission, that give an insight into the interaction between the host and vector population. Several mathematical models of malaria transmission have been developed considering the impact of temperature and rainfall variability on mosquito birth rate, contact rate, and death rate (Ngarakana-Gwasira et al., 2016; Abiodun et al., 2018; Bhuju et al., 2018; Okuneye et al., 2019; Gashaw et al., 2019; Garba and Danbaba, 2020; Traoré et al., 2020; Yiga et al., 2020). For instances, Bhuju et al. (2018) proposed an SEIRS model for human population and SEI for malaria. They also derived malaria transmission model by incorporating the effect of temperature on the biting rate and birth rate of the vector population. Gashaw et al. (2019) studied SIRS a mathematical model for human population and SI for malaria. Their study shown the effect of temperature on the biting rate and both temperature and rainfall on the birth rate and death rate of the mosquito.

However, all of these studies did not consider the impact of temperature variability on malaria epidemics with a logistic growth of temperature variation with respect to mosquitoes breeding and malaria infection. Motivated by the recent works of (Ngarakana-Gwasira et al., 2016; Abiodun et al., 2018; Bhuju et al., 2018; Okuneye et al., 2019; Gashaw et al., 2019; Garba and Danbaba, 2020; Traoré et al., 2020; Yiga et al., 2020), we consider a malaria transmission model with the impact of temperature variability on malaria epidemics considering a logistic model for temperature variation with respect to mosquitoes breeding and malaria infection. Therefore, this study proposed a mathematical model for the impact of temperature variability on the malaria epidemics with optimal control strategy and cost-effectiveness analysis.

1.3 Objectives of the study

1.3.1 General objective

The general objective of this study is to investigate the impact of temperature variability on malaria epidemics using a mathematical model and propose an optimal control strategy with cost-effectiveness analysis.

1.3.2 Specific objectives

The specific objectives are to:

- develop SIRS mathematical model of malaria dynamics with temperature variability.
- extend the SIRS model into optimal control and cost effectiveness analysis.
- develop SEIRS mathematical model of malaria dynamics with temperature variability.
- extend the SEIRS model into optimal control and cost effectiveness analysis.

1.4 Significance of the study

The study is significant for the following reasons:

- it will help to improve control strategies for the occurrence of malaria epidemics in a community.
- the output of this study will serve as an input for public health policymakers.

- the study will also serve as a reference for further research on optimal control of malaria and form a base for further studies of related problems.
- further, the study will also help researchers to create awareness of the impact of temperature variability on malaria epidemics.

1.5 The scope of the study

This study mainly focus on developing a deterministic mathematical models to investigate the impact of temperature variation on the malaria epidemics. Further the developed mathematical models were extended to optimal control strategies with cost-effectiveness analysis. During applying optimal control theories to the model it is not possible to apply each and every control measure due to the time constraint. Thus, the study will be limited to the main governing control strategies depending on the disease dynamics. Pontraygin's minimum principle is applied to obtain the necessary condition for the optimal control and the cost-effectiveness analysis is described with all the various combinations of the controls. In this dissertation, we used the data obtained from the East Shawa Zone.

1.6 Organization of the study

The dissertation is organized into 8 chapters. The structure of each chapter is presented as follows. Chapter 1 presents general overview. That is, background of the study, statement of the problem, objectives of the study and significance of the study. In Chapter 2 we presented the relevant related review of the literature. Chapter 3 illustrates the research methodology of the study. Chapter 4 describes a basic deterministic model that describes the impact of temperature variability on malaria epidemics. This model analyzed both qualitatively and quantitatively. Chapter 5 proposes and analyzes a deterministic model of the transmission dynamics of malaria in the presence of temperature variability factor. Chapter 6 deals with optimal control strategy and cost-effectiveness analysis of the malaria epidemics model. Chapter 7 is devoted to the optimal control analysis of the malaria epidemics in the presence of temperature variability. Finally, the conclusions, recommendations and future research are presented in the last chapter 8.

CHAPTER 2
LITERATURE REVIEW

Malaria is a serious health problem in many African countries. Many studies have been conducted on understanding how this disease is transmitted and its control by proposing various types of Mathematical models. In this chapter, we reviewed some researches that were studied a mathematical model of malaria transmission with optimal control and cost effectiveness analysis that are directly related to the objectives of our study.

2.1 Malaria transmission models

A number of studies have been conducted to emphasize the control of the diseases and their dynamic by building different types of Mathematical models. The study on malaria using mathematical model began in 1911 by Ronald Ross (Ross, 1911). He considered the first deterministic two-dimensional model with one variable representing humans and the other representing mosquitoes. Later, he introduced the first deterministic mathematical model of malaria by dividing the human population into susceptible and infected compartments, with the infected class returning to susceptible class again leading to the SIS structure. The mosquito population also has only two compartments susceptible and infected, but they do not recover from infection due to their short life span, and there by follow the SI structure (Mandal et al., 2011). The major advantage in Ross model was his ability to provide a suitable control strategy through the transmission threshold criterion which is based on the reproductive capacity of the parasite and is termed as basic reproductive number.

After about 40 years, Macdonald et al. (1957) termed the latency period and introduced the exposed class in the mosquitoes. As a result, in their model the mosquito population is divided into three compartments SEI and the model studies the time evolution of the exposed and infected classes in mosquito. Thus, their model takes the form SIS-SEI. Aron and May (1982) proposed SIRS model by introducing the recovery group in the human population

and their model was structure SIRS-SEI. Later, Anderson and May (1992) proposed the latency of infection by making additional exposed class in humans and their model followed by SEIS-SEI. This modification further reduces the long term prevalence of both the infected humans and mosquitoes.

Yang (2000) introduced a mathematical model based on the human host immunity with separate immune class in human population and mosquito vector taking into account that the average period of development from egg to adult mosquito are dependent on the temperature. In the same year, Ngwa and Shu (2000) proposed a model for malaria transmission in which human hosts follow a susceptible-exposed-infected-recovered-susceptible pattern and vector hosts follow the susceptible-exposed-infected pattern due to their short life cycle. Authors introduce in their model, a class of persons who are partially immune to the disease malaria. Besides, the inclusion of acquired immunity proposed by Chitnis et al. (2006) was a major point of malaria transmission model. In their model, they considered that the susceptible mosquitoes can become infected when they bite infectious or recovered humans. The authors also showed that for basic reproduction number is greater than unity, the disease free equilibrium is unstable while the endemic equilibrium is stable. Author's numerical simulations showed for larger values of the disease-induced death rate, a backward bifurcation is possible at basic reproduction number equal to unity. Chitnis et al. (2008) extended the model of Ngwa and Shu (2000) by assuming that individuals in the recovered class are immune, in the sense that they do not suffer from serious illness, they still have low levels of *Plasmodium* parasite in their bloodstream and so that can infect the susceptible mosquitoes. Authors suggested that minimizing the mosquito biting rate and increasing the human recovery rate can be successful in controlling malaria.

Yang et al. (2010) proposed SIR for the human population and SI for vector compartment. The authors computed disease free equilibrium and derived a basic reproduction number for model and through stability analysis, that is the disease free equilibrium is stable for basic reproduction number is less than unity. They also derived an expression for an endemic equilibrium that is biologically relevant only when basic reproduction number greater than one. The authors also proved that for basic reproduction number is greater than unity, the disease free equilibrium is unstable while the endemic equilibrium is stable. Their numerical simulation result has an agreement with the analytical results. From the contribution point of view, all other mathematical models that exist for malaria dynamics are developed from the three basic models (Ross, 1911; Macdonald et al., 1957; Anderson and May, 1992) by

incorporating different factors to make them biologically more realistic in explaining disease prevalence and prediction (Mandal et al., 2011).

In recent decades, many studies reveal that the transmission of malaria is determined by the climatic factors such that temperature and rainfall. For instance, Mordecai et al. (2013) presented the optimal temperature for malaria transmission. Their model includes empirically derived nonlinear thermal responses, predicts optimal malaria transmission at 25^oC. The result of their studies showed that the transmission of malaria is very low at temperature below 16^oC and decreases for temperature greater than 28^oC. Ngarakana-Gwasira et al. (2016) proposed the role of climate change in malaria transmission in Africa. Their mathematical model incorporated rainfall and temperature to study the transmission dynamics of malaria. They have also studied the impact of temperature on the death rate of the mosquito population. The rest of their study suggested that malaria transmission is sensitive to climate change in the sense that the vector that spread malaria and the parasite that causes the disease are sensitive to climate variables especially temperature and rainfall. The analysis of the model suggested that the optimum temperature malaria transmission is $30-32^oC$. Moreover, Abiodun et al. (2016) derived a deterministic malaria transmission model that gives the influence of temperature and rainfall on the dynamics of mosquito populations. They concluded that climatic changes have a high influence on the vector population birth rate and the dynamics are negatively influenced by temperature below 15^oC and above 30^oC.

Bhuju et al. (2018) proposed a mathematical model for the study of the impact of temperature on malaria transmission dynamics. They have studied the effect of temperature variability in the biting rate and birth rate of the vector population. Their analysis concluded that the mosquito bite rate is very minimum in temperature below 16^oC, optimum in 28^oC and greater than 32^oC have negative impact on the survival of the mosquitoes and the transmission dynamics of the disease. Abiodun et al. (2018) presented SEIRS-SEI compartment of mathematical model for impact of temperature and rainfall variables on malaria transmission. The author incorporated the effect of temperature in the biting rate and death rate of the vector population. Their findings suggest that the biting rate of mosquito is very low in temperature below 12^oC; gradually increasing with a slight declination at upper thermal limit of 35^oC and when greater than 35^oC have negative impact on the mosquito death rate. Mosquito death rate is high at temperature below 18^oC, low between $18-25^oC$ and increases temperature beyond 25^oC.

Gashaw et al. (2019) proposed SIRS for the human population and SI malaria model for the climate-dependent malaria disease transmission model and it's analysis. Authors investigated a model by incorporating the effect of temperature in the biting rate and the effects of both temperature and rainfall in the birth rate and death rate of the vector population. They have showed that the mosquito bite rate is low at temperature below 18^oC and increases at a temperature beyond 25^oC. They also verified that the parasite birth rate increases along with moderate temperature, while mosquito death rate is constrained at high temperature. Okuneye et al. (2019) presented weather-driven malaria transmission model. In their study death rate of mosquito is mainly depend on temperature. The authors suggested that malaria burden peaks at 29.5^oC when daily ambient temperature is held constant, but this peak decreases with increasing daily temperature variation to about $23^oC - 25^oC$. Malaria burden also varies nonlinearly with temperature such that small temperature changes can increase or decrease the dynamics transmission of the disease.

Traoré et al. (2020) modified the Okuneye et al. (2019) malaria transmission model by formulating a mosquito-stage-structured to take the four metamorphic stages of mosquitoes which is subject to temperature variations. They confirmed that, climate factors have a great impact on the mosquito life cycle and parasite survival in mosquitoes. Also, using the reported monthly mean temperature of Burkina Faso, they perform some numerical simulations to illustrate their theoretical results. Further more, Garba and Danbaba (2020) presented a mathematical model that shows the effect of temperature variability on malaria control strategies. Their model assess the impact of temperature changes on various control strategies. The authors introduced the impact of temperature variation on death rate and birth rate mosquito population. They have shown that, the model exhibit the phenomenon of backward bifurcation when an associated reproduction number is less than unity. Yiga et al. (2020) proposed and analyzed the impact of seasonal factors on malaria transmission dynamics. They incorporated the role of temperature in death rate of the vector and impact of both temperature and rainfall in the birth rate of mosquito. Their study concluded that temperature has more influence on death rate of mosquito.

2.2 Malaria transmission models with optimal controls

The theory of optimal control has been widely applied in the study of malaria transmission. Many scholars have developed mathematical models that aim at studying the dynamics of malaria while incorporating a combination of control strategies. For instance, Blayneh et al.

(2009) formulated a mathematical model with optimal control problem to study the role of prevention and treatment on the vector borne disease. The authors concluded that the combination of prevention and treatment control measures is the best optimal strategy to combat the vector borne diseases. Makinde and Okosun (2011) presented a malaria model for the impact of chemo-therapy on optimal control of malaria using three time dependent continuous controls. Using the Pontryagin's minimum principle, the optimal control problem was constructed with combination of four control strategies. They showed that the most efficient and best strategy to control the malaria transmission is the combination of screening, infected human treatment using drugs and indoor spraying of insecticide. Okosun et al. (2011) proposed a malaria model with optimal control strategies of malaria spread using two measures that control treatment infectious and vaccination. The authors obtained the necessary conditions of optimal control problem using Pontryagin's minimum principle to determined optimal strategies to reduce the spread of the disease and least cost effective strategy. Authors concluded that the best optimal strategy and least cost to control malaria is the combination of treatment and vaccination.

Agusto et al. (2012) studied a malaria transmission model that includes the optimal control problem to investigate optimal strategies. To minimize the spread of malaria, they used treated bed net, treatment infectious and indoor insecticide spraying. Authors performed an optimal control strategy with the use of one control at a time, two controls at a time and the combination of more than two controls at a time, to compare the effects of the control strategies on malaria eradication. Their study reveal that the combination of the treated bed net, treatment and indoor spraying of insecticides is the best strategy for controlling of the disease. Moreover, Okosun et al. (2013) presented the malaria transmission dynamics with optimal control and analysis of cost-effectiveness. The authors applied the combinations of three malaria control measures such are treated bed net, treatment of infected humans with ant-malarial drugs and indoor insecticides spraying. In the time-dependent control case, they derived necessary conditions for the optimal control of the disease. In their conclusion, the best optimal and least cost-effective controls to prevent malaria spread is the combination of treatment of infected human using drugs and indoor insecticides spraying.

Mwamtobe et al. (2015) formulated a deterministic a SEIRS-SEI compartment model for malaria transmission by considering three optimal control strategies. These controls are treated bed net, treatment infectious and indoor insecticide spraying. Authors obtained the necessary conditions for the optimal control of the disease. Their numerical simulations in-

dicate that the prevention strategies lead to the reduction of both the mosquito population and infected human individuals. The results showed that the combination of the three intervention strategies has a positive and greater impact in reducing the epidemics of malaria. Abdullahi et al. (2015) studied a deterministic mathematical model for malaria transmission with two control strategies. The model was extended by applying the optimal control theory that investigated the optimal control strategies for controlling the spread of malaria using treatment and culling. The authors suggested that the most effective and least cost strategy to control malaria is the combination of treatment and culling.

Otieno et al. (2016) presented malaria transmission model with optimal control problem, using four control measures that time-dependent. The Pontryagin's minimum principle was described to derive the necessary conditions for the optimal control of the malaria. The existence of optimal control problem is proved. Their result concluded that the combinations of treated bed nets and treatment is the most optimal strategy to minimize the disease. Gashaw et al. (2018) presented SIRS for the human population and SI malaria model for the malaria transmission that climate-dependent by introducing triples controls. The authors suggested that the mixed of three controls treated bed net, treatment of infected human using drugs and insecticide spraying is the best strategies for the prevention of malaria.

Olaniyi et al. (2018) presented a SEIRS-SEI model with an optimal control analysis using four time dependent controls, namely personal protection, chemo-prophylaxis, chemotherapy and mosquito-reduction effort to describe the dynamics of malaria transmission. Their results concluded that the combinations of all these controls are the best measure for minimizing the spread of malaria. Mohammed-Awel et al. (2018) proposed nonlinear deterministic mathematical model for the malaria spread and optimal control strategies in a community. Their study presented a new deterministic model for assessing the population-level impact of mosquito insecticide resistance on malaria transmission dynamics. The optimal control problem was designed by applying Pontryagin's minimum principle with two control strategies, namely, the prevention strategy through insecticide-treated bed-nets and indoor residual spraying; which is the best cost-effective strategy to minimize the disease. Kyere et al. (2018) presented the optimal control strategies for the malaria model to reduce the spread of disease using treated bed net, treatment of infected human and indoor insecticide spraying. The authors suggested that the combination of the treated bed nets, treatment and indoor spraying of insecticides is the best strategy for control of the disease.

Romero-Leiton et al. (2018) studied an SEIRS-SI optimal control model for malaria transmission in Colombia considering three optimal control strategies. The authors concluded that integrated of control measures treated bed net, intermittent prophylactic treatment in pregnancy and effective case management is the best strategy for the prevention of malaria disease. Romero-Leiton et al. (2019) proposed SEIRS for the human population and SI malaria model with optimal control and cost-effectiveness analysis in Colombia using four time dependent controls. They suggested that the combination of treat bed net, antimalarial treatment, intermittent prophylactic treatment in pregnancy and spraying of insecticides strategy is the most cost-effective approach to control malaria in rural Tumaco.

Oke et al. (2020) proposed the mathematical model for malaria transmission that includes the optimal control analysis using three time dependent controls. The author's numerical simulations results showed that the combination of the three controls, treated bed-net, medication and insecticides spraying, has the highest impact on the control of the disease. Agusto (2020) presented the model of the impact temperature variations on malaria transmission dynamics with the optimal control using the time dependent control variables namely personal protection, larvaciding and insecticides spraying. This study presented the results obtained from investigating the optimal control strategies for malaria in the presence of temperature variation using a temperature-dependent malaria model. Thus, they concluded that personal protection, particularly the use of treated bed net, should be encouraged not only at low temperatures but particularly at high temperatures when individuals are driven not to use the nets.

Ghosh et al. (2020) investigated a malaria model for the spread of disease with optimal control and cost-effectiveness analysis using three control measures. Their model with time-dependent control strategies was analyzed to find the optimal solutions of the optimal control problem. Cost-effectiveness analysis was conducted to support the results of the optimal control problem by using the average cost-effectiveness ratio and incremental cost-effectiveness ratio methods. The authors demonstrated the numerical simulations to enhance the theoretical results. Finally, they suggested that the combinations of treated bed net, treatment using drugs and an insecticides spraying is the most effective and less costly interventions strategy. Olaniyi et al. (2020) presented a mathematical model of malaria dynamics with naturally acquired immunity in the presence of protected travellers. An optimal control theory used to analyses an optimal control model by incorporating four control variables, which minimizes malaria infection and costs of implementation. Furthermore, the cost-effectiveness analysis was carried out to identify the less costly strategy that could be implemented to prevent

the spread of malaria with limited resources. Their study reveal that the combination of the optimal use of treat bed net, prophylaxis and indoor residual spraying is the optimal cost-effective intervention.

Bakare and Hoskova-Mayerova (2021) formulated a susceptible-exposed-infected-recovered-susceptible compartment for the human population and susceptible-exposed-infected malaria model with optimal control analysis incorporating the presence of five different time dependent controls namely, treated bed net, treatment, educational campaigns, indoor residual spray and regular destruction of mosquito breeding sites to reduce the number of new mosquitoes. The authors concluded that multiple control interventions of those strategies were an optimal strategy for malaria controlling in the community. Herdicho et al. (2021) proposed an optimal control of malaria transmission model with mosquito seasonal factor using three time dependent controls such are treated bed net, treatment and insecticide spraying. Furthermore, they determined the existence of the optimal control variable in the malaria model with seasonal factor. The combination of three controls treated bed net, treatment of infected human using drugs and insecticide spraying is an optimal strategy and effective in reducing the disease. Aldila and Angelina (2021) presented a mathematical model of malaria transmission by extending to the optimal control problem. The optimal control problem was constructed by introducing the treating fumigation and medical treatment strategy as the time-dependent variable. The author's numerical simulations of the optimal control problem was concluded that time-dependent fumigation and medical treatment could suppress the spread of malaria more efficiently at minimum cost.

Generally, there are plenty of mathematical studies that have been undertaken for malaria transmission model with optimal control, but there are no studies that have been undertaken for modeling the impact of temperature variability on malaria epidemics with optimal control and cost effectiveness analysis considering logistic growth of temperature variation with respect to mosquitoes breeding and malaria infection in their models. Hence, to fill this gap, we considered the impact of temperature variability on malaria epidemics with a logistic growth of temperature variation with respect to mosquitoes breeding and malaria infection. This study is therefore designed and proposed malaria transmission dynamics with the impact of temperature variability on malaria epidemics with optimal control strategies and cost-effectiveness analysis.

CHAPTER 3
RESEARCH METHODOLOGY

In this chapter we present the study area, data collection and mathematical procedures.

3.1 Study area

East Shewa is one of the Zones of Oromia regional states. It is located in the middle of Oromia, connecting the western regions to the eastern ones. This zone is bordered on the south by the west Arsi Zone, on the south west by the Sidama Regions, on the west by South west Shewa and Oromia Special Zone surrounding Finfinne, on the North west by North Shewa, on the north by the Amhara Region, on the North east by the Afar Region and on the south east by Arsi. According to East Shewa administrative zone, the current (2019) estimated total population in the zone is about 2,130,372.

3.2 Data collection

East Shewa Zone is malaria endemic area located in the Great Rift Valley in Ethiopia. This study provided data collected from East Shewa Zone Health office. The data is a year, secondary data reported of malaria infectious between 2010 and 2019 in East Shewa zone.

3.3 Mathematical methods

Mathematical models provide descriptions of the behavior of the systems using mathematical concepts. It begins with a clear description of the processes based on the understanding of the system. Then translate into mathematical equations should be made with a specific goal. We present a mathematical model which describes the impact of temperature variability on malaria epidemics using a logistic growth for temperature variation with respect to mosquito breeding rate and malaria infection rate.

Firstly, the domain in which the model is mathematically well posed and epidemiologically meaningful was determined. Qualitative and quantitative analysis of the model is presented. Both local and global stability analysis of the equilibrium points of the model have been performed using Jacobian matrix and Lyapunov functions respectively. Also, the nature of the bifurcation is identified using the method described by Castillo-Chavez and Song that is based on centre manifold theory (Castillo-Chavez and Song, 2004a). Sensitivity analyses of basic reproduction numbers have been studied to determine which parameter plays greater role in the transmission of malaria. Some of the parameter values were estimated with real data using least square method to validate our model.

Moreover, a malaria transmission model is extended to the optimal control problem. The existence of the optimal controls is illustrated. Then the necessary conditions of the optimal control have been derived by using the Pontryagin's minimum principle. Numerical methods for solving ordinary differential equations and boundary value problems can then be employed to solve the resulting two-point boundary value problem. The method called fourth forward-backward Runge-Kutta sweep is used to solve the optimality system. Lastly, numerical simulations of the models are done using the MATLAB software to supplement the analytical solution of the model. A cost-effectiveness analysis is described with the purpose of finding the most cost-effective strategy for the prevention of malaria. The most effective and less costly strategy is obtained using the method called incremental cost-effectiveness ratio which is defined as the ratio between the difference in averted costs between two strategies and the difference in infections averted between two strategies. In this method, a combination of more than one control at a time is implemented to identify the most optimal and least-cost strategy which minimizes the disease.

CHAPTER 4
MODELING SIRS MATHEMATICAL MODEL OF MALARIA DYNAMICS WITH TEMPERATURE VARIABILITY

Mathematical modeling is an essential tool in the study of disease transmission and decision for the disease control. In this chapter, we proposed a malaria transmission model that describes the impact of temperature variability on malaria epidemics.

4.1 Model description and formulation

The model we are introducing for the malaria transmission divides the human and mosquito population with the total human populations denoted by $N_h(t)$ and mosquito populations denoted by $N_m(t)$ respectively. The model sub-divides the total human population into sub-populations with respect to their disease status in the system into susceptible human denoted by $\mathtt{S}_h(t)$, infected human denoted by $\mathtt{I}_h(t)$ and recovered individuals with temporary immunity denoted by $\mathtt{R}_h(t)$. The human population is assumed the SIRS compartment model since humans would be repeatedly infected because there is no acquiring permanent immunity. Thus, the total population of human is given by $N_h(t) = \mathtt{S}_h(t) + \mathtt{I}_h(t) + \mathtt{R}_h(t)$. The female anopheles mosquitoes considered as the transmission vector since only female mosquito bites human for blood meals. The total vector (mosquito) population denoted by $N_m(t)$ is sub-divided into susceptible mosquito denoted by $\mathtt{S}_m(t)$ and infected mosquito denoted by $\mathtt{I}_m(t)$. We assume mosquitoes do not recover from the *Plasmodium* parasite and the mosquito population is followed by the SI compartment model. Hence, the total population of mosquito is given by $N_m(t) = \mathtt{S}_m(t) + \mathtt{I}_m(t)$.

The recruitment rate of human enter the susceptible human population at a rate Ψ. Susceptible human becomes infected if it contacts with the infected mosquito at the rate $\beta_h(\mathtt{T})$

is temperature-dependent and β_{0h} is contact rate of human with mosquito when there is no variation in temperature and β_{1h} is incremental contact rate of human with mosquito due to temperature variation. The natural death rate of all human populations is μ_h and the human induced death rate due to disease is δ. Infected human recovery due to the use of anti-malarial drugs through treatment at a rate γ_h. Recovered human could be lost temporary immunity and then becomes susceptible to reinfection at a rate ω_h.

The recruitment of mosquito population at a rate $\Phi(\mathrm{T})$ is temperature-dependent and Φ_0 is the birth rate of mosquito if there is no variation in temperature and Φ_{1m} is the incremental birth rate of mosquito due to temperature variation. Susceptible mosquito population becomes infected if it contacts with an infected human at a rate $\beta_m(\mathrm{T})$ is temperature-dependent and β_{0m} is contact rate of mosquito with a human when there is no variation in temperature whereas β_{1m} is incremental contact rate of mosquito with human due temperature variation. The natural death rate of all mosquitoes population is μ_m. We assumed mosquitoes do not recover from malaria. Also, mosquitoes do not die due to disease infection. The growth rate of the temperature is r, maximum temperature for a mosquito to be most active is denoted by $\mathrm{T}_{\max}$ and the minimum temperature for the mosquito to be less active is T_0. We assume that all parameters in the model are positive.

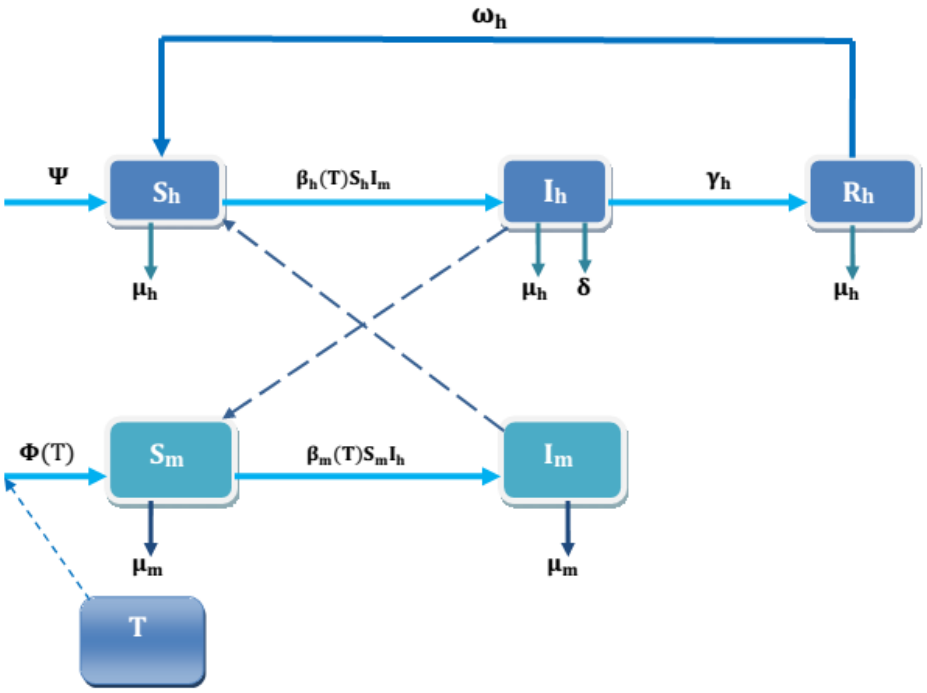

Figure 4.1: Flow diagram of malaria transmission model

From the flow diagram depicted in Figure 4.1, the governing mathematical model is described by the following system of differential equations

$$\begin{cases} \frac{dS_h}{dt} &= \Psi - \beta_h(\mathtt{T})S_h I_m - \mu_h S_h + \omega_h \mathtt{R}_h, \\ \frac{dI_h}{dt} &= \beta_h(\mathtt{T})S_h I_m - (\mu_h + \delta + \gamma_h)I_h, \\ \frac{dR_h}{dt} &= \gamma_h I_h - (\mu_h + \omega_h)\mathtt{R}_h, \\ \frac{dS_m}{dt} &= \Phi(\mathtt{T}) - \beta_m(\mathtt{T})S_m I_h - \mu_m S_m, \\ \frac{dI_m}{dt} &= \beta_m(\mathtt{T})S_m I_h - \mu_m I_m, \\ \frac{d\mathtt{T}}{dt} &= \mathrm{r}(1 - \frac{\mathtt{T}}{\mathtt{T}_{\max}})(\mathtt{T} - \mathtt{T}_0), \end{cases} \tag{4.1}$$

where,
$\beta_h(\mathtt{T}) = \beta_{0h} + \beta_{1h}\left(\frac{\mathtt{T}-\mathtt{T}_0}{\mathtt{T}_{\max}}\right)$, $\beta_m(\mathtt{T}) = \beta_{0m} + \beta_{1m}\left(\frac{\mathtt{T}-\mathtt{T}_0}{\mathtt{T}_{\max}}\right)$ and $\Phi(\mathtt{T}) = \Phi_0 + \Phi_{1m}\left(\frac{\mathtt{T}-\mathtt{T}_0}{\mathtt{T}_{\max}}\right)$.

With conditions $\mathtt{S}_h(0) = \mathtt{S}_{h0}, \mathtt{I}_h(0) = \mathtt{I}_{h0}, \mathtt{R}_h(0) = \mathtt{R}_{h0}, \mathtt{S}_m(0) = S_{m0}, \mathtt{I}_m(0) = \mathtt{I}_{m0}, \mathtt{T}(0) = \mathtt{T}_{\mathrm{m0}}$.

Table 4.1: Parameters description used for the model (4.1)

Parameters	**Parameters description**
β_{0h}	Contact rate of human with mosquito
Φ_{1m}	Incremental breeding rate of mosquito
Ψ	Human recruitment rate
Φ_0	Mosquito recruitment rate
γ_h	Recover rate of infected human
μ_h	Human natural death rate
δ	Human induced death rate
μ_m	Natural death rate for mosquito
ω_h	Rate of loss of immunity in human
β_{0m}	Contact rate of mosquito with human
β_{1m}	Incremental contact rate of mosquito
β_{1h}	Incremental contact rate of human
r	Growth rate of temperature
$\mathtt{T}_0$	Minimum temperature for the mosquito to be less active
$\mathtt{T}_{\max}$	Maximum temperature for the mosquito to be most active

4.2 Qualitative analysis of the model

In this section, we investigate the invariant region, positivity of the solution, disease free equilibrium point, basic reproduction number, endemic equilibrium point, local and global stability of equilibrium points of the system (4.1).

4.2.1 Invariant region

It is basic to find the invariant region of the model (4.1) that is a biologically meaningful and mathematically well posed such that the solution of the model (4.1) is bounded.

Theorem 4.1 The solution of the model (4.1) enter into invariant region and stay in Θ, where

$$\Theta = \Theta_h \times \Theta_m = \left\{ (\mathtt{S}_h, \mathtt{I}_h, \mathtt{R}_h, \mathtt{S}_m, \mathtt{I}_m) \in \mathbb{R}^5_+ : N_h \leq \frac{\Psi}{\mu_h}, N_m \leq \frac{\Phi(\mathtt{T})}{\mu_m} \right\}. \tag{4.2}$$

Proof: The model (4.1) represents two groups, namely, the human population and mosquito population. Firstly, the total population of human is given by $N_h(t) = \mathtt{S}_h(t) + \mathtt{I}_h(t) + \mathtt{R}_h(t)$. Then, differentiate $N_h(t)$ both sides with respect to time and adding the first three equations of system (4.1) we got,

$$\begin{aligned} \frac{dN_h}{dt} &= \Psi - \mu_h N_h - \delta \mathtt{I}_h, \\ \frac{dN_h}{dt} &\leq \Psi - \mu_h N_h. \end{aligned} \tag{4.3}$$

Integrating both sides of equation (4.3) with respect to time and simplifying, we obtain,

$$\Psi - \mu_h N_h \geq \mathscr{A} e^{-\mu_h t} \tag{4.4}$$

where $\mathscr{A}$ is a constant. Using the initial conditions at $t = 0$, $N_h(0) = N_{h0}$ in (4.4) and rearranging equation, we got

$$N_h \leq \frac{\Psi}{\mu_h} - \left(\frac{\Psi - \mu_h N_{h0}}{\mu_h} \right) e^{-\mu_h t}. \tag{4.5}$$

From equation (4.5) the population of human $N_h \to \frac{\Psi}{\mu_h}$ as time (t) tends to infinity that indicates $N_h \leq \frac{\Psi}{\mu_h}$. So that, the invariant region of the system (4.1) for human population that is positively invariant is given by

$$\Theta_h = \left\{ (\mathtt{S}_h, \mathtt{I}_h, \mathtt{R}_h) \in \mathbb{R}^3_+ : \mathtt{S}_h + \mathtt{I}_h + \mathtt{R}_h \leq \frac{\Psi}{\mu_h} \right\}.$$

Secondly, the total mosquito population from the system (4.1) is given as

$$N_m(t) = \mathtt{S}_m(t) + \mathtt{I}_m(t).$$

Thus, differentiating $N_m(t)$ both sides with respect to time (t) the result obtain as

$$\frac{dN_m}{dt} = \Phi(\mathtt{T}) - \mu_m N_m. \tag{4.6}$$

By solving equation (4.6), we obtain $N_m \leq \frac{\Phi(\mathtt{T})}{\mu_m}$. Hence, the positive invariant region of the system (4.1) for mosquito population is given as

$$\Theta_m = \left\{ (\mathtt{S}_m, \mathtt{I}_m) \in \mathbb{R}^2_+ : \mathtt{S}_m + \mathtt{I}_m \leq \frac{\Phi(\mathtt{T})}{\mu_m} \right\}.$$

Consequently, the invariant region of the system (4.1) is given by

$$\Theta = \Theta_h \times \Theta_m = \left\{ (\mathtt{S}_h, \mathtt{I}_h, \mathtt{R}_h, \mathtt{S}_m, \mathtt{I}_m) \in \mathbb{R}^5_+ : N_h \leq \frac{\Psi}{\mu_h}, N_m \leq \frac{\Phi(\mathtt{T})}{\mu_m} \right\} \tag{4.7}$$

is positive invariant and therefore, all the solution set of system (4.1) is bounded in Θ.

4.2.2 Positivity of the solutions

In this subsection, we are going to show that all solutions of system (4.1) with non-negative initial data will remain non-negative for all time $t \geq 0$.

Theorem 4.2 Let $\Theta = \left\{ (\mathtt{S}_h, \mathtt{I}_h, \mathtt{R}_h, \mathtt{S}_m, \mathtt{I}_m) \in \mathbb{R}^5_+ : \mathtt{S}_h(0), \mathtt{I}_h(0), \mathtt{R}_h(0), \mathtt{S}_m(0), \mathtt{I}_m(0) \right\}$ are positive, then the solution $\{\mathtt{S}_h(t), \mathtt{I}_h(t), \mathtt{R}_h(t), \mathtt{S}_m(t), \mathtt{I}_m(t)\}$ of the system (4.1) are positive for $t \geq 0$.

Proof. Take the second equation of system (4.1) we have,

$$\begin{aligned} \frac{d\mathtt{I}_h}{dt} &= \beta_h(\mathtt{T}) S_h I_m - (\mu_h + \delta + \gamma_h) I_h, \\ \frac{d\mathtt{I}_h}{dt} &\geq -(\mu_h + \delta + \gamma_h) I_h. \end{aligned} \tag{4.8}$$

Integrating equation (4.8) with respect to time and applying separation of variable, we obtain

$$\mathtt{I}_h(t) \geq \mathtt{I}_h(0) e^{-(\mu_h + \delta + \gamma_h)t} \geq 0.$$

Next, from the third equation of system (4.1) we have,

$$\begin{aligned} \frac{d\mathtt{R}_h}{dt} &= \gamma_h I_h - (\mu_h + \omega_h)\mathtt{R}_h, \\ \frac{d\mathtt{R}_h}{dt} &\geq -(\mu_h + \omega_h)\mathtt{R}_h. \end{aligned} \tag{4.9}$$

Applying separation of variable after integrating equation (4.9) with respect to time, we get

$$\mathtt{R}_h(t) \geq \mathtt{R}_h(0)e^{-(\omega_h+\mu_h)t} \geq 0.$$

Thirdly, from the sixth equation of system (4.1) we have,

$$\begin{aligned} \frac{d\mathtt{I}_m}{dt} &= \beta_m(\mathtt{T})S_m I_h - \mu_m I_m, \\ \frac{d\mathtt{I}_m}{dt} &\geq -\mu_m I_m. \end{aligned} \tag{4.10}$$

Integrating equation (4.10) with respect to time and solving separation of variable with applying initial condition, we obtain

$$\mathtt{I}_m(t) \geq \mathtt{I}_m(0)e^{-(\mu_m)t} \geq 0.$$

Continuing from the first equation of system (4.1) that is given as

$$\begin{aligned} \frac{d\mathtt{S}_h}{dt} &= \Psi - \beta_h(\mathtt{T})S_h I_m - \mu_h S_h + \omega_h \mathtt{R}_h, \\ \frac{d\mathtt{S}_h}{dt} &\geq -(\beta_h(\mathtt{T})I_m + \mu_h)S_h. \end{aligned} \tag{4.11}$$

Integrating equation (4.11) with respect to time and solving separation of variable with applying initial condition, we obtain

$$\mathtt{S}_h(t) \geq \mathtt{S}_h(0)e^{-(\beta_h(\mathtt{T})I_m+\mu_h)t} > 0.$$

Lastly, from the fourth equation of the model (4.1)

$$\begin{aligned} \frac{d\mathtt{S}_m}{dt} &= \Phi(\mathtt{T}) - \beta_m(\mathtt{T})S_m I_h - \mu_m S_m, \\ \frac{d\mathtt{S}_m}{dt} &\geq -(\beta_m(\mathtt{T})I_h + \mu_m)S_m. \end{aligned} \tag{4.12}$$

Integrating equation (4.12) with respect to time and using separation of variable with applying initial condition, we obtain

$$\mathtt{S}_m(t) \geq \mathtt{S}_m(0)e^{-(\beta_m(\mathtt{T})I_h+\mu_m)t} > 0.$$

Thus, this shows that the all solutions of system (4.1) are non-negative for all $t \geq 0$. Hence, the proposed model (4.1) is both epidemiologically meaningful and mathematically well posed in Θ.

4.2.3 Disease free equilibrium point

An equilibrium point of the dynamic system that occurs in the absence of the disease is known as the disease free equilibrium (DFE). The model (4.1) has a disease free equilibrium that occurs in the absence of the malaria. Then the disease free equilibrium points are obtained by setting the left-hand side of model (4.1) to zero, that is given as;

$$\begin{aligned}
\Psi - \beta_h(\mathtt{T})S_h I_m - \mu_h S_h + \omega_h \mathtt{R}_h &= 0,\\
\beta_h(\mathtt{T})S_h I_m - (\mu_h + \delta + \gamma_h)I_h &= 0,\\
\gamma_h I_h - (\mu_h + \omega_h)\mathtt{R}_h &= 0,\\
\Phi(\mathtt{T}) - \beta_m(\mathtt{T})S_m I_h - \mu_m S_m &= 0,\\
\beta_m(\mathtt{T})S_m I_h - \mu_m I_m &= 0,\\
\mathrm{r}(1 - \frac{\mathtt{T}}{\mathtt{T}_{\max}})(\mathtt{T} - \mathtt{T}_0) &= 0.
\end{aligned} \tag{4.13}$$

The model has a steady state in the absence of the malaria that is $\mathtt{I}_h = 0$, $\mathtt{I}_m = 0$ and the disease free equilibrium of system (4.1) is denoted by $\mathtt{E}_1$ or $\mathtt{E}_2$ given by

$$\mathtt{E}_1 = \left(\frac{\Psi}{\mu_h}, 0, 0, \frac{\Phi(\mathtt{T}_0)}{\mu_m}, 0, \mathtt{T}_0\right) \text{ or } \mathtt{E}_2 = \left(\frac{\Psi}{\mu_h}, 0, 0, \frac{\Phi(\mathtt{T}_{\max})}{\mu_m}, 0, \mathtt{T}_{\max}\right). \tag{4.14}$$

4.2.4 Basic reproduction number

The basic reproduction number ($\mathtt{R}_0$) is defined as the average number of secondary infections caused by a single individual in totally susceptible environment (Van den Driessche and Watmough, 2002). It is crucial in determining whether the disease persists in the population or eliminated. The $\mathtt{R}_0$ is computed using the next-generation matrix method (Olaniyi et al., 2020; Huo and Qiu, 2014). Thus, to compute we should rewriting the system (4.1) with starting the infective human and mosquito population classes

$$\begin{aligned}
\frac{d\mathtt{I}_h}{dt} &= \beta_h(\mathtt{T}^*)S_h I_m - (\mu_h + \delta + \gamma_h)I_h,\\
\frac{d\mathtt{I}_m}{dt} &= \beta_m(\mathtt{T}^*)S_m I_h - \mu_m I_m.
\end{aligned} \tag{4.15}$$

Then next the right hand side of system (4.15) can be written as the form of $\mathscr{F} - \mathscr{V}$, where

$$\mathscr{F} = \begin{pmatrix} \beta_h(\mathtt{T}^*)S_h I_m \\ \beta_m(\mathtt{T}^*)S_m I_h \end{pmatrix} \text{ and } \mathscr{V} = \begin{pmatrix} (\mu_h + \delta + \gamma_h)I_h \\ \mu_m I_m \end{pmatrix}.$$

Finding the partial derivatives of $\mathscr{F}$ and $\mathscr{V}$ at the disease free equilibrium points gives $\mathtt{f}$ and $\mathtt{v}$ respectively, where,

$$\mathtt{f} = \begin{pmatrix} 0 & \beta_h(\mathtt{T}^*)\frac{\Psi}{\mu_h} \\ \beta_m(\mathtt{T}^*)\frac{\Phi(\mathtt{T}^*)}{\mu_m} & 0 \end{pmatrix} \text{ and } \mathtt{v} = \begin{pmatrix} \mu_h+\delta+\gamma_h & 0 \\ 0 & \mu_m \end{pmatrix}.$$

The inverse of $\mathtt{v}$ is obtained as

$$\mathtt{v}^{-1} = \begin{pmatrix} \frac{1}{\mu_h+\delta+\gamma_h} & 0 \\ 0 & \frac{1}{\mu_m} \end{pmatrix}. \tag{4.16}$$

Then the product of $\mathtt{f}v^{-1}$ is

$$\mathtt{f}v^{-1} = \begin{pmatrix} 0 & \frac{\beta_h(\mathtt{T}^*)\Psi}{\mu_h\mu_m} \\ \frac{\beta_m(\mathtt{T}^*)\Phi(\mathtt{T}^*)}{\mu_m(\mu_h+\delta+\gamma_h)} & 0 \end{pmatrix}. \tag{4.17}$$

The eigenvalues are computed from the determinant of $|\mathtt{f}v^{-1} - \mathtt{I}\lambda_2| = 0$ as given

$$\begin{vmatrix} -\lambda & \frac{\beta_h(\mathtt{T}^*)\Psi}{\mu_h\mu_m} \\ \frac{\beta_m(\mathtt{T}^*)\Phi(\mathtt{T}^*)}{\mu_m(\mu_h+\delta+\gamma_h)} & -\lambda \end{vmatrix} = 0. \tag{4.18}$$

Obviously, the eigenvalues of $\mathtt{f}v^{-1}$ are obtained as

$$-\sqrt{\frac{\beta_h(\mathtt{T}^*)\Psi\beta_m(\mathtt{T}^*)\Phi_m(\mathtt{T}^*)}{\mu_h\mu_m^2(\mu_h+\delta+\gamma_h)}} \text{ and } \sqrt{\frac{\beta_h(\mathtt{T}^*)\Psi\beta_m(\mathtt{T}^*)\Phi_m(\mathtt{T}^*)}{\mu_h\mu_m^2(\mu_h+\delta+\gamma_h)}}. \tag{4.19}$$

Hence, the basic reproduction number, $\mathtt{R}_0 = \rho(\mathtt{f}v^{-1})$, is the largest eigenvalue of the product matrix and the $\mathtt{R}_0$ at $\mathtt{E}_1$ and $\mathtt{E}_2$ are given respectively, by the equation (4.20) and (4.21) as given

$$\mathtt{R}_{01} = \sqrt{\frac{\beta_{0h}\Psi\beta_{0m}\Phi_0}{\mu_h\mu_m^2(\mu_h+\delta+\gamma_h)}} \tag{4.20}$$

and

$$\mathtt{R}_{02} = \sqrt{\frac{(\beta_{0h}+\beta_{2h})\Psi(\beta_{0m}+\beta_{2m})(\Phi_0+\Phi_{2m})}{\mu_h\mu_m^2(\mu_h+\delta+\gamma_h)}} \tag{4.21}$$

where, $\beta_{2h} = \beta_{1h}k$, $\beta_{2m} = \beta_{1m}k$, $\Phi_{2m} = \Phi_{1m}k$ and $k = \left(\frac{\mathtt{T}_{\max}-\mathtt{T}_0}{\mathtt{T}_{\max}}\right)$.

Consequently, the basic reproduction number ($\mathtt{R}_{02}$) at maximum temperature ($\mathtt{T}_{\max}$) can be written by equation (4.22) as

$$\mathtt{R}_{02} = \sqrt{\mathtt{R}_{01}^2 + \frac{\Phi_0\beta_{0m}\beta_{2m}\Psi + \Psi(\beta_{0m}+\beta_{2m})[\beta_{2h}(\Phi_0+\Phi_{2m}) + \Phi_{2m}\beta_{0h}]}{\mu_h\mu_m^2(\mu_h+\delta+\gamma_h)}} \tag{4.22}$$

where, $\mathtt{R}_{01}$ is the reproduction number at $\mathtt{T}_0$ for the mosquito to be less active to breed.

4.2.5 Local stability of disease free equilibrium

Theorem 4.3. The disease free equilibrium points of the system (4.1) is locally asymptotically stable in Θ if $\mathtt{R}_{01} < \mathtt{R}_{02} < 1$.

Proof. To prove, we started by finding the Jacobian matrix of the system (4.1) obtain as

$$\mathtt{J} = \begin{pmatrix} -\beta_h(\mathtt{T}^*)I_h - \mu_h & 0 & \omega_h & 0 & -\beta_h(\mathtt{T}^*)S_h \\ \beta_h(\mathtt{T}^*)I_m & -(\mu_h+\delta+\gamma_h) & 0 & 0 & \beta_h(\mathtt{T}^*)S_h \\ 0 & \gamma_h & \mathtt{J}_{33} & 0 & 0 \\ 0 & -\beta_m(\mathtt{T}^*)S_m & 0 & \mathtt{J}_{44} & 0 \\ 0 & \beta_m(\mathtt{T}^*)S_m & 0 & \beta_m(\mathtt{T}^*)I_h & \mathtt{J}_{55} \end{pmatrix} \tag{4.23}$$

where $\mathtt{J}_{33} = -(\omega_h+\mu_h), \mathtt{J}_{44} = -\beta_m(\mathtt{T}^*)I_h - \mu_m, \mathtt{J}_{55} = -\mu_m$ and $\mathtt{T}^* = \mathtt{T}_0$ or $\mathtt{T}_{\max}$.

The Jacobian matrix (4.23) at the disease free equilibrium points is given as

$$\mathtt{J}(\mathtt{E}_*) = \begin{pmatrix} -\mu_h & 0 & \omega_h & 0 & -\beta_h(\mathtt{T}^*)\frac{\Psi}{\mu_h} \\ 0 & -(\mu_h+\delta+\gamma_h) & 0 & 0 & \beta_h(\mathtt{T}^*)\frac{\Psi}{\mu_h} \\ 0 & \gamma_h & -(\omega_h+\mu_h) & 0 & 0 \\ 0 & -\beta_m(\mathtt{T}^*)\frac{\Phi(\mathtt{T}^*)}{\mu_m} & 0 & -\mu_m & 0 \\ 0 & \beta_m(\mathtt{T}^*)\frac{\Phi(\mathtt{T}^*)}{\mu_m} & 0 & 0 & -\mu_m \end{pmatrix}. \tag{4.24}$$

The eigenvalues of equation (4.24) are obtained from the characteristic equation $|\mathtt{J}(\mathtt{E}_*) - \mathtt{I}\lambda| = 0$ given as

$$\begin{vmatrix} -\mu_h-\lambda & 0 & \omega_h & 0 & -\beta_h(\mathtt{T}^*)\frac{\Psi}{\mu_h} \\ 0 & -(\mu_h+\delta+\gamma_h)-\lambda & 0 & 0 & \beta_h(\mathtt{T}^*)\frac{\Psi}{\mu_h} \\ 0 & \gamma_h & -(\omega_h+\mu_h)-\lambda & 0 & 0 \\ 0 & -\beta_m(\mathtt{T}^*)\frac{\Phi(\mathtt{T}^*)}{\mu_m} & 0 & -\mu_m-\lambda & 0 \\ 0 & \beta_m(\mathtt{T}^*)\frac{\Phi(\mathtt{T}^*)}{\mu_m} & 0 & 0 & -\mu_m-\lambda \end{vmatrix} = 0. \tag{4.25}$$

Now, all are zero except the first entry in the first column of (4.25) that is $-\mu_h - \lambda$ and we have the first eigenvalue $\lambda = -\mu_h$. The other eigenvalues are obtained from the equation as follows;

$$\begin{vmatrix} -(\mu_h+\delta+\gamma_h)-\lambda & 0 & 0 & \beta_h(\mathtt{T}^*)\frac{\Psi}{\mu_h} \\ \gamma_h & -(\omega_h+\mu_h)-\lambda & 0 & 0 \\ -\beta_m(\mathtt{T}^*)\frac{\Phi(\mathtt{T}^*)}{\mu_m} & 0 & -\mu_m-\lambda & 0 \\ \beta_m(\mathtt{T}^*)\frac{\Phi(\mathtt{T}^*)}{\mu_m} & 0 & 0 & -\mu_m-\lambda \end{vmatrix} = 0. \tag{4.26}$$

Also all are zero except the third entry in the third column of (4.26) that is $-\mu_m - \lambda$. Hence, we have the second eigenvalue $\lambda = -\mu_m$. The other eigenvalues are computed using the equation described as;

$$\begin{vmatrix} -(\mu_h + \delta + \gamma_h) - \lambda & 0 & \beta_h(\mathtt{T}^*)\frac{\Psi}{\mu_h} \\ \gamma_h & -(\omega_h + \mu_h) - \lambda & 0 \\ \beta_m(\mathtt{T}^*)\frac{\Phi(\mathtt{T}^*)}{\mu_m} & 0 & -\mu_m - \lambda \end{vmatrix} = 0. \tag{4.27}$$

Again the second column is zero except in its diagonal. The third eigenvalue of (4.27) found to be $\lambda = -(\mu_h + \omega_h)$. The remaining eigenvalues are obtain using the equation given by

$$\begin{vmatrix} -(\mu_h + \delta + \gamma_h) - \lambda & \beta_h(\mathtt{T}^*)\frac{\Psi}{\mu_h} \\ \beta_m(\mathtt{T}^*)\frac{\Phi(\mathtt{T}^*)}{\mu_m} & -\mu_m - \lambda \end{vmatrix} = 0. \tag{4.28}$$

From the equation (4.28), we have the last characteristic equation as;

$$\lambda^2 + a_1\lambda + a_2 = 0 \tag{4.29}$$

where,

$$\begin{aligned} a_1 &= \mu_m + \mu_h + \delta + \gamma_h, \\ a_2 &= \mu_m\gamma_h + \mu_m\delta + \mu_m\mu_h - \frac{\beta_h(\mathtt{T}^*)\Psi\beta_m(\mathtt{T}^*)\Phi(\mathtt{T}^*)}{\mu_m\mu_h}. \end{aligned} \tag{4.30}$$

By using Routh-Hurwitz criteria (Mojeeb and Adu, 2017), the equation (4.29) has real root that strictly negative if $a_1 > 0$ and $a_2 > 0$. So that, we see that $a_1 > 0$ since it is the sum of positive parameters. The value of a_2 at $\mathtt{T}^* = \mathtt{T}_{\max}$ is derived as

$$a_2 = \mu_m\gamma_h + \mu_m\delta + \mu_m\mu_h - \frac{(\beta_{0h} + \beta_{2h})\Psi(\beta_{0m} + \beta_{2m})(\Phi_0 + \Phi_{2m})}{\mu_m\mu_h} = 1 - \mathtt{R}_{02}^2.$$

This implies that a_2 to be positive, $1 - \mathtt{R}_{02}^2$ must be positive, which leads to $\mathtt{R}_{02} < 1$. However, a_2 will be negative if $\mathtt{R}_{02} > 1$. Since $\mathtt{R}_{01} < \mathtt{R}_{02}$ hence the DFE is locally asymptotically stable in Θ if $\mathtt{R}_{01} < \mathtt{R}_{02} < 1$.

4.2.6 Global stability of disease free equilibrium

Theorem 4.4 The disease free equilibrium points of the system (4.1) is globally asymptotically stable in Θ if $\mathtt{R}_{01} < \mathtt{R}_{02} < 1$.

Proof. To prove, we first developed the following Lyapunov function defined as

$$\mathtt{L} = \frac{\mu_m}{\beta_h(\mathtt{T}^*)}\mathtt{I}_h + \mathtt{I}_m \quad \text{where, } \mathtt{T}^* = \mathtt{T}_0 \text{ or } \mathtt{T}_{\max}. \tag{4.31}$$

By differentiating the above Lyapunov function with respect to time (t) we obtain,

$$\begin{aligned}
\frac{d\mathtt{L}}{dt} &= \frac{\mu_m}{\beta_h(\mathtt{T}^*)}\frac{d\mathtt{I}_h}{dt} + \frac{d\mathtt{I}_m}{dt}, \\
&= \frac{\mu_m}{\beta_h(\mathtt{T}^*)}\left(\beta_h(\mathtt{T}^*)S_hI_m - (\mu_h+\delta+\gamma_h)I_h\right) + \beta_m(\mathtt{T}^*)S_mI_h - \mu_mI_m, \\
&= \mu_mS_hI_m - \frac{\mu_m}{\beta_h(\mathtt{T}^*)}(\mu_h+\delta+\gamma_h)I_h + \beta_m(\mathtt{T}^*)S_mI_h - \mu_mI_m, \\
&= \left(\beta_m(\mathtt{T}^*)S_m - \frac{\mu_m}{\beta_h(\mathtt{T}^*)}(\mu_h+\delta+\gamma_h)\right)\mathtt{I}_h - \mu_m(1-s_h)\mathtt{I}_m, \\
&\leq \left(\beta_m(\mathtt{T}^*)S_m - \frac{\mu_m}{\beta_h(\mathtt{T}^*)}(\mu_h+\delta+\gamma_h)\right)\mathtt{I}_h, \\
&= \left(\beta_m(\mathtt{T}^*)\frac{\Phi(\mathtt{T}^*)}{\mu_m} - \frac{\mu_m}{\beta_h(\mathtt{T}^*)}(\mu_h+\delta+\gamma_h)\right)\mathtt{I}_h, \\
&= \frac{\mu_m(\mu_h+\delta+\gamma_h)}{(\beta_{0h}+\beta_{2h})}\left(\frac{\mu_h}{\Psi}\mathtt{R}_{02}^2 - 1\right)\mathtt{I}_h \text{ at } \mathtt{T}^* = \mathtt{T}_{\max}.
\end{aligned} \tag{4.32}$$

So, we have that $\frac{d\mathtt{L}}{dt} < 0$ if $\mathtt{R}_{02} < 1$ and $\frac{d\mathtt{L}}{dt} = 0$ if and only if $\mathtt{I}_h = 0,\ \mathtt{I}_m = 0$, since $\frac{\mu_h}{\Psi}$ is less than one. Thus, the dominant invariant set in $\{(\mathtt{S}_h, \mathtt{I}_h, \mathtt{R}_h, \mathtt{S}_m, \mathtt{I}_m) \in \Theta : \frac{d\mathtt{L}}{dt} = 0\}$ is the singleton set DFE in Θ. Therefore, from LaSalle's invariant principle (La Salle, 1976), one concludes that every solution begin in the domain approaches DFE as $t \to \infty$ and since $\mathtt{R}_{01} < \mathtt{R}_{02}$ the DFE is globally asymptotically stable in Θ for $\mathtt{R}_{01} < \mathtt{R}_{02} < 1$.

4.2.7 Endemic equilibrium point

An endemic equilibrium point occur when the malaria persist in the community. The endemic equilibrium point denoted by $\mathtt{E}^* = (\mathtt{S}_h^*, \mathtt{I}_h^*, \mathtt{R}_h^*, \mathtt{S}_m^*, \mathtt{I}_m^*, \mathtt{T}^*)$ can be obtained by setting the right hand side of the model (4.1) equal to zero. Thus, we used the following approach to find the endemic equilibrium point(s) of the model (4.1) by equating the right hand side equal to zero.

Firstly, solving the third equation of the model (4.1), we obtain

$$\mathtt{R}_h^* = \frac{\gamma_hI_h^*}{\omega_h+\mu_h}. \tag{4.33}$$

Secondly, solving the fourth equation of the model (4.1), we got

$$\mathtt{S}_m^* = \frac{\Phi(\mathtt{T}^*)}{\beta_m(\mathtt{T}^*)I_h^*+\mu_m}. \tag{4.34}$$

Thirdly, solving the fifth equation of the model (4.1) gives

$$\mathtt{I}_m^* = \frac{\beta_m(\mathtt{T}^*)\Phi(\mathtt{T}^*)I_h^*}{\mu_m(\beta_m(\mathtt{T}^*)I_h^*+\mu_m)}. \tag{4.35}$$

Continuing solving the first equation of the model (4.1), we obtain

$$\mathrm{S}_h^* = \frac{\Psi + \omega_h \mathrm{R}_h^*}{\beta_h(\mathrm{T}^*) I_m^* + \mu_h}. \tag{4.36}$$

The endemic equilibrium point of the model (4.1) at $\mathrm{T}^* = \mathrm{T}_0$ is obtain as

$$\begin{cases} \mathrm{S}_h^* = \frac{\Psi+\omega_h \mathrm{R}_h^*}{\beta_{0h} I_m^* + \mu_h}, \\ \mathrm{R}_h^* = \frac{\gamma_h I_h^*}{\omega_h + \mu_h}, \\ \mathrm{S}_m^* = \frac{\Phi_0}{\beta_{0m} I_h^* + \mu_m}, \\ \mathrm{I}_m^* = \frac{\beta_{0m} \Phi_0 I_h^*}{\mu_m(\beta_{0m} I_h^* + \mu_m)}. \end{cases} \tag{4.37}$$

From equation (4.37) by substituting S_h^* and I_m^* into the second equation of model (4.1), then the I_h^* is computed by solving the equation

$$\mathrm{A}_1 (\mathrm{I}_h^*)^2 + \mathrm{B}_1 (\mathrm{I}_h^*) = 0 \tag{4.38}$$

$$\begin{aligned} \text{where, } \mathrm{A}_1 &= \beta_{0m}(\beta_{0h}\Phi_0(\omega_h\delta + \mu_h(\gamma_h + \omega_h + \delta + \mu_h)) + \mu_h(\omega_h + \mu_h)(\gamma_h + \delta + \mu_h)\mu_m), \\ \mathrm{B}_1 &= (\omega_h + \mu_h)\left[\mu_h \mu_m^2 (\gamma_h + \delta + \mu_h)(1 - \mathrm{R}_{01}^2)\right]. \end{aligned} \tag{4.39}$$

Thus, $\mathrm{A}_1 > 0$ and $\mathrm{B}_1 > 0$ whenever $\mathrm{R}_{01} < 1$. Solving for I_h^* , we have that $\mathrm{I}_h^* = -\frac{B_1}{A_1} < 0$. Hence, there is no positive endemic equilibrium whenever $\mathfrak{R}_{01} < 1$.

Similarly, using the same procedure, the endemic equilibrium point at $\mathrm{T}^* = \mathrm{T}_{\max}$ is given as

$$\begin{cases} \mathrm{S}_h^* = \frac{\Psi+\omega_h \mathrm{R}_h^*}{(\beta_{0h}+\beta_{2h}) I_m^* + \mu_h}, \\ \mathrm{R}_h^* = \frac{\gamma_h I_h^*}{\omega_h + \mu_h}, \\ \mathrm{S}_m^* = \frac{(\Phi_0+\Phi_{2m})}{(\beta_{0m}+\beta_{2m}) I_h^* + \mu_m}, \\ \mathrm{I}_m^* = \frac{(\beta_{0m}+\beta_{2m})(\Phi_0+\Phi_{2m}) I_h^*}{\mu_m((\beta_{0m}+\beta_{2m}) I_h^* + \mu_m)}, \end{cases} \tag{4.40}$$

where $\beta_{2h} = \beta_{1h}k$, $\beta_{2m} = \beta_{1m}k$, $\Phi_{2m} = \Phi_{1m}k$ and $k = \left(\frac{\mathrm{T}_{\max} - \mathrm{T}_0}{\mathrm{T}_{\max}}\right)$.

From equation (4.40) by substituting S_h^* and I_m^* into the second equation of model (4.1), then the I_h^* is obtained by solving the equation

$$\mathrm{A} (\mathrm{I}_h^*)^2 + \mathrm{B} (\mathrm{I}_h^*) = 0 \tag{4.41}$$

$$\begin{aligned} \text{where, } \mathrm{A} &= \beta_{3m}(\beta_{3h}\Phi_{2m}(\omega_h\delta + \mu_h(\gamma_h + \omega_h + \delta + \mu_h)) + \mu_h(\omega_h + \mu_h)(\gamma_h + \delta + \mu_h)\mu_m), \\ \mathrm{B} &= (\omega_h + \mu_h)\left[\mu_h \mu_m^2 (\gamma_h + \delta + \mu_h)(1 - \mathrm{R}_{02}^2)\right], \end{aligned} \tag{4.42}$$

where $\beta_{3h} = \beta_{0h} + \beta_{2h}$, $\beta_{3m} = \beta_{0m} + \beta_{2m}$ and $\Phi_{3m} = \Phi_0 + \Phi_{2m}$.
Hence, if $\mathtt{R}_{02} < 1$ then automatically implies that $\mathtt{R}_{01} < 1$ (see equation 4.22). However, $\mathtt{R}_{01} < 1$ does not automatically implies $\mathtt{R}_{02} < 1$, since the value of $\mathtt{R}_{02}$ may be greater than unity, which implies that while $\mathtt{R}_{01}$ present disease free equilibrium $\mathtt{R}_{02}$ may be become endemic situation or present backward bifurcation while $\mathtt{R}_{01}$ only present forward bifurcation.

4.2.8 Local stability of endemic equilibrium

Theorem 4.5. The endemic equilibrium points of system (4.1) is locally asymptotically stable in Θ if $\mathtt{R}_{02} > \mathtt{R}_{01} > 1$.

Proof. The Jacobian matrix of the model (4.1) at an endemic equilibrium points is

$$Q(\mathtt{E}^*) = \begin{pmatrix} Q_{11} - \mu_h & 0 & \omega_h & 0 & -\beta_h(\mathtt{T}^*)S_h^* \\ \beta_h(\mathtt{T}^*)I_m^* & -(\mu_h + \delta + \gamma_h) & 0 & 0 & \beta_h(\mathtt{T}^*)S_h^* \\ 0 & \gamma_h & Q_{33} & 0 & 0 \\ 0 & -\beta_m(\mathtt{T}^*)S_m^* & 0 & Q_{44} & 0 \\ 0 & \beta_m(\mathtt{T}^*)S_m^* & 0 & \beta_m(\mathtt{T}^*)I_h^* & Q_{55} \end{pmatrix} \tag{4.43}$$

where, $Q_{11} = -\beta_h(\mathtt{T}^*)\mathtt{I}_h^*$, $Q_{33} = -(\omega_h + \mu_h)$, $Q_{44} = -\beta_m(\mathtt{T}^*)\mathtt{I}_h^* - \mu_m$ and $Q_{55} = -\mu_m$.
The eigenvalues of equation (4.43) are the characteristic equation of $|Q(\mathtt{E}^*) - \lambda\,\mathtt{I}_5| = 0$ is given as

$$\begin{vmatrix} Q_{11} - \lambda & 0 & \omega_h & 0 & -\beta_h(\mathtt{T}^*)S_h^* \\ \beta_h(\mathtt{T}^*)I_m^* & -(\mu_h + \delta + \gamma_h) - \lambda & 0 & 0 & \beta_h(\mathtt{T}^*)S_h^* \\ 0 & \gamma_h & Q_{33} - \lambda & 0 & 0 \\ 0 & -\beta_m(\mathtt{T}^*)S_m^* & 0 & Q_{44} - \lambda & 0 \\ 0 & \beta_m(\mathtt{T}^*)S_m^* & 0 & \beta_m(\mathtt{T}^*)I_h^* & Q_{55} - \lambda \end{vmatrix} = 0 \tag{4.44}$$

where,
$Q_{11} = -(\beta_h(\mathtt{T}^*)\mathtt{I}_h^* + \mu_h)$, $Q_{33} = -(\omega_h + \mu_h)$, $Q_{44} = -(\beta_m(\mathtt{T}^*)\mathtt{I}_h^* + \mu_m)$ and $Q_{55} = -\mu_m$.

Letting $c_{11} = -(\beta_h(\mathtt{T}^*)I_h^* + \mu_h)$, $c_{21} = \beta_h(\mathtt{T}^*)I_m^*$, $c_{22} = -(\mu_h + \delta + \gamma_h)$, $c_{32} = \gamma_h$, $c_{42} = -\beta_m(\mathtt{T}^*)S_m^*$, $c_{52} = \beta_m(\mathtt{T}^*)S_m^*$, $c_{13} = \omega_h$, $c_{33} = -(\omega_h + \mu_h)$, $c_{44} = -(\beta_m(\mathtt{T}^*)I_h^* + \mu_m)$, $c_{54} = \beta_m(\mathtt{T}^*)I_h^*$, $c_{15} = -\beta_h(\mathtt{T}^*)S_h^*$, $c_{25} = \beta_h(\mathtt{T}^*)S_h^*$, $c_{55} = -\mu_m$ and the characteristic equation of the Jacobian matrix (4.44) at endemic equilibrium point is given by

$$\lambda^5 + \mathtt{D}_1\lambda^4 + \mathtt{D}_2\lambda^3 + \mathtt{D}_3\lambda^2 + \mathtt{D}_4\lambda + \mathtt{D}_5 = 0 \tag{4.45}$$

where,

$$
\begin{aligned}
\mathrm{D}_1 &= -(c_{11}+c_{22}+c_{33}+c_{44}+c_{55}), \qquad (4.46)\\
\mathrm{D}_2 &= c_{55}(c_{11}+c_{22}+c_{33}+c_{44})+c_{11}(c_{22}+c_{33}+c_{44})+c_{22}(c_{33}+c_{44})-c_{11}c_{25}c_{52},\\
\mathrm{D}_3 &= c_{11}c_{25}(c_{52}+c_{33}c_{52})-c_{11}c_{25}(c_{42}c_{54}+c_{42}c_{44})-(c_{13}c_{21}c_{33})+(c_{15}c_{21}c_{52})-c_{55}\\
&\quad [(c_{11}c_{22}+c_{33}c_{44})+(c_{11}+c_{22})(c_{33}+c_{44})]-[(c_{33}+c_{44})c_{11}c_{22}+(c_{11}c_{22})c_{33}c_{44}],\\
\mathrm{D}_4 &= c_{13}c_{21}c_{33}(c_{44}+c_{55})+c_{15}c_{21}(c_{33}c_{52}+c_{52}c_{44}-c_{42}c_{54})+c_{11}c_{25}(c_{52}c_{44}+c_{42}c_{54}-c_{33}c_{52})\\
&\quad + c_{11}c_{25}c_{33}(c_{42}c_{54}-c_{52}c_{44})+(c_{33}+c_{44})c_{11}c_{22}c_{55}+(c_{11}+c_{22})c_{33}c_{44}c_{55}+c_{11}c_{22}c_{33}c_{44},\\
\mathrm{D}_5 &= c_{15}c_{21}c_{33}(c_{42}c_{54}-c_{52}c_{44})-c_{13}c_{21}c_{44}c_{55}+c_{11}c_{25}c_{33}(c_{52}c_{44}-c_{42}c_{54})-c_{11}c_{22}c_{33}c_{44}c_{55}.
\end{aligned}
$$

Using the Routh-Hurwitz criterion (Mojeeb and Adu, 2017), for $\mathrm{R}_{02} > \mathrm{R}_{01} > 1$ the endemic equilibrium points is locally asymptotically stable if $\mathrm{D}_i > 0,\ i = 1,...5$ and

$$
\begin{aligned}
\mathrm{D}_1\mathrm{D}_2 - \mathrm{D}_3 &> 0,\\
\mathrm{D}_1\mathrm{D}_2\mathrm{D}_3 + \mathrm{D}_1\mathrm{D}_5 - \mathrm{D}_3^2 - \mathrm{D}_4\mathrm{D}_1^2 &> 0, \qquad (4.47)\\
(\mathrm{D}_3\mathrm{D}_4 - \mathrm{D}_2\mathrm{D}_5)(\mathrm{D}_1\mathrm{D}_2 - \mathrm{D}_3) - (\mathrm{D}_1\mathrm{D}_4 - \mathrm{D}_5)^2 &> 0,\\
\mathrm{D}_5((\mathrm{D}_3\mathrm{D}_4 - \mathrm{D}_2\mathrm{D}_5)(\mathrm{D}_1\mathrm{D}_2 - \mathrm{D}_3) - (\mathrm{D}_1\mathrm{D}_4 - \mathrm{D}_5)^2) &> 0.
\end{aligned}
$$

Therefore, according to the Routh Hurwitz criterion, the characteristic equation (4.45) will have negative roots or imaginary roots with negative real part for $\mathrm{R}_{02} > \mathrm{R}_{01} > 1$, the point E^* is locally asymptotically stable.

4.2.9 Global stability of endemic equilibrium

Theorem 4.6. The endemic equilibrium points of the model (4.1) is globally asymptotically stable in Θ if $\mathrm{R}_{02} > \mathrm{R}_{01} > 1$.

Proof. First, we consider the following Lyapunov function constructed as

$$
\mathrm{V} = \frac{1}{2}[(\mathrm{S}_h - \mathrm{S}_h^*) + (\mathrm{I}_h - \mathrm{I}_h^*) + (\mathrm{R}_h - \mathrm{R}_h^*)]^2 + \frac{1}{2}[(\mathrm{S}_m - \mathrm{S}_m^*) + (\mathrm{I}_m - \mathrm{I}_m^*)]^2. \qquad (4.48)
$$

The partial derivative of (4.48) with respect to time (t) corresponding to system (4.1) is,

$$
\begin{aligned}
\frac{d\mathrm{V}}{dt} &= [(\mathrm{S}_h - \mathrm{S}_h^*) + (\mathrm{I}_h - \mathrm{I}_h^*) + (\mathrm{R}_h - \mathrm{R}_h^*)]\frac{d}{dt}[\mathrm{S}_h + \mathrm{I}_h + \mathrm{R}_h] + [(\mathrm{S}_m - \mathrm{S}_m^*) + (\mathrm{I}_m - \mathrm{I}_m^*)]\frac{d}{dt}[\mathrm{S}_m + \mathrm{I}_m].\\
&= [(\mathrm{S}_h - \mathrm{S}_h^*) + (\mathrm{I}_h - \mathrm{I}_h^*) + (\mathrm{R}_h - \mathrm{R}_h^*)]\frac{dN_h}{dt} + [(\mathrm{S}_m - \mathrm{S}_m^*) + (\mathrm{I}_m - \mathrm{I}_m^*)]\frac{dN_m}{dt}. \qquad (4.49)
\end{aligned}
$$

However, from equations (4.3) and (4.6) we have,

$$
\begin{aligned}
\frac{dN_h}{dt} &= \frac{d}{dt}[\mathrm{S}_h + \mathrm{I}_h + \mathrm{R}_h] \leq \Psi - \mu_h N_h,\\
\frac{dN_m}{dt} &= \frac{d}{dt}[\mathrm{S}_m + \mathrm{I}_m] = \Phi(\mathrm{I}^*) - \mu_m N_m. \qquad (4.50)
\end{aligned}
$$

By substituting equations of model (4.50) into the equation (4.49), we have that

$$\begin{aligned}\frac{d\mathrm{V}}{dt} &= [(\mathrm{S}_h - \mathrm{S}_h^*) + (\mathrm{I}_h - \mathrm{I}_h^*) + (\mathrm{R}_h - \mathrm{R}_h^*)]\frac{dN_h}{dt} + [(\mathrm{S}_m - \mathrm{S}_m^*) + (\mathrm{I}_m - \mathrm{I}_m^*)]\frac{dN_m}{dt},\\ &\leq [(\mathrm{S}_h - \mathrm{S}_h^*) + (\mathrm{I}_h - \mathrm{I}_h^*) + (\mathrm{R}_h - \mathrm{R}_h^*)][\Psi - \mu_h N_h] + [(\mathrm{S}_m - \mathrm{S}_m^*) + (\mathrm{I}_m - \mathrm{I}_m^*)][\Phi(\mathrm{T}^*) - \mu_m N_m],\\ &\leq \left[N_h - \frac{\Psi}{\mu_h}\right][\Psi - \mu_h N_h] + \left[N_m - \frac{\Phi(\mathrm{T}^*)}{\mu_m}\right][\Phi(\mathrm{T}^*) - \mu_m N_m]. \end{aligned} \tag{4.51}$$

By re-arranging and simplify the equation (4.51), we obtain the following result

$$\frac{d\mathrm{V}}{dt} \leq -\frac{1}{\mu_h}[\Psi - \mu_h N_h]^2 - \frac{1}{\mu_m}[\Phi(\mathrm{T}^*) - \mu_m N_m]^2. \tag{4.52}$$

Therefore, $(\frac{d\mathrm{V}}{dt})(\mathrm{S}_h, \mathrm{I}_h, \mathrm{R}_h, \mathrm{S}_m, \mathrm{I}_m) \leq 0$ and $\frac{dV}{dt} = 0$, if and only if $\mathrm{S}_h = \mathrm{S}_h^*, \mathrm{I}_h = \mathrm{I}_h^*, \mathrm{R}_h = \mathrm{R}_h^*, \mathrm{S}_m = \mathrm{S}_m^*, \mathrm{I}_m = \mathrm{I}_m^*$. Thus, the dominant invariant set in $\{(\mathrm{S}_h^*, \mathrm{I}_h^*, \mathrm{R}_h^*, \mathrm{S}_m^*, \mathrm{I}_m^*) \in \Theta : \frac{d\mathrm{V}}{dt} = 0\}$ is the singleton point E^*. Hence, from LaSalle's invariant principle (La Salle, 1976), this indicates that the endemic equilibrium point E^* is globally asymptotically stable in Θ.

4.2.10 Bifurcation analysis

In this sub-section, we can identify the nature of the bifurcation using the method described by Castillo-Chavez and Song that is based on centre manifold theory (Castillo-Chavez and Song, 2004a). This approach helps us to determine the bifurcation analysis of model (4.1) at R_0 is equal to unity. Then the following result can be obtained.

Theorem 4.7. The system (4.1) exhibits forward bifurcation at $\mathrm{R}_{01} = 1$.

Proof. Let β_{0h} be consider as bifurcation parameter such that $\mathrm{R}_{01} = 1$ if and only if

$$\beta_{0h} = \beta_{0h}^* = \frac{\mu_h \mu_m^2 (\mu_h + \delta + \gamma_h)}{\Psi \beta_{0m} \Phi_0}. \tag{4.53}$$

Using the changes of variables $S_h = x_1, I_h = x_2, \mathrm{R}_h = x_3, S_m = x_4, I_m = x_5, \mathrm{T} = x_6$ and vector notation $X = (x_1, x_2, x_3, x_4, x_5, x_6)^{\mathrm{T}}$ of the model (4.1) can be written in the form $\frac{dx}{dt} = (f_1, f_2, f_3, f_4, f_5, f_6)^{\mathrm{T}}$ as

$$\begin{cases} \frac{dx_1}{dt} = \Psi - \beta_{0h} x_1 x_5 - \mu_h x_1 + \omega_h x_3, \\ \frac{dx_2}{dt} = \beta_{0h} x_1 x_5 - (\mu_h + \delta + \gamma_h) x_2, \\ \frac{dx_3}{dt} = \gamma_h x_2 - (\omega_h + \mu_h) x_3, \\ \frac{dx_4}{dt} = \Phi_0 - \beta_{0m} x_4 x_2 - \mu_m x_4, \\ \frac{dx_5}{dt} = \beta_{0m} x_4 x_2 - \mu_m x_5, \\ \frac{dx_6}{dt} = \mathrm{r}(1 - \frac{x_6}{\mathrm{T}_{\max}})(x_6 - \mathrm{T}_0). \end{cases} \tag{4.54}$$

The Jacobian matrix of (4.54) at a disease free equilibrium point E_1 with β_{0h}^* is given as

$$\mathrm{J}(\mathrm{E}_1) = \begin{pmatrix} -\mu_h & 0 & \omega_h & 0 & -\beta_{0h}\frac{\Psi}{\mu_h} & 0 \\ 0 & -(\mu_h+\delta+\gamma_h) & 0 & 0 & \beta_{0h}\frac{\Psi}{\mu_h} & 0 \\ 0 & \gamma_h & -(\omega_h+\mu_h) & 0 & 0 & 0 \\ 0 & -\beta_{0m}\frac{\Phi_0}{\mu_m} & 0 & -\mu_m & 0 & 0 \\ 0 & \beta_{0m}\frac{\Phi_0}{\mu_m} & 0 & 0 & -\mu_m & 0 \\ 0 & 0 & 0 & 0 & 0 & \mathrm{r}(1-\frac{\mathrm{T}_0}{\mathrm{T}_{\max}}) \end{pmatrix} \tag{4.55}$$

The Jacobian matrix (4.55) has right eigenvectors, $w = (w_1, w_2, w_3, w_4, w_5, w_6)^{\mathrm{T}}$ associated to simple zero eigenvalue near $\beta_{0h} = \beta_{0h}^*$ will obtain from equation $\mathrm{J}w = 0$ can be described as

$$\begin{pmatrix} -\mathrm{J}_{11} & 0 & \omega_h & 0 & -\beta_{0h}\frac{\Psi}{\mu_h} & 0 \\ 0 & -\mathrm{J}_{22} & 0 & 0 & \beta_{0h}\frac{\Psi}{\mu_h} & 0 \\ 0 & \gamma_h & -\mathrm{J}_{33} & 0 & 0 & 0 \\ 0 & -\beta_{0m}\frac{\Phi_0}{\mu_m} & 0 & -\mathrm{J}_{44} & 0 & 0 \\ 0 & \beta_{0m}\frac{\Phi_0}{\mu_m} & 0 & 0 & -\mathrm{J}_{55} & 0 \\ 0 & 0 & 0 & 0 & 0 & \mathrm{J}_{66} \end{pmatrix} \begin{pmatrix} w_1 \\ w_2 \\ w_3 \\ w_4 \\ w_5 \\ w_6 \end{pmatrix} = \begin{pmatrix} 0 \\ 0 \\ 0 \\ 0 \\ 0 \\ 0 \end{pmatrix} \tag{4.56}$$

where,

$\mathrm{J}_{11} = \mu_h, \mathrm{J}_{22} = (\mu_h+\delta+\gamma_h), \mathrm{J}_{33} = (\omega_h+\mu_h), \mathrm{J}_{44} = \mathrm{J}_{55} = \mu_m,$ and $\mathrm{J}_{66} = \mathrm{r}(1-\frac{\mathrm{T}_0}{\mathrm{T}_{\max}})$.

From equation (4.56), we obtain,

$$\begin{cases} w_1 = -\frac{((\mu_h+\delta+\gamma_h)\mu_h+\omega_h(\mu_h+\delta))w_2}{\omega_h+\mu_h}, \\ w_2 = w_2 > 0, \\ w_3 = \frac{\gamma_h}{\omega_h+\mu_h}w_2, \\ w_4 = -\frac{\beta_{0m}\Phi_0}{\mu_m}w_2, \\ w_5 = \frac{\beta_{0m}\Phi_0}{\mu_m}w_2, \\ w_6 = 0. \end{cases} \tag{4.57}$$

The left eigenvectors, $v = (v_1, v_2, v_3, v_4, v_5, v_6)$ corresponding to zero eigenvalue will be obtain by equating $v\mathrm{J} = 0$ and the equation is arranged in the simple form

$$\begin{pmatrix} v_1 \\ v_2 \\ v_3 \\ v_4 \\ v_5 \\ v_6 \end{pmatrix}^{\mathrm{T}} \begin{pmatrix} -\mathrm{J}_{11} & 0 & \omega_h & 0 & -\beta_{0h}\frac{\Psi}{\mu_h} & 0 \\ 0 & -\mathrm{J}_{22} & 0 & 0 & \beta_{0h}\frac{\Psi}{\mu_h} & 0 \\ 0 & \gamma_h & -\mathrm{J}_{33} & 0 & 0 & 0 \\ 0 & -\beta_{0m}\frac{\Phi_0}{\mu_m} & 0 & -\mathrm{J}_{44} & 0 & 0 \\ 0 & \beta_{0m}\frac{\Phi_0}{\mu_m} & 0 & 0 & -\mathrm{J}_{55} & 0 \\ 0 & 0 & 0 & 0 & 0 & \mathrm{J}_{66} \end{pmatrix} = \begin{pmatrix} 0 \\ 0 \\ 0 \\ 0 \\ 0 \\ 0 \end{pmatrix} \tag{4.58}$$

where,

$\mathtt{J}_{11} = \mu_h, \mathtt{J}_{22} = (\mu_h + \delta + \gamma_h), \mathtt{J}_{33} = (\omega_h + \mu_h), \mathtt{J}_{44} = \mathtt{J}_{55} = \mu_m$, and $\mathtt{J}_{66} = \mathtt{r}(1 - \frac{\mathtt{T}_0}{\mathtt{T}_{\max}})$.

From the equation (4.58), we obtain

$$\begin{aligned} v_1 &= v_3 = v_4 = v_6 = 0, \\ v_5 &= \frac{(\mu_m(\mu_h + \delta + \gamma_h))v_2}{\beta_{0m}\Phi_0}. \end{aligned} \tag{4.59}$$

Using the center manifold theorem Castillo-Chavez and Song (2004a), the values of constant numbers a and b such that

$$\begin{aligned} a &= \sum_{i,j,k=1}^{6} v_k w_i w_j \frac{\partial^2 f_k}{\partial x_i \partial x_j}(\mathtt{E}_1, \beta^*_{0h}), \\ b &= \sum_{k,i=1}^{6} v_k w_i \frac{\partial^2 f_k}{\partial x_i \partial \beta_{0h}}(\mathtt{E}_1, \beta^*_{0h}). \end{aligned} \tag{4.60}$$

From equation (4.58), taking the account only partial derivative of f_2 and f_5 that are nonzero the result is given as

$$\begin{aligned} \frac{\partial^2 f_2}{\partial x_1 \partial x_5} &= \beta^*_{0h} = \frac{\partial^2 f_2}{\partial x_5 \partial x_1}, \\ \frac{\partial^2 f_2}{\partial \beta^*_{0h} \partial x_5} &= x^*_1 = \frac{\partial^2 f_2}{\partial x_5 \partial \beta^*_{0h}}, \\ \frac{\partial^2 f_5}{\partial x_4 \partial x_2} &= \beta^*_{0m} = \frac{\partial^2 f_5}{\partial x_2 \partial x_4}. \end{aligned} \tag{4.61}$$

Having the partial derivatives of (4.61) the type of bifurcation at $\mathtt{R}_{01} = 1$ is obtain as

$$\begin{aligned} a &= v_2 w_5 w_1 \beta^*_{0h} + v_2 w_1 w_5 \beta^*_{0h} + v_5 w_4 w_2 \beta_{0\mathrm{m}} + v_5 w_2 w_4 \beta_{0m}, \\ b &= v_2 w_5 x^*_1 = v_2 w_5 \frac{\Psi}{\mu_h}. \end{aligned} \tag{4.62}$$

Thus, substituting values of eigenvalues and eigenvectors into (4.62), we got

$$a = -2v_2\beta_{0m}\Phi_0 w_2^2 \left(\frac{(\mu_h(\mu_h + \delta + \gamma_h) + \omega_h(\mu_h + \delta))\mu_h\mu_m^2(\mu_h + \delta + \gamma_h)}{\mu_m(\omega_h + \mu_h)\Psi\beta_{0m}\Phi_0} + \frac{\mu_m(\mu_h + \delta + \gamma_h)}{\mu_m\Phi_0} \right) < 0,$$

$$b = v_2 w_5 x^*_1 = v_2 w_5 \frac{\Psi}{\mu_h} = v_2 w_2 \frac{\beta_{0m}\Phi_0\Psi}{\mu_m\mu_h} > 0.$$

Obviously, the constant b is positive and a is negative, the malaria transmission model, therefore, the system (4.1) may exhibits forward bifurcation at $\mathtt{R}_{01} = 1$ and which implies that at least one stable endemic equilibrium exist when $\mathtt{R}_{01} > 1$.

Theorem 4.8. If $\mathtt{R}_{02} < 1$, then the system (4.1) exhibits backward bifurcation at $\mathtt{R}_{02} = 1$.

Proof. We consider β_{3h} as bifurcation parameter so that $\mathfrak{R}_{02} = 1$ if and only if

$$\beta_{3h} = \beta_{3h}^{*} = \left(\frac{\mu_h \mu_m^2 (\mu_h + \delta + \gamma_h)(1 - \mathtt{R}_{01}^2) - \Psi \Phi_0 \beta_{0m} \beta_{2h}}{\Psi(\beta_{0m}\Phi_{2m} + \beta_{2m}\Phi_{0m} + \beta_{2m}\Phi_{2m})} \right), \tag{4.63}$$

Let $S_h = x_1, I_h = x_2, \mathtt{R}_h = x_3, S_m = x_4, I_m = x_5, \mathtt{T} = x_6$ and $X = (x_1, x_2, x_3, x_4, x_5, x_6)^{\mathtt{T}}$. Then the system (4.1) can be illustrated in the form $\frac{dx}{dt} = (f_1, f_2, f_3, f_4, f_5, f_6)^{\mathtt{T}}$ as

$$\begin{cases} \frac{dx_1}{dt} = \Psi - \beta_{3h} x_1 x_5 - \mu_h x_1 + \omega_h x_3, \\ \frac{dx_2}{dt} = \beta_{3h} x_1 x_5 - (\mu_h + \delta + \gamma_h) x_2, \\ \frac{dx_3}{dt} = \gamma_h x_2 - (\omega_h + \mu_h) x_3, \\ \frac{dx_4}{dt} = \Phi_{3m} - \beta_{3m} x_4 x_2 - \mu_m x_4, \\ \frac{dx_5}{dt} = \beta_{3m} x_4 x_2 - \mu_m x_5, \\ \frac{dx_6}{dt} = \mathtt{r}(1 - \frac{x_6}{\mathtt{T}_{\max}})(x_6 - \mathtt{T}_0). \end{cases} \tag{4.64}$$

The Jacobian matrix of (4.64) at a disease free equilibrium point $(\mathtt{E}_2)$ is given by

$$\mathtt{J}(\mathtt{E}_2) = \begin{pmatrix} -\mu_h & 0 & \omega_h & 0 & -\beta_{3h}\frac{\Psi}{\mu_h} & 0 \\ 0 & -(\mu_h + \delta + \gamma_h) & 0 & 0 & \beta_{3h}\frac{\Psi}{\mu_h} & 0 \\ 0 & \gamma_h & -(\omega_h + \mu_h) & 0 & 0 & 0 \\ 0 & -\beta_{3m}\frac{\Phi_{3m}}{\mu_m} & 0 & -\mu_m & 0 & 0 \\ 0 & \beta_{3m}\frac{\Phi_{3m}}{\mu_m} & 0 & 0 & -\mu_m & 0 \\ 0 & 0 & 0 & 0 & 0 & -\mathtt{r}(1 - \frac{\mathtt{T}_0}{\mathtt{T}_{\max}}) \end{pmatrix} \tag{4.65}$$

The right eigenvectors, $w = (w_1, w_2, w_3, w_4, w_5, w_6)^{\mathtt{T}}$ corresponding to zero eigenvalue will be obtain from the equation $\mathtt{J}w = 0$. The equation can be written in the form

$$\begin{pmatrix} -\mathtt{J}_{11} & 0 & \omega_h & 0 & -\beta_{3h}\frac{\Psi}{\mu_h} & 0 \\ 0 & -\mathtt{J}_{22} & 0 & 0 & \beta_{3h}\frac{\Psi}{\mu_h} & 0 \\ 0 & \gamma_h & -\mathtt{J}_{33} & 0 & 0 & 0 \\ 0 & -\beta_{3m}\frac{\Phi_{3m}}{\mu_m} & 0 & -\mathtt{J}_{44} & 0 & 0 \\ 0 & \beta_{3m}\frac{\Phi_{3m}}{\mu_m} & 0 & 0 & -\mathtt{J}_{55} & 0 \\ 0 & 0 & 0 & 0 & 0 & \mathtt{J}_{66} \end{pmatrix} \begin{pmatrix} w_1 \\ w_2 \\ w_3 \\ w_4 \\ w_5 \\ w_6 \end{pmatrix} = \begin{pmatrix} 0 \\ 0 \\ 0 \\ 0 \\ 0 \\ 0 \end{pmatrix} \tag{4.66}$$

where,

$\mathtt{J}_{11} = \mu_h, \mathtt{J}_{22} = (\mu_h + \delta + \gamma_h), \mathtt{J}_{33} = (\omega_h + \mu_h), \mathtt{J}_{44} = \mathtt{J}_{55} = \mu_m, \mathtt{J}_{66} = -\mathtt{r}(1 - \frac{\mathtt{T}_0}{\mathtt{T}_{\max}})$.

From equation (4.66), we obtain

$$\begin{cases} w_1 = -\frac{((\mu_h+\delta+\gamma_h)\mu_h+\omega_h(\mu_h+\delta))w_2}{\omega_h+\mu_h}, \\ w_2 = w_2 > 0, \\ w_3 = \frac{\gamma_h}{\omega_h+\mu_h}w_2, \\ w_4 = -\frac{\beta_{3m}\Phi_{3m}}{\mu_m}w_2, \\ w_5 = \frac{\beta_{3m}\Phi_{3m}}{\mu_m}w_2, \\ w_6 = 0. \end{cases} \tag{4.67}$$

The left eigenvectors, $v = (v_1, v_2, v_3, v_4, v_5, v_6)$ corresponding with zero eigenvalue obtain by equating $v\mathrm{J} = 0$. This equation can simplify and becomes

$$\begin{pmatrix} v_1 \\ v_2 \\ v_3 \\ v_4 \\ v_5 \\ v_6 \end{pmatrix}^{\mathrm{T}} \begin{pmatrix} -\mathrm{J}_{11} & 0 & \omega_h & 0 & -\beta_{3h}\frac{\Psi}{\mu_h} & 0 \\ 0 & -\mathrm{J}_{22} & 0 & 0 & \beta_{3h}\frac{\Psi}{\mu_h} & 0 \\ 0 & \gamma_h & -\mathrm{J}_{33} & 0 & 0 & 0 \\ 0 & -\beta_{3m}\frac{\Phi_{3m}}{\mu_m} & 0 & -\mathrm{J}_{44} & 0 & 0 \\ 0 & \beta_{3m}\frac{\Phi_{3m}}{\mu_m} & 0 & 0 & -\mathrm{J}_{55} & 0 \\ 0 & 0 & 0 & 0 & 0 & J_{66} \end{pmatrix} = \begin{pmatrix} 0 \\ 0 \\ 0 \\ 0 \\ 0 \\ 0 \end{pmatrix} \tag{4.68}$$

where,

$\mathrm{J}_{11} = \mu_h, \mathrm{J}_{22} = (\mu_h + \delta + \gamma_h), \mathrm{J}_{33} = (\omega_h + \mu_h), \mathrm{J}_{44} = \mathrm{J}_{55} = \mu_m, \mathrm{J}_{66} = -\mathrm{r}(1 - \frac{\mathrm{T}_0}{\mathrm{T}_{\max}})$.

By solving the equation (4.68), we got

$$\begin{aligned} v_1 = v_3 = v_4 = v_6 = 0, \\ v_5 = \frac{\mu_m(\mu_h + \delta + \gamma_h)}{\beta_{3m}\Phi_{3m}}v_2. \end{aligned} \tag{4.69}$$

Using the center manifold theorem Castillo-Chavez and Song (2004a), the value of constant numbers c and d are;

$$\begin{aligned} c &= \sum_{i,j,k=1}^{6} v_k u_i u_j \frac{\partial^2 f_k}{\partial x_i \partial x_j}(\mathrm{E}_2, \beta_{3h}^*), \\ d &= \sum_{k,i=1}^{6} v_k u_i \frac{\partial^2 f_k}{\partial x_i \partial \beta_{2h}}(\mathrm{E}_2, \beta_{3h}^*). \end{aligned} \tag{4.70}$$

From equation (4.68) as the first, third, fourth and sixth parts of v are zero, then we can omit derivative of $f_i (i = 1, 3, 4, 6)$ and from the derivative of f_2 and f_5, the only nonzero values

are

$$\begin{aligned}
\frac{\partial^2 f_2}{\partial x_1 \partial x_5} &= \beta^*_{3h} = \frac{\partial^2 f_2}{\partial x_5 \partial x_1}, \\
\frac{\partial^2 f_2}{\partial \beta^*_{3h} \partial x_5} &= x^*_1 = \frac{\partial^2 f_2}{\partial x_5 \partial \beta^*_{3h}}, \\
\frac{\partial^2 f_5}{\partial x_4 \partial x_2} &= \beta_{3m} = \frac{\partial^2 f_5}{\partial x_2 \partial x_4}.
\end{aligned} \tag{4.71}$$

The direction of the bifurcation can be determined from the value of c and d using the above partial derivatives, which is given as

$$\begin{aligned}
c &= v_2 u_5 u_1 \beta^*_{3h} + v_2 u_1 u_5 \beta^*_{3h} + v_5 u_4 u_2 \beta_{3\mathrm{m}} + v_5 u_2 u_4 \beta_{3m}, \\
d &= v_2 u_5 x^*_1 = v_2 u_5 \frac{\Psi}{\mu_h}.
\end{aligned} \tag{4.72}$$

From the above, the value of c and d are obtain as given by

$$\begin{aligned}
c =& -2v_2\beta_{3m}\Phi_{3m}u_2^2 \left(\frac{(\mu_h(\mu_h+\delta+\gamma_h)+\omega_h(\mu_h+\delta))(\mu_h\mu_m^2(\mu_h+\delta+\gamma_h)-\Psi\Phi_0\beta_{0m}(\beta_{0h}-\beta_{1h}k))}{\mu_m(\omega_h+\mu_h)\Psi(\beta_{0m}\Phi_{2m}+\beta_{2m}\Phi_{0m}+\beta_{2m}\Phi_{2m})} \right) \\
& -2v_2\beta_{3m}\Phi_{3m}u_2^2 \left(\frac{\mu_m(\mu_h+\delta+\gamma_h)}{\mu_m\Phi_{3m}} \right), \\
d =& v_2u_5x^*_1 = v_2u_5\frac{\Psi}{\mu_h} = v_2u_2\frac{\beta_{3m}\Phi_{3m}\Psi}{\mu_m\mu_h} > 0.
\end{aligned} \tag{4.73}$$

Therefore, since the value of d is always positive, it follows that the model (4.1) exhibits backward bifurcation at $\mathrm{R}_{02} = 1$, which implies that R_{02} may be become endemic situation if the coefficient c is positive.

4.3 Local sensitivity analysis

In this section, we have computed the sensitivity indices of the basic reproduction number with respect to the parameter values in the malaria model. The sensitivity indices serve as determinants of the significance of each parameter in the prevalence of the diseases and help us to determine the parameters that have a high impact on the basic reproduction number (R_0). Thus, to find the sensitivity indices, we followed the approach outlined in (Makinde and Okosun, 2011; Chitnis et al., 2008). To obtain the sensitivity index of all the basic parameters, the developed techniques defined as follows.

Definition 4.1 The normalized forward sensitivity index of R_0 that depends differentiable on a parameter Q is defined as

$$\vartheta_Q^{\mathrm{R}_0} = \frac{\partial \mathrm{R}_0}{\partial Q} \times \frac{Q}{\mathrm{R}_0} \tag{4.74}$$

for Q represents all the parameters.

Notice that $\vartheta_Q^{\mathrm{R}_0} = 1$ shows that decreasing (increasing) of Q by $m\%$ decreases (increases) of R_0 by $m\%$. Similarly, $\vartheta_Q^{\mathrm{R}_0} = -1$ implies that decreasing (increasing) of Q by $m\%$ increases (decreases) of R_0 by $m\%$.

For instance, the sensitivity index of R_{01} with respect to basic parameters is computed as

$$
\begin{aligned}
\vartheta_{\beta_{0h}}^{\mathrm{R}_{01}} &= \frac{\partial \mathrm{R}_{01}}{\partial \beta_{0h}} \frac{\beta_{0h}}{\mathrm{R}_{01}} = \frac{1}{2\sqrt{\frac{\beta_{0h}\Psi\beta_{0m}\Phi_0}{\mu_h\mu_m^2(\mu_h+\delta+\gamma_h)}}} \frac{\beta_{0m}\Phi_0\Psi}{\mu_h\mu_m^2(\mu_h+\delta+\gamma_h)} \frac{\beta_{0h}}{\mathrm{R}_{01}} = \frac{1}{2} > 0,\\
\vartheta_{\beta_{0m}}^{\mathrm{R}_{01}} &= \frac{\partial \mathrm{R}_{01}}{\partial \beta_{0m}} \frac{\beta_{0m}}{\mathrm{R}_{01}} = \frac{1}{2\sqrt{\frac{\beta_{0h}\Psi\beta_{0m}\Phi_0}{\mu_h\mu_m^2(\mu_h+\delta+\gamma_h)}}} \frac{\beta_{0h}\Phi_0\Psi}{\mu_h\mu_m^2(\mu_h+\delta+\gamma_h)} \frac{\beta_{0m}}{\mathrm{R}_{01}} = \frac{1}{2} > 0,\\
\vartheta_{\Phi_0}^{\mathrm{R}_{01}} &= \frac{\partial \mathrm{R}_{01}}{\partial \Phi_0} \frac{\Phi_0}{\mathrm{R}_{01}} = \frac{1}{2\sqrt{\frac{\beta_{0h}\Psi\beta_{0m}\Phi_0}{\mu_h\mu_m^2(\mu_h+\delta+\gamma_h)}}} \frac{\beta_{0m}\beta_{0h}\Psi}{\mu_h\mu_m^2(\mu_h+\delta+\gamma_h)} \frac{\Phi_0}{\mathrm{R}_{01}} = \frac{1}{2} > 0,\\
\vartheta_{\Psi}^{\mathrm{R}_{01}} &= \frac{\partial \mathrm{R}_{01}}{\partial \Psi} \frac{\psi}{\mathrm{R}_{01}} = \frac{1}{2\sqrt{\frac{\beta_{0h}\Psi\beta_{0m}\Phi_0}{\mu_h\mu_m^2(\mu_h+\delta+\gamma_h)}}} \frac{\beta_{0m}\beta_{0h}\Phi_0}{\mu_h\mu_m^2(\mu_h+\delta+\gamma_h)} \frac{\Psi}{\mathrm{R}_{01}} = \frac{1}{2} > 0,\\
\vartheta_{\mu_m}^{\mathrm{R}_{01}} &= \frac{\partial \mathrm{R}_{01}}{\partial \mu_m} \frac{\mu_m}{\mathrm{R}_{01}} = \frac{1}{2\sqrt{\frac{\beta_{0h}\Psi\beta_{0m}\Phi_0}{\mu_h\mu_m^2(\mu_h+\delta+\gamma_h)}}} \frac{-2\beta_{0m}\Psi\beta_{0h}\Phi_0}{\mu_h\mu_m^3(\mu_h+\delta+\gamma_h)} \frac{\mu_m}{\mathrm{R}_{01}} = -1 < 0,\\
\vartheta_{\mu_h}^{\mathrm{R}_{01}} &= \frac{\partial \mathrm{R}_{01}}{\partial \mu_h} \frac{\mu_h}{\mathrm{R}_{01}} = \frac{1}{2\sqrt{\mathscr{B}}} \frac{-\mu_m^2(2\mu_h+\delta+\gamma_h)\beta_{0m}\Psi\beta_{0h}\Phi_0}{[\mu_h\mu_m^2(\mu_h+\delta+\gamma_h)]^2} \frac{\mu_h}{\mathrm{R}_{01}} = \frac{-(2\mu_h+\delta+\gamma_h)}{2(\mu_h+\delta+\gamma_h))} < 0,\\
\vartheta_{\delta}^{\mathrm{R}_{01}} &= \frac{\partial \mathrm{R}_{01}}{\partial \delta} \frac{\delta}{\mathrm{R}_{01}} = \frac{1}{2\sqrt{\frac{\beta_{0h}\Psi\beta_{0m}\Phi_0}{\mu_h\mu_m^2(\mu_h+\delta+\gamma_h)}}} \frac{-\mu_h\mu_m^2\beta_{0m}\Psi\beta_{0h}\Phi_0}{[\mu_h\mu_m^2(\mu_h+\delta+\gamma_h)]^2} \frac{\delta}{\mathrm{R}_{01}} = \frac{-\delta}{2(\mu_h+\delta+\gamma_h))} < 0,\\
\vartheta_{\gamma_h}^{\mathrm{R}_{01}} &= \frac{\partial \mathrm{R}_{01}}{\partial \gamma_h} \frac{\delta}{\mathrm{R}_{01}} = \frac{1}{2\sqrt{\frac{\beta_{0h}\Psi\beta_{0m}\Phi_0}{\mu_h\mu_m^2(\mu_h+\delta+\gamma_h)}}} \frac{-\mu_h\mu_m^2\beta_{0m}\Psi\beta_{0h}\Phi_0}{[\mu_h\mu_m^2(\mu_h+\delta+\gamma_h)]^2} \frac{\gamma_h}{\mathrm{R}_{01}} = \frac{-\gamma_h}{2(\mu_h+\delta+\gamma_h))} < 0,
\end{aligned}
\tag{4.75}
$$

where $\mathscr{B} = \frac{\beta_{0h}\Psi\beta_{0m}\Phi_0}{\mu_h\mu_m^2(\mu_h+\delta+\gamma_h)}$.

Consequently, their sensitivity indices were written in Table 4.2 after evaluated the parameter value as given by

Table 4.2: Sensitivity indices of parameters with respect to R_{01}

Parameters symbol	**Sensitivity index**
Ψ	0.5
Φ_0	0.5
β_{0h}	0.5
β_{0m}	0.5
μ_m	-1
μ_h	-0.092541
δ	-0.475258
γ_h	-0.024462

By the same procedure the sensitivity index of R_{02} with respect to parameter Ψ is

$$\vartheta_{\Psi}^{\mathrm{R}_{02}} = \frac{\partial \mathrm{R}_{02}}{\partial \Psi}\frac{\Psi}{\mathrm{R}_{02}} = \frac{1}{2\sqrt{\frac{\beta_{3h}\Psi\beta_{3m}\Phi_{3m}}{\mu_h\mu_m^2(\mu_h+\delta+\gamma_h)}}}\frac{\beta_{3h}\beta_{3m}\Phi_{3m}}{\mu_h\mu_m^2(\mu_h+\delta+\gamma_h)}\frac{\Psi}{\mathrm{R}_{02}} = \frac{1}{2} > 0$$

Similarly, with respect to others basic parameters, $\vartheta_{\beta_{0h}}^{\mathrm{R}_{02}}$, $\vartheta_{\beta_{0m}}^{\mathrm{R}_{02}}$, $\vartheta_{\Phi_0}^{\mathrm{R}_{02}}$, $\vartheta_{\beta_{1m}}^{\mathrm{R}_{02}}$, $\vartheta_{\Phi_{1m}}^{\mathrm{R}_{02}}$, $\vartheta_{\beta_{1h}}^{\mathrm{R}_{02}}$, $\vartheta_{\mu_h}^{\mathrm{R}_{02}}$, $\vartheta_{\mu_m}^{\mathrm{R}_{02}}$, $\vartheta_{\delta}^{\mathrm{R}_{02}}$ are obtained and their sensitivity indices were written in Table 4.3 as given by

Table 4.3: Sensitivity indices of parameters with respect to R_{02}

Parameters symbol	**Sensitivity index**
Ψ	0.5
Φ_0	0.072438
β_{0h}	0.291659
β_{0m}	0.285714
Φ_{1m}	0.069169
β_{1h}	0.208341
β_{1m}	0.214286
μ_m	-1
μ_h	-0.092541
δ	-0.475258
γ_h	-0.024462

4.3.1 Interpretation of sensitivity indices

In Table 4.2, we described sensitivity indices of the basic reproductive number $\mathtt{R}_{01}$ with respect to parameters. This output shows that the parameters Ψ, Φ_0, β_{0h}, and β_{0m} have positive sensitivity indices. They can increase value of $\mathtt{R}_{01}$ if their values increases while keeping other parameters constant. But, the parameters μ_m, μ_h, δ and γ_h have negative sensitivity indices, decreases the value of $\mathtt{R}_{01}$ if their values were increased while keeping the other parameters constant. For examples, $\vartheta_{\beta_{0m}}^{\mathtt{R}_{01}} = 0.5$, shows that decreasing (increasing) the mosquito contact rate by 10%, decreases (increases) the $\mathtt{R}_{01}$ by 5%, in the same way, $\vartheta_{\mu_m}^{\mathtt{R}_{01}}$ = -1, indicates that decreasing (increasing) the mosquitoes death rate by 10%, increases (decreases) $\mathtt{R}_{01}$, by 10%.

Similarly, in Table 4.3, the sensitivity indices of $\mathtt{R}_{02}$ with respect to basic parameters were shown. From this, the parameters that have positive (negative) sensitivity indices respectively, are increase the malaria if their value increases (decreases) respectively, while the others parameters stay constant. For instances, $\vartheta_{\beta_{0m}}^{\mathtt{R}_{02}} = 0.285714$, shows that decreasing (increasing) the contact rate of the mosquitoes by 10%, decreases (increases) the basic reproduction number $\mathtt{R}_{02}$ by 2.85714%, similarly, $\vartheta_{\gamma_h}^{\mathtt{R}_{02}}$ = -0.024462, indicates that decreasing (increasing) the rate of the recovery human by 10%, increases (decreases) the basic reproduction number $\mathtt{R}_{02}$, by 0.24462%.

4.4 Numerical simulations

In this section, we performed the numerical simulation to illustrate the dynamical properties of the model to show the stability of the disease free equilibrium points and endemic equilibrium points, and bifurcation analysis of the study. We verified the analytical results of our model by numerical simulations. Also, the numerical simulations of the model (4.1) were conducted by Matlab software using parameters values found in Table 4.4 to show the role of these parameters in the transmission of the malaria. Most of those parameters are taken from published papers whereas few of them are taken as assumed and we used the initial values $\mathtt{S}_h(0) = 800, \mathtt{I}_h(0) = 20, \mathtt{R}_h(0) = 0, \mathtt{S}_m(0) = 1000, \mathtt{I}_m(0) = 30$ and $\mathrm{T}(0) = 16.1^oC$ for simulation of malaria transmission model. Moreover, to show the impact of each parameter on the disease persists in the community, the convergence of the infected human and infected mosquito to the disease free equilibrium and endemic equilibrium points were shown. These numerical simulations are demonstrated to enhance the analytical results of the model.

Table 4.4: Parameters from literature value and assumed values used for model (4.1).

Parameters	Parameters description	Values	References
μ_h	Human natural death rate	0.00004	Agusto et al. (2012)
Ψ	Recruitment rate of humans	0.041	Chitnis et al. (2006)
δ	Induced death rate for human	0.068	Mojeeb and Adu (2017)
γ_h	Recover rate of infected humans	0.0035	Mojeeb and Adu (2017)
Φ_0	Recruitment rate of mosquito	0.071	Olaniyi et al. (2020)
μ_m	Natural death rate for mosquito	0.05	Mojeeb and Adu (2017)
ω_h	Immunity loss rate of human	0.005	Abiodun et al. (2018)
β_{1m}	Mosquito incremental contact rate	0.07	Assumed
β_{1h}	Incremental contact rate of human	0.05	Assumed
Φ_{1m}	Incremental birth rate of mosquito	0.09	Assumed
β_{0h}	Contact rate of human	0.03	Olaniyi et al. (2018)
β_{0m}	Mosquito contact rate	0.09	Olaniyi et al. (2020)
r	Growth rate of temperature	0.007	Assumed
T_0	Minimum temperature	16^oC	Abiodun et al. (2016)
$\mathrm{T}_{\max}$	Maximum temperature	28^oC	Bhuju et al. (2018)

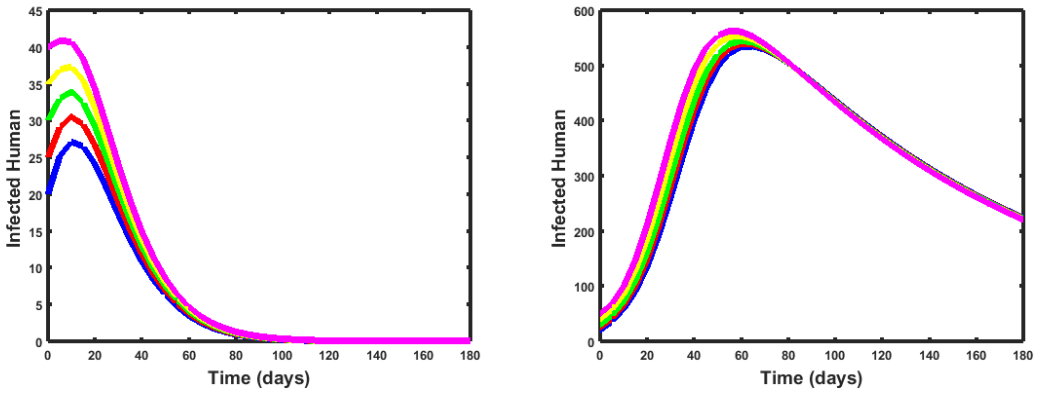

(**a**) (**b**)

Figure 4.2: Convergence of solutions for infected human to the equilibrium points

Figure 4.2**a**, describes that the simulation of convergence of the infected human at the disease free equilibrium point of the model (4.1) such that $\mathrm{R}_{01} = 0.85$ where the malaria disease dies out. In a contrast, Figure 4.2**b** shows the convergence of the infected human at the endemic equilibrium point of the model (4.1), in which the basic reproduction number

($\mathbb{R}_{02}$) greater than unity such that the disease persists in the community.

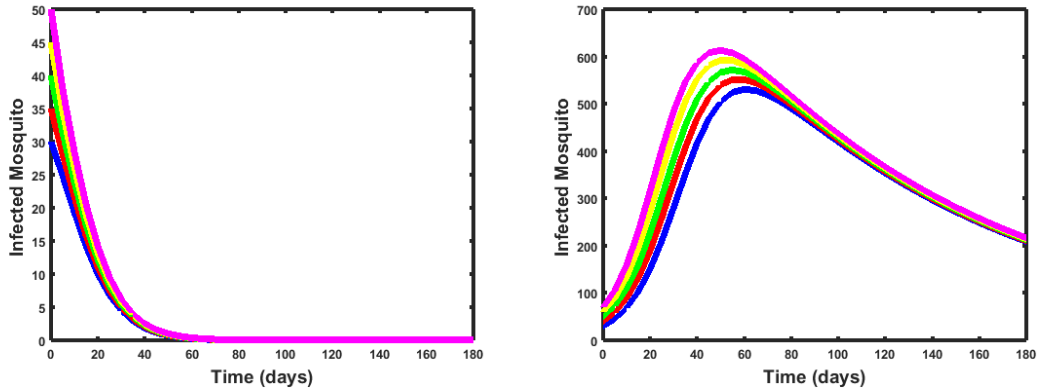

(**a**) (**b**)

Figure 4.3: Convergence of solutions for infected mosquitoes to the equilibrium points

Figure 4.3**a**, describes that the simulation of convergence of the infected mosquito at the disease free equilibrium point of the model (4.1) such that $\mathfrak{R}_{01} = 0.85$ where the malaria disease dies out. In a contrast, Figure 4.3**b** shows the dynamics of the infected mosquito at the endemic equilibrium point of the model (4.1) in which the basic reproduction number ($\mathbb{R}_{02}$) greater than unity such that the disease persists in the community.

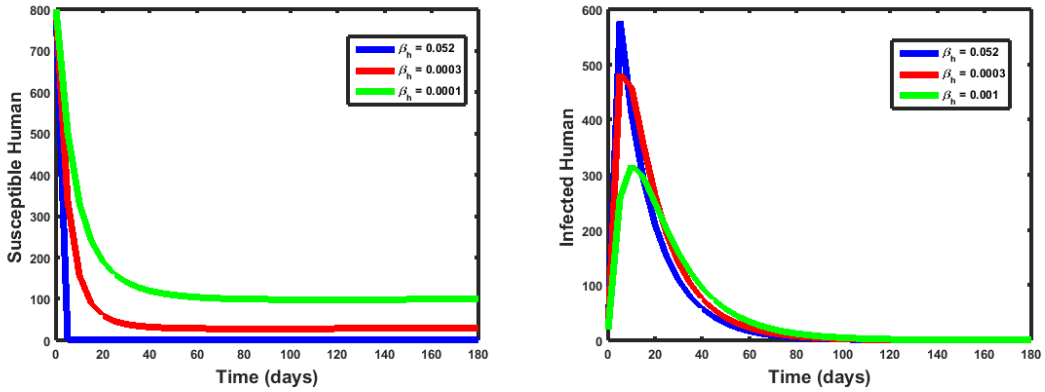

(**a**) (**b**)

Figure 4.4: Simulation results of susceptible and infected human with vary values of β_h

Figure 4.4 shows the results of susceptible human and infected human with a vary value of β_h. In the Figures 4.4**a** and 4.4**b**, we observed that an increase the infection rate of infected mosquito on susceptible human β_h, the secondary case number increases, which implies that an increase the amount of infected human while the susceptible human population decreases in number.

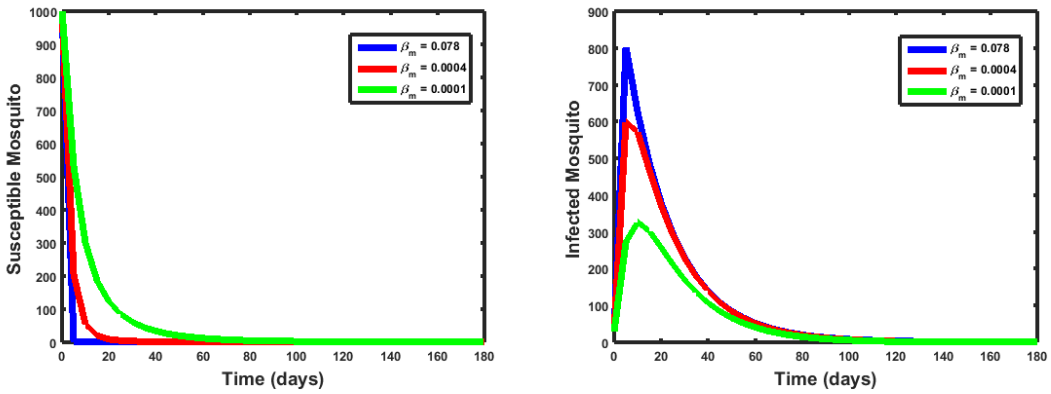

(**a**) (**b**)

Figure 4.5: Simulation results of susceptible and infected mosquitoes with vary values of β_m

Figure 4.5 describes the simulation results with infected mosquito and susceptible mosquito for vary value of β_m. Figures 4.5**a** and 4.5**b** described that increase the infection rate of infected human on susceptible mosquito β_m, the endemic of disease increases, which indicates that an increase the amount of infected mosquito while the amount of susceptible population mosquito decreases in number.

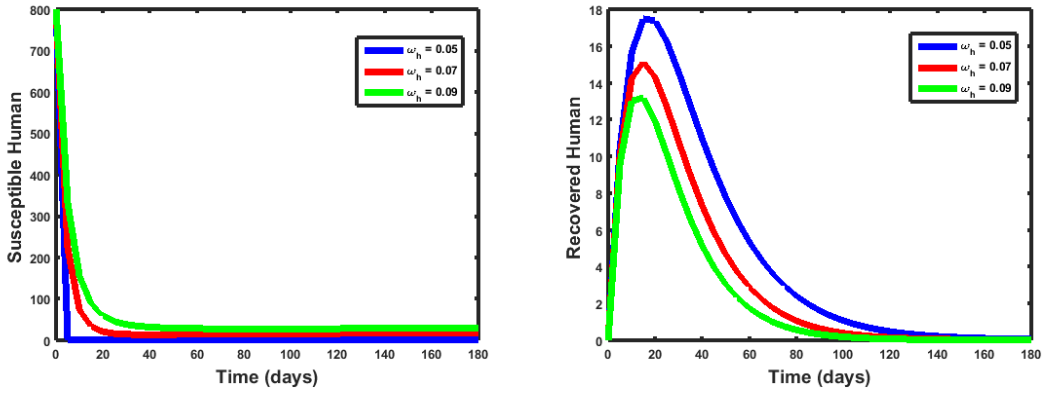

(**a**) (**b**)

Figure 4.6: Simulation results of susceptible and recovered human for different value of ω_h

Figure 4.6 shows the results of susceptible human and recovered human for vary value of ω_h. From the Figures 4.6**a** and 4.6**b**, we can see that an increase the rate of loss of immunity in human which leads to an again increase number of susceptible human population, whereas an increase the loss of immunity rate is decrease the number of recovered human population.

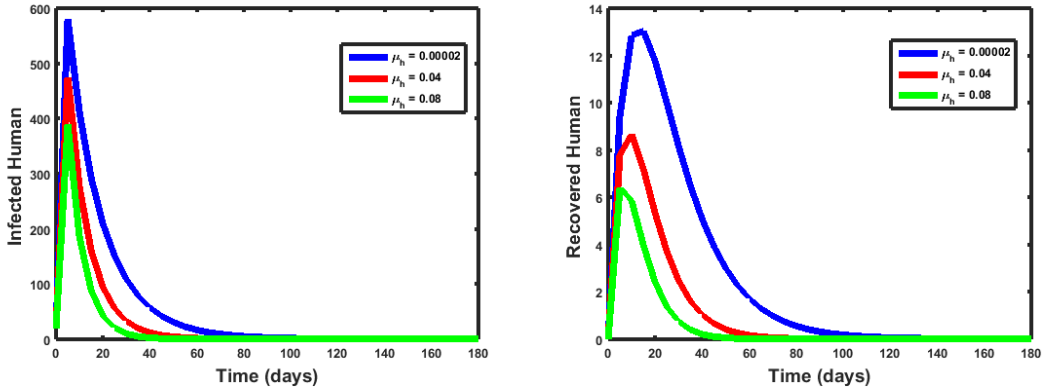

(**a**) (**b**)

Figure 4.7: Simulation results of infected and recovered human with different values of μ_h

Figure 4.7 describes variations results of infected and recovered human population for a different value of natural death μ_h. From the Figure 4.7**a** it can be observed that increase the death rate of the infected human reduces the number infected human and increase death rate of recovered human decreases number of recovered human populations as described in Figure 4.7**b**.

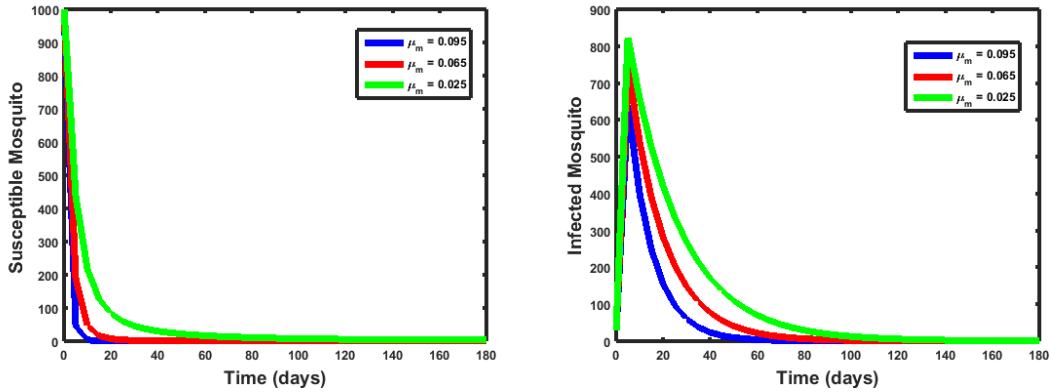

(**a**) (**b**)

Figure 4.8: Simulation results of susceptible and infected mosquito with vary values of μ_m

Figure 4.8 shows variation results with susceptible mosquito and infected population of mosquito for a various value of μ_m. In the Figures 4.8**a** and 4.8**b**, we observed that increase the death rate of the mosquito population decrease the amount of secondary case infection. Hence, as death rate increase, this leads to a decrease both susceptible and infected population of the mosquito.

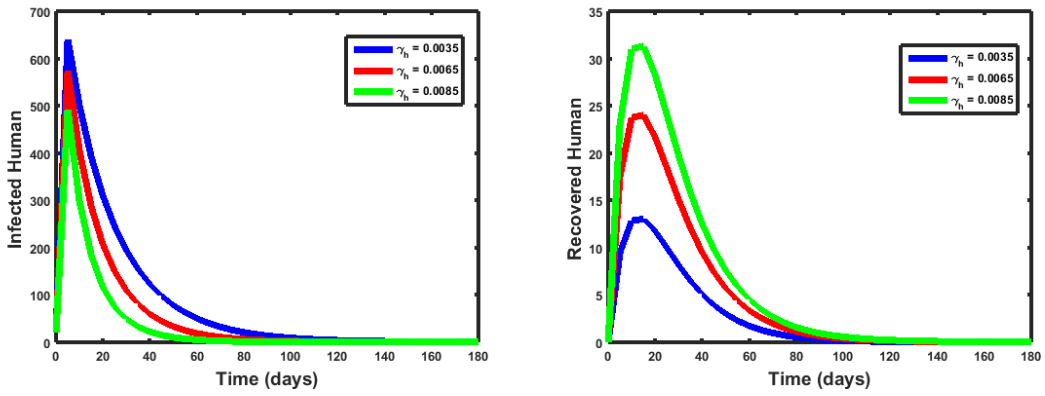

(**a**) (**b**)

Figure 4.9: Simulation results of infected and recovered of human with different value of γ_h

Figure 4.9 illustrates variation results of infected human and recovered human for a different value of γ_h. From the Figures 4.9**a** and 4.9**b**, we can see that increase the recovery rate of population of infected human due to using the anti-malaria drugs, which makes the decreases the infected human population while increases recovered human population. Note that since the reverse relation between basic reproduction number and recover rate leads to reduces the basic reproduction number.

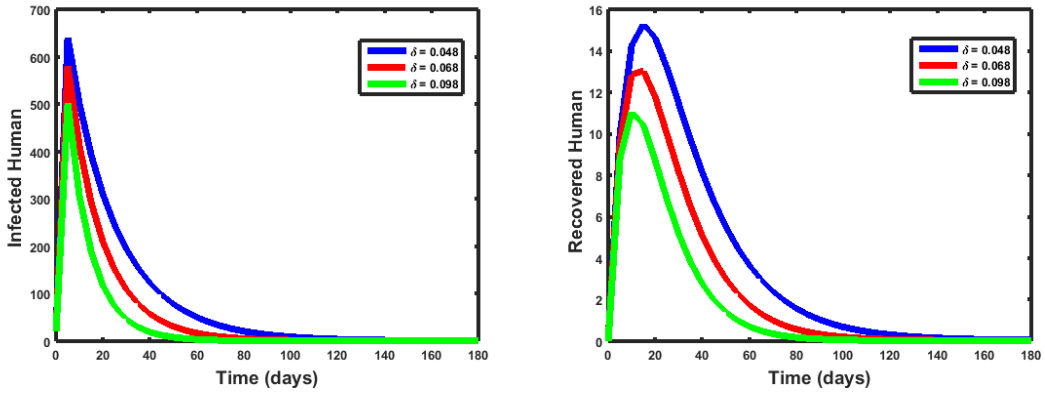

(**a**) (**b**)

Figure 4.10: Simulation results of infected and recovered human with different values of δ

Figure 4.10 shows the simulation result is illustrated that the difference of infected human for a different value of death rate. From Figure 4.10**a**, it can observe that increase the death rate of the human due to disease, decreases the number of infected human population. Figure 4.10**b** shows that increase the death rate of human due to disease decreases the number of recovered human population.

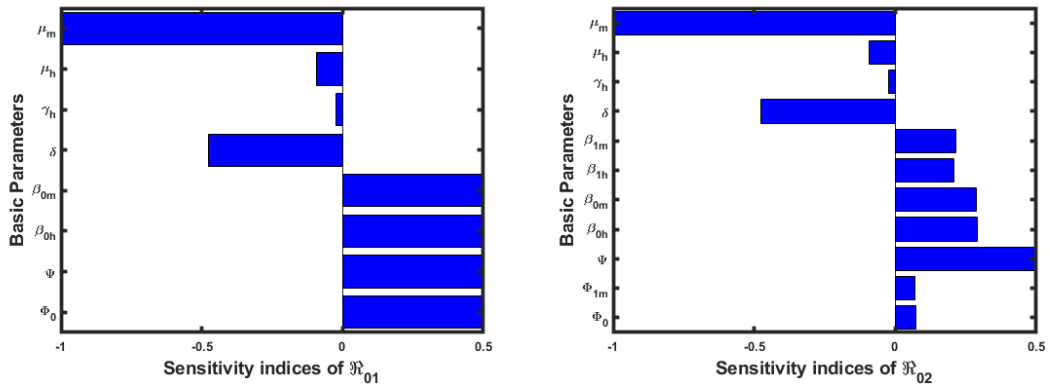

(**a**) (**b**)

Figure 4.11: Sensitivity indices of basic reproduction number R_{01} and R_{02} respectively

Figure 4.11 shows numerical simulation of the sensitivity analysis of model parameters. Note that the parameters that have positive (negative) sensitivity indices respectively, were increase the basic reproduction number R_0 if their value increases (decreases) respectively, while the others parameters stay constant.

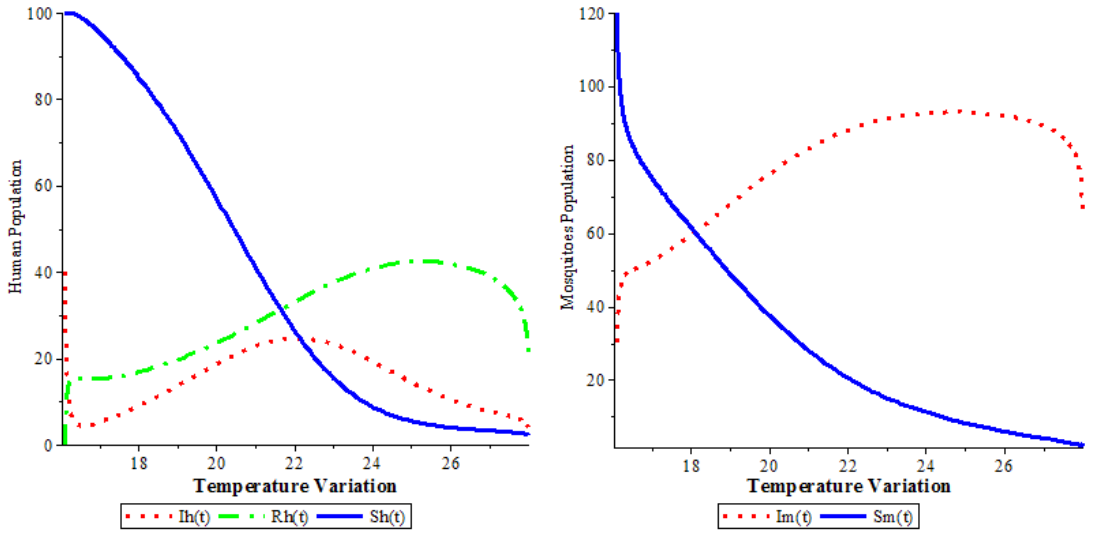

(**a**) (**b**)

Figure 4.12: Human population and mosquitoes population with rise in temperature

Figure 4.12 describes human population and mosquito population with rise in temperature. It can be observed that from the Figure 4.12**a**, the susceptible human, recovered human and infected human are decreasing. From Figure 4.12**b**, we can see that infected mosquito increase to a maximum point then decrease and susceptible mosquito decreases and tends to its lowest value at maximum temperature ($\mathrm{T}_{\max} = 28^{o}C$).

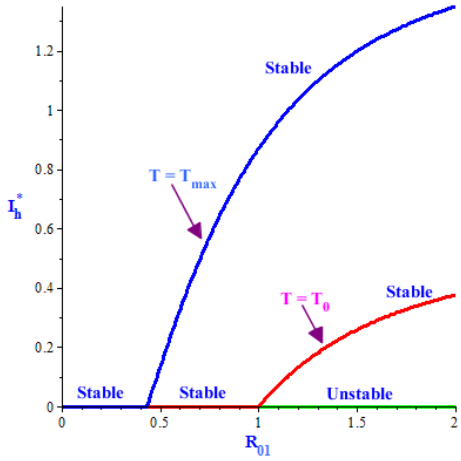

Figure 4.13: Bifurcation diagram of malaria transmission model with temperature variation

Figure 4.13 shows the bifurcation diagram for the case when $\mathtt{T} = \mathtt{T}_0$ and $\mathtt{T} = \mathtt{T}_{\max}$ that the model is exhibits forward and backward bifurcation respectively, for malaria transmission model. This implies that $\mathtt{R}_{01} < 1$ does not automatically implies $\mathtt{R}_{02} < 1$, since the value of $\mathtt{R}_{02}$ may be greater than 1, which implies that $\mathtt{R}_{02}$ present backward bifurcation while $\mathtt{R}_{01}$ only present forward bifurcation.

CHAPTER 5
MODELING SEIRS MATHEMATICAL MODEL OF MALARIA TRANSMISSION WITH TEMPERATURE VARIABILITY

Plasmodium parasite requires both human and mosquito for its life cycle to complete, and the infection is transferred between susceptible human through the bite of infected mosquitoes, which acquire infection through a blood meal from infected humans. The period from the point of infection to the beginning of the state of infectiousness is known as latent period during which the infected individuals stay in the exposed (E) class (Mandal et al., 2011). In this chapter we considered exposed class and presented a mathematical model that describes malaria dynamics in the presence of temperature variability.

5.1 Mathematical model formulation

In this section, we have extended the model introduced in section (4.1) by including the exposed class on the human and mosquito populations. The total population of human denoted by $\mathtt{N}_h(t)$ and population of mosquito denoted by $\mathtt{N}_m(t)$. The human population is described by the SEIRS model and sub-divided at the time (t) into the following sub-population of susceptible human $\mathtt{S}_h(t)$ those are do not have malaria, exposed humans $\mathtt{E}_h(t)$ those are infected but can not transmit disease, infected humans $\mathtt{I}_h(t)$ those can transmit the disease to mosquitoes, and recovered $\mathtt{R}_h(t)$ are whose recovered from infected compartment. Thus, the total human population size is $\mathtt{N}_h(t) = \mathtt{S}_h(t) + \mathtt{E}_h(t) + \mathtt{I}_h(t) + \mathtt{R}_h(t)$.

New recruitment that enters the population of humans by born or migrate at the rate Ψ (assumed that it is susceptible). An infected mosquito can transmit the malaria to the susceptible human and moved to the exposed human at a rate $\beta_h(\mathtt{T})$ is temperature-dependent and β_{0h} is the contact rate of human with mosquito when there is no variation in temperature

and β_{1h} is incremental contact rate of human with mosquito due temperature variation. The exposed human moved to an infected human at the rate α_h. All humans die with a natural death rate μ_h. An infected human can die due to disease at an induced death rate δ. This death can be reduces the infect human. An infected human can be recovered due to the use of anti-malarial drugs through treatment at the rate γ_h. The recovered human has lost their temporary immunity and becomes susceptible to reinfection at the rate ω_h.

Moreover, the population of mosquito is followed the SEI compartment model and the total population of mosquito at time (t) is denoted by $\mathtt{N}_m(t)$ is sub-divided into susceptible mosquito $\mathtt{S}_m(t)$, exposed mosquito $\mathtt{E}_m(t)$ and infected mosquito $\mathtt{I}_m(t)$. So that the total adult female *Anopheles* mosquito population at time is given by $\mathtt{N}_m(t) = \mathtt{S}_m(t) + \mathtt{E}_m(t) + \mathtt{I}_m(t)$. The susceptible mosquito is recruited at the rate $\Phi(\mathtt{T})$ is temperature-dependent and Φ_0 is the birth rate of mosquito if there is no variation in temperature and Φ_{1m} is the incremental birth rate of mosquito due to temperature variation. An infected human can transmit the disease to a susceptible mosquito and the mosquito population gets an infection when it contacts the infected human by malaria is moved to the exposed mosquito at the rate $\beta_m(\mathtt{T})$ is temperature-dependent and β_{0m} is contact rate of mosquito with a human when there is no variation in temperature and β_{1m} is incremental contact rate of mosquito with human due temperature variations. The exposed mosquito moved to an infected mosquito at a rate α_m. A natural death rate of all mosquitoes is μ_m. We suppose mosquitoes do not recover from malaria until death. A mosquito does not die due to disease infection.

The temperature growth rate represented by $\mathtt{r}$, mosquito to be most active at maximum temperature denoted by $\mathtt{T}_{\max}$ and minimum temperature for the mosquito to be less active is denoted by $\mathtt{T}_0$. Also we assume that all parameters in the model are nonnegative. Figure 5.1 shows the flow diagram of malaria transmission so that the state variables and parameters of the model are described in Table 5.1.

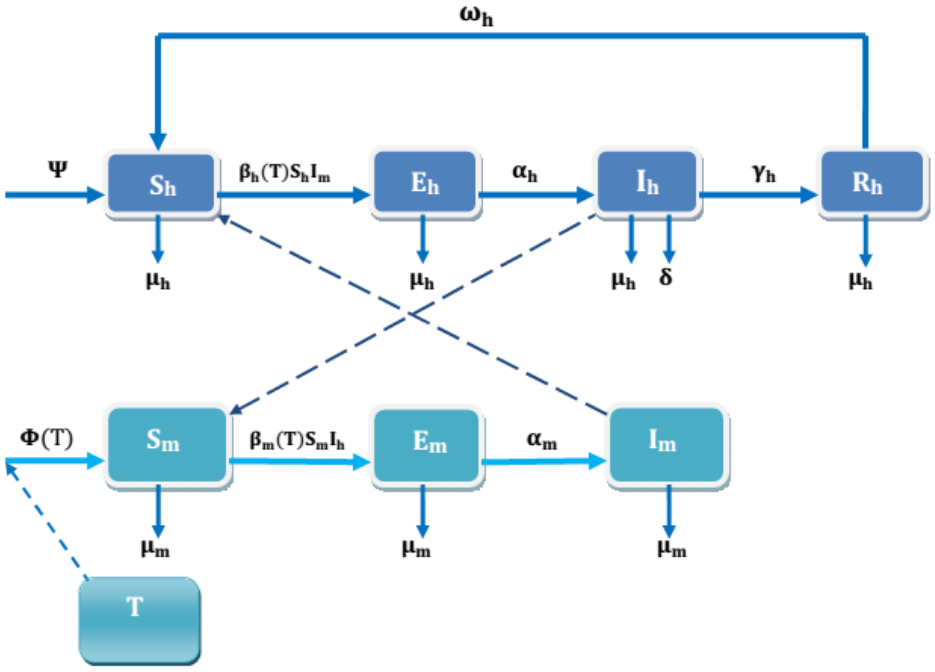

Figure 5.1: Flow diagram of malaria transmission with exposed compartment

From the schematic diagram depicted in Figure 5.1, the dynamics of malaria transmission is illustrated by the system of non-linear differential equations

$$\begin{cases} \frac{dS_h}{dt} = \Psi - \beta_h(\mathrm{T})S_hI_m - \mu_hS_h + \omega_h\mathrm{R}_h, \\ \frac{d\mathrm{E}_h}{dt} = \beta_h(\mathrm{T})S_hI_m - (\mu_h+\alpha_h)\mathrm{E}_h, \\ \frac{dI_h}{dt} = \alpha_h\mathrm{E}_h - (\mu_h+\delta+\gamma_h)I_h, \\ \frac{d\mathrm{R}_h}{dt} = \gamma_hI_h - (\mu_h+\omega_h)\mathrm{R}_h, \\ \frac{dS_m}{dt} = \Phi(\mathrm{T}) - \beta_m(\mathrm{T})S_mI_h - \mu_mS_m, \\ \frac{d\mathrm{E}_m}{dt} = \beta_m(\mathrm{T})S_mI_h - (\mu_m+\alpha_m)\mathrm{E}_m, \\ \frac{dI_m}{dt} = \alpha_m\mathrm{E}_m - \mu_mI_m, \\ \frac{d\mathrm{T}}{dt} = \mathrm{r}(1-\frac{\mathrm{T}}{\mathrm{T}_{\max}})(\mathrm{T}-\mathrm{T}_0), \end{cases} \tag{5.1}$$

where ,

$\beta_h(\mathrm{T}) = \beta_{0h} + \beta_{1h}\left(\frac{\mathrm{T}-\mathrm{T}_0}{\mathrm{T}_{\max}}\right)$, $\beta_m(\mathrm{T}) = \beta_{0m} + \beta_{1m}\left(\frac{\mathrm{T}-\mathrm{T}_0}{\mathrm{T}_{\max}}\right)$ and $\Phi(\mathrm{T}) = \Phi_0 + \Phi_{1m}\left(\frac{\mathrm{T}-\mathrm{T}_0}{\mathrm{T}_{\max}}\right)$.

With initial conditions $S_h(0) = S_{h0}, \mathrm{E}_h(0) = \mathrm{E}_{h0}, I_h(0) = I_{h0}, \mathrm{R}_h(0) = \mathrm{R}_{h0}, S_m(0) = S_{m0}$,

$\mathrm{E}_m(0) = \mathrm{E}_{m0}, I_m(0) = I_{m0}, \mathrm{T}(0) = \mathrm{T}_{\mathrm{m0}}$.

Table 5.1: Parameters description used for the model (5.1)

Parameters	**Parameters description**
α_h	Exposed human rate of progression
α_m	Rate of progression for exposed mosquito
β_{0h}	Contact rate of human with infected mosquito
Φ_{1m}	Incremental breeding rate of mosquito population
Ψ	The rate of new human enter to population
Φ_0	Recruitment rate of mosquito
γ_h	Recover rate of infected human
μ_h	Natural death rate of human population
δ	Induced death rate for human population
μ_m	Natural death rate for mosquito
ω_h	Humans immunity loss rate
β_{0m}	Contact rate of mosquito with infected human
β_{1m}	Incremental contact rate of mosquito
β_{1h}	Incremental contact rate of human
r	Growth rate of temperature
$\mathtt{T}_0$	Minimum temperature for the mosquito to be less active
$\mathtt{T}_{\max}$	Maximum temperature for the mosquito to be most active

5.2 Qualitative analysis of the model

In this section, we have shown the fundamental properties of the malaria dynamics model such as invariant region, positivity of the solutions, disease free-equilibrium point, basic reproduction number, endemic equilibrium point, local and global stability of equilibrium points of the model (5.1).

5.2.1 Invariant region

In this sub-section, we will see biologically meaningful and mathematically well posed on condition that all the solutions with non-negative initial data remain non-negative at every time.

Theorem 5.1 If the initial conditions of the model (5.1) are non-negative in Ω where

$$\Omega = \Omega_h \times \Omega_m = \left\{ (\mathrm{S}_h, \mathrm{E}_h, \mathrm{I}_h, \mathrm{R}_h, \mathrm{S}_m, \mathrm{E}_m, \mathrm{I}_m) \in \mathbb{R}^7_+ : \mathrm{N}_h \leq \frac{\Psi}{\mu_h}, \mathrm{N}_m \leq \frac{\Phi(\mathrm{T})}{\mu_m} \right\} \tag{5.2}$$

then the solutions of the model (5.1) enter and stay in Ω.

Proof: The total human population from the model (5.1) is given $N_h = S_h + \mathrm{E}_h + I_h + \mathrm{R}_h$. Then differentiate N_h both sides with respect to time (t) gives

$$\frac{d\mathrm{N}_h}{dt} = \frac{d\mathrm{S}_h}{dt} + \frac{d\mathrm{E}_h}{dt} + \frac{d\mathrm{I}_h}{dt} + \frac{d\mathrm{R}_h}{dt}. \tag{5.3}$$

By substituting equations (5.1) into (5.3), we got

$$\frac{d\mathrm{N}_h}{dt} = \Psi - \mu_h \mathrm{N}_h - \delta \mathrm{I}_h. \tag{5.4}$$

In fact, the equation (5.4) becomes,

$$\frac{d\mathrm{N}_h}{dt} \leq \Psi - \mu_h \mathrm{N}_h. \tag{5.5}$$

Integrating both sides of equation (5.5) and simplify the expression, we obtain

$$\Psi - \mu_h \mathrm{N}_h \geq \mathscr{B} e^{-\mu_h t} \tag{5.6}$$

where $\mathscr{B}$ is a constant. Using the initial conditions $\mathrm{N}_h(0) = \mathrm{N}_{h0}$ in equation (5.6) we got,

$$\Psi - \mu_h \mathrm{N}_h \geq (\Psi - \mu_h \mathrm{N}_{h0}) e^{-\mu_h t}. \tag{5.7}$$

Then rearranging equation (5.7), that gives

$$\mathrm{N}_h \leq \frac{\Psi}{\mu_h} - \left(\frac{\Psi - \mu_h \mathrm{N}_{h0}}{\mu_h} \right) e^{-\mu_h t}. \tag{5.8}$$

From equation (5.8) as time (t) approaches to infinity, the human population size $\mathrm{N}_h \to \frac{\Psi}{\mu_h}$ implies that $\mathrm{N}_h \leq \frac{\Psi}{\mu_h}$. Hence, the invariant region of the system (5.1) for human population is given by

$$\Omega_h = \left\{ (\mathrm{S}_h, \mathrm{E}_h, \mathrm{I}_h, \mathrm{R}_h) \in \mathbb{R}^4_+ : \mathrm{S}_h + \mathrm{E}_h + \mathrm{I}_h + \mathrm{R}_h \leq \frac{\Psi}{\mu_h} \right\}. \tag{5.9}$$

Similarly, we consider the total mosquito population from the system (5.1) given by

$$\mathrm{N}_m(t) = \mathrm{S}_m(t) + \mathrm{E}_m(t) + \mathrm{I}_m(t). \tag{5.10}$$

After the differentiating $\mathrm{N}_m(t)$ both sides with respect to time (t), we got

$$\frac{d}{dt}(\mathrm{S}_m + \mathrm{E}_m + \mathrm{I}_m) = \Phi(\mathrm{T}) - \mu_m \mathrm{N}_m. \tag{5.11}$$

By solving equation (5.11), we obtain $\mathtt{N}_m \leq \frac{\Phi(\mathtt{T})}{\mu_m}$. Hence, the invariant region of the system (5.1) for mosquito population is given by

$$\Omega_m = \left\{ (\mathtt{S}_m, \mathtt{E}_m, \mathtt{I}_m) \in \mathbb{R}^3_+ : \mathtt{S}_m + \mathtt{E}_m + \mathtt{I}_m \leq \frac{\Phi(\mathtt{T})}{\mu_m} \right\}. \tag{5.12}$$

Therefore, the invariant region of the system (5.1) is given by

$$\Omega = \Omega_h \times \Omega_m = \left\{ (\mathtt{S}_h, \mathtt{E}_h, \mathtt{I}_h, \mathtt{R}_h, \mathtt{S}_m, \mathtt{E}_m, \mathtt{I}_m) \in \mathbb{R}^7_+ : \mathtt{N}_h \leq \frac{\Psi}{\mu_h}, \mathtt{N}_m \leq \frac{\Phi(\mathtt{T})}{\mu_m} \right\} \tag{5.13}$$

is positive invariant and all the solution set of system (5.1) is bounded in Ω.

5.2.2 Positivity of the solutions

In this sub-section, we are going to show all solutions of the model system (5.1) with non-negative initial data will remain non-negative for all time $t \geq 0$.

Theorem 5.2 The solution of model (5.1) given as $\mathtt{S}_h(t)$, $\mathtt{E}_h(t)$, $\mathtt{I}_h(t)$, $\mathtt{R}_h(t)$, $\mathtt{S}_m(t)$, $\mathtt{E}_m(t)$ and $\mathtt{I}_m(t)$ with non-negative initial conditions, $S_h(0)$, $\mathtt{E}_h(0)$, $I_h(0)$, $\mathtt{R}_h(0)$, $S_m(0)$, $\mathtt{E}_m(0)$ and $I_m(0)$ are remain non-negative for all time $t \geq 0$.

Proof: Take the first equation from model (5.1) given as follows

$$\frac{d\mathtt{S}_h}{dt} = \Psi - \beta_h(\mathtt{T}) S_h I_m - \mu_h S_h + \omega_h \mathtt{R}_h. \tag{5.14}$$

It is true that the equation (5.14) becomes

$$\frac{d\mathtt{S}_h}{dt} \geq -(\beta_h(\mathtt{T}) I_m + \mu_h) S_h. \tag{5.15}$$

Integrating equation (5.15) with respect to time and using technique separation of variables with applying initial condition, we obtain

$$\mathtt{S}_h(t) \geq \mathtt{S}_h(0) e^{-(\beta_h(\mathtt{T}) I_m + \mu_h)t} \geq 0.$$

From the model (5.1) the second equation is given as

$$\frac{d\mathtt{E}_h}{dt} = \beta_h(\mathtt{T}) S_h I_m - (\mu_h + \alpha_h)\mathtt{E}_h,$$
$$\frac{d\mathtt{E}_h}{dt} \geq -(\mu_h + \alpha_h)\mathtt{E}_h.$$

Using the approaches of separation of variable, we get

$$\mathtt{E}_h(t) \geq \mathtt{E}_h(0) e^{-(\mu_h + \alpha_h)t} \geq 0. \tag{5.16}$$

From the third equation of the model (5.1), we have

$$\frac{d\mathtt{I}_h}{dt} = \alpha_h \mathtt{E}_h - (\mu_h + \delta + \gamma_h) I_h,$$
$$\frac{d\mathtt{I}_h}{dt} \geq -(\mu_h + \delta + \gamma_h) I_h.$$

Applying the separation of variable, we get

$$\mathtt{I}_h(t) \geq \mathtt{I}_h(0) e^{-(\mu_h+\delta+\gamma_h)t} \geq 0. \tag{5.17}$$

From the model (5.1) the fourth equation is given as

$$\frac{d\mathtt{R}_h}{dt} = \gamma_h I_h - (\mu_h + \omega_h)\mathtt{R}_h,$$
$$\frac{d\mathtt{R}_h}{dt} \geq -(\mu_h + \omega_h)\mathtt{R}_h.$$

Applying the separation of variable, we get

$$\mathtt{R}_h(t) \geq \mathtt{R}_h(0) e^{-(\mu_h+\omega_h)t} \geq 0. \tag{5.18}$$

From the model (5.1) fifth equation, we have

$$\frac{d\mathtt{S}_m}{dt} = \Phi(\mathtt{T}) - \beta_m(\mathtt{T}) S_m I_h - \mu_m S_m,$$
$$\frac{d\mathtt{S}_m}{dt} \geq -(\beta_m(\mathtt{T}) I_h - \mu_m) S_m.$$

Applying the separation of variable, we get

$$\mathtt{S}_m(t) \geq \mathtt{S}_m(0) e^{-(\beta_m(\mathtt{T})I_h-\mu_m)t} \geq 0. \tag{5.19}$$

From the model (5.1) sixth equation, we have

$$\frac{d\mathtt{E}_m}{dt} = \beta_m(\mathtt{T}) S_m I_h - (\mu_m + \alpha_m)\mathtt{E}_m,$$
$$\frac{d\mathtt{E}_m}{dt} \geq -(\mu_m + \alpha_m)\mathtt{E}_m.$$

Applying the separation of variable, we obtain

$$\mathtt{E}_m(t) \geq \mathtt{E}_m(0) e^{-(\mu_m+\alpha_m)t} \geq 0. \tag{5.20}$$

Finally, from the seventh equation of the model (5.1), we get

$$\mathtt{I}_m(t) \geq \mathtt{I}_m(0) e^{-\mu_m t} \geq 0. \tag{5.21}$$

This shows that the solution of the model (5.1) with non-negative initial data will remain non-negative for all time $t \geq 0$. Obviously, the malaria transmission model (5.1) is both meaningful epidemiologically and well-posed mathematically in Ω.

5.2.3 Disease free equilibrium

A disease free equilibrium point of the model is a steady-state solution in the absence of malaria. To compute the equilibrium solution of the system (5.1), setting the right-hand side of the system (5.1) to zero, that is given as

$$\begin{aligned}
\Psi - \beta_h(\mathrm{T})S_h I_m - \mu_h S_h + \omega_h \mathrm{R}_h = 0,\\
\beta_h(\mathrm{T})S_h I_m - (\mu_h + \alpha_h)\mathrm{E}_h = 0,\\
\alpha_h \mathrm{E}_h - (\mu_h + \delta + \gamma_h) I_h = 0,\\
\gamma_h I_h - (\mu_h + \omega_h)\mathrm{R}_h = 0,\\
\Phi(\mathrm{T}) - \beta_m(\mathrm{T})S_m I_h - \mu_m S_m = 0,\\
\beta_m(\mathrm{T})S_m I_h - (\mu_m + \alpha_m)\mathrm{E}_m = 0,\\
\alpha_m \mathrm{E}_m - \mu_m I_m = 0,\\
\mathrm{r}(1 - \frac{\mathrm{T}}{\mathrm{T}_{\max}})(\mathrm{T} - \mathrm{T}_0) = 0.
\end{aligned} \tag{5.22}$$

Thus, if there is no malaria, then the value of $\mathrm{E}_h = 0, I_h = 0, \mathrm{E}_m = 0, \mathrm{I}_m = 0$ and the disease free equilibrium of system (5.1) denoted by ξ_1 or ξ_2, where

$$\xi_1 = \left(\frac{\Psi}{\mu_h}, 0, 0, 0, \frac{\Phi(\mathrm{T}_0)}{\mu_m}, 0, 0, \mathrm{T}_0\right) \text{ or } \xi_2 = \left(\frac{\Psi}{\mu_h}, 0, 0, 0, \frac{\Phi(\mathrm{T}_{\max})}{\mu_m}, 0, 0, \mathrm{T}_{\max}\right). \tag{5.23}$$

5.2.4 Basic reproduction number

In this sub-section, we computed a basic reproduction number that determine the spread of a malaria. A basic reproduction number is interpreted as the average number of new infections that will be generate by one infected case during their entire infectious life-time (Agusto et al., 2012). It has computed using the next-generation matrix approach (John et al., 2020). Accordingly, using next-generation matrix, we re-writing the model (5.1) beginning with newly infective classes:

$$\begin{cases}
\frac{d\mathrm{E}_h}{dt} = \beta_h(\mathrm{T}^*)S_h I_m - (\mu_h + \alpha_h)\mathrm{E}_h,\\
\frac{dI_h}{dt} = \alpha_h \mathrm{E}_h - (\mu_h + \delta + \gamma_h) I_h,\\
\frac{d\mathrm{E}_m}{dt} = \beta_m(\mathrm{T}^*)S_m I_h - (\mu_m + \alpha_m)\mathrm{E}_m,\\
\frac{dI_m}{dt} = \alpha_m \mathrm{E}_m - \mu_m I_m.
\end{cases} \tag{5.24}$$

From equation (5.24), using the next generation matrix, the rate of appearance of new infection in sub-populations $\mathtt{E}_h$ and $\mathtt{E}_m$ is

$$\mathscr{F} = \begin{pmatrix} \beta_h(\mathtt{T}^*)S_h I_m \\ 0 \\ \beta_m(\mathtt{T}^*)S_m I_h \\ 0 \end{pmatrix}. \tag{5.25}$$

The Jacobian matrix of $\mathscr{F}$ at the disease free-equilibrium points gives f as

$$f = \begin{pmatrix} 0 & 0 & 0 & \beta_h(\mathtt{T}^*)\frac{\Psi}{\mu_h} \\ 0 & 0 & 0 & 0 \\ 0 & \beta_m(\mathtt{T}^*)\frac{\Phi(\mathtt{T}^*)}{\mu_m} & 0 & 0 \\ 0 & 0 & 0 & 0 \end{pmatrix}. \tag{5.26}$$

The transfer of individuals out of the compartments of the system (5.24) by all other means,

$$\mathscr{V} = \begin{pmatrix} (\mu_h + \alpha_h)\mathtt{E}_h \\ (\mu_h + \delta + \gamma_h)I_h - \alpha_h \mathtt{E}_h \\ (\mu_m + \alpha_m)\mathtt{E}_m \\ \mu_m I_m - \alpha_m \mathtt{E}_m \end{pmatrix}. \tag{5.27}$$

The Jacobian matrix of $\mathscr{V}$ at the disease free-equilibrium points gives υ as

$$\upsilon = \begin{pmatrix} \alpha_h + \mu_h & 0 & 0 & 0 \\ -\alpha_h & \mu_h + \delta + \gamma_h & 0 & 0 \\ 0 & 0 & \alpha_m + \mu_m & 0 \\ 0 & 0 & -\alpha_m & \mu_m \end{pmatrix}. \tag{5.28}$$

The inverse of υ is obtain as

$$\upsilon^{-1} = \begin{pmatrix} \frac{1}{\alpha_h+\mu_h} & 0 & 0 & 0 \\ \frac{\alpha_h}{(\alpha_h+\mu_h)(\mu_h+\delta+\gamma_h)} & \frac{1}{\mu_h+\delta+\gamma_h} & 0 & 0 \\ 0 & 0 & \frac{1}{\alpha_m+\mu_m} & 0 \\ 0 & 0 & \frac{\alpha_m}{\mu_m(\alpha_m+\mu_m)} & \frac{1}{\mu_m} \end{pmatrix}. \tag{5.29}$$

The next matrix generation is computed as

$$f\upsilon^{-1} = \begin{pmatrix} 0 & 0 & \frac{\beta_h(\mathtt{T}^*)\Psi\alpha_m}{\mu_h\mu_m(\alpha_m+\mu_m)} & \frac{\beta_h(\mathtt{T}^*)\Psi}{\mu_h\mu_m} \\ 0 & 0 & 0 & 0 \\ \frac{\beta_m(\mathtt{T}^*)\Phi(\mathtt{T}^*)\alpha_h}{\mu_m(\alpha_h+\mu_h)(\mu_h+\delta+\gamma_h)} & \frac{\beta_m(\mathtt{T}^*)\Phi(\mathtt{T}^*)}{\mu_m(\mu_h+\delta+\gamma_h)} & 0 & 0 \\ 0 & 0 & 0 & 0 \end{pmatrix}. \tag{5.30}$$

The eigenvalues are obtain from the determinant given by

$$\begin{vmatrix} -\lambda & 0 & \frac{\beta_h(\mathrm{T}^*)\Psi\alpha_m}{\mu_h\mu_m(\alpha_m+\mu_m)} & \frac{\beta_h(\mathrm{T}^*)\Psi}{\mu_h\mu_m} \\ 0 & -\lambda & 0 & 0 \\ \frac{\beta_m(\mathrm{T}^*)\Phi(\mathrm{T}^*)\alpha_h}{\mu_m(\alpha_h+\mu_h)(\mu_h+\delta+\gamma_h)} & \frac{\beta_m(\mathrm{T}^*)\Phi(\mathrm{T}^*)}{\mu_m(\mu_h+\delta+\gamma_h)} & -\lambda & 0 \\ 0 & 0 & 0 & -\lambda \end{vmatrix} = 0. \tag{5.31}$$

The eigenvalues from the matrix (5.31) gives

$$\begin{pmatrix} 0 \\ 0 \\ \sqrt{\frac{\beta_h\Psi(\mathrm{T}^*)\beta_m(\mathrm{T}^*)\Phi(\mathrm{T}^*)\alpha_h\alpha_m}{\mu_h\mu_m^2(\alpha_h+\mu_h)(\mu_h+\delta+\gamma_h)(\alpha_m+\mu_m)}} \\ -\sqrt{\frac{\beta_h\Psi(\mathrm{T}^*)\beta_m(\mathrm{T}^*)\Phi(\mathrm{T}^*)\alpha_h\alpha_m}{\mu_h\mu_m^2(\alpha_h+\mu_h)(\mu_h+\delta+\gamma_h)(\alpha_m+\mu_m)}} \end{pmatrix}. \tag{5.32}$$

Hence, the basic reproduction number computed by $\mathrm{R}_0 = \rho(f\upsilon^{-1})$ where ρ is the spectral radius of the product $f\upsilon^{-1}$ are obtained, respectively, by the equation (5.33) and (5.34) as given by

$$\mathrm{R}_{0\mathrm{l}} = \sqrt{\frac{\beta_{0h}\Psi\beta_{0m}\Phi_0\alpha_h\alpha_m}{\mu_h\mu_m^2(\mu_h+\delta+\gamma_h)(\alpha_h+\mu_h)(\alpha_m+\mu_m)}} \tag{5.33}$$

and

$$\mathrm{R}_{0\mathrm{m}} = \sqrt{\frac{(\beta_{0h}+\beta_{2h})\Psi(\beta_{0m}+\beta_{2m})(\Phi_0+\Phi_{2m})\alpha_h\alpha_m}{\mu_h\mu_m^2(\mu_h+\delta+\gamma_h)(\alpha_h+\mu_h)(\alpha_m+\mu_m)}} \tag{5.34}$$

where, $\beta_{2h} = \beta_{1h}k$, $\beta_{2m} = \beta_{1m}k$, $\Phi_{2m} = \Phi_{1m}k$ and $k = \left(\frac{\mathrm{T}_{\max}-\mathrm{T}_0}{\mathrm{T}_{\max}}\right)$.

Hence, the basic reproduction number at maximum temperature can be written as;

$$\mathrm{R}_{0\mathrm{m}} = \sqrt{\mathrm{R}_{0\mathrm{l}}^2 + \frac{\Phi_0\beta_{0m}\beta_{2m}\Psi\alpha_h\alpha_m + \Psi(\beta_{0m}+\beta_{2m})[\beta_{2h}(\Phi_0+\Phi_{2m})+\Phi_{2m}\beta_{0h}]\alpha_h\alpha_m}{\mu_h\mu_m^2(\mu_h+\delta+\gamma_h)(\alpha_h+\mu_h)(\alpha_m+\mu_m)}} \tag{5.35}$$

where, $\mathrm{R}_{0\mathrm{l}}$ is the basic reproduction number at T_0 for the mosquito to be less active to breed.

5.2.5 Local stability of disease free equilibrium

Theorem 5.3 If $\mathrm{R}_{0\mathrm{l}} < \mathrm{R}_{0\mathrm{m}} < 1$, then the disease free-equilibrium points of the system (5.1) is locally asymptotically stable in Ω.

Proof: To begin, first find the Jacobian matrix of the system (5.1) given as

$$z = \begin{pmatrix} z_{11} & 0 & 0 & \omega_h & 0 & 0 & -\beta_h(\mathtt{T}^*)S_h \\ \beta_h(\mathtt{T}^*)I_m & z_{22} & 0 & 0 & 0 & 0 & \beta_h(\mathtt{T}^*)S_h \\ 0 & \alpha_h & z_{33} & 0 & 0 & 0 & 0 \\ 0 & 0 & \gamma_h & z_{44} & 0 & 0 & 0 \\ 0 & 0 & -\beta_m(\mathtt{T}^*)S_m & 0 & z_{55} & \beta_m(\mathtt{T}^*)I_h & 0 \\ 0 & 0 & \beta_m(\mathtt{T}^*)S_m & 0 & \beta_m(\mathtt{T}^*)I_h & z_{66} & 0 \\ 0 & 0 & 0 & 0 & 0 & \alpha_m & z_{77} \end{pmatrix} \tag{5.36}$$

where,

$z_{11} = -(\beta_h(\mathtt{T}^*)I_h + \mu_h), z_{22} = -(\alpha_h + \mu_h)$, $z_{33} = -(\mu_h + \delta + \gamma_h)$, $z_{44} = -(\mu_h + \omega_h)$,
$z_{55} = -(\beta_m(\mathtt{T}^*)I_h + \mu_m), z_{66} = -(\alpha_m + \mu_m)$, and $z_{77} = -\mu_m$.

The Jacobian matrix of system (5.36) at the disease free equilibrium point is given by

$$z(\mathtt{E}_*) = \begin{pmatrix} z_{11} & 0 & 0 & \omega_h & 0 & 0 & -\beta_h(\mathtt{T}^*)\frac{\Psi}{\mu_h} \\ 0 & z_{22} & 0 & 0 & 0 & 0 & \beta_h(\mathtt{T}^*)\frac{\Psi}{\mu_h} \\ 0 & \alpha_h & z_{33} & 0 & 0 & 0 & 0 \\ 0 & 0 & \gamma_h & z_{44} & 0 & 0 & 0 \\ 0 & 0 & -\beta_m(\mathtt{T}^*)\frac{\Phi(\mathtt{T}^*)}{\mu_m} & 0 & z_{55} & 0 & 0 \\ 0 & 0 & \beta_m(\mathtt{T}^*)\frac{\Phi(\mathtt{T}^*)}{\mu_m} & 0 & 0 & z_{66} & 0 \\ 0 & 0 & 0 & 0 & 0 & \alpha_m & z_{77} \end{pmatrix} \tag{5.37}$$

where, $z_{11} = -\mu_h, z_{22} = -(\alpha_h + \mu_h)$, $z_{33} = -(\mu_h + \delta + \gamma_h)$, $z_{44} = -(\mu_h + \omega_h), z_{55} = -\mu_m$,
$z_{66} = -(\alpha_m + \mu_m)$, and $z_{77} = -\mu_m$.

The eigenvalues of (5.45) are the solutions of the characteristic equation $|z(\mathtt{E}_*) - \mathtt{I}_7\lambda| = 0$ is

$$\begin{vmatrix} z_{11}-\lambda & 0 & 0 & \omega_h & 0 & 0 & -\beta_h(\mathtt{T}^*)\frac{\Psi}{\mu_h} \\ 0 & z_{22}-\lambda & 0 & 0 & 0 & 0 & \beta_h(\mathtt{T}^*)\frac{\Psi}{\mu_h} \\ 0 & \alpha_h & z_{33}-\lambda & 0 & 0 & 0 & 0 \\ 0 & 0 & \gamma_h & z_{44}-\lambda & 0 & 0 & 0 \\ 0 & 0 & -\beta_m(\mathtt{T}^*)\frac{\Phi(\mathtt{T}^*)}{\mu_m} & 0 & z_{55}-\lambda & 0 & 0 \\ 0 & 0 & \beta_m(\mathtt{T}^*)\frac{\Phi(\mathtt{T}^*)}{\mu_m} & 0 & 0 & z_{66}-\lambda & 0 \\ 0 & 0 & 0 & 0 & 0 & \alpha_m & z_{77}-\lambda \end{vmatrix} = 0, \tag{5.38}$$

The first column of (5.38) has only one non-zero $-\mu_h - \lambda$ that is in its diagonal. This implies that the first eigenvalue is $\lambda_1 = -\mu_h$. Then the others of the eigenvalues are obtain

from equation

$$\begin{vmatrix} z_{22}-\lambda & 0 & 0 & 0 & 0 & \beta_h(\mathtt{T}^*)\frac{\Psi}{\mu_h} \\ \alpha_h & z_{33}-\lambda & 0 & 0 & 0 & 0 \\ 0 & \gamma_h & z_{44}-\lambda & 0 & 0 & 0 \\ 0 & -\beta_m(\mathtt{T}^*)\frac{\Phi(\mathtt{T}^*)}{\mu_m} & 0 & z_{55}-\lambda & 0 & 0 \\ 0 & \beta_m(\mathtt{T}^*)\frac{\Phi(\mathtt{T}^*)}{\mu_m} & 0 & 0 & z_{66}-\lambda & 0 \\ 0 & 0 & 0 & 0 & \alpha_m & z_{77}-\lambda \end{vmatrix} = 0. \tag{5.39}$$

The third and the fourth columns have diagonal entries. Hence, we have obtained two eigenvalues $\lambda_2 = -(\mu_h + \omega_h)$ and $\lambda_3 = -\mu_m$ respectively. Then the other eigenvalues are computed using the equation

$$\begin{vmatrix} z_{22}-\lambda & 0 & 0 & \beta_h(\mathtt{T}^*)\frac{\Psi}{\mu_h} \\ \alpha_h & z_{33}-\lambda & 0 & 0 \\ 0 & \beta_m(\mathtt{T}^*)\frac{\Phi(\mathtt{T}^*)}{\mu_m} & z_{66}-\lambda & 0 \\ 0 & 0 & \alpha_m & z_{77}-\lambda \end{vmatrix} = 0. \tag{5.40}$$

Setting $c_1 = \alpha_h + \mu_h$, $c_2 = \mu_h + \delta + \gamma_h$, $c_3 = \alpha_m + \mu_m$, $c_4 = \mu_m$ and the remaining eigenvalues are calculated from equation (5.40) with the characteristic given by

$$\lambda^4 + b_1\lambda^3 + b_2\lambda^2 + b_3\lambda + b_4 = 0 \tag{5.41}$$

where,

$$\begin{aligned} b_1 &= c_1 + c_2 + c_3 + c_4, \\ b_2 &= c_1c_2 + c_2c_3 + 2c_1c_4 + c_3c_4 + c_2c_4, \\ b_3 &= 2c_1c_2c_3 + c_1c_2c_4 + c_2c_3c_4, \\ b_4 &= c_1c_2c_3c_4 - \frac{\beta_h(\mathtt{T}^*)\Psi\beta_m(\mathtt{T}^*)\Phi(\mathtt{T}^*)\alpha_h\alpha_m}{\mu_m\mu_h}. \end{aligned} \tag{5.42}$$

By applying Routh-Hurwitz criteria (Ibrahim et al., 2020) the eigenvalues of the equation (5.41) is negative roots or imaginary roots with negative real part if

$$b_1 > 0,\ b_2 > 0,\ b_3 > 0,\ b_4 > 0, b_1b_2 - b_3 > 0, b_1b_2b_3 - b_3^2 - b_4b_1^2 > 0, b_4(b_1b_2b_3 - b_3^2 - b_4b_1^2) > 0.$$

Obviously, we have seen that $b_1 > 0$, $b_2 > 0$, and $b_3 > 0$, because they are the sum of positive parameters. Secondly, the value of b_4, at $\mathtt{T}^* = \mathtt{T}_{\max}$ is given by

$$b_4 = \mu_m(\mu_h + \delta + \gamma_h)(\alpha_h + \mu_h)(\alpha_m + \mu_m) - \frac{(\beta_{0h} + \beta_{2h})\Psi(\beta_{0m} + \beta_{2m})(\Phi_0 + \Phi_{2m})}{\mu_m\mu_h} = 1 - \mathtt{R}_{0m}^2.$$

This implies b_4 to be positive $1 - \mathtt{R}_{0m}^2$ could be positive, which shows $\mathtt{R}_{0m} < 1$. But, if $\mathtt{R}_{0m} > 1$ then $b_4 < 0$ shows that equation (5.41) has non-negative real solution and DFE is unstable. Since $\mathtt{R}_{0l} < \mathtt{R}_{0m}$ the DFE is locally asymptotically stable in Ω if $\mathtt{R}_{0l} < \mathtt{R}_{0m} < 1$.

5.2.6 Global stability of disease free equilibrium

Theorem 5.4. The disease free equilibrium points of the system (5.1) is globally asymptotically stable in Ω if $\mathtt{R}_{0l} < \mathtt{R}_{0m} < 1$.

Proof: First we developed the following Lyapunov function $\mathtt{V}$ that is defined as

$$\mathtt{V} = \left(\frac{\alpha_h \mathtt{E}_h}{(\alpha_h+\mu_h)(\mu_h+\delta+\gamma_h)}\right) + \left(\frac{\mathtt{I}_h}{\mu_h+\delta+\gamma_h}\right) + \left(\frac{\mu_m \mathtt{R}_{0m}}{\beta_{3m}\Phi_{3m}}\right)\mathtt{E}_m + \left(\frac{\mu_m(\alpha_m+\mu_m)\mathtt{R}_{0m}}{\beta_{3m}\Phi_{3m}\alpha_m}\right)\mathtt{I}_m \tag{5.43}$$

By differentiating the above Lyapunov function with respect to time (t) we obtain

$$\begin{aligned}
\frac{d\mathtt{V}}{dt} &= \left(\frac{\alpha_h \dot{\mathtt{E}}_h}{(\alpha_h+\mu_h)(\mu_h+\delta+\gamma_h)}\right) + \left(\frac{\dot{\mathtt{I}}_h}{\mu_h+\delta+\gamma_h}\right) + \left(\frac{\mu_m \mathtt{R}_{0m}}{\beta_{3m}\Phi_{3m}}\right)\dot{\mathtt{E}}_m + \left(\frac{\mu_m(\alpha_m+\mu_m)\mathtt{R}_{0m}}{\beta_{3m}\Phi_{3m}\alpha_m}\right)\dot{\mathtt{I}}_m \\
&= \left(\frac{\alpha_h}{(\alpha_h+\mu_h)(\mu_h+\delta+\gamma_h)}\right)(\beta_{3h}S_h I_m - (\mu_h+\alpha_h)\mathtt{E}_h) + \left(\frac{(\alpha_h \mathtt{E}_h - (\mu_h+\delta+\gamma_h)I_h)}{\mu_h+\delta+\gamma_h}\right) \\
&+ \left(\frac{\mu_m \mathtt{R}_{0m}}{\beta_{3m}\Phi_{3m}}\right)(\beta_{3m}S_m I_h - (\mu_m+\alpha_m)\mathtt{E}_m) + \left(\frac{\mu_m(\alpha_m+\mu_m)\mathtt{R}_{0m}}{\beta_{3m}\Phi_{3m}\alpha_m}\right)(\alpha_m \mathtt{E}_m - \mu_m)I_m, \\
&= \frac{\beta_{3h}\alpha_h S_h I_m}{(\alpha_h+\mu_h)(\mu_h+\delta+\gamma_h)} - I_h + \frac{\mu_m S_m I_h \mathtt{R}_{0m}}{\Phi_{3m}} - \left(\frac{\mu_m^2(\alpha_m+\mu_m)\mathtt{R}_{0m} I_m}{\beta_{3m}\alpha_m\Phi_{3m}}\right), \\
&\leq \left(\frac{\beta_{3h}\alpha_h\Psi}{(\alpha_h+\mu_h)(\mu_h+\delta+\gamma_h)\mu_h} - \frac{\mu_m^2(\alpha_m+\mu_m)\mathtt{R}_{0m}}{\beta_{3m}\alpha_m\Phi_{3m}}\right) I_m + (\mathtt{R}_{0m}-1)I_h, \\
&= \left[\left(\frac{\mu_m^2(\alpha_m+\mu_m)}{\beta_{3m}\alpha_m\Phi_{3m}}\sqrt{\frac{\beta_{3h}\alpha_h\Psi\beta_{3m}\Phi_{3m}\alpha_m}{\mu_h\mu_m^2(\alpha_h+\mu_h)(\mu_h+\delta+\gamma_h)(\alpha_m+\mu_m)}}\right) I_m + I_h\right](\mathtt{R}_{0m}-1)
\end{aligned} \tag{5.44}$$

where, $\beta_{3h} = \beta_{0h} + \beta_{2h}$, $\beta_{3m} = \beta_{0m} + \beta_{2m}$ and $\Phi_{3m} = \Phi_0 + \Phi_{2m}$.

Thus, $\frac{d\mathtt{V}}{dt} < 0$ if $\mathtt{R}_{0m} < 1$ and $\frac{dV}{dt} = 0$ if and only if $\mathtt{I}_h = 0$ and $\mathtt{I}_m = 0$. It shows that the largest compact invariant set in $\{(\mathtt{S}_h, \mathtt{E}_h, \mathtt{I}_h, \mathtt{R}_h, \mathtt{S}_m, \mathtt{E}_m, \mathtt{I}_m) \in \Omega : \frac{d\mathtt{V}}{dt} = 0\}$ is the singleton set DFE in Ω. Therefore, by LaSalle's invariant principle (La Salle, 1976) every solution which begins in the domian approaches DFE as time (t) tends to infinity. Therefore, since $\mathtt{R}_{0l} < \mathtt{R}_{0m}$ the DFE is globally asymptotically stable in Ω if $\mathtt{R}_{0l} < \mathtt{R}_{0m} < 1$.

5.2.7 Endemic equilibrium point

An equilibrium point of the dynamic system that shows existence of the disease is the endemic equilibrium point (EEP). The endemic equilibrium point $\mathtt{E}^* = (\mathtt{S}_h^*, \mathtt{E}_h^*, \mathtt{I}_h^*, \mathtt{R}_h^*, \mathtt{S}_m^*, \mathtt{E}_m^*, \mathtt{I}_m^*, \mathtt{T}^*)$ is the solution of the system from the equations (5.22). At this point let $\lambda_h^* = \beta_h(\mathtt{T}^*)\mathtt{I}_m^*$ and $\lambda_m^* = \beta_m(\mathtt{T}^*)\mathtt{I}_h^*$ be, respectively, infection force of human and infection force of mosquito. To compute the endemic equilibrium point of the model (5.1), we used the following procedure:

Firstly, solving the fourth equation of the model (5.1), we obtain

$$\mathrm{R}_h^* = \frac{\gamma_h I_h^*}{\omega_h + \mu_h}. \tag{5.45}$$

Secondly, solving the first equation of the model (5.1), we got

$$\mathrm{S}_h^* = \frac{\Psi + \omega_h \mathrm{R}_h^*}{\lambda_h^* + \mu_h}. \tag{5.46}$$

Thirdly, solving the second equation of the model (5.1) gives

$$\mathrm{E}_h^* = \frac{\lambda_h^* S_h^*}{\alpha_h + \mu_h}. \tag{5.47}$$

Similarly, solving the third equation of the model (5.1) gives the result,

$$\mathrm{I}_h^* = \frac{\alpha_h \mathrm{E}_h^*}{\mu_h + \delta + \gamma_h}. \tag{5.48}$$

After substituting and re-arranging the expression of the equation (5.48), we obtain

$$\mathrm{I}_h^* = \frac{\Psi \alpha_h (\mu_h + \omega_h) \lambda_h^*}{(\alpha_h + \mu_h)(\mu_h + \delta + \gamma_h)(\mu_h + \omega_h)(\lambda_h^* + \mu_h) - (\omega_h \alpha_h \gamma_h \lambda_h^*)}. \tag{5.49}$$

Continuing solving the fifth equation of the model (5.1) gives the result,

$$\mathrm{S}_m^* = \frac{\Phi(\mathrm{T}^*)}{\lambda_m^* + \mu_m}. \tag{5.50}$$

Again solving the sixth equation of the model (5.1) gives the result,

$$\mathrm{E}_m^* = \frac{\lambda_m^* S_m^*}{\alpha_m + \mu_m}. \tag{5.51}$$

Lastly, solving the seventh equation of the model (5.1) gives the result,

$$\mathrm{I}_m^* = \frac{\alpha_m \mathrm{E}_m^*}{\mu_m}. \tag{5.52}$$

After substituting and re-arranging the expression of the equation (5.52), we obtain

$$\mathrm{I}_m^* = \frac{\lambda_m^* \alpha_m \Phi(\mathrm{T}^*)}{(\lambda_m^* + \mu_m)(\alpha_m + \mu_m)\mu_m}. \tag{5.53}$$

Using the infected human, the infection force of mosquito is computed as

$$\lambda_m^* = \beta_m(\mathrm{T}^*)\mathrm{I}_h^* = \beta_m(\mathrm{T}^*)\left[\frac{\Psi \alpha_h (\mu_h + \omega_h) \lambda_h^*}{(\alpha_h + \mu_h)(\mu_h + \delta + \gamma_h)(\mu_h + \omega_h)(\lambda_h^* + \mu_h) - (\omega_h \alpha_h \gamma_h \lambda_h^*)}\right]. \tag{5.54}$$

And also using the infectious mosquito, the infection force of human is obtained as

$$\lambda_h^* = \beta_h(\mathrm{T}^*)\mathrm{I}_m^* = \beta_h(\mathrm{T}^*)\left[\frac{\lambda_m^* \alpha_m \Phi(\mathrm{T}^*)}{(\lambda_m^* + \mu_m)(\alpha_m + \mu_m)\mu_m}\right]. \tag{5.55}$$

Hence, the system (5.1) has the endemic equilibrium point at $\mathtt{T}^* = \mathtt{T}_0$ is given by

$$\begin{aligned}
S_h^* &= \frac{\Psi(\alpha_h+\mu_h)(\mu_h+\delta+\gamma_h)(\mu_h+\omega_h)}{(\alpha_h+\mu_h)(\mu_h+\delta+\gamma_h)(\mu_h+\omega_h)(\lambda_h^*+\mu_h)-(\omega_h\alpha_h\gamma_h\lambda_h^*)},\\
\mathtt{E}_h^* &= \frac{\Psi(\mu_h+\delta+\gamma_h)(\mu_h+\omega_h)\lambda_h^*}{(\alpha_h+\mu_h)(\mu_h+\delta+\gamma_h)(\mu_h+\omega_h)(\lambda_h^*+\mu_h)-(\omega_h\alpha_h\gamma_h\lambda_h^*)},\\
\mathtt{I}_h^* &= \frac{\Psi\alpha_h(\mu_h+\omega_h)\lambda_h^*}{(\alpha_h+\mu_h)(\mu_h+\delta+\gamma_h)(\mu_h+\omega_h)(\lambda_h^*+\mu_h)-(\omega_h\alpha_h\gamma_h\lambda_h^*)},\\
\mathtt{R}_h^* &= \frac{\Psi\alpha_h\gamma_h\lambda_h^*}{(\alpha_h+\mu_h)(\mu_h+\delta+\gamma_h)(\mu_h+\omega_h)(\lambda_h^*+\mu_h)-(\omega_h\alpha_h\gamma_h\lambda_h^*)},\\
S_m^* &= \frac{\Phi_0}{\lambda_m^*+\mu_m},\\
\mathtt{E}_m^* &= \frac{\lambda_m^*\Phi_0}{(\lambda_m^*+\mu_m)(\alpha_m+\mu_m)},\\
\mathtt{I}_m^* &= \frac{\lambda_m^*\alpha_m\Phi_0}{(\lambda_m^*+\mu_m)(\alpha_m+\mu_m)\mu_m}.
\end{aligned} \tag{5.56}$$

By substituting $\mathtt{I}_h^*$ and $\mathtt{I}_m^*$ from equation (5.56) into λ_m^* and λ_h^* respectively, and λ_h^* is obtained by solving the equation

$$\mathtt{C}_1(\lambda_h^*)^2 + \mathtt{C}_2(\lambda_h^*) = 0 \tag{5.57}$$

where,

$$\begin{aligned}
\mathtt{C}_1 &= \mu_m(\alpha_m+\mu_m)[(\mu_h+\omega_h)[\beta_{0m}\alpha_h\Psi+\mu_m((\mu_h+\delta+\gamma_h)(\alpha_h+\mu_h))]+\mu_m(\omega_h\gamma_h\alpha_h)],\\
\mathtt{C}_2 &= (\omega_h+\mu_h)\left[\mu_h\mu_m^2(\alpha_h+\mu_h)(\alpha_m+\mu_m)(\mu_h+\delta+\gamma_h)(1-\mathtt{R}_{0l}^2)\right].
\end{aligned} \tag{5.58}$$

Therefore, $\mathtt{C}_1 > 0$ and $\mathtt{C}_2 > 0$ whenever $\mathtt{R}_{0l} < 1$, so that $\lambda_h^* = -\frac{\mathtt{C}_2}{\mathtt{C}_1} < 0$. Hence, positive endemic equilibrium does not occurs whenever $\mathtt{R}_{0l} < 1$. But, the endemic equilibrium is exist if $\mathtt{C}_2$ is less than zero.

By the same procedure, the model (5.1) has the endemic equilibrium point at maximum

temperature ($\mathtt{T}^* = \mathtt{T}_{\max}$) computed as

$$
\begin{aligned}
S_h^* &= \frac{\Psi(\alpha_h+\mu_h)(\mu_h+\delta+\gamma_h)(\mu_h+\omega_h)}{(\alpha_h+\mu_h)(\mu_h+\delta+\gamma_h)(\mu_h+\omega_h)(\lambda_h^*+\mu_h)-(\omega_h\alpha_h\gamma_h\lambda_h^*)},\\
\mathtt{E}_h^* &= \frac{\Psi(\mu_h+\delta+\gamma_h)(\mu_h+\omega_h)\lambda_h^*}{(\alpha_h+\mu_h)(\mu_h+\delta+\gamma_h)(\mu_h+\omega_h)(\lambda_h^*+\mu_h)-(\omega_h\alpha_h\gamma_h\lambda_h^*)},\\
\mathtt{I}_h^* &= \frac{\Psi\alpha_h(\mu_h+\omega_h)\lambda_h^*}{(\alpha_h+\mu_h)(\mu_h+\delta+\gamma_h)(\mu_h+\omega_h)(\lambda_h^*+\mu_h)-(\omega_h\alpha_h\gamma_h\lambda_h^*)},\\
\mathtt{R}_h^* &= \frac{\Psi\alpha_h\gamma_h\lambda_h^*}{(\alpha_h+\mu_h)(\mu_h+\delta+\gamma_h)(\mu_h+\omega_h)(\lambda_h^*+\mu_h)-(\omega_h\alpha_h\gamma_h\lambda_h^*)},\\
S_m^* &= \frac{(\Phi_0+\Phi_{2m})}{\lambda_m^*+\mu_m},\\
\mathtt{E}_m^* &= \frac{\lambda_m^*(\Phi_0+\Phi_{2m})}{(\lambda_m^*+\mu_m)(\alpha_m+\mu_m)},\\
\mathtt{I}_m^* &= \frac{\lambda_m^*\alpha_m(\Phi_0+\Phi_{2m})}{(\lambda_m^*+\mu_m)(\alpha_m+\mu_m)\mu_m}.
\end{aligned}
\tag{5.59}
$$

Similarly, substituting $\mathtt{I}_h^*$ and $\mathtt{I}_m^*$ from equation (5.59) into λ_m^* and λ_h^* respectively, and λ_h^* is obtained by solving the equation

$$
\mathtt{C}(\lambda_h^*)^2 + \mathtt{D}(\lambda_h^*) = 0 \tag{5.60}
$$

where,

$$
\begin{aligned}
&\mathtt{C} = \mu_m(\alpha_m+\mu_m)[(\mu_h+\omega_h)[(\beta_{0m}+\beta_{2m})\alpha_h\Psi+\mu_m((\mu_h+\delta+\gamma_h)(\alpha_h+\mu_h))]+\mu_m(\omega_h\gamma_h\alpha_h)],\\
&\mathtt{D} = (\omega_h+\mu_h)\left[\mu_h\mu_m^2(\alpha_h+\mu_h)(\alpha_m+\mu_m)(\mu_h+\delta+\gamma_h)(1-\mathtt{R}_{0m}^2)\right],
\end{aligned}
\tag{5.61}
$$

where, $\beta_{2h} = \beta_{1h}k$, $\beta_{2m} = \beta_{1m}k$, $\Phi_{2m} = \Phi_{1m}k$ and $k = \left(\frac{\mathtt{T}_{\max}-\mathtt{T}_0}{\mathtt{T}_{\max}}\right)$.

Hence, if $\mathtt{R}_{0m} < 1$ then automatically implies that $\mathtt{R}_{0l} < 1$ (see equation 5.35) and DFE exists for both $\mathtt{R}_{0l}$ and $\mathtt{R}_{0m}$. However, $\mathtt{R}_{0l} < 1$ does not automatically implies $\mathtt{R}_{0m} < 1$, since the value of $\mathtt{R}_{0m}$ may be greater than 1, which implies that while $\mathtt{R}_{0l}$ present DFE, $\mathtt{R}_{0m}$ may be become endemic situation or present backward bifurcation while $\mathtt{R}_{0l}$ only present forward bifurcation.

5.2.8 Global stability of endemic equilibrium

Theorem 5.5. The endemic equilibrium points of the system (5.1) is globally asymptotically stable in Θ if $\mathtt{R}_{0\mathtt{m}} > \mathtt{R}_{0\mathtt{l}} > 1$.

Proof: To illustrate the global stability, we constructed the following Lyapunov function;

$$\begin{aligned}\mathtt{L} &= [\mathtt{S}_h - \mathtt{S}_h^* - \mathtt{S}_h^* ln(\frac{\mathtt{S}_h}{\mathtt{S}_h^*})] + [\mathtt{E}_h - \mathtt{E}_h^* - \mathtt{E}_h^* ln(\frac{\mathtt{E}_h}{\mathtt{E}_h^*})] + [\mathtt{I}_h - \mathtt{I}_h^* - \mathtt{I}_h^* ln(\frac{\mathtt{I}_h}{\mathtt{I}_h^*})] \\ &+ [\mathtt{R}_h - \mathtt{R}_h^* - \mathtt{R}_h^* ln(\frac{\mathtt{R}_h}{\mathtt{R}_h^*})] + [\mathtt{S}_m - \mathtt{S}_m^* - \mathtt{S}_m^* ln(\frac{\mathtt{S}_m}{\mathtt{S}_m^*})] + [\mathtt{E}_m - \mathtt{E}_m^* - \mathtt{E}_m^* ln(\frac{\mathtt{E}_m}{\mathtt{E}_m^*})] \\ &+ [\mathtt{I}_m - \mathtt{I}_m^* - \mathtt{I}_m^* ln(\frac{\mathtt{I}_m}{\mathtt{I}_m^*})]. \end{aligned} \tag{5.62}$$

Computing the derivative of $\mathtt{L}$ along the solutions of system (5.1) and the result is

$$\frac{d\mathtt{L}}{dt} = [1 - \frac{\mathtt{S}_h^*}{\mathtt{S}_h}]\dot{\mathtt{S}_h} + [1 - \frac{\mathtt{E}_h^*}{\mathtt{E}_h}]\dot{\mathtt{E}_h} + [1 - \frac{\mathtt{I}_h^*}{\mathtt{I}_h}]\dot{\mathtt{I}_h} + [1 - \frac{\mathtt{R}_h^*}{\mathtt{R}_h}]\dot{\mathtt{R}_h} + [1 - \frac{\mathtt{S}_m^*}{\mathtt{S}_m}]\dot{S_m} + [1 - \frac{\mathtt{E}_m^*}{\mathtt{E}_m}]\dot{\mathtt{E}_m} + [1 - \frac{\mathtt{I}_m^*}{\mathtt{I}_m}]\dot{\mathtt{I}_m}.$$

By substituting equations of model (5.1) into the above equation, we got

$$\begin{aligned}\frac{d\mathtt{L}}{dt} =& [1 - \frac{\mathtt{S}_h^*}{\mathtt{S}_h}]\underbrace{(\Psi - \beta_h(\mathtt{T}^*)S_h I_m - \mu_h S_h + \omega_h \mathtt{R}_h)}_{\dot{S}_h} + [1 - \frac{\mathtt{E}_h^*}{\mathtt{E}_h}]\underbrace{(\beta_h(\mathtt{T}^*)S_h I_m - (\mu_h + \alpha_h)\mathtt{E}_h)}_{\dot{\mathtt{E}}_h} \\ &+ [1 - \frac{\mathtt{I}_h^*}{\mathtt{I}_h}]\underbrace{(\alpha_h \mathtt{E}_h - (\mu_h + \delta + \gamma_h)I_h)}_{\dot{\mathtt{I}}_h} + [1 - \frac{\mathtt{R}_h^*}{\mathtt{R}_h}]\underbrace{(\gamma_h I_h - (\mu_h + \omega_h)\mathtt{R}_h)}_{\dot{\mathtt{R}}_h} \\ &+ [1 - \frac{\mathtt{S}_m^*}{\mathtt{S}_m}]\underbrace{(\Phi(\mathtt{T}^*) - \beta_m(\mathtt{T}^*)S_m I_h - \mu_m S_m)}_{\dot{\mathtt{S}}_m} + [1 - \frac{\mathtt{E}_m^*}{\mathtt{E}_m}]\underbrace{(\beta_m(\mathtt{T}^*)S_m I_h - (\mu_m + \alpha_m)\mathtt{E}_m)}_{\dot{\mathtt{E}}_m} \\ &+ [1 - \frac{\mathtt{I}_m^*}{\mathtt{I}_m}]\underbrace{(\alpha_m \mathtt{E}_m - \mu_m I_m)}_{\dot{\mathtt{I}}_m}. \end{aligned} \tag{5.63}$$

Consequently, by re-arranging and collecting like terms equation (5.63) becomes

$$\begin{aligned}\frac{d\mathtt{L}}{dt} =& \underbrace{\Psi + \beta_h(\mathtt{T}^*)\mathtt{I}_m(\mathtt{S}_h^* + \mathtt{S}_h) + \omega_h(\mathtt{R}_h^* + \mathtt{R}_h) + \mu_h \mathtt{N}_h^* + \alpha_h(\mathtt{E}_h^* + \mathtt{E}_h) + \gamma_h \mathtt{I}_h + (\delta + \gamma_h)\mathtt{I}_h^*}_{\mathbf{M}} \\ &\underbrace{+\Phi(\mathtt{T}^*) + \beta_m(\mathtt{T}^*)\mathtt{I}_h(\mathtt{S}_m^* + \mathtt{S}_m) + \mu_m \mathtt{N}_m^* + \alpha_h(\mathtt{E}_m^* + \mathtt{E}_m)}_{\mathbf{M}} \underbrace{- [\Psi \frac{\mathtt{S}_h^*}{\mathtt{S}_h}] + \beta_h(\mathtt{T}^*)\mathtt{S}_h \mathtt{I}_m(\frac{\mathtt{E}_h^* + \mathtt{E}_h}{\mathtt{E}_h})}_{\mathbf{Q}} \\ &\underbrace{+\omega_h(\mathtt{R}_h^* + \mathtt{R}_h(\frac{\mathtt{S}_h^*}{\mathtt{S}_h})) + \mu_h \mathtt{N}_h + \alpha_h \frac{(\mathtt{I}_h^* + \mathtt{I}_h)}{\mathtt{I}_h} + \gamma_h \mathtt{I}_h \frac{\mathtt{R}_h^*}{\mathtt{R}_h} + (\delta + \gamma_h)\mathtt{I}_h + \Phi(\mathtt{T}^*)\frac{\mathtt{S}_m^*}{\mathtt{S}_m} + \mu_h \mathtt{N}_m}_{\mathbf{Q}} \\ &\underbrace{+\beta_m(\mathtt{T}^*)\mathtt{S}_m^* \mathtt{I}_h(\frac{\mathtt{E}_m^* + \mathtt{E}_m}{\mathtt{E}_m}) + \alpha_m \mathtt{E}_m(\frac{\mathtt{I}_m^* + \mathtt{I}_m}{\mathtt{I}_m})}_{\mathbf{Q}}. \end{aligned} \tag{5.64}$$

Hence, if $\mathtt{M} < Q$ then $\frac{d\mathtt{L}}{dt} < 0$ and $\frac{dL}{dt} = 0$, if and only if $\mathtt{S}_h = S_h^*, \mathtt{E}_h = \mathtt{E}_h^*, \mathtt{I}_h = \mathtt{I}_h^*, \mathtt{R}_h = \mathtt{R}_h^*, \mathtt{S}_m = \mathtt{S}_m^*, \mathtt{E}_m = \mathtt{E}_m^*, \mathtt{I}_m = \mathtt{I}_m^*$. Thus, the dominant positive invariant set in $\{(\mathtt{S}_h^*, \mathtt{E}_h^*, \mathtt{I}_h^*, \mathtt{R}_h^*, \mathtt{S}_m^*, \mathtt{E}_m^*, \mathtt{I}_m^*) \in \Omega : \frac{d\mathtt{L}}{dt} = 0\}$ is the singleton point $(\mathtt{E}^*)$. Hence, from LaSalle's invariant principle (La Salle, 1976), this indicates that the point $\mathtt{E}^*$ is globally asymptotically stable in Ω if $\mathtt{M} < Q$.

5.2.9 Bifurcation analysis

In this section, we investigated the nature of the bifurcation with the use of the center manifold theory (Castillo-Chavez and Song, 2004a) that identify the bifurcation analysis of the model (5.1) at $\mathtt{R}_0$ is equal to unity. Then we can obtain the following result.

Theorem 5.6 The system (5.1) exhibits forward bifurcation at $\mathtt{R}_{0l} = 1$.

Proof: First take transmission rate β_{0h} as bifurcation parameter so that $\mathtt{R}_{0l} = 1$ if and only if

$$\beta_{0h} = \beta_{0h}^{*} = \frac{\mu_h \mu_m^2 (\mu_h + \delta + \gamma_h)(\alpha_h + \mu_h)(\alpha_m + \mu_m)}{\Psi \beta_{0m} \Phi_0 \alpha_h \alpha_m}. \tag{5.65}$$

Moreover, by changing the variables $\mathtt{S}_h = x_1, \mathtt{E}_h = x_2, \mathtt{I}_h = x_3, \mathtt{R}_h = x_4, \mathtt{S}_m = x_5, \mathtt{E}_m = x_6, \mathtt{I}_m = x_7, \mathtt{T} = x_8$ and using vector $X = (x_1, x_2, x_3, x_4, x_5, x_6, x_7, x_8)^{\mathtt{T}}$ of the system (5.1) can be written in the form $\frac{dx}{dt} = (g_1, g_2, g_3, g_4, g_5, g_6, g_7, g_8)^{\mathtt{T}}$ as obtain

$$\begin{cases} \frac{dx_1}{dt} = \Psi - \beta_{0h} x_1 x_7 - \mu_h x_1 + \omega_h x_4, \\ \frac{dx_2}{dt} = \beta_{0h} x_1 x_7 - (\mu_h + \alpha_h) x_2, \\ \frac{dx_3}{dt} = \alpha_h x_2 - (\mu_h + \delta + \gamma_h) x_3, \\ \frac{dx_4}{dt} = \gamma_h x_3 - (\omega_h + \mu_h) x_4, \\ \frac{dx_5}{dt} = \Phi_0 - \beta_{0m} x_5 x_3 - \mu_m x_5, \\ \frac{dx_6}{dt} = \beta_{0m} x_5 x_3 - (\alpha_m + \mu_m) x_6, \\ \frac{dx_7}{dt} = \alpha_m x_7 - \mu_m x_7, \\ \frac{dx_8}{dt} = \mathtt{r}(1 - \frac{x_8}{\mathtt{T}_{\max}})(x_8 - \mathtt{T}_0). \end{cases} \tag{5.66}$$

The Jacobian matrix of (5.66) at the disease free equilibrium ξ_1 with $\beta_{0h} = \beta_{0h}^{*}$ is given

$$\mathtt{J}(\xi_1) = \begin{pmatrix} -\mathtt{J}_{11} & 0 & 0 & \omega_h & 0 & 0 & -\beta_{0h}\frac{\Psi}{\mu_h} & 0 \\ 0 & -\mathtt{J}_{22} & 0 & 0 & 0 & 0 & \beta_{0h}\frac{\Psi}{\mu_h} & 0 \\ 0 & \alpha_h & -\mathtt{J}_{33} & 0 & 0 & 0 & 0 & 0 \\ 0 & 0 & \gamma_h & -\mathtt{J}_{44} & 0 & 0 & 0 & 0 \\ 0 & 0 & -\beta_{0m}\frac{\Phi_0}{\mu_m} & 0 & -\mathtt{J}_{55} & 0 & 0 & 0 \\ 0 & 0 & \beta_{0m}\frac{\Phi_0}{\mu_m} & 0 & 0 & -\mathtt{J}_{66} & 0 & 0 \\ 0 & 0 & 0 & 0 & 0 & \alpha_m & -\mathtt{J}_{77} & 0 \\ 0 & 0 & 0 & 0 & 0 & 0 & 0 & \mathtt{J}_{88} \end{pmatrix} \tag{5.67}$$

where, $\mathtt{J}_{11} = \mu_h, \mathtt{J}_{22} = \alpha_h + \mu_h, \mathtt{J}_{33} = \mu_h + \delta + \gamma_h, \mathtt{J}_{44} = \mu_h + \omega_h, \mathtt{J}_{55} = \mu_m, \mathtt{J}_{66} = \alpha_m + \mu_m, \mathtt{J}_{77} = \mu_m$, and $\mathtt{J}_{88} = \mathtt{r}(1 - \frac{\mathtt{T}_0}{\mathtt{T}_{\max}})$.

Further the right eigenvectors, $w = (w_1, w_2, w_3, w_4, w_5, w_6, w_7, w_8)^{\mathrm{T}}$ corresponding to zero eigenvalue of equation (5.67) obtain from equation $\mathrm{J}w = 0$.

$$\begin{pmatrix} -\mathrm{J}_{11} & 0 & 0 & \omega_h & 0 & 0 & -\beta_{0h}\frac{\Psi}{\mu_h} & 0 \\ 0 & \mathrm{J}_{22} & 0 & 0 & 0 & 0 & \beta_{0h}\frac{\Psi}{\mu_h} & 0 \\ 0 & \alpha_h & -\mathrm{J}_{33} & 0 & 0 & 0 & 0 & 0 \\ 0 & 0 & \gamma_h & -\mathrm{J}_{44} & 0 & 0 & 0 & 0 \\ 0 & 0 & -\beta_{0m}\frac{\Phi_0}{\mu_m} & 0 & -\mathrm{J}_{55} & 0 & 0 & 0 \\ 0 & 0 & \beta_{0m}\frac{\Phi_0}{\mu_m} & 0 & 0 & -\mathrm{J}_{66} & 0 & 0 \\ 0 & 0 & 0 & 0 & 0 & \alpha_m & -\mathrm{J}_{77} & 0 \\ 0 & 0 & 0 & 0 & 0 & 0 & 0 & \mathrm{J}_{88} \end{pmatrix} \begin{pmatrix} w_1 \\ w_2 \\ w_3 \\ w_4 \\ w_5 \\ w_6 \\ w_7 \\ w_8 \end{pmatrix} = \begin{pmatrix} 0 \\ 0 \\ 0 \\ 0 \\ 0 \\ 0 \\ 0 \\ 0 \end{pmatrix} \tag{5.68}$$

where, $\mathrm{J}_{11} = \mu_h, \mathrm{J}_{22} = \alpha_h + \mu_h, \mathrm{J}_{33} = \mu_h + \delta + \gamma_h, \mathrm{J}_{44} = \mu_h + \omega_h, \mathrm{J}_{55} = \mu_m, \mathrm{J}_{66} = \alpha_m + \mu_m,$ $\mathrm{J}_{77} = \mu_m,$ and $\mathrm{J}_{88} = \mathrm{r}(1 - \frac{\mathrm{T}_0}{\mathrm{T}_{\max}})$.

From equation (5.68), we obtain

$$\begin{cases} w_1 = -\frac{((\alpha_h+\mu_h)+(\mu_h+\delta+\gamma_h)\alpha_h)w_2}{\mu_h^2}, \\ w_2 = w_2 > 0, \\ w_3 = \frac{\alpha_h}{(\mu_h+\delta+\gamma_h)}w_2, \\ w_4 = \frac{\alpha_h\gamma_h}{(\mu_h+\omega_h)(\mu_h+\delta+\gamma_h)}w_2, \\ w_5 = -\frac{\alpha_h^2\beta_{0m}\Phi_0}{\mu_m^2\mu_h(\mu_h+\delta+\gamma_h)}w_2, \\ w_6 = \frac{\alpha_h^2\beta_{0m}\Phi_0}{\mu_m\mu_h(\mu_h+\delta+\gamma_h)}w_2, \\ w_7 = \frac{\alpha_h^2\alpha_m\beta_{0m}\Phi_0}{\mu_m^2\mu_h(\alpha_m+\mu_m)}w_2, \\ w_8 = 0. \end{cases} \tag{5.69}$$

Similarly, the left eigenvectors, $v = (v_1, v_2, v_3, v_4, v_5, v_6, v_7, v_8)$ corresponding to zero eigenvalue were obtain from the equating $v\mathtt{J} = 0$.

$$\begin{pmatrix} v_1 \\ v_2 \\ v_3 \\ v_4 \\ v_5 \\ v_6 \\ v_7 \\ v_8 \end{pmatrix}^{\mathtt{T}} \begin{pmatrix} -\mathtt{J}_{11} & 0 & 0 & \omega_h & 0 & 0 & -\beta_{0h}\frac{\Psi}{\mu_h} & 0 \\ 0 & -\mathtt{J}_{22} & 0 & 0 & 0 & 0 & \beta_{0h}\frac{\Psi}{\mu_h} & 0 \\ 0 & \alpha_h & -\mathtt{J}_{33} & 0 & 0 & 0 & 0 & 0 \\ 0 & 0 & \gamma_h & -\mathtt{J}_{44} & 0 & 0 & 0 & 0 \\ 0 & 0 & -\beta_{0m}\frac{\Phi_0}{\mu_m} & 0 & -\mathtt{J}_{55} & 0 & 0 & 0 \\ 0 & 0 & \beta_{0m}\frac{\Phi_0}{\mu_m} & 0 & 0 & -\mathtt{J}_{66} & 0 & 0 \\ 0 & 0 & 0 & 0 & 0 & \alpha_m & -\mathtt{J}_{77} & 0 \\ 0 & 0 & 0 & 0 & 0 & 0 & 0 & J_{88} \end{pmatrix} = \begin{pmatrix} 0 \\ 0 \\ 0 \\ 0 \\ 0 \\ 0 \\ 0 \\ 0 \end{pmatrix} \tag{5.70}$$

where, $\mathtt{J}_{11} = \mu_h, \mathtt{J}_{22} = \alpha_h + \mu_h, \mathtt{J}_{33} = \mu_h + \delta + \gamma_h, \mathtt{J}_{44} = \mu_h + \omega_h, \mathtt{J}_{55} = \mu_m, \mathtt{J}_{66} = \alpha_m + \mu_m,$ $\mathtt{J}_{77} = \mu_m,$ and $\mathtt{J}_{88} = \mathtt{r}(1 - \frac{\mathtt{T}_0}{\mathtt{T}_{\max}})$.

From the equation (5.70), we got

$$\begin{aligned} v_1 &= v_4 = v_5 = v_8 = 0, \\ v_3 &= \frac{(\alpha_h + \mu_h)}{\alpha_h} v_2, \\ v_6 &= \frac{\beta_{0h}\Psi}{\mu_h \mu_m (\alpha_m + \mu_m)} v_2, \\ v_7 &= \frac{\beta_{0h}\Psi}{\mu_h \mu_m} v_2. \end{aligned} \tag{5.71}$$

The second partial derivatives of functions $g_i (i = 1,2,3,4,5,6,7,8)$ at the point (ξ_1, β^*_{0h}) are

$$\begin{aligned} \frac{\partial^2 g_2}{\partial x_1 \partial x_7} &= \beta^*_{0h} = \frac{\partial^2 g_2}{\partial x_7 \partial x_1} \\ \frac{\partial^2 g_2}{\partial \beta^*_{0h} \partial x_7} &= x^*_1 = \frac{\partial^2 g_2}{\partial x_7 \partial \beta^*_{0h}} \\ \frac{\partial^2 g_6}{\partial x_5 \partial x_3} &= \beta^*_{0m} = \frac{\partial^2 g_6}{\partial x_3 \partial x_5}. \end{aligned} \tag{5.72}$$

Thus, the nature of bifurcation at $\mathtt{R}_{01} = 1$ obtained from the above partial derivatives is given

$$\begin{aligned} a &= v_2 w_7 w_1 \beta^*_{0h} + v_2 w_1 w_7 \beta^*_{0h} + v_6 w_5 w_3 \beta_{0\mathrm{m}} + v_6 w_3 w_5 \beta_{0m}, \\ b &= v_2 w_7 x^*_1 = v_2 w_7 \frac{\Psi}{\mu_h}. \end{aligned} \tag{5.73}$$

By substituting the parameter values, we have the following expression

$$a = -2v_2\alpha_h^2\beta_{0m}\Phi_0 w_2^2\left(\frac{((\alpha_h+\mu_h)(\mu_h+\delta+\gamma_h))^2}{\mu_h^2\Psi\beta_{0m}\Phi_0}+\frac{(\alpha_h+\mu_h)}{\alpha_m\Phi_0\mu_h\mu_m(\mu_h+\delta+\gamma_h)}\right)<0,$$
$$b = v_2w_7x_1^* = v_2w_7\frac{\Psi}{\mu_h} = v_2w_2\frac{(\alpha_h^2\alpha_m)\beta_{0m}\Phi_0\Psi}{\mu_m^2\mu_h^2(\alpha_m+\mu_m)}>0. \tag{5.74}$$

Obviously, the coefficient of b is always positive and a is negative. This implies that the system (5.1) exhibits forward bifurcation at $\mathtt{R}_{0l}=1$ and which implies that at least one stable endemic equilibrium exist when $\Re_{0l}>1$.

Theorem 5.7 If $\mathtt{R}_{0m}<1$, then the system (5.1) exhibits backward bifurcation at $\mathtt{R}_{0m}=1$.

Proof. Considering rate β_{3h} as bifurcation parameter so that $\mathtt{R}_{0m}=1$ if and only if

$$\beta_{3h}=\beta_{3h}^*=\left(\frac{\mu_h\mu_m^2(\mu_h+\delta+\gamma_h)(\alpha_h+\mu_h)(\alpha_m+\mu_m)(1-\Re_{0l}^2)-\Psi\Phi_0\beta_{0h}\beta_{2h}\alpha_h\alpha_m}{\Psi(\Phi_{2m}\beta_{0m}+\beta_{2m}\Phi_0+\Phi_{2m}\beta_{2m})\alpha_h\alpha_m}\right). \tag{5.75}$$

Let renaming the variables $\mathtt{S}_h=x_1,\mathtt{E}_h=x_2,\mathtt{I}_h=x_3,\mathtt{R}_h=x_4,\mathtt{S}_m=x_5,\mathtt{E}_m=x_6,\mathtt{I}_m=x_7,\mathtt{T}=x_8$ and using vector $X=(x_1,x_2,x_3,x_4,x_5,x_6,x_7,x_8)^{\mathtt{T}}$. Then the model (5.1) can be written in the form $\frac{dx}{dt}=(g_1,g_2,g_3,g_4,g_5,g_6,g_7,g_8)^{\mathtt{T}}$ as described by

$$\begin{cases}
\frac{dx_1}{dt} = \Psi-\beta_{3h}x_1x_7-\mu_hx_1+\omega_hx_4,\\
\frac{dx_2}{dt} = \beta_{3h}x_1x_7-(\mu_h+\alpha_h)x_2,\\
\frac{dx_3}{dt} = \alpha_hx_2-(\mu_h+\delta+\gamma_h)x_3,\\
\frac{dx_4}{dt} = \gamma_hx_3-(\omega_h+\mu_h)x_4,\\
\frac{dx_5}{dt} = \Phi_{3m}-\beta_{3m}x_5x_3-\mu_mx_5,\\
\frac{dx_6}{dt} = \beta_{3m}x_5x_3-(\alpha_m+\mu_m)x_6,\\
\frac{dx_7}{dt} = \alpha_mx_7-\mu_mx_7,\\
\frac{dx_8}{dt} = \mathtt{r}(1-\frac{x_8}{\mathtt{T}_{\max}})(x_8-\mathtt{T}_0).
\end{cases} \tag{5.76}$$

where, $\beta_{3h}=\beta_{0h}+\beta_{1h}k$, $\beta_{3m}=\beta_{0m}+\beta_{1m}k$, $\Phi_{3m}=\Phi_0+\Phi_{1m}k$ and $k=\left(\frac{\mathtt{T}_{\max}-\mathtt{T}_0}{\mathtt{T}_{\max}}\right)$.

The Jacobian matrix of equation (5.76) at a disease free equilibrium ξ_2 with β_{3h}^* is given;

$$\mathtt{J}(\xi_2) = \begin{pmatrix} -\mathtt{J}_{11} & 0 & 0 & \omega_h & 0 & 0 & -\beta_{3h}\frac{\Psi}{\mu_h} & 0 \\ 0 & -\mathtt{J}_{22} & 0 & 0 & 0 & 0 & \beta_{3h}\frac{\Psi}{\mu_h} & 0 \\ 0 & \alpha_h & -\mathtt{J}_{33} & 0 & 0 & 0 & 0 & 0 \\ 0 & 0 & \gamma_h & -\mathtt{J}_{44} & 0 & 0 & 0 & 0 \\ 0 & 0 & -\beta_{3m}\frac{\Phi_{3m}}{\mu_m} & 0 & -\mathtt{J}_{55} & 0 & 0 & 0 \\ 0 & 0 & \beta_{3m}\frac{\Phi_{3m}}{\mu_m} & 0 & 0 & -\mathtt{J}_{66} & 0 & 0 \\ 0 & 0 & 0 & 0 & 0 & \alpha_m & -\mathtt{J}_{77} & 0 \\ 0 & 0 & 0 & 0 & 0 & 0 & 0 & -\mathtt{J}_{88} \end{pmatrix} \tag{5.77}$$

where, $\mathtt{J}_{11} = \mu_h, \mathtt{J}_{22} = \alpha_h + \mu_h, \mathtt{J}_{33} = \mu_h + \delta + \gamma_h, \mathtt{J}_{44} = \mu_h + \omega_h, \mathtt{J}_{55} = \mu_m, \mathtt{J}_{66} = \alpha_m + \mu_m,$ $\mathtt{J}_{77} = \mu_m,$ and $\mathtt{J}_{88} = \mathtt{r}(1 - \frac{\mathtt{T}_0}{\mathtt{T}_{\max}})$.

The right eigenvectors, $w = (w_1, w_2, w_3, w_4, w_5, w_6, w_7, w_8)^{\mathtt{T}}$ associated to simple zero eigenvalue of equation (5.77) obtain from equation $Jw = 0$.

$$\begin{pmatrix} -\mathtt{J}_{11} & 0 & 0 & \omega_h & 0 & 0 & -\beta_{3h}\frac{\Psi}{\mu_h} & 0 \\ 0 & -\mathtt{J}_{22} & 0 & 0 & 0 & 0 & \beta_{3h}\frac{\Psi}{\mu_h} & 0 \\ 0 & \alpha_h & -\mathtt{J}_{33} & 0 & 0 & 0 & 0 & 0 \\ 0 & 0 & \gamma_h & -\mathtt{J}_{44} & 0 & 0 & 0 & 0 \\ 0 & 0 & -\beta_{3m}\frac{\Phi_{3m}}{\mu_m} & 0 & -\mathtt{J}_{55} & 0 & 0 & 0 \\ 0 & 0 & \beta_{3m}\frac{\Phi_{3m}}{\mu_m} & 0 & 0 & -\mathtt{J}_{66} & 0 & 0 \\ 0 & 0 & 0 & 0 & 0 & \alpha_m & -\mathtt{J}_{77} & 0 \\ 0 & 0 & 0 & 0 & 0 & 0 & 0 & -\mathtt{J}_{88} \end{pmatrix} \begin{pmatrix} w_1 \\ w_2 \\ w_3 \\ w_4 \\ w_5 \\ w_6 \\ w_7 \\ w_8 \end{pmatrix} = \begin{pmatrix} 0 \\ 0 \\ 0 \\ 0 \\ 0 \\ 0 \\ 0 \\ 0 \end{pmatrix} \tag{5.78}$$

where, $\mathtt{J}_{11} = \mu_h, \mathtt{J}_{22} = \alpha_h + \mu_h, \mathtt{J}_{33} = \mu_h + \delta + \gamma_h, \mathtt{J}_{44} = \mu_h + \omega_h, \mathtt{J}_{55} = \mu_m, \mathtt{J}_{66} = \alpha_m + \mu_m,$ $\mathtt{J}_{77} = \mu_m,$ and $\mathtt{J}_{88} = \mathtt{r}(1 - \frac{\mathtt{T}_0}{\mathtt{T}_{\max}})$.

From equation (5.78), we obtain

$$\begin{cases} w_1 = -\frac{((\alpha_h+\mu_h)+(\mu_h+\delta+\gamma_h)\alpha_h)w_2}{\mu_h^2}, \\ w_2 = w_2 > 0, \\ w_3 = \frac{\alpha_h}{(\mu_h+\delta+\gamma_h)}w_2, \\ w_4 = \frac{\alpha_h\gamma_h}{(\mu_h+\omega_h)(\mu_h+\delta+\gamma_h)}w_2, \\ w_5 = -\frac{\alpha_h^2\beta_{3m}\Phi_{3m}}{\mu_m^2\mu_h(\mu_h+\delta+\gamma_h)}w_2, \\ w_6 = \frac{\alpha_h^2\beta_{3m}\Phi_{3m}}{\mu_m\mu_h(\mu_h+\delta+\gamma_h)}w_2, \\ w_7 = \frac{\alpha_h^2\alpha_m\beta_{3m}\Phi_{3m}}{\mu_m^2\mu_h(\alpha_m+\mu_m)}w_2, \\ w_8 = 0. \end{cases} \tag{5.79}$$

Similarly, the left eigenvectors, $v = (v_1, v_2, v_3, v_4, v_5, v_6, v_7, v_8)$ corresponding to simple zero eigenvalue can be obtained from the equating $vJ = 0$ and the system can be written in the form

$$\begin{pmatrix} v_1 \\ v_2 \\ v_3 \\ v_4 \\ v_5 \\ v_6 \\ v_7 \\ v_8 \end{pmatrix}^{\mathrm{T}} \begin{pmatrix} -\mathrm{J}_{11} & 0 & 0 & \omega_h & 0 & 0 & -\beta_{3h}\frac{\Psi}{\mu_h} & 0 \\ 0 & -\mathrm{J}_{22} & 0 & 0 & 0 & 0 & \beta_{3h}\frac{\Psi}{\mu_h} & 0 \\ 0 & \alpha_h & -\mathrm{J}_{33} & 0 & 0 & 0 & 0 & 0 \\ 0 & 0 & \gamma_h & -\mathrm{J}_{44} & 0 & 0 & 0 & 0 \\ 0 & 0 & -\beta_{3m}\frac{\Phi_{3m}}{\mu_m} & 0 & -\mathrm{J}_{55} & 0 & 0 & 0 \\ 0 & 0 & \beta_{3m}\frac{\Phi_{3m}}{\mu_m} & 0 & 0 & -\mathrm{J}_{66} & 0 & 0 \\ 0 & 0 & 0 & 0 & 0 & \alpha_m & -\mathrm{J}_{77} & 0 \\ 0 & 0 & 0 & 0 & 0 & 0 & 0 & -\mathrm{J}_{88} \end{pmatrix} = \begin{pmatrix} 0 \\ 0 \\ 0 \\ 0 \\ 0 \\ 0 \\ 0 \\ 0 \end{pmatrix} \tag{5.80}$$

where, $\mathrm{J}_{11} = \mu_h, \mathrm{J}_{22} = \alpha_h + \mu_h, \mathrm{J}_{33} = \mu_h + \delta + \gamma_h, \mathrm{J}_{44} = \mu_h + \omega_h, \mathrm{J}_{55} = \mu_m, \mathrm{J}_{66} = \alpha_m + \mu_m, \mathrm{J}_{77} = \mu_m,$ and $\mathrm{J}_{88} = \mathrm{r}(1 - \frac{\mathrm{T}_0}{\mathrm{T}_{\max}})$.

From the equation (5.80), we got,

$$\begin{aligned} v_1 &= v_4 = v_5 = v_8 = 0, \\ v_3 &= \frac{(\alpha_h + \mu_h)}{\alpha_h}v_2, \\ v_6 &= \frac{\beta_{3h}\Psi}{\mu_h\mu_m(\alpha_m + \mu_m)}v_2, \\ v_7 &= \frac{\beta_{3h}\Psi}{\mu_h\mu_m}v_2. \end{aligned} \tag{5.81}$$

From the second partial derivatives of functions g_2 and g_6, with the ones that are nonzero at the point ξ_2 with β_{3h}^* are obtain from

$$\begin{aligned}
\frac{\partial^2 g_2}{\partial x_1 \partial x_7} &= \beta_{3h}^* = \frac{\partial^2 g_2}{\partial x_7 \partial x_1} \\
\frac{\partial^2 g_2}{\partial \beta_{3h}^* \partial x_7} &= x_1^* = \frac{\partial^2 g_2}{\partial x_7 \partial \beta_{3h}^*} \\
\frac{\partial^2 g_6}{\partial x_5 \partial x_3} &= \beta_{3m}^* = \frac{\partial^2 g_6}{\partial x_3 \partial x_5}
\end{aligned} \tag{5.82}$$

and all the other partial derivative of g_2 and g_6 are zero. The direction of bifurcation at $\mathrm{R}_{0l} = 1$ obtained from the above partial derivatives given as

$$\begin{aligned}
a &= v_2 w_7 w_1 \beta_{3h}^* + v_2 w_1 w_7 \beta_{3h}^* + v_6 w_5 w_3 \beta_{3m} + v_6 w_3 w_5 \beta_{3m}, \\
b &= v_2 w_7 x_1^* = v_2 w_7 \frac{\Psi}{\mu_h}.
\end{aligned} \tag{5.83}$$

By substituting the parameter values, we have the following expression

$$\begin{aligned}
a &= (-2v_2 \alpha_h^2 \beta_{3m} \Phi_{3m} w_2^2) \left(\frac{\mu_h \mu_m^2 (\alpha_m + \mu_m)(\alpha_h + \mu_h)(\mu_h + \delta + \gamma_h) - \Psi \alpha_h \alpha_m \Phi_0 \beta_{0m} (\beta_{0h} + \beta_{1h} k)}{\Psi(\beta_{0m} \Phi_{2m} + \beta_{2m} \Phi_0 + \beta_{2m} \Phi_{2m})} \right) \\
&\cdot \left(\frac{(\alpha_h + \mu_h)(\mu_h + \delta + \gamma_h)}{\mu_h \mu_m^2 (\alpha_m + \mu_m)} \right) - 2v_2 \alpha_h^2 \beta_{3m} \Phi_{3m} w_2^2 \left(\frac{(\alpha_h + \mu_h)}{\alpha_m \Phi_{3m} \mu_h \mu_m (\mu_h + \delta + \gamma_h)} \right), \\
b &= v_2 w_7 x_1^* = v_2 w_7 \frac{\Psi}{\mu_h} = v_2 w_2 \frac{\alpha_h^2 \alpha_m \beta_{3m} \Phi_{3m} \Psi}{\mu_m^2 \mu_h^2 (\alpha_m + \mu_m)} > 0.
\end{aligned} \tag{5.84}$$

Therefore, the coefficient b is always positive since all parameters are non-negative. The malaria transmission model (5.1) may exhibit backward bifurcation at $\mathrm{R}_{0m} = 1$, if the constant coefficient a is positive.

5.3 Local sensitivity analysis

In this section, we apply same approach implemented in section (4.3) for sensitivity analysis of some basic parameters of the model. The sensitivity analysis of the model parameter is to illustrate the parameters that affected on the basic reproduction number. The approach we followed is outlined in (Okosun and Makinde, 2014; Berhe, 2020) to find the sensitivity analysis. These sensitivity indices tell us how crucial each parameter is on the transmission of the disease.

Definition 5.1 The normalized forward sensitivity index of R_0 that depends differentiable on a parameter p is defined as

$$\Pi_p^{\mathrm{R}_0} := \frac{\partial \mathrm{R}_0}{\partial p} \frac{p}{\mathrm{R}_0}. \tag{5.85}$$

For instance, the sensitivity index of R_{0l} with respect to all parameters is computed as

$$
\begin{aligned}
\Pi_{\beta_{0m}}^{\mathrm{R}_{0l}} &= \frac{\partial \mathrm{R}_{0l}}{\partial \beta_{0m}} \frac{\beta_{0m}}{\mathrm{R}_{0l}} = \frac{1}{2} > 0, \\
\Pi_{\beta_{0h}}^{\mathrm{R}_{0l}} &= \frac{\partial \mathrm{R}_{0l}}{\partial \beta_{0h}} \frac{\beta_{0h}}{\mathrm{R}_{0l}} = \frac{1}{2} > 0 \\
\Pi_{\Phi_0}^{\mathrm{R}_{0l}} &= \frac{\partial \mathrm{R}_{0l}}{\partial \Phi_0} \frac{\Phi_0}{\mathrm{R}_{0l}} = \frac{1}{2} > 0, \\
\Pi_{\Psi}^{\mathrm{R}_{0l}} &= \frac{\partial \mathrm{R}_{0l}}{\partial \Psi} \frac{\Psi}{\mathrm{R}_{0l}} = \frac{1}{2} > 0, \\
\Pi_{\alpha_h}^{\mathrm{R}_{0l}} &= \frac{\partial \mathrm{R}_{0l}}{\partial \alpha_h} \frac{\alpha_h}{\mathrm{R}_{0l}} = \frac{\mu_h}{2(\alpha_h + \mu_h)} > 0, \\
\Pi_{\alpha_m}^{\mathrm{R}_{0l}} &= \frac{\partial \mathrm{R}_{0l}}{\partial \alpha_m} \frac{\alpha_m}{\mathrm{R}_{0l}} = \frac{\mu_m}{2(\alpha_m + \mu_m)} > 0, \\
\Pi_{\mu_m}^{\mathrm{R}_{0l}} &= \frac{\partial \mathrm{R}_{0l}}{\partial \mu_m} \frac{\mu_m}{\mathrm{R}_{0l}} = -\frac{2\alpha_m + 3\mu_m}{2(\alpha_m + \mu_m)} < 0, \\
\Pi_{\delta}^{\mathrm{R}_{0l}} &= \frac{\partial \mathrm{R}_{0l}}{\partial \delta} \frac{\delta}{\mathrm{R}_{0l}} = -\frac{\delta}{2(\mu_h + \delta + \gamma_h)} < 0, \\
\Pi_{\gamma_h}^{\mathrm{R}_{0l}} &= \frac{\partial \mathrm{R}_{0l}}{\partial \gamma_h} \frac{\gamma_h}{\mathrm{R}_{0l}} = -\frac{\gamma_h}{2(\mu_h + \delta + \gamma_h)} < 0, \\
\Pi_{\mu_h}^{\mathrm{R}_{0l}} &= \frac{\partial \mathrm{R}_{0l}}{\partial \mu_h} \frac{\mu_h}{\mathrm{R}_{0l}} = -\frac{1}{2} - \frac{\mu_h(\alpha_h + 2\mu_h + \delta + \gamma_h)}{2(\mu_h + \delta + \gamma_h)(\alpha_h + \mu_h)} < 0.
\end{aligned}
\tag{5.86}
$$

As a result, after evaluated the parameters values, their sensitivity indices were written in Table 5.2 as given by

Table 5.2: Sensitivity indices of parameters with respect to R_{0l}

Parameters symbol	**Sensitivity index**
α_h	0.000345
α_m	0.238095
Ψ	0.5
Φ_0	0.5
β_{0h}	0.5
β_{0m}	0.5
μ_m	-0.013650
μ_h	-0.092541
δ	-0.475258
γ_h	-0.024462

Applying similar method, the sensitivity index of R_{0m} with respect to parameter Ψ is given by

$$\Pi_{\Psi}^{\mathrm{R}_{0m}} = \frac{\partial \mathrm{R}_{0m}}{\partial \Psi} \times \frac{\Psi}{\mathrm{R}_{0m}} = \frac{1}{2} > 0. \tag{5.87}$$

Similarly, with respect to others basic parameters, $\Pi_{\beta_{0h}}^{\mathrm{R}_{0m}}$, $\Pi_{\beta_{0m}}^{\mathrm{R}_{0m}}$, $\Pi_{\Phi_0}^{\mathrm{R}_{0m}}$, $\Pi_{\beta_{1m}}^{\mathrm{R}_{0m}}$, $\Pi_{\Phi_{1m}}^{\mathrm{R}_{0m}}$, $\Pi_{\beta_{1h}}^{\mathrm{R}_{0m}}$, $\Pi_{\mu_h}^{\mathrm{R}_{0m}}$, $\Pi_{\mu_m}^{\mathrm{R}_{0m}}$, $\Pi_{\delta}^{\mathrm{R}_{0m}}$, $\Pi_{\alpha_h}^{\mathrm{R}_{0m}}$, $\Pi_{\gamma_h}^{\mathrm{R}_{0m}}$, $\Pi_{\alpha_m}^{\mathrm{R}_{0m}}$are obtained and their sensitivity indices were written in Table 5.3 as given by

Table 5.3: Sensitivity indices of parameters with respect to R_{0m}

Parameters symbol	**Sensitivity index**
α_h	0.000345
α_m	0.238095
Ψ	0.5
Φ_0	0.072438
β_{0h}	0.291659
β_{0m}	0.285714
Φ_{1m}	0.069169
β_{1h}	0.208341
β_{1m}	0.214286
μ_m	-0.013650
μ_h	-0.092541
δ	-0.475258
γ_h	-0.024462

5.3.1 Interpretation of the sensitivity indices

In this study, using the given parameter values we have described the sensitivity indices of different parameters as given in Table 5.2 and Table 5.3 respectively. In Table 5.2 the sensitivity indices of the basic reproductive number R_{0l} with respect to ten basic parameters are described. This indicates that the parameters α_m, α_h, Ψ, Φ_0, β_{0h} and β_{0m} have positive sensitivity indices. The value of R_{0l} increases if their value increases while keeping other parameters constant. This shows that the total amount of secondary cases of infection increases in the population. The parameters $\alpha_m, \alpha_h, \delta$ and γ_h have negative indices. They decrease the value of R_{0l} if their value are increased while stay the other parameters constant. For examples, $\Pi_{\beta_{0m}}^{\mathrm{R}_{0l}}$ = 0.5, shows that decreasing (increasing) the mosquito contact rate by

10%, decreases (increases) the $\mathtt{R}_{0l}$ by 5%, in the same way, $\Pi_{\mu_m}^{\mathtt{R}_{0l}}$ = -0.013650, indicates that decreasing (increasing) the mosquitoes death rate by 10%, increases (decreases) $\mathtt{R}_{0l}$, by 0.13650%.

By the same approach in Table 5.3, we have illustrated the sensitivity indices of the basic reproductive number $\mathtt{R}_{0m}$ with respect to thirteen basic parameters. The output of the parameters α_m, α_h, Ψ, Φ_0, Φ_{1m}, β_{0h}, β_{1h}, β_{0m} and β_{1m} have positive sensitivity indices will have a high role on the spread of the disease in the population if their values are increased. The parameters $\alpha_m, \alpha_h, \delta$ and γ_h have negative sensitivity indices. Those parameters have an ability to minimize the existence of the malaria disease as their value increases with others keep constant. For instance, $\Pi_{\beta_{0m}}^{\mathtt{R}_{0m}}$ = 0.285714, implies that decreasing (increasing) the mosquito contact rate by 10% decreases (increases) the $\mathtt{R}_{0m}$ by 2.85714%. In contrast, $\Pi_{\mu_m}^{\mathtt{R}_{0m}}$ = -0.013650, shows that decreasing (increasing) the mosquito's death rate by 10% increases (decreases) the basic reproduction number $\mathtt{R}_{0m}$ by 0.13650%.

5.4 Parameter estimation

A standard dynamic model for system (5.1) is the ordinary differential equation given as

$$\frac{dx}{dt} = f(t,x,\upsilon), \qquad x(t_0) = x_0 \tag{5.88}$$

where t represents independent variables, x is the state vector of the system, υ is the vector of unknown parameters and x_0 is the initial condition of the system. The representation of the error is sum of squares error given as the form

$$\Theta(\upsilon) = \sum_{i=1} (x_i - x_i^*)^2 \tag{5.89}$$

where x_i is the real data and x_i^* is the solution of ordinary differential equation (5.88) for the given υ. Our main goal is to find the least square estimators υ to minimize the errors of equation (5.89) under the constraint equation (5.88) to obtain the best estimated parameters using least-square method. The procedure that used to estimate the basic parameters is summarized in Table 5.4 as follows.

Table 5.4: Procedures that used to estimate the model parameters

Input:	Setting the initial parameter values of the model (5.1).
Step 1.	The system (5.88) is solved with the initial parameters values using MATLAB **ode45**.
Step 2.	The model solution is compared with the real data and algorithm of an optimization (**fminsearch**) is applied to obtain the estimated parameter values to fit malaria data.
Step 3.	After obtained the update parameters' values, using this values the **Ode** (5.88) is solved and the real data is compared with the model solution.
Step 4.	The iteration between updating the values of parameter and solutions of the model (5.88) continues till the minimize error in equation (5.89) is obtained.

5.4.1 Data

Malaria is one of the most serious infectious disease in Ethiopia. East Shewa Zone is one of the malaria endemic area located in the Great Rift Valley in southeast Ethiopia. This study provided data collected from East Shewa Zone of Oromiya Region, Ethiopia. The data is a year reported of malaria infectious between 2010 and 2019 in East Shewa Zone.

Table 5.5: Total number of malaria infectious in East Shewa between 2010 and 2019.

Year	Malaria infectious	Year	Malaria infectious
2010	32102	2015	52266
2011	38650	2016	37452
2012	51663	2017	25280
2013	52659	2018	18325
2014	54676	2019	12094

Table 5.6: The estimated parameters used for the model (5.1)

Parameters	Parameters Description	Value	Reference
α_h	Exposed human progression rate	0.058	Olaniyi et al. (2018)
α_m	Exposed mosquito progression rate	0.055	Yiga et al. (2020)
μ_h	Natural death rate for human	0.015074	United Nation (2019)
δ	Induced death rate for human	0.068	Mojeeb and Adu (2017)
γ_h	Recover rate of infected human	0.0035	Mojeeb and Adu (2017)
Ψ	Recruitment rate of human	32112.93	Estimated
Φ_0	Recruitment rate of mosquito	1000	Ghosh et al. (2020)
μ_m	Mosquito natural death rate	0.05	Mojeeb and Adu (2017)
ω_h	Human loss of immunity rate	0.09	Abiodun et al. (2018)
β_{1m}	Incremental contact rate of mosquito	0.07	Assumed
β_{1h}	Incremental contact rate of human	0.05	Assumed
Φ_{1m}	Incremental birth rate of mosquito	0.09	Assumed
β_{0h}	Contact rate of human with mosquito	0.0482	Estimated
β_{0m}	Contact rate of mosquito with human	0.0932	Estimated
r	Growth rate of temperature	0.007	Assumed
$\mathtt{T}_0$	Minimum temperature	16^oC	Abiodun et al. (2016)
$\mathtt{T}_{\max}$	Maximum temperature	28^oC	Bhuju et al. (2018)

5.5 Numerical simulations

A numerical simulation is important to justify the theoretical result of the model. In this section, we use numerical tools to illustrate the theoretical results obtained in the mathematical model analysis sections for our model. Then we investigate the simulation of the model (5.1) with parameter values in Table 5.6 using the Runge Kutta fourth order to show the impact of the basic parameters in the transmission of the disease. Some of the parameters value are obtained from literature whereas few of the them were estimated as described Table 5.6. For instance, the parameter value of natural death rate $\mu_h = \frac{1}{66.34}$ per year where 66.34 years is the average life span in Ethiopia (United Nation and affairs population dynamics report, 2019). Based on the 2007 Census conducted by the Central Statistical Agency of Ethiopia (CSA), East Shewa zone has a total population of 2130372 (Zone, 2019). The recruitment rate Ψ is then estimated as $\Psi = \mu_h \mathtt{N}(0) = 32112.93$ per year. The initial infected humans are taken as the infected human ones the first year of 2010. Numerical

simulation is shown with the initial values $\mathrm{S}_h(0) = 50000, \mathrm{E}_h(0) = 34000, \mathrm{I}_h(0) = 32102$, $\mathrm{R}_h(0) = 1000, \mathrm{S}_m(0) = 52000, \mathrm{E}_m(0) = 35000, \mathrm{I}_m(0) = 2000$ and $\mathrm{T}(0) = 16.1^oC$ in malaria transmission model.

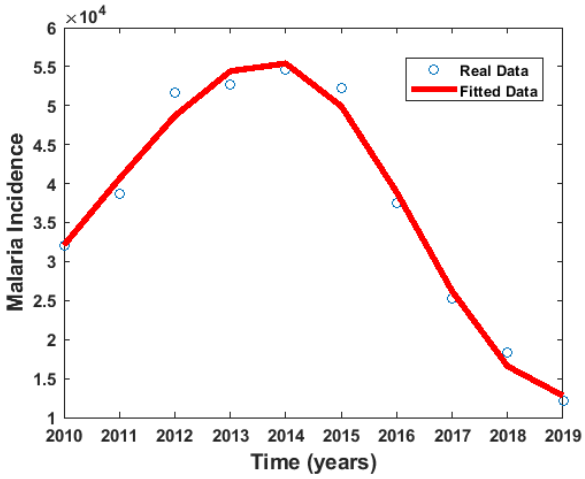

Figure 5.2: Fitting of the model equation (5.1) to the real data in Table 5.5

Figure 5.2 demonstrates the results of fitting the model (5.1) to the malaria data in Table 5.5. From Figure 5.2, the continuous line and points are represent, respectively, the model output of infected human and the malaria infected real data. Overall, the model fits well with the real data.

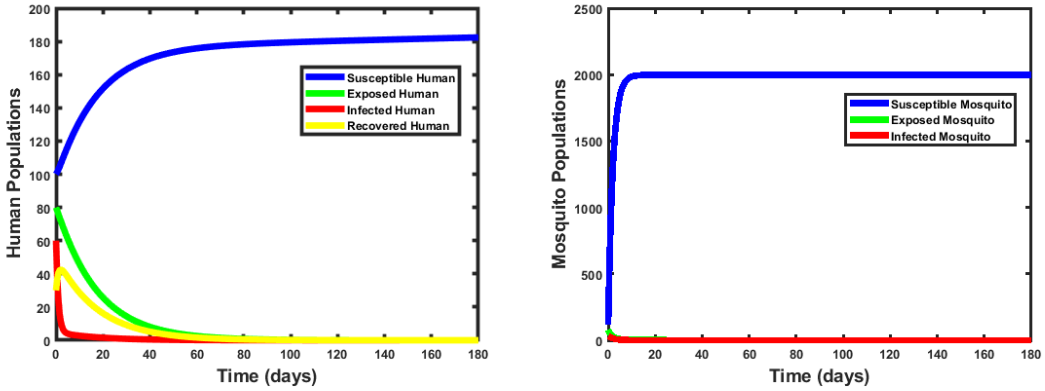

(**a**) (**b**)

Figure 5.3: Human population and mosquitoes population group when $\mathrm{R}_{0l} = 0.183$

In Figure 5.3**a**, the susceptible human population increases, recovered human population increase to a certain point then decrease while exposed and infected human population are decreased. From Figure 5.3**b**, the susceptible mosquito population increase while the population of exposed mosquito and infected mosquito are decreased due to natural death.

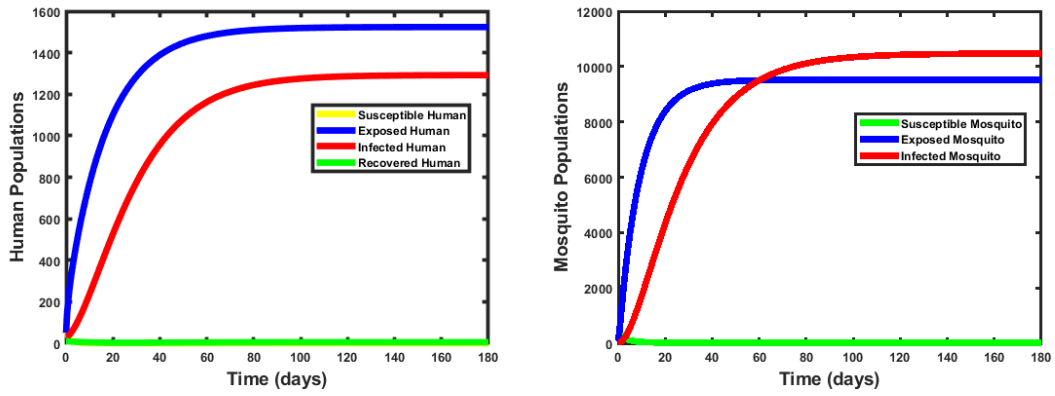

(**a**) (**b**)

Figure 5.4: Human population and mosquitoes population group when $\mathrm{R}_{0m} = 13.758$

From Figure 5.4**a**, the susceptible human population decelerates to zero due to the infected mosquito population. The exposed and infected human population increases to an endemic point due to malaria disease. Recovered human immediately decreases. It can be seen that in Figure 5.4**b**, susceptible mosquitoes are decreased because of natural death. The exposed mosquito and infected mosquito population are increases exponentially to a certain endemic point level.

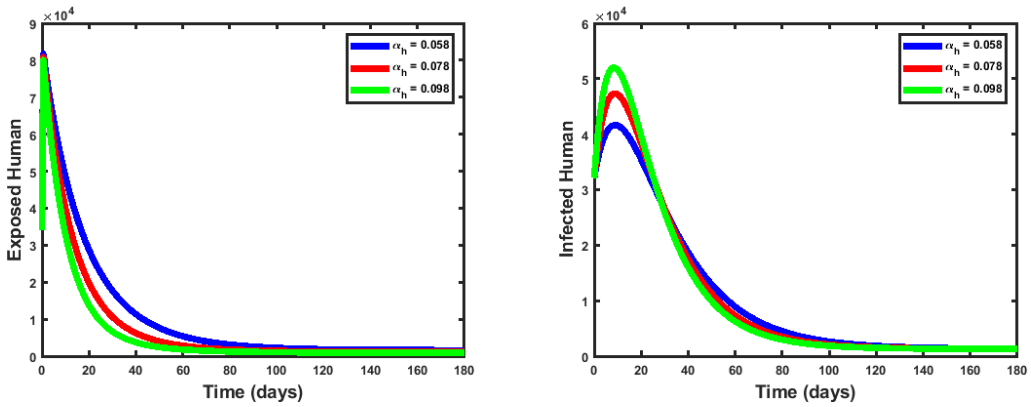

(**a**) (**b**)

Figure 5.5: Variation results of the exposed and infected humans for different value of α_h

Figure 5.5 describes the variation results of exposed and infected populations of human for different value of α_h. From the Figures 5.5**a** and 5.5**b**, we observed that an increase the rate of progression for exposed human increase the infection of secondary cases. Thus, increase the rate of progression for exposed human, decreases the exposed human population while increases the number of infected humans due to disease.

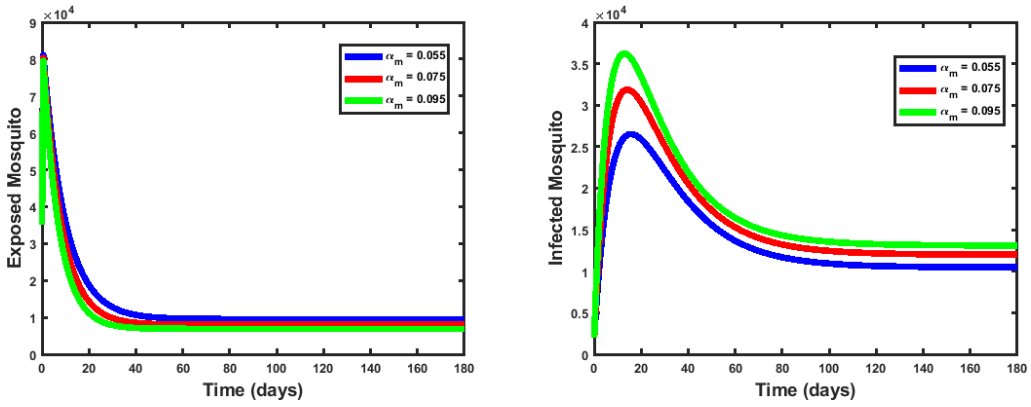

(**a**) (**b**)

Figure 5.6: Variation results of exposed and infected mosquitoes for a vary value of α_m

Figure 5.6 shows the variation results of exposed and infected population of mosquito for different value of α_m. From the Figures 5.6**a** and 5.6**b**, we can see that an increase the rate of progression exposed mosquito increases basic reproduction number. Hence, as increase the rate of progression exposed mosquito, the exposed mosquito population decreases while an increases the number of infected mosquito.

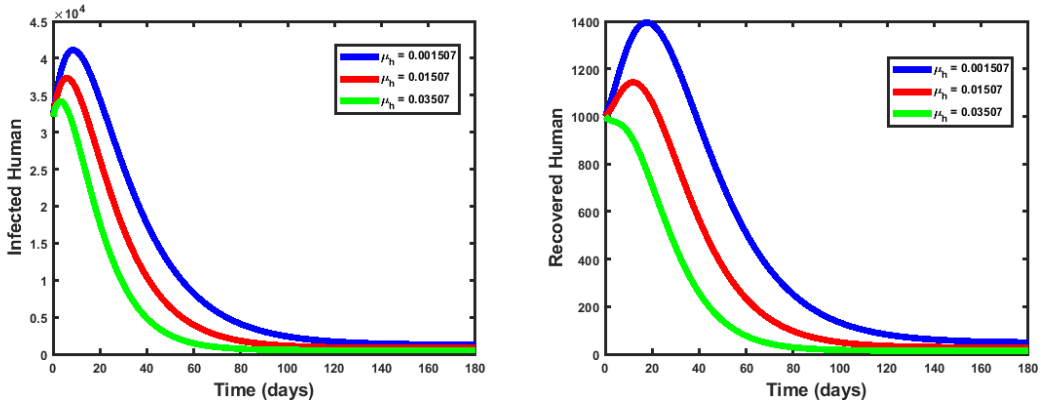

(**a**) (**b**)

Figure 5.7: Variation of the infected and recovered humans with different values of μ_h

Figure 5.7 describes variations results of infected population and recovered human population for a different value of natural death μ_h. From the Figures 5.7**a** and 5.7**b**, it can be observed that increase the death rate of the infected and recovered population of human which makes that the infected and recovered human population decreases in number.

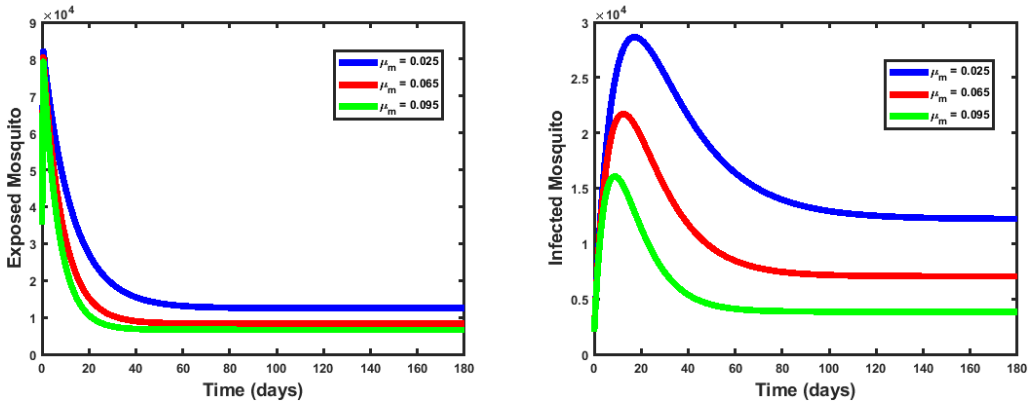

(**a**) (**b**)

Figure 5.8: Variation of the exposed and infected mosquitoes with different value of μ_m

Figure 5.8 shows variation results with exposed mosquito and infected population of mosquito for a different value of μ_m. In Figures 5.8**a** and 5.8**b**, we can see that the increase in the death rate of the mosquito population decreases the amount of secondary case infection. This implies that as death rate increases both susceptible and infected population of the mosquito leads to decreases in number.

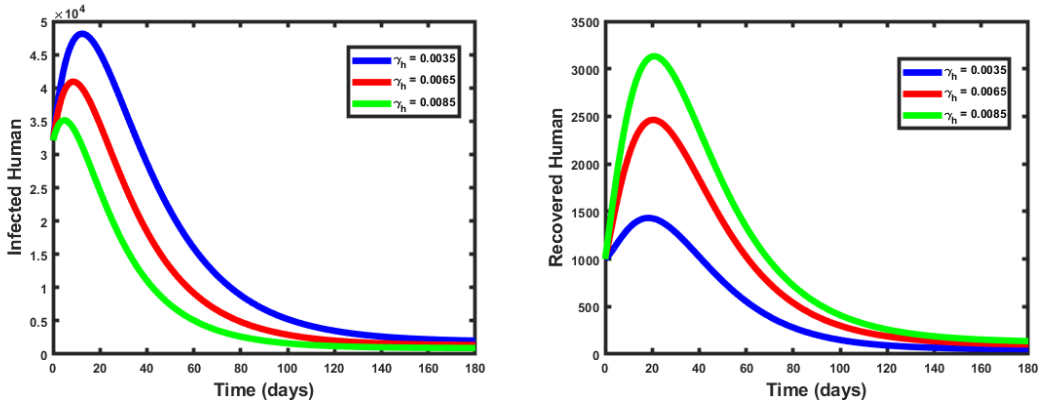

(**a**) (**b**)

Figure 5.9: Variation of infected and recovered humans with different value of γ_h

Figure 5.9 illustrates variation results of infected human and recovered human for a different value of γ_h. From the Figures 5.9**a** and 5.9**b**, we can see that an increase the recovery rate of the infected population due to the use of anti-malaria drugs increases the recovered human population. However, an increase the recovery rate of infected human, decreases number of the infected human.

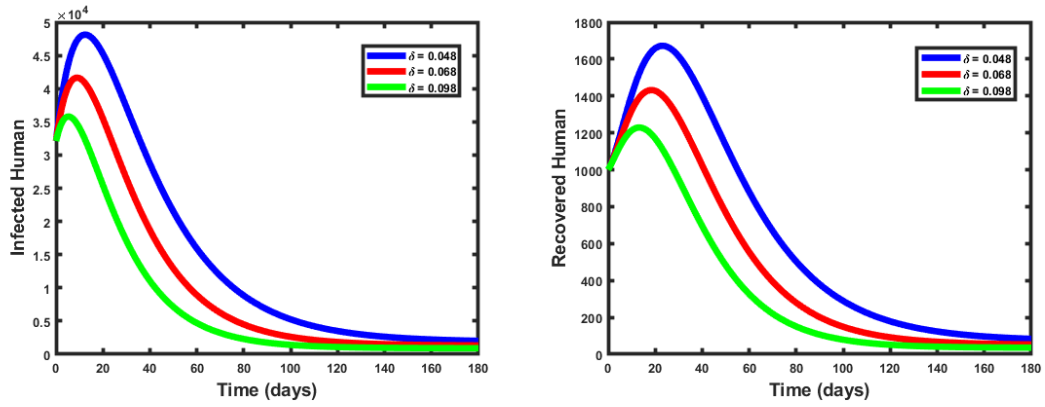

(**a**) (**b**)

Figure 5.10: Variation of infected human and recovered human with varies values of δ

Figure 5.10 describes the variation results of infected and recovered population of human for a different values of δ. From Figure 5.10**a**, we can see that increasing the death rate of the human population due to disease, decrease the number of the infected human population. Figure 5.10**b** shows that if death rate of the human increases then the number of recovered human population decreases.

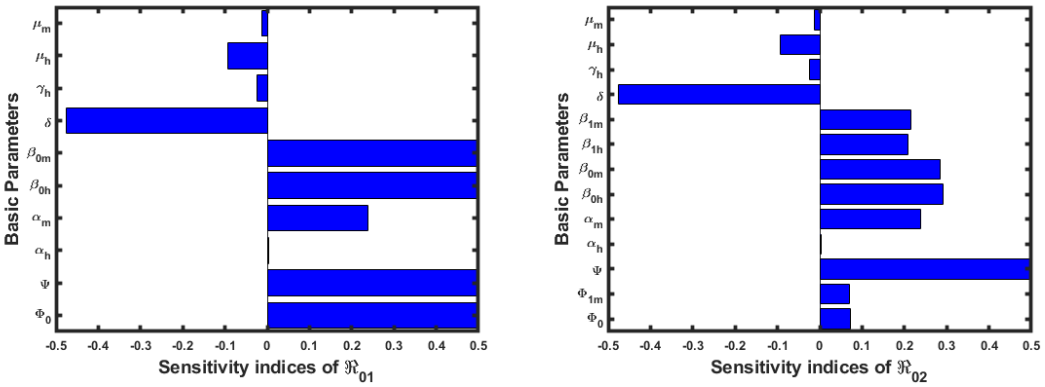

(**a**) (**b**)

Figure 5.11: Sensitivity indices of basic reproduction number R_{0l} and R_{0m} respectively

Figure 5.11 shows numerical simulation of the sensitivity analysis of model parameters. Note that the parameters that have positive (negative) sensitivity indices respectively, were increase the basic reproduction number R_0 if their value increases (decreases) respectively, while the others parameters stay constant.

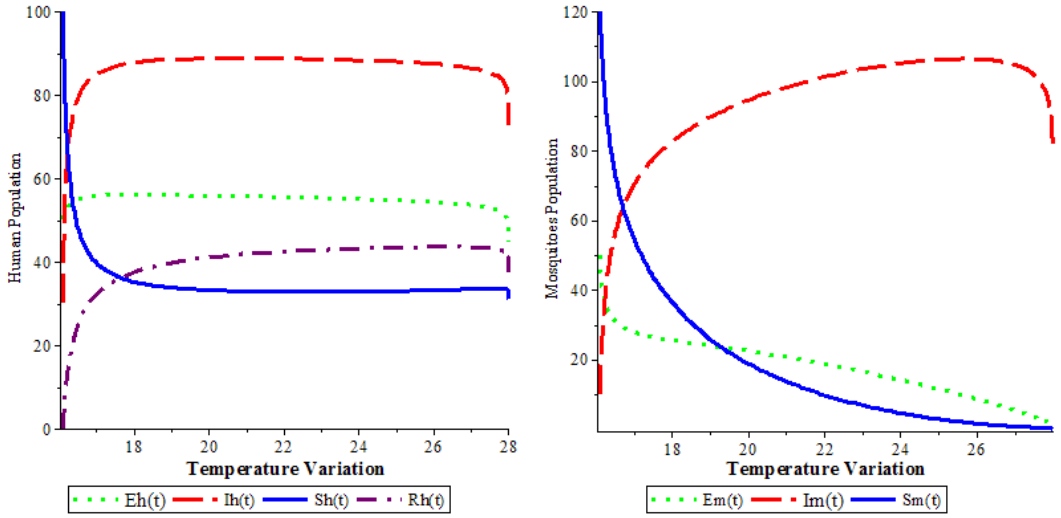

(**a**) (**b**)

Figure 5.12: Human and mosquitoes populations with rise in temperature respectively

Figure 5.12 indicates the human population and mosquitoes population group with rise in temperature. From the Figure 5.12**a**, we can see that all the humans populations are decreasing at maximum temperature ($\mathrm{T}_{\max} = 28^{o}C$). Figure 5.12**b** shows that all mosquitoes populations are decreasing at maximum temperature ($\mathrm{T}_{\max} = 28^{o}C$).

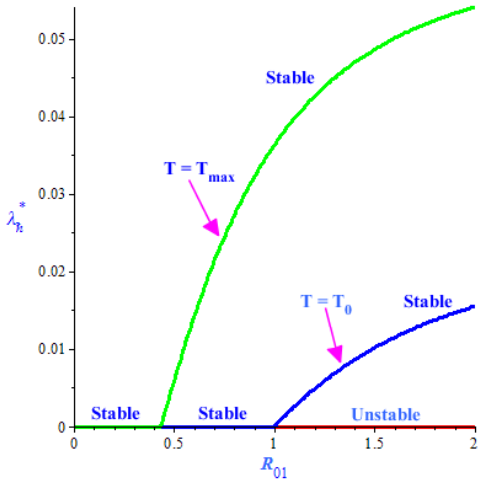

Figure 5.13: Bifurcation diagram of the model when $\mathrm{T} = \mathrm{T}_0$ and $\mathrm{T} = \mathrm{T}_{\max}$

Figure 5.13 illustrates the diagram of bifurcation for the case when $\mathrm{T} = \mathrm{T}_0$ and $\mathrm{T} = \mathrm{T}_{\max}$ for malaria transmission model. Basically, $\mathrm{R}_{0l} < 1$ does not automatically implies $\mathrm{R}_{0m} < 1$, since the value of R_{0m} may be greater than 1, which implies that while R_{02} present backward bifurcation while R_{0l} only present forward bifurcation.

CHAPTER 6
OPTIMAL CONTROL AND COST EFFECTIVENESS ANALYSIS OF SIRS MALARIA DYNAMICS MODEL WITH TEMPERATURE VARIABILITY

Optimal control theory is used to make a decision that involves a mathematical model on the biological situations (Lenhart and Workman, 2007). In this chapter, we want to implement the optimal control strategy to prevent malaria transmission. Thus, we proposed a non-linear deterministic optimal control model for malaria transmission described by systems of ordinary differential equation and using optimal control theory to determine an optimal control and least cost strategy with limited resources.

6.1 Optimal control problem formulation

In this section, we extended the malaria model in section (4.1) to optimal control model with introduced time dependent controls. The optimal control strategies on the malaria model (4.1) was formulated using the controls; the force of infection in the human and mosquitoes populations in the model (4.1) is decreased by a factor $(1-u_1(t))$ where $u_1(t)$ denotes treated bed net that used to minimize the contacts between susceptible human and susceptible mosquitoes populations with infected mosquitos and infected human respectively. The next control function $u_2(t)$ represents the control effort on the treatment of infected human with anti-malarial drugs. The third control function $u_3(t)$ is indoor residual spraying used to increase the mosquito death rate that reduce the number of mosquitoes. The control functions are performed on the time interval $[0,t_f]$. After incorporating the controls into the malaria

transmission model (4.1), the state equations becomes

$$\begin{cases} \frac{dS_h}{dt} &= \Psi - (1-u_1)\beta_h(\mathtt{T})S_h I_m - \mu_h S_h + \omega_h \mathtt{R}_h, \\ \frac{dI_h}{dt} &= (1-u_1)\beta_h(\mathtt{T})S_h I_m - (\mu_h + \delta + \gamma_h + u_2)I_h, \\ \frac{dR_h}{dt} &= (\gamma_h + u_2)I_h - (\mu_h + \omega_h)\mathtt{R}_h, \\ \frac{dS_m}{dt} &= \Phi(\mathtt{T}) - (1-u_1)\beta_m(\mathtt{T})S_m I_h - (\mu_m + u_3)S_m, \\ \frac{dI_m}{dt} &= (1-u_1)\beta_m(\mathtt{T})S_m I_h - (\mu_m + u_3)I_m, \\ \frac{d\mathtt{T}}{dt} &= \mathrm{r}(1 - \frac{\mathtt{T}}{\mathtt{T}_{\max}})(\mathtt{T} - \mathtt{T}_0), \end{cases} \tag{6.1}$$

where,
$\beta_h(\mathtt{T}) = \beta_{0h} + \beta_{1h}\left(\frac{\mathtt{T}-\mathtt{T}_0}{\mathtt{T}_{\max}}\right)$, $\beta_m(\mathtt{T}) = \beta_{0m} + \beta_{1m}\left(\frac{\mathtt{T}-\mathtt{T}_0}{\mathtt{T}_{\max}}\right)$ and $\Phi(\mathtt{T}) = \Phi_0 + \Phi_{1m}\left(\frac{\mathtt{T}-\mathtt{T}_0}{\mathtt{T}_{\max}}\right)$.
The main objective is to reduce the total amount of infected human $\mathtt{I}_h(t)$, infected mosquito $\mathtt{I}_m(t)$ and costs of controls $u_i(t)$ associated with treated bed nets to protect the mosquito, treatment of infected human with anti-malaria drugs to reduces the infected human and indoor residual spraying to kill the mosquitoes. The objective functional we formulated for model (6.1) is given by

$$\mathtt{J}(u_1,u_2,u_3) = \underbrace{min}_{\mathtt{u}_1,\mathtt{u}_2,\mathtt{u}_3} \int_0^{t_f} \left(\mathtt{A}_1 I_h + \mathtt{A}_2 I_m + \frac{1}{2}(\mathtt{B}_1 u_1^2 + \mathtt{B}_2 u_2^2 + \mathtt{B}_3 u_3^2)\right) dt \tag{6.2}$$

where the quantity t_f denoted the final time, quantities $\mathtt{A}_1$ and $\mathtt{A}_2$ are weights constants for the infected human and infected mosquito respectively, while $\mathtt{B}_1, \mathtt{B}_2$ and $\mathtt{B}_3$ are weight constants for each controls respectively. The expression $\frac{1}{2}\mathtt{B}_i u_i^2$ stands for cost functions that corresponding to the controls $u_i(t)$ is quadratic in similar within the literature (Abioye et al., 2020; Bakare and Hoskova-Mayerova, 2021; Ghosh et al., 2020; Handari et al., 2019; Wang et al., 2021). The basic goal is to compute a triple optimal controls u_1^*, u_2^* and u_3^* such that

$$\mathtt{J}(u_1^*,u_2^*,u_3^*) = \min\{\mathtt{J}(u_1,u_2,u_3) : u_1,u_2,u_3 \in \vartheta\} \tag{6.3}$$

where $\vartheta = (u_1,u_2,u_3) : u_i(t)$ such that u_1,u_2 and u_3 are Lebesgue measurable on $t \in [0,t_f]$ with $0 \le u_i(t) \le 1$ for $i = 1,2,3$ is the control set. Next the basic setup of the optimal control problem starts by checking the existence of the optimal control triples and characterization of the optimal pair.

6.2 Existence of the optimal controls

In this section, we prove the existence of an optimal control triples that optimize the objective functional given in (6.2). Thus, we have the following result.

Theorem 6.1: Given a cost functional $\mathtt{J}(u_1,u_2,u_3)$ subject to control induced state system (6.1), then there exists an optimal control triples $u^* = (u_1^*,u_2^*,u_3^*)$ and the corresponding to the optimal solution $(\mathtt{S}_h^*,\mathtt{I}_h^*,\mathtt{R}_h^*,\mathtt{S}_m^*,\mathtt{I}_m^*,\mathtt{T}^*)$ such that

$$\mathtt{J}(u_1^*,u_2^*,u_3^*) = \min\{\mathtt{J}(u_1,u_2,u_3) : u_1,u_2,u_3 \in \vartheta\}. \tag{6.4}$$

Proof: To prove the existence of optimal controls triples we need to verify the following five conditions based on the result given in (Fleming and Rishel, 1975).

1. The set of controls and corresponding state variables is non-empty.
2. The measurable control set is convex and closed.
3. The right hand side of the state system is bounded by a linearized function in the state and control variables.
4. The integrand of the cost functional is convex on ϑ.
5. There exist constants $d_1,d_2 > 0$ and $d_3 > 1$ such that the integrand of the objective functional satisfies $g(x,u) \geq d_1(|u_1|^2+|u_2|^2+|u_3|^2)^{\frac{d_3}{2}} - d_2$.

1. Note that we have shown the boundedness of the malaria model in section (4.1). It follows that the solutions of the state system are continuous and bounded for each admissible control functions in ϑ. Moreover, the right hand side functions of the model equation (6.1) satisfies the Lipschitz condition with respect to state variables. Thus, the solutions of system (6.1) exist (Lukes, 1982). Thus, the set ϑ is non-empty.

2. Given that the control set $\vartheta = [0,1]^3$, then ϑ is closed by definition. Moreover, we consider

$$\vartheta = \{u \in \mathbb{R}^3 : ||u|| \leq 1\}.$$

Let $u_1,u_2 \in \vartheta$ such that $||u_1|| \leq 1$ and $||u_2|| \leq 1$. It follows, by the definition of a convex set (Beck, 2014), that for any $\lambda \in [0,1]$,

$$||\lambda u_1 + (1-\lambda)u_2|| \leq \lambda||u_1|| + (1-\lambda)||u_2|| \leq 1.$$

Thus, $\lambda u_1 + (1-\lambda)u_2 \in \vartheta$ implies that ϑ is a convex set.

3. In order to verify this condition, we used the approach adopted by (Berhe, 2020; Laarabi et al., 2012). Let the right hand side of the system equation (6.1) and it's

solution be represented by h and θ respectively. It follows that

$$|h(t,\theta_1,u)-h(t,\theta_2,u)| = \left| \begin{pmatrix} -(1-u_1)\lambda_h(S_{h1}-S_{h2})-\mu_h(S_{h1}-S_{h2})+\omega_h(\mathrm{R}_{h1}-\mathrm{R}_{h2}) \\ (1-u_1)\lambda_h(S_{h1}-S_{h2})-(\mu_h+\delta+\gamma_h+u_2)(I_{h1}-I_{h2}) \\ (\gamma_h+u_2)(I_{h1}-I_{h2})-(\mu_h+\omega_h)(\mathrm{R}_{h1}-\mathrm{R}_{h2}) \\ -(1-u_1)\lambda_m(S_{m1}-S_{m2})-(\mu_m+u_3)(S_{m1}-S_{m2}) \\ (1-u_1)\lambda_m(S_{m1}-S_{m2})-(\mu_m+u_3)(I_{m1}-I_{m2}) \end{pmatrix} \right|$$

$$\begin{aligned} |h(t,\theta_1,u)-h(t,\theta_2,u)| \leq\ & (2(1-u_1)\lambda_h+\mu_h)|S_{h1}-S_{h2}|+(\mu_h+\delta+2\gamma_h+2u_2)|I_{h1}-I_{h2}| \\ & +(2\omega_h+\mu_h)|\mathrm{R}_{h1}-\mathrm{R}_{h2}|+(2(1-u_1)\lambda_m+\mu_m+u_3)|S_{m1}-S_{m2}| \\ & +(\mu_m+u_3)|I_{m1}-I_{m2}| \\ \leq\ & \mathrm{L}_1|S_{h1}-S_{h2}|+\mathrm{L}_2|I_{h1}-I_{h2}|+\mathrm{L}_3|\mathrm{R}_{h1}-\mathrm{R}_{h2}|+\mathrm{L}_4|S_{m1}-S_{m2}| \\ & +\mathrm{L}_5|I_{m1}-I_{m2}| \\ \leq\ & \mathrm{M}|\theta_1-\theta_2| \end{aligned}$$

where $\mathrm{L}_1 = 2(1-u_1)\lambda_h, \mathrm{L}_2 = (\mu_h+\delta+2\gamma_h+2u_2), \mathrm{L}_3 = (2\omega_h+\mu_h)$,
$\mathrm{L}_4 = (2(1-u_1)\lambda_m)+\mu_m+u_3, \mathrm{L}_5 = (\mu_m+u_3)$ and $\mathrm{M} = \max\{\mathrm{L}_1,\mathrm{L}_2,\mathrm{L}_3,\mathrm{L}_4,\mathrm{L}_5\}$.
Thus, the state system (6.1) is clearly uniformly Lipschitz continuous and with this condition (3) is satisfied.

4. Let the integrand of the cost functional is given by

$$g(x,u) = \mathrm{A}_1 I_h + \mathrm{A}_2 I_m + \frac{1}{2}(\mathrm{B}_1 u_1^2 + \mathrm{B}_2 u_2^2 + \mathrm{B}_3 u_3^2).$$

Let $w = (w_1,w_2,w_3) \in \vartheta, z = (z_1,z_2,z_3) \in \vartheta$ and $\tau \in [0,1]$. Then we have

$$\begin{aligned} & g(x,(1-\tau)w+\tau z)-[(1-\tau)g(x,w)+\tau g(x,z)] \\ & = \frac{\mathrm{B}_1}{2}[(1-\tau)^2 w_1^2+2\tau(1-\tau)w_1z_1+\tau^2 z_1^2]+\frac{\mathrm{B}_2}{2}[(1-\tau)^2 w_2^2+2\tau(1-\tau)w_2z_2+\tau^2 z_2^2] \\ & + \frac{\mathrm{B}_3}{2}[(1-\tau)^2 w_2^3+2\tau(1-\tau)w_3z_3+\tau^2 z_3^2]-[(1-\tau)(\frac{\mathrm{B}_1}{2}w_1^2+\frac{\mathrm{B}_2}{2}w_2^2+\frac{\mathrm{B}_3}{2}w_3^2)] \\ & -[\tau(\frac{\mathrm{B}_1}{2}z_1^2+\frac{\mathrm{B}_2}{2}z_2^2+\frac{\mathrm{B}_3}{2}z_3^2)] \\ & = \underbrace{(\tau^2-\tau)}_{\leq 0}\left(\frac{\mathrm{B}_1}{2}(w_1-z_1)^2+\frac{\mathrm{B}_2}{2}(w_2-z_2)^2+\frac{\mathrm{B}_3}{2}(w_1-z_1)^2\right) \leq 0. \end{aligned} \tag{6.5}$$

Hence,

$$g(x,(1-\tau)w+\tau z) \leq [(1-\tau)g(x,w)+\tau g(x,z)]$$

which proves that $g(x,u)$ is a convex function (Beck, 2014).

5. Finally, we get

$$\begin{aligned} g(x,u) &= \mathtt{A}_1 I_h + \mathtt{A}_2 I_m + \frac{1}{2}(\mathtt{B}_1 u_1^2 + \mathtt{B}_2 u_2^2 + \mathtt{B}_3 u_3^2), \\ &\geq \frac{1}{2}(\mathtt{B}_1 u_1^2 + \mathtt{B}_2 u_2^2 + \mathtt{B}_3 u_3^2), \\ &\geq \frac{d_1}{2}(u_1^2 + u_2^2 + u_3^2) - d_2, \end{aligned}$$

where $d_1 = \min\{\mathtt{B}_1, \mathtt{B}_2, \mathtt{B}_3\}$, $d_2 > 0$ and $d_3 = 2$. Hence, there exists an optimal control triples that minimizes the objective functional.

6.3 Hamiltonian system

In this section, we use the Pontryagin's minimum principle (Pontryagin, 2018) to obtain the necessary conditions for the optimal control model (6.1). The defined Hamiltonian function of the optimal control problem that consists of equations (6.1) and (6.2) is represented as

$$\mathscr{H} = [\mathtt{A}_1 I_h + \mathtt{A}_2 I_m + \frac{1}{2}\sum_{i=1}^{3} \mathtt{B}_i u_i^2] + \lambda_1 \frac{dS_h}{dt} + \lambda_2 \frac{dI_h}{dt} + \lambda_3 \frac{d\mathtt{R}_h}{dt} + \lambda_4 \frac{dS_m}{dt} + \lambda_5 \frac{dI_m}{dt} + \lambda_6 \frac{d\mathtt{T}}{dt}. \quad (6.6)$$

It follows that the system of equations (6.1) and (6.2) are substituted into a minimize Hamiltonian function with respect to u_1, u_2, u_3 is given by

$$\begin{aligned} \mathscr{H} =& [A_1 I_h + A_2 I_m + \frac{1}{2}(\mathtt{B}_1 u_1^2 + \mathtt{B}_2 u_2^2 + \mathtt{B}_3 u_3^2)] \\ &+ \lambda_1[\Psi - (1-u_1)\beta_h(\mathtt{T}) S_h I_m - \mu_h S_h + \omega_h \mathtt{R}_h] \\ &+ \lambda_2[(1-u_1)\beta_h(\mathtt{T}) S_h I_m - (\mu_h + \delta + \gamma_h + u_2) I_h] \\ &+ \lambda_3[(\gamma_h + u_2) I_h - (\mu_h + \omega_h)\mathtt{R}_h] \\ &+ \lambda_4[\Phi(\mathtt{T}) - (1-u_1)\beta_m(\mathtt{T}) S_m I_h - (\mu_m + u_3) S_m] \\ &+ \lambda_5[(1-u_1)\beta_m(\mathtt{T}) S_m I_h - (\mu_m + u_3) I_m] \\ &+ \lambda_6[r(1 - \frac{\mathtt{T}}{\mathtt{T}_{\max}})(\mathtt{T} - \mathtt{T}_0)], \end{aligned} \quad (6.7)$$

where $\lambda_1, \lambda_2, \lambda_3, \lambda_4, \lambda_5$ and λ_6 are adjoint variables. Next to obtain the adjoint variables by applying Pontryagin's minimum principle (Pontryagin, 2018), with existence result of (Fleming and Rishel, 1975), the following theorem is stated.

Theorem 6.2. For a given optimal control triples u_1^*, u_2^*, u_3^* and solutions $\mathtt{S}_h^*, \mathtt{I}_h^*, \mathtt{R}_h^*, \mathtt{S}_m^*, \mathtt{I}_m^*$, $\mathtt{T}^*$ of the corresponding state system that minimize $\mathtt{J}(u_1, u_2, u_3)$ over ϑ subject to the equation (6.1), then there exist co-state variables $\lambda_1, \lambda_2, \lambda_3, \lambda_4, \lambda_5$ and λ_6 satisfying the adjoint

system

$$\begin{cases} \frac{d\lambda_1}{dt} &= -((1-u_1)\beta_h(\mathtt{T})I_m(\lambda_2-\lambda_1))+\mu_h\lambda_1, \\ \frac{d\lambda_2}{dt} &= -((1-u_1)\beta_m(\mathtt{T})S_m(\lambda_5-\lambda_4))+\lambda_2(\mu_h+\delta+\gamma_h+u_2)-\lambda_3(u_2+\gamma_h)-\mathtt{A}_1, \\ \frac{d\lambda_3}{dt} &= -\omega_h\lambda_1+\lambda_3(\mu_h+\omega_h), \\ \frac{d\lambda_4}{dt} &= -((1-u_1)\beta_m(\mathtt{T})I_h(\lambda_5-\lambda_4))+\lambda_4(u_3+\mu_m), \\ \frac{d\lambda_5}{dt} &= -((1-u_1)\beta_h(\mathtt{T})S_h(\lambda_2-\lambda_1))+\lambda_5(u_3+\mu_m)-\mathtt{A}_2, \\ \frac{d\lambda_6}{dt} &= -r\lambda_6-r\lambda_6(\frac{\mathtt{T}_0}{\mathtt{T}_{\max}}-\frac{2\mathtt{T}}{\mathtt{T}_{\max}}), \end{cases} \tag{6.8}$$

with transversality conditions

$$\lambda_1(t_f)=\lambda_2(t_f)=\lambda_3(t_f)=\lambda_4(t_f)=\lambda_5(t_f)=\lambda_6(t_f)=0. \tag{6.9}$$

Further more, the optimal controls u_1^*, u_2^* and u_3^* are represented by

$$\begin{aligned} u_1^* &= \max\left\{0, \min\left\{1, \frac{(\lambda_2-\lambda_1)\beta_h(\mathtt{T})S_h^*I_m^*+(\lambda_5-\lambda_4)\beta_m(\mathtt{T})S_m^*I_h^*}{\mathtt{B}_1}\right\}\right\}, \\ u_2^* &= \max\left\{0, \min\left\{1, \frac{(\lambda_2-\lambda_3)I_h^*}{\mathtt{B}_2}\right\}\right\}, \\ u_3^* &= \max\left\{0, \min\left\{1, \frac{\lambda_4S_m^*+\lambda_5I_m^*}{\mathtt{B}_3}\right\}\right\}. \end{aligned} \tag{6.10}$$

Proof. To obtain the form of the adjoint equations we compute the derivative of the Hamiltonian function (6.7) with respect to $\mathtt{S}_h, \mathtt{I}_h, \mathtt{R}_h, \mathtt{S}_m, \mathtt{I}_m$ and $\mathtt{T}$ respectively. Then the adjoint equations obtained are given by

$$\begin{cases} \frac{d\lambda_1}{dt} &= -\frac{\partial\mathscr{H}}{\partial S_h} = -((1-u_1)\beta_h(\mathtt{T})I_m(\lambda_2-\lambda_1))+\mu_h\lambda_1, \\ \frac{d\lambda_2}{dt} &= -\frac{\partial\mathscr{H}}{\partial I_h} = -((1-u_1)\beta_m(\mathtt{T})S_m(\lambda_5-\lambda_4))+\lambda_2(\mu_h+\delta+\gamma_h+u_2)-\lambda_3(u_2+\gamma_h)-\mathtt{A}_1, \\ \frac{d\lambda_3}{dt} &= -\frac{\partial\mathscr{H}}{\partial R_h} = -\omega_h\lambda_1+\lambda_3(\mu_h+\omega_h), \\ \frac{d\lambda_4}{dt} &= -\frac{\partial\mathscr{H}}{\partial S_m} = -((1-u_1)\beta_m(\mathtt{T})I_h(\lambda_5-\lambda_4))+\lambda_4(u_3+\mu_m), \\ \frac{d\lambda_5}{dt} &= -\frac{\partial\mathscr{H}}{\partial I_m} = -((1-u_1)\beta_h(\mathtt{T})S_h(\lambda_2-\lambda_1))+\lambda_5(u_3+\mu_m)-\mathtt{A}_2, \\ \frac{d\lambda_6}{dt} &= -\frac{\partial\mathscr{H}}{\partial \mathtt{T}} = -r\lambda_6-r\lambda_6(\frac{\mathtt{T}_0}{\mathtt{T}_{\max}}-\frac{2\mathtt{T}}{\mathtt{T}_{\max}}), \end{cases} \tag{6.11}$$

with transversality conditions

$$\lambda_1(t_f)=\lambda_2(t_f)=\lambda_3(t_f)=\lambda_4(t_f)=\lambda_5(t_f)=\lambda_6(t_f)=0. \tag{6.12}$$

To obtain the controls value, we compute the partial derivative of Hamiltonian given by

$$\frac{\partial\mathscr{H}}{\partial u_i}=0, \quad \texttt{for } i=1,2,3. \tag{6.13}$$

Obviously, after derivation of Hamiltonian $(\mathscr{H})$ with respect to each control the result becomes

$$\begin{aligned}
0 = \frac{\partial \mathscr{H}}{\partial u_1} &= (\lambda_1 - \lambda_2)\beta_h(\mathtt{T})S_h^* I_m^* + (\lambda_4 - \lambda_5)\beta_m(\mathtt{T})S_m^* I_h^* + u_1 \mathtt{B}_1, \\
0 = \frac{\partial \mathscr{H}}{\partial u_2} &= \lambda_3 I_h^* - \lambda_2 I_h^* + u_2 \mathtt{B}_2, \\
0 = \frac{\partial \mathscr{H}}{\partial u_3} &= -(\lambda_4 S_m^* + \lambda_5 I_m^*) + u_3 \mathtt{B}_3.
\end{aligned} \tag{6.14}$$

Moreover, solving for control variables from the equation (6.14), we obtain

$$\begin{cases}
u_1^* &= \frac{(\lambda_2 - \lambda_1)\beta_h(\mathtt{T})S_h^* I_m^* + (\lambda_5 - \lambda_4)\beta_m(\mathtt{T})S_m^* I_h^*}{\mathtt{B}_1}, \\
u_2^* &= \frac{(\lambda_2 - \lambda_3)I_h^*}{\mathtt{B}_2}, \\
u_3^* &= \frac{\lambda_4 S_m^* + \lambda_5 I_m^*}{\mathtt{B}_3}.
\end{cases} \tag{6.15}$$

By standard control arguments involving bounds on the control, it becomes

$$u_i^* = \begin{cases}
0 & \text{if} \quad \vartheta_i^* \leq 0 \\
\vartheta_i^* & \text{if} \quad 0 < \vartheta_i^* < 1 \\
1 & \text{if} \quad \vartheta_i^* \geq 1
\end{cases} \tag{6.16}$$

and the compact notation of (6.16) is written as the compact form of the controls

$$\begin{aligned}
u_1^* &= \max\left\{0, \min\left\{1, \underbrace{\frac{(\lambda_2 - \lambda_1)\beta_h(\mathtt{T})S_h^* I_m^* + (\lambda_5 - \lambda_4)\beta_m(\mathtt{T})S_m^* I_h^*}{\mathtt{B}_1}}_{=\vartheta_1^*}\right\}\right\}, \\
u_2^* &= \max\left\{0, \min\left\{1, \underbrace{\frac{(\lambda_2 - \lambda_3)I_h^*}{\mathtt{B}_2}}_{=\vartheta_2^*}\right\}\right\}, \\
u_3^* &= \max\left\{0, \min\left\{1, \underbrace{\frac{\lambda_4 S_m^* + \lambda_5 I_m^*}{\mathtt{B}_3}}_{=\vartheta_3^*}\right\}\right\}.
\end{aligned} \tag{6.17}$$

6.4 Optimality system

The optimality system is obtained from the optimal control system (6.1) and the adjoint system (6.8) by incorporating the optimality condition on control set (6.10), the initial value

of (6.1) and transversal condition of (6.9). And after incorporated, the optimality system is given by

$$
\begin{cases}
\frac{dS_h}{dt} = \Psi - (1-u_1^*)\beta_h(\mathtt{T})S_hI_m - \mu_hS_h + \omega_h\mathtt{R}_h, \\
\frac{dI_h}{dt} = (1-u_1^*)\beta_h(\mathtt{T})S_hI_m - (\mu_h+\delta+\gamma_h+u_2^*)I_h, \\
\frac{dR_h}{dt} = (\gamma_h+u_2^*)I_h - (\mu_h+\omega_h)\mathtt{R}_h, \\
\frac{dS_m}{dt} = \Phi(\mathtt{T}) - (1-u_1^*)\beta_m(\mathtt{T})S_mI_h - (\mu_m+u_3^*)S_m, \\
\frac{dI_m}{dt} = (1-u_1^*)\beta_m(\mathtt{T})S_mI_h - (\mu_m+u_3^*)I_m, \\
\frac{d\mathtt{T}}{dt} = \mathrm{r}(1-\frac{\mathtt{T}}{\mathtt{T}_{\max}})(\mathtt{T}-\mathtt{T}_0), \\
\frac{d\lambda_1}{dt} = -((1-u_1^*)\beta_h(\mathtt{T})I_m(\lambda_2-\lambda_1)) + \mu_h\lambda_1, \\
\frac{d\lambda_2}{dt} = -((1-u_1^*)\beta_m(\mathtt{T})S_m(\lambda_5-\lambda_4)) + \lambda_2(\mu_h+\delta+\gamma_h+u_2^*) - \lambda_3(u_2^*+\gamma_h) - \mathtt{A}_1, \\
\frac{d\lambda_3}{dt} = -\omega_h\lambda_1 + \lambda_3(\mu_h+\omega_h), \\
\frac{d\lambda_4}{dt} = -((1-u_1^*)\beta_m(\mathtt{T})I_h(\lambda_5-\lambda_4)) + \lambda_4(u_3^*+\mu_m), \\
\frac{d\lambda_5}{dt} = -((1-u_1^*)\beta_h(\mathtt{T})S_h(\lambda_2-\lambda_1)) + \lambda_5(u_3^*+\mu_m) - \mathtt{A}_2, \\
\frac{d\lambda_6}{dt} = -r\lambda_6 - r\lambda_6(\frac{\mathtt{T}_0}{\mathtt{T}_{\max}} - \frac{2\mathtt{T}}{\mathtt{T}_{\max}}), \\
u_1^* = \max\left\{0, \min\left\{1, \frac{(\lambda_2-\lambda_1)\beta_h(\mathtt{T})S_h^*I_m^* + (\lambda_5-\lambda_4)\beta_m(\mathtt{T})S_m^*I_h^*}{\mathtt{B}_1}\right\}\right\}, \\
u_2^* = \max\left\{0, \min\left\{1, \frac{(\lambda_2-\lambda_3)I_h^*}{\mathtt{B}_2}\right\}\right\}, \\
u_3^* = \max\left\{0, \min\left\{1, \frac{\lambda_4S_m^*+\lambda_5I_m^*}{\mathtt{B}_3}\right\}\right\},
\end{cases}
\tag{6.18}
$$

$\lambda_1(t_f) = \lambda_2(t_f) = \lambda_3(t_f) = \lambda_4(t_f) = \lambda_5(t_f) = \lambda_6(t_f) = 0, \mathtt{S}_h(0) = S_{h0}, I_h(0) = I_{h0},$
$\mathtt{R}_h(0) = \mathtt{R}_{h0}, S_m(0) = S_{m0}, I_m(0) = I_{m0}, \mathtt{T}(0) = \mathtt{T}_{\mathrm{m0}}.$

6.5 Numerical simulations

Most optimal control problems can not be solved analytically and instead numerical solution approach is used. Then to get optimal strategy we solved the optimality system (6.18) that contains two systems such are state system and the adjoint system. The iterative method called the forward-backward sweep is implemented to solve the optimality system. In solving state equations (6.1) using the initial value of state variables, the forward fourth order Runge-Kutta was used. Due to the transversality condition (6.9) with the solution of state functions and the value of optimal controls, the adjoint equations are solved using backward fourth order Runge-Kutta. Using a convex combination of the previous controls and the value from the optimality conditions (6.10) then the controls were updated. Until two consecutive iterations are close enough to each other this situation continues (Lenhart and Workman, 2007). The expected time of control strategies was approximately 6 months (180 days). For numerical simulation of the optimal control problem the initial condition

$\mathtt{S}_h(0) = 100, \mathtt{I}_h(0) = 10, \mathtt{R}_h(0) = 0, \mathtt{S}_m(0) = 300, \mathtt{I}_m(0) = 30,\ \mathtt{T}(0) = 16.1^oC$ and the parameter values from Table 4.4 were used. The weight constants values chosen for the state and controls that we used are $\mathtt{A}_1 = 60, \mathtt{A}_2 = 100, \mathtt{B}_1 = 60, \mathtt{B}_2 = 100$, and $\mathtt{B}_3 = 80$.
Next, we proposed four strategies with different combination of more than two controls at a time to illustrate the influence of each control on reducing of malaria.

Strategy A: Combination of treated bed net (u_1) and treatment of infected human (u_2)
Strategy B: Combination of treated bed net (u_1) and indoor residual spraying (u_3)
Strategy C: Combination of treatment of human (u_2) and indoor residual spraying (u_3)
Strategy D: Combination of treated (u_1), treatment (u_2) and insecticides spraying (u_3)

6.1 Strategy A: Combination of treated bed net (u_1) and treatment with drugs (u_2)

Under this strategy we optimize the objective function equation 6.2 using the treated bed net as control u_1 and the treatment of infected human as control u_2 with the value of the indoor insecticides spraying as control u_3 set to zero. From Figure 6.1**a** we can observe that if there is use the control, the number of infected humans $\mathtt{I}_h$ reduces whereas the infected of human increases if control is not used. Similarly, in Figure 6.1**b** we can see that the infected mosquitoes $\mathtt{I}_m$ is decreased in the use of control strategy tends to its lower point whereas for the uncontrolled case an infected mosquito increases. The control profiles are given in Figure 6.1**c** with this strategy suggest that controls on treated bed nets u_1 maintain maximum level (100%) until the end of the implementation while the treatment of infected with anti-malaria drugs u_2 is retained its maximum bound for 5 days then gradually tends to the minimum value in the end of day.

6.2 Strategy B: Combination of treated bed net (u_1) and indoor spraying (u_3).

This strategy combined the treated bed net as control u_1 and indoor insecticides spraying as control u_3 that used to reduce the total populations of infected and cost associated without the value of the treatment of infected human as control u_2. In Figure 6.2**a**, we can see that the amount of infected humans $\mathtt{I}_h$ declines with use of controls, in contrast, the infected human increases to certain point when there is no controls. From Figure 6.2**b** we observed that the infected mosquitoes $\mathtt{I}_m$ is decrease in there is control strategy whereas an infected mosquitoes increase for the uncontrolled case. The control profiles described in Figure 6.2**c** suggest that controls on treated bed nets u_1 is maintain upper bound (100%) for 175 days of the intervention period before dropping slowly to the lower bound while the indoor insecticides spraying u_3 is kept its maximum for 10 days and gradually drops to its minimum value

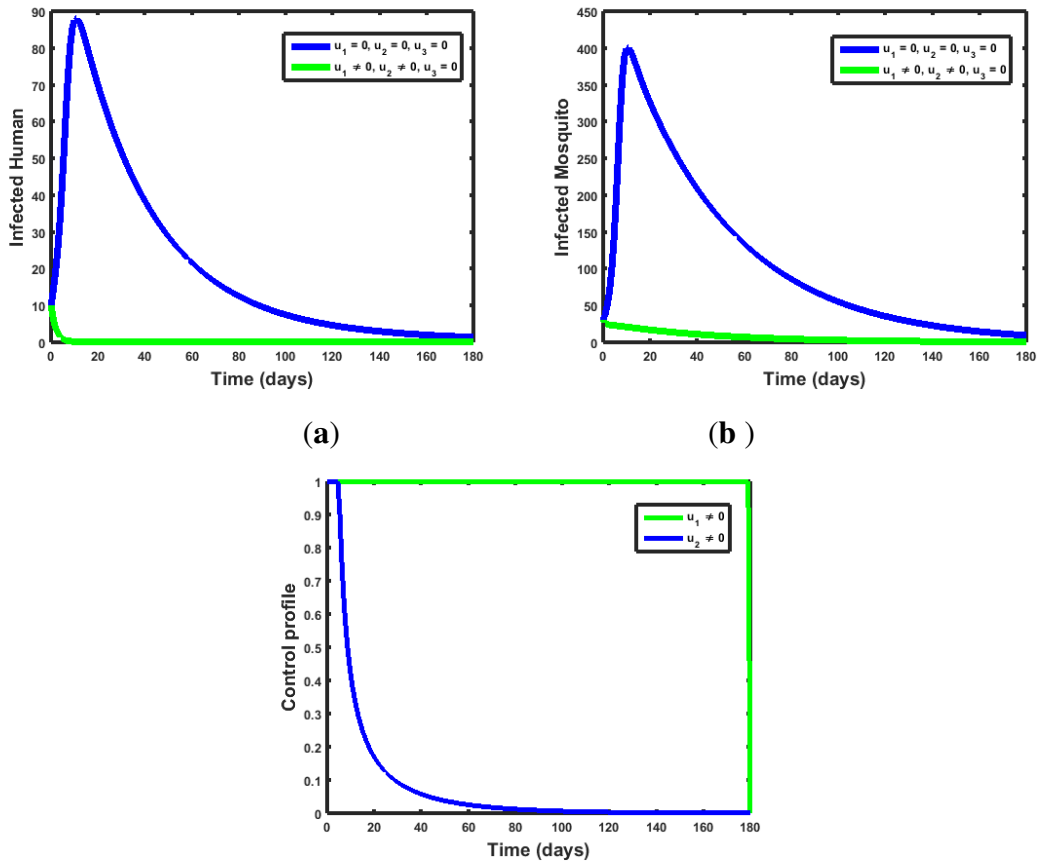

Figure 6.1: Simulations use of treated bed net (u_1) and treatment of infected human (u_2)

at the end of the intervention.

6.3 Strategy C: Combination of treatment (u_2) and indoor insecticides spraying (u_3)

In this strategy, we used the combination of treatment of infected human as control u_2 and indoor insecticides spraying as control u_3 to minimize the total infected populations and cost averted. From Figure 6.3**a** we observed that using this control strategy, the number of infected human $\mathtt{I}_h$ becomes smaller if there is the use of controls than without controls and declines to its lowest value. The infected mosquitoes $\mathtt{I}_m$ is decreased in the occurrence of control strategy then drops whereas for the uncontrolled case infected mosquitoes increase is observed in Figure 6.3**b**. In Figure 6.3**c** with this approach, the control profiles conclude that controls on the treatment of infected human u_2 maintain upper bound (100%) for 5 days while the indoor spraying u_3 is retained maximum for 6 days and gradually declines to lower bound at the end of the 180th day.

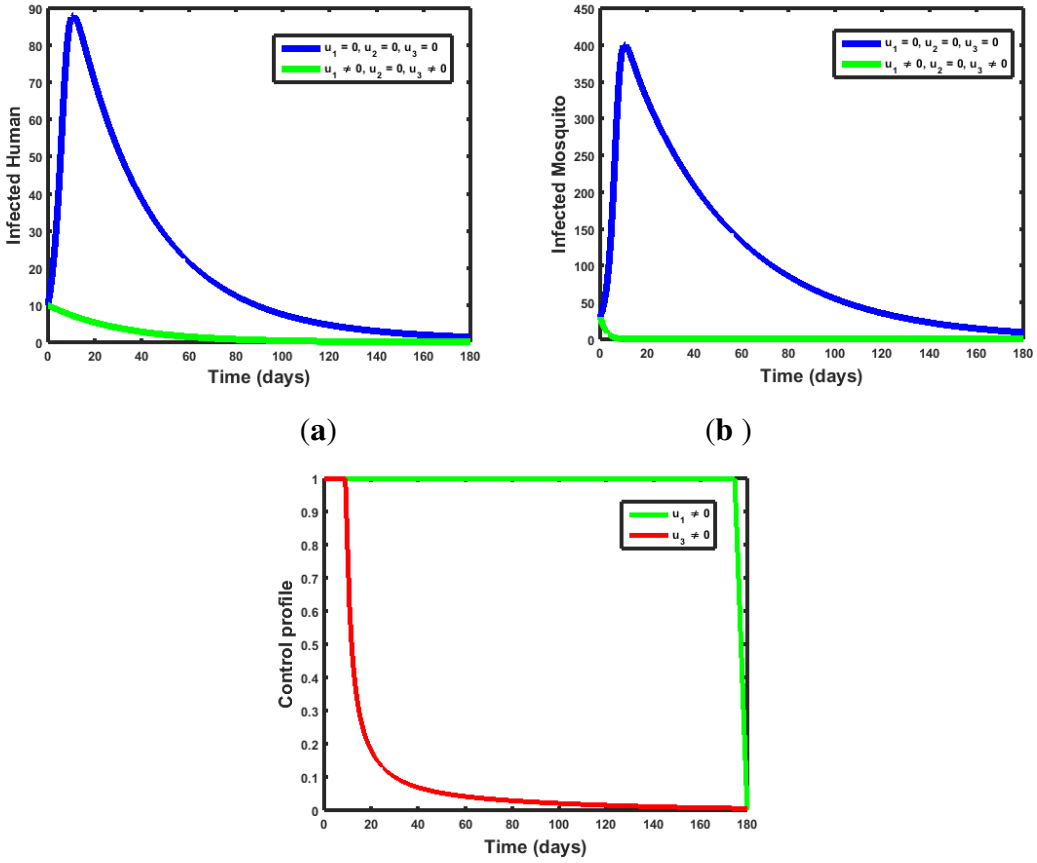

Figure 6.2: Simulations use of treatment (u_1) and indoor spraying of insecticides (u_3)

6.4 Strategy D: Using treated (u_1), treatment (u_2) and indoor spraying (u_3)

In order to minimize the objective functional (6.2) we used all controls on the treated bed net u_1, treatment of infected human u_2 and an indoor insecticides spraying u_3. From Figure 6.4**a**, we observed that the number of infected humans $\mathtt{I}_h$ decreases in the presence of controls as the infected human increases if there is no use of control. It can be described that the infected population of mosquitoes $\mathtt{I}_m$ decreases in the use of control strategy whereas in the absence of control strategy an infected mosquitoes increases are observed in Figure 6.4**b**. Using this strategy, in Figure 6.4**c** the control profile depicted that controls on treated bed nets u_1 and the treatment u_2 were kept their maximum coverage (100%) for 160 days and 5 days respectively, while insecticides spray u_3 is retained its upper bound (100%) for 8 days, then all reduces to their minimum level in the last day.

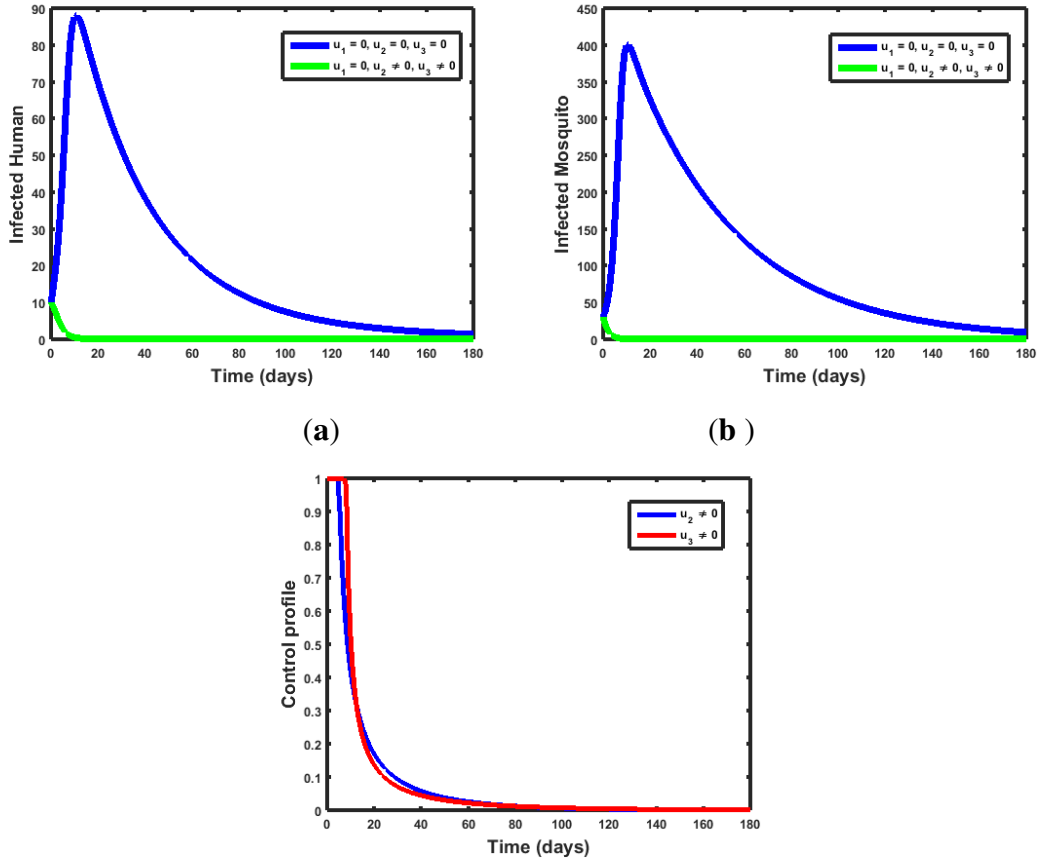

(a) (b) (c)

Figure 6.3: Simulations use of treatment (u_2) and spraying of insecticides (u_3)

6.6 Cost effectiveness analysis

From the above Figures (6.1-6.4) it is not possible to determine the most efficient strategy as their patterns are similar. Based upon the numerical simulation of the optimality system using the parameter values in Table 4.4, we can obtain the most effective and least-cost strategy. To obtain this strategy, we used the method called incremental cost-effectiveness ratio (ICER). Applying this technique we compare more than one competing strategy incrementally, one intervention should be compared with the next less effective alternative. This approach was defined as the ratio of the difference in averted costs between two strategies to the difference in the total number of infections averted (Tilahun et al., 2018). The total infected averted during the intervention period $\mathtt{t}_f$ is given by

$$\text{total infection averted } = \int_0^{t_f} \mathtt{I}_h^{'} dt - \int_0^{t_f} \mathtt{I}_h^{*} dt, \tag{6.19}$$

where $\mathtt{I}_h^{'}$ is the solution of the system (6.1) without controls and $\mathtt{I}_h^{*}$ is the optimal solution of system (6.1) with controls. This implies that the total number of infections averted is

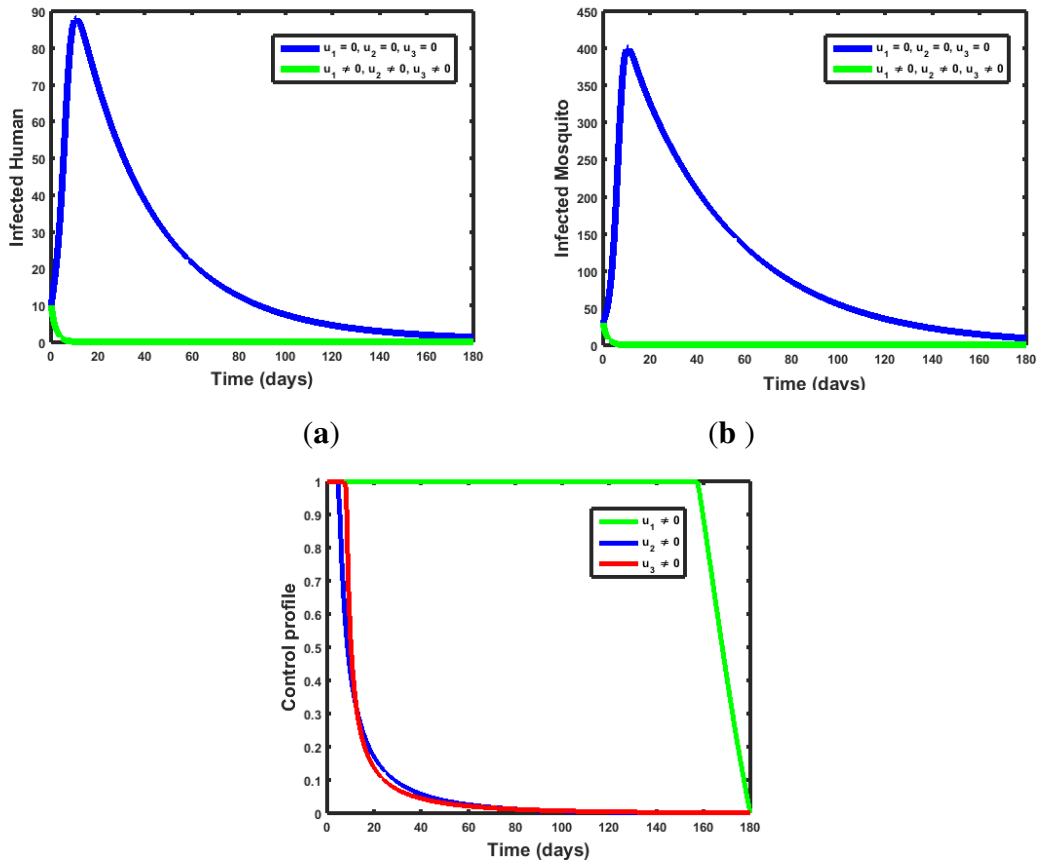

Figure 6.4: Using the treated bed net (u_1), treatment (u_2) and indoor spraying (u_3)

obtained by subtracting the total number of the infected human populations by malaria with control from the total number of the infected human population by malaria without control. And whereas the total cost of each strategy was obtained by using cost functional represented by $\frac{1}{2}\mathrm{B}_1 u_1^2, \frac{1}{2}\mathrm{B}_2 u_2^2$ and $\frac{1}{2}\mathrm{B}_3 u_3^2$ over the time (Berhe et al., 2019). But, we did not consider a strategy that applies single control, since alone control is not effective to reduce the malaria at all from the human population. From the simulation of numerical result, the calculated total cost averted, total infections saved, and control strategy order in increasing based on the total infections saved as listed in Table 6.1.

Table 6.1: Total amount of the infections saved and cost averted for all strategies

Strategy	**Description**	**Total averted**	**Total cost**($)
B	Treated bed net and indoor spraying	3792.797	6420.361
C	Treatment and indoor spraying	4094.558	1955.467
A	Treated bed net and treatment of infected	4115.460	6474.615
D	Treated, treatment and indoor spraying	4115.486	6490.286

Using the total number of saved population and total cost of averted for each strategy given in Table 6.1, the calculated value of the incremental cost effectiveness ratio (ICER) used for comparing different two strategies is obtained and given by

$$\begin{aligned}
\text{ICER}(\mathbf{B}) &= \frac{6420.361}{3792.797} = 1.693 \\
\text{ICER}(\mathbf{C}) &= \frac{1955.467 - 6420.361}{4094.558 - 3792.797} = -14.796 \\
\text{ICER}(\mathbf{A}) &= \frac{6474.615 - 1955.467}{4115.460 - 4094.5584} = 216.211 \\
\text{ICER}(\mathbf{D}) &= \frac{6490.286 - 6474.615}{4115.486 - 4115.460} = 602.725
\end{aligned}$$

From the above result the number of infection saved with ICER for four strategy is given in Table 6.2.

Table 6.2: Total amount of the infection averted and total cost with their ICER

Strategies	**Total infections averted**	**Total cost** ($)	**ICER**
B	3792.797	6420.361	1.693
C	4094.558	1955.467	-14.796
A	4115.460	6474.615	216.211
D	4115.486	6490.286	602.725

In Table 6.2 we have compared the interventions **B** and **C**. It can observed that ICER(**C**) is less than ICER(**B**). This shows that strategy **B** is expensive and less in saving people. Thus, strategy **C** save people more than strategy **B**. So that we have omitted **B** from the the competing strategies. Then re-calculate the ICER for the competing strategies **C**, **A** and **D** as given in Table 6.3.

Table 6.3: Total infection averted and total cost of the strategies **C**, **A** and **D**

Strategies	**Total infections averted**	**Total cost** ($)	**ICER**
C	4094.558	1955.467	0.478
A	4115.460	6474.615	216.211
D	4115.486	6490.286	602.725

As we have seen in Table 6.3 from the competing intervention strategies **C** and **A**, the ICER(**C**) is less than ICER(**A**). This illustrate that strategy **C** dominates **A**. Thus, strategy **A** is less effective and more costly than strategy **C**. Hence, we have dropped strategy **A** from the list of competing and re-calculate the ICER as given in Table 6.4.

Table 6.4: Total infection averted and total cost of the strategies **C** and **D**

Strategies	**Total infections averted**	**Total cost** ($)	**ICER**
C	4094.558	1955.467	0.478
D	4115.486	6490.286	216.687

In Table 6.4 comparison between intervention strategies **C** and **D** indicates that ICER(**C**) is less than ICER(**D**). This shows that strategy **C** strongly dominates **D**. So that the strategy **C** provided the least total cost and the most effective. From the result of the analysis, therefore, we suggest that strategy **C** that is a combination of treatment of infected human and indoor residual spraying is the most effective and least-cost strategy to minimize the disease.

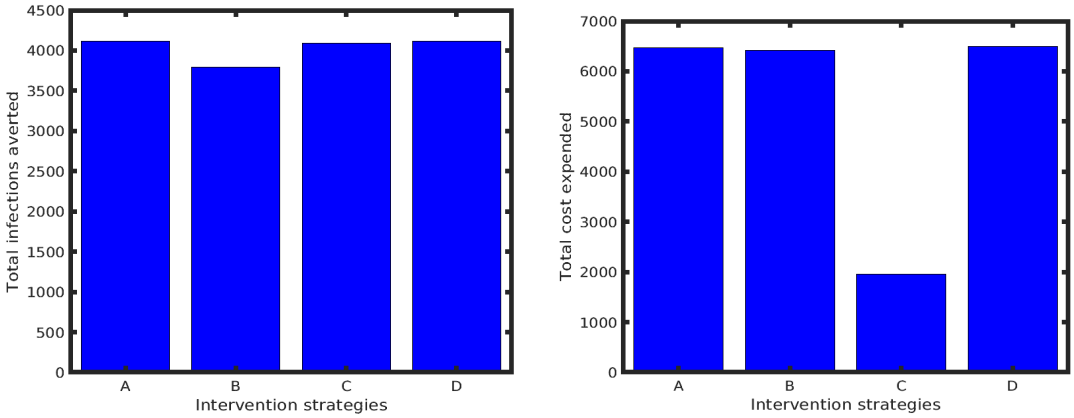

(**a**) (**b**)

Figure 6.5: The total people averted with their respect total cost used for strategies

CHAPTER 7
OPTIMAL CONTROL AND COST EFFECTIVENESS ANALYSIS OF SEIRS MALARIA TRANSMISSION MODEL IN THE PRESENCE OF TEMPERATURE VARIABILITY

In this chapter, we have extended the malaria model introduced in (5.1) into an optimal control model. The Pontryagin's minimum principle is used to determine the necessary condition for the controls to be optimal. The study compares the combination of different controls strategies and cost-effectiveness analysis is implemented to identify the least-cost strategy that helps to minimize the disease in the specified time.

7.1 Formulation of optimal control model

In this section, we incorporated the time-dependent controls into the malaria transmission model (5.1) to study the optimal strategies that prevent malaria epidemics. The control functions $u_1(t)$ represents protective control using insecticide treated bed net, where the infection force of susceptible human and mosquitoes populations are reduced by a factor $(1-u_1(t))$. The second, $u_2(t)$ represents treatment control of infected human using anti-malaria drugs, whereas $u_3(t)$ denotes a mosquito reducing control using indoor spraying of insecticides. Time is specified, that is given by $t \in [0, t_f]$ where t_f is the terminal time. Then by extending malaria transmission model (5.1) into the optimal control problem, then the associated state

system is obtain and given by

$$\begin{cases} \frac{dS_h}{dt} &= \Psi - (1-u_1)\beta_h(\mathtt{T})S_h I_m - \mu_h S_h + \omega_h \mathtt{R}_h, \\ \frac{dE_h}{dt} &= (1-u_1)\beta_h(\mathtt{T})S_h I_m - (\mu_h + \alpha_h)\mathtt{E}_h, \\ \frac{dI_h}{dt} &= \alpha_h \mathtt{E}_h - (\mu_h + \delta + \gamma_h + u_2)I_h, \\ \frac{dR_h}{dt} &= (\gamma_h + u_2)I_h - (\mu_h + \omega_h)\mathtt{R}_h, \\ \frac{dS_m}{dt} &= \Phi(\mathtt{T}) - (1-u_1)\beta_m(\mathtt{T})S_m I_h - (\mu_m + u_3)S_m, \\ \frac{dE_m}{dt} &= (1-u_1)\beta_m(\mathtt{T})S_m I_h - (\mu_m + \alpha_m + u_3)\mathtt{E}_m, \\ \frac{dI_m}{dt} &= \alpha_m \mathtt{E}_m - (\mu_m + u_3)I_m, \\ \frac{d\mathtt{T}}{dt} &= \mathtt{r}(1 - \frac{\mathtt{T}}{\mathtt{T}_{\max}})(\mathtt{T} - \mathtt{T}_0), \end{cases} \tag{7.1}$$

where
$\beta_h(\mathtt{T}) = \beta_{0h} + \beta_{1h}\left(\frac{\mathtt{T}-\mathtt{T}_0}{\mathtt{T}_{\max}}\right)$, $\beta_m(\mathtt{T}) = \beta_{0m} + \beta_{1m}\left(\frac{\mathtt{T}-\mathtt{T}_0}{\mathtt{T}_{\max}}\right)$ and $\Phi(\mathtt{T}) = \Phi_0 + \Phi_{1m}\left(\frac{\mathtt{T}-\mathtt{T}_0}{\mathtt{T}_{\max}}\right)$.
The analysis of optimal control problem is described by the Pontryagin's minimum principle (Boltyanskiy et al., 1961), with the aim of reducing the exposed human $\mathtt{E}_h(t)$, infected human $\mathtt{I}_h(t)$, infected mosquito $\mathtt{I}_m(t)$ and costs of controls $u_i(t)$. The problem (7.1) has objective functional given by

$$\mathtt{J}(u_1,u_2,u_3) = \underbrace{min}_{\mathtt{u}_1,\mathtt{u}_2,\mathtt{u}_3} \int_0^{t_f} \left(\mathtt{B}_1\mathtt{E}_h + \mathtt{B}_2 I_h + \mathtt{B}_3 I_m + \frac{1}{2}(\mathtt{D}_1 u_1^2 + \mathtt{D}_2 u_2^2 + \mathtt{D}_3 u_3^2) \right) dt, \tag{7.2}$$

where t_f represents the final time of control implementation, parameters $\mathtt{B}_1$, $\mathtt{B}_2$ and $\mathtt{B}_3$ are weights constants of the exposed human population, infected human population and infected mosquito population respectively, while $\mathtt{D}_1, \mathtt{D}_2$ and $\mathtt{D}_3$ are weight constants for use treated bed nets, treatment control using anti-malaria drug and indoor insecticides spraying respectively. In this work, as in other studies (Kyere et al., 2018; Chukwu et al., 2020; Okosun and Makinde, 2013; Tchoumi et al., 2021; Srivastav and Ghosh, 2021), we make the expression $\frac{1}{2}\mathtt{D}_i u_i^2$ is to be a quadratic for the cost control functions in order to obtain a unique optimal expression for each of the control variables from the optimality condition. The specific goal is to obtain an optimal control triple u_1^*, u_2^* and u_3^* of that

$$\mathtt{J}(u_1^*,u_2^*,u_3^*) = \min\{\mathtt{J}(u_1,u_2,u_3) : u_1,u_2,u_3 \in \Theta\} \tag{7.3}$$

and it is assumed that there is limitations on the maximum rate of treated bed nets, using anti-malaria drug and indoor insecticides spraying where $\Theta = \{(u_1,u_2,u_3) : u_i(t)$ is Lebesgue measurable on $t \in [0,t_f]$ with $0 \le u_i(t) \le 1\}$.

7.2 Existence of the optimal controls

In this section, the boundedness of solutions of system for a finite time interval is used to prove the existence of an optimal controls. As the result, the existence of an optimal control triples treated bed nets, treatment of infected human and indoor insecticides spray can be proven based on the result (Fleming and Rishel, 1975).

Theorem 7.1: Given $\mathtt{J}(u_1,u_2,u_3)$ subject to state system equation (7.1), then there exist optimal controls $u^* = (u_1^*,u_2^*,u_3^*)$ and corresponding to the optimal solution $(\mathtt{S}_h^*,\mathtt{E}_h^*,\mathtt{I}_h^*,\mathtt{R}_h^*,\mathtt{S}_m^*,\mathtt{E}_m^*,\mathtt{I}_m^*,\mathtt{T}^*)$ such that

$$\mathtt{J}(u_1^*,u_2^*,u_3^*) = \min\{\mathtt{J}(u_1,u_2,u_3) : u_1,u_2,u_3 \in \Theta\}. \tag{7.4}$$

Proof: To prove the existence of an optimal controls triples we need to verify the following five conditions based on the result given in (Fleming and Rishel, 1975).

i. The set of controls and corresponding state variables is nonempty.

ii. The measurable control set is convex and closed.

iii. The state system can be written as linear function of control variables with coefficients depending on time and state variables.

iv. The integrand of the cost functional is convex on ϑ.

v. There exist constants $b_1,b_2 > 0$ and $b_3 > 1$ such that the integrand of the objective functional satisfies $g(x,u) \geq b_1(|u_1|^2+|u_2|^2+|u_3|^2)^{\frac{b_3}{2}} - b_2$.

i. It is clear that Θ is an nonempty set of measurable functions on $0 \leq t_f$ in real numbers $\mathbb{R}$. Since the system (7.1) has bounded coefficients, any solutions are bounded on $[0,t_f]$. The corresponding solutions for the system (7.1) exist (Lukes, 1982).

ii. We consider

$$\Theta = \{u \in \mathbb{R}^3 : ||u|| \leq 1\}.$$

Let $u_1,u_2 \in \Theta$ such that $||u_1|| \leq 1$ and $||u_2|| \leq 1$. It follows, by the definition of a convex set (Chong and Zak, 2004), that for any $\delta \in [0,1]$,

$$||\delta u_1 + (1-\delta)u_2|| \leq \delta||u_1|| + (1-\delta)||u_2|| \leq 1.$$

Thus, $\delta u_1 + (1-\delta)u_2 \in \Theta$ implies that Θ is a convex set.

iii. The state system (7.1) is clearly linear in control variables u_1, u_2 and u_3 with coefficients depending on state variables. With this condition (iii) is satisfied.

iv. Let the integrand of the cost functional is given by

$$g(t,x,u) = \underbrace{\mathtt{B}_1\mathtt{E}_h + \mathtt{B}_2 I_h + \mathtt{B}_3 I_m}_{f(t,\,x)} + \underbrace{\frac{1}{2}(\mathtt{D}_1 u_1^2 + \mathtt{D}_2 u_2^2 + \mathtt{D}_3 u_3^2)}_{h(t,\,u)}.$$

Thus, $g(t,x,u)$ is the sum two convex functions. Since linear function is a convex, $f(t,x)$ is convex. Obviously, $h(t,u)$ is a finite linear combination with positive coefficients of the functions $h_i(u) = \frac{1}{2}u_i^2$. It is more better to show that the function $h_1 : \Theta \to R$ defined by $h_1(u) = \frac{1}{2}u^2$ is convex. Let $v, z \in \Theta$ and $\varpi \in [0,1]$. Then we have

$$\begin{aligned} & h_1(t,(1-\varpi)v + \varpi z) - [(1-\varpi)g(t,v) + \varpi g(t,z)] \\ &= \frac{1}{2}((1-\varpi)v + \varpi z)^2 - \frac{1}{2}((1-\varpi)v^2 + \varpi z^2), \\ &= \frac{1}{2}(\varpi^2 - \varpi)(v-z)^2 \leq 0. \end{aligned} \tag{7.5}$$

Hence,

$$h_1(t,(1-\varpi)v + \varpi z) \leq [(1-\varpi)h_1(t,v) + \varpi h_1(t,z)]$$

which proves that $h_1(t,u)$ is a convex function (Chong and Zak, 2004). Since the sum of two convex functions is convex, so $g(t,x,u)$ is convex function.

v. Lastly, we have

$$\begin{aligned} g(x,u) &= \mathtt{B}_1\mathtt{E}_h + \mathtt{B}_2 I_h + \mathtt{B}_3 I_m + \frac{1}{2}(\mathtt{D}_1 u_1^2 + \mathtt{D}_2 u_2^2 + \mathtt{D}_3 u_3^2), \\ &\geq \frac{1}{2}\sum_{i=1}^{3} \mathtt{D}_i u_i^2, \\ &\geq b_1 \left(\sum_{i=1}^{3} u_i^2\right)^{\frac{b_3}{2}} - b_2, \end{aligned}$$

where $b_1 = \frac{1}{2}\min\{\mathtt{D}_1, \mathtt{D}_2, \mathtt{D}_3\}$, $b_2 > 0$ and $b_3 = 2$.
Hence, there exists an optimal control that minimizes the objective function. This completes the proof.

7.3 Hamiltonian system

By using the Pontryagin's minimum principle (Boltyanskiy et al., 1961) to obtain the necessary condition, the Hamiltonian $(\mathscr{H})$, which consists of the state equations (7.1) and inte-

grand of the objective functional (7.2) is given by

$$\mathscr{H} = [\mathtt{B}_1\mathtt{E}_h + \mathtt{B}_2\mathtt{I}_h + \mathtt{B}_3\mathtt{I}_m + \frac{1}{2}\sum_{i=1}^{3}\mathtt{D}_i u_i^2] + \lambda_i\left[\frac{d\mathtt{S}_h}{dt} + \frac{d\mathtt{E}_h}{dt} + \frac{d\mathtt{I}_h}{dt} + \frac{d\mathtt{R}_h}{dt} + \frac{d\mathtt{S}_m}{dt} + \frac{d\mathtt{E}_m}{dt} + \frac{d\mathtt{I}_m}{dt} + \frac{d\mathtt{T}}{dt}\right]. \tag{7.6}$$

By substituting the stated equations (7.1) and (7.2) into a minimizing problem of a Hamiltonian function $(\mathscr{H})$ with respect to controls u_1, u_2, u_3 is given by

$$\begin{aligned}
\mathscr{H} =& [\mathtt{B}_1\mathtt{E}_h + \mathtt{B}_2 I_h + \mathtt{B}_3 I_m + \frac{1}{2}(\mathtt{D}_1 u_1^2 + \mathtt{D}_2 u_2^2 + \mathtt{D}_3 u_3^2)] \\
&+ \lambda_1[\Psi - (1-u_1)\beta_h(\mathtt{T})S_h I_m - \mu_h S_h + \omega_h \mathtt{R}_h] \\
&+ \lambda_2[(1-u_1)\beta_h(\mathtt{T})S_h I_m - (\mu_h + \alpha_h)\mathtt{E}_h] \\
&+ \lambda_3[\alpha_h \mathtt{E}_h - (\mu_h + \delta + \gamma_h + u_2)I_h] \\
&+ \lambda_4[(\gamma_h + u_2)I_h - (\mu_h + \omega_h)\mathtt{R}_h] \\
&+ \lambda_5[\Phi(\mathtt{T}) - (1-u_1)\beta_m(\mathtt{T})S_m I_h - (\mu_m + u_3)S_m] \\
&+ \lambda_6[(1-u_1)\beta_m(\mathtt{T})S_m I_h - (\mu_m + \alpha_m + u_3)\mathtt{E}_m] \\
&+ \lambda_7[\alpha_m \mathtt{E}_m - (\mu_m + u_3)I_m] \\
&+ \lambda_8[r(1 - \frac{\mathtt{T}}{\mathtt{T}_{\max}})(\mathtt{T} - \mathtt{T}_0)],
\end{aligned} \tag{7.7}$$

where, $\lambda_1, \lambda_2, \lambda_3, \lambda_4, \lambda_5, \lambda_6, \lambda_7$ and λ_8 are adjoint variables. In the next we present the adjoint variables and control characterizations by applying Pontryagin's minimum principle (Boltyanskiy et al., 1961), with existence of the optimal controls (Fleming and Rishel, 1975) the following result can be obtain.

Theorem 7.2. For an optimal control set $u^* = (u_1^*, u_2^*, u_3^*)$ and a solution $(\mathtt{S}_h^*, \mathtt{E}_h^*, \mathtt{I}_h^*, \mathtt{R}_h^*, \mathtt{S}_m^*, \mathtt{E}_m^*, \mathtt{I}_m^*, \mathtt{T}^*)$ to the corresponding state system (7.1) that minimize $\mathtt{J}(u_1, u_2, u_3)$ over $\mathtt{U}$, then there exist adjoint variables $\lambda_1, \lambda_2, \lambda_3, \lambda_4, \lambda_5, \lambda_6, \lambda_7$ and λ_8 such that

$$\begin{cases}
\frac{d\lambda_1}{dt} &= -((1-u_1)\beta_h(\mathtt{T})I_m(\lambda_2 - \lambda_1)) + \mu_h\lambda_1, \\
\frac{d\lambda_2}{dt} &= -\mathtt{B}_1 + \lambda_2(\mu_h + \alpha_h) - \alpha_h\lambda_3, \\
\frac{d\lambda_3}{dt} &= -\mathtt{B}_2 - ((1-u_1)\beta_m(\mathtt{T})S_m(\lambda_6 - \lambda_5)) + \lambda_3(\mu_h + \delta + \gamma_h + u_2) - \lambda_4(u_2 + \gamma_h), \\
\frac{d\lambda_4}{dt} &= -\omega_h\lambda_1 + \lambda_4(\mu_h + \omega_h), \\
\frac{d\lambda_5}{dt} &= -((1-u_1)\beta_m(\mathtt{T})I_h(\lambda_6 - \lambda_5)) + \lambda_5(u_3 + \mu_m), \\
\frac{d\lambda_6}{dt} &= \lambda_6(u_3 + \mu_m + \alpha_m) - \lambda_7\alpha_m, \\
\frac{d\lambda_7}{dt} &= -\mathtt{B}_3 - ((1-u_1)\beta_h(\mathtt{T})S_h(\lambda_2 - \lambda_1)) + \lambda_7(u_3 + \mu_m), \\
\frac{d\lambda_8}{dt} &= -r\lambda_8 - r\lambda_8(\frac{\mathtt{T}_0}{\mathtt{T}_{\max}} - \frac{2\mathtt{T}}{\mathtt{T}_{\max}}),
\end{cases} \tag{7.8}$$

with full time (transversality) conditions

$$\lambda_1(t_f) = \lambda_2(t_f) = \lambda_3(t_f) = \lambda_4(t_f) = \lambda_5(t_f) = \lambda_6(t_f) = \lambda_7(t_f) = \lambda_8(t_f) = 0. \tag{7.9}$$

Moreover, the optimal controls u_1^*, u_2^*, u_3^* with the optimality condition are represented by

$$\begin{aligned}
u_1^* &= \max\left\{0, \min\left\{1, \frac{(\lambda_2-\lambda_1)\beta_h(\mathtt{T})S_h^*I_m^* + (\lambda_6-\lambda_5)\beta_m(\mathtt{T})S_m^*I_h^*}{\mathtt{D}_1}\right\}\right\},\\
u_2^* &= \max\left\{0, \min\left\{1, \frac{(\lambda_3-\lambda_4)I_h^*}{\mathtt{D}_2}\right\}\right\},\\
u_3^* &= \max\left\{0, \min\left\{1, \frac{\lambda_5 S_m^* + \lambda_6 \mathtt{E}_m^* + \lambda_7 I_m^*}{\mathtt{D}_3}\right\}\right\}.
\end{aligned} \tag{7.10}$$

Proof: By finding the partial derivatives of the Hamiltonian function (7.7) with respect to the state variables $\mathtt{S}_h, \mathtt{E}_h, \mathtt{I}_h, \mathtt{R}_h, \mathtt{S}_m, \mathtt{E}_m, \mathtt{I}_m$, and $\mathtt{T}$ respectively, the adjoint equations stated at the system (7.8) are obtained. So that the adjoint equations are given by

$$\begin{cases}
\frac{d\lambda_1}{dt} = -\frac{\partial \mathscr{H}}{\partial S_h} = -((1-u_1)\beta_h(\mathtt{T})I_m(\lambda_2-\lambda_1)) + \mu_h\lambda_1,\\
\frac{d\lambda_2}{dt} = -\frac{\partial \mathscr{H}}{\partial \mathtt{E}_h} = -\mathtt{B}_1 + \lambda_2(\mu_h+\alpha_h) - \alpha_h\lambda_3,\\
\frac{d\lambda_3}{dt} = -\frac{\partial \mathscr{H}}{\partial I_h} = -\mathtt{B}_2 - ((1-u_1)\beta_m(\mathtt{T})S_m(\lambda_6-\lambda_5)) + \lambda_3(\mu_h+\delta+\gamma_h+u_2) - \lambda_4(u_2+\gamma_h),\\
\frac{d\lambda_4}{dt} = -\frac{\partial \mathscr{H}}{\partial R_h} = -\omega_h\lambda_1 + \lambda_4(\mu_h+\omega_h),\\
\frac{d\lambda_5}{dt} = -\frac{\partial \mathscr{H}}{\partial S_m} = -((1-u_1)\beta_m(\mathtt{T})I_h(\lambda_6-\lambda_5)) + \lambda_5(u_3+\mu_m),\\
\frac{d\lambda_6}{dt} = -\frac{\partial \mathscr{H}}{\partial E_m} = \lambda_6(u_3+\mu_m+\alpha_m) - \lambda_7\alpha_m,\\
\frac{d\lambda_7}{dt} = -\frac{\partial \mathscr{H}}{\partial I_m} = -\mathtt{B}_3 - ((1-u_1)\beta_h(\mathtt{T})S_h(\lambda_2-\lambda_1)) + \lambda_7(u_3+\mu_m),\\
\frac{d\lambda_8}{dt} = -\frac{\partial \mathscr{H}}{\partial \mathtt{T}} = -r\lambda_8 - r\lambda_8\left(\frac{\mathtt{T}_0}{\mathtt{T}_{\max}} - \frac{2\mathtt{T}}{\mathtt{T}_{\max}}\right).
\end{cases} \tag{7.11}$$

with transversality conditions

$$\lambda_1(t_f) = \lambda_2(t_f) = \lambda_3(t_f) = \lambda_4(t_f) = \lambda_5(t_f) = \lambda_6(t_f) = \lambda_7(t_f) = \lambda_8(t_f) = 0. \tag{7.12}$$

Further, the optimality conditions with respect to the controls is given by

$$\frac{\partial \mathscr{H}}{\partial u_i} = 0, \quad \text{for } i = 1,2,3. \tag{7.13}$$

The optimal controls value that calculated by the above condition is follows that

$$\begin{aligned}
0 &= \frac{\partial \mathscr{H}}{\partial u_1} = (\lambda_1-\lambda_2)\beta_h(\mathtt{T})S_h^*I_m^* + (\lambda_5-\lambda_6)\beta_m(\mathtt{T})S_m^*I_h^* + u_1\mathtt{D}_1,\\
0 &= \frac{\partial \mathscr{H}}{\partial u_2} = \lambda_4 I_h^* - \lambda_3 I_h^* + u_2\mathtt{D}_2,\\
0 &= \frac{\partial \mathscr{H}}{\partial u_2} = -(\lambda_5 S_m^* + \lambda_6 \mathtt{E}_m^* + \lambda_7 I_m^*) + u_3\mathtt{D}_3.
\end{aligned} \tag{7.14}$$

From equation (7.14) solving for control variables then we obtain,

$$\begin{cases} u_1^* &= \frac{(\lambda_2-\lambda_1)\beta_h(\mathtt{T})S_h^*I_m^*+(\lambda_6-\lambda_5)\beta_m(\mathtt{T})S_m^*I_h^*}{\mathtt{D}_1}, \\ u_2^* &= \frac{(\lambda_3-\lambda_4)I_h^*}{\mathtt{D}_2}, \\ u_3^* &= \frac{(\lambda_5 S_m^*+\lambda_6 \mathtt{E}_m^*+\lambda_7 I_m^*)}{\mathtt{D}_3}. \end{cases} \tag{7.15}$$

By standard control arguments involving bounds on the control, then becomes

$$u_i^* = \begin{cases} 0 & \text{if} \quad z_i^* \leq 0 \\ z_i^* & \text{if} \quad 0 < z_i^* < 1 \\ 1 & \text{if} \quad z_i^* \geq 1 \end{cases} \tag{7.16}$$

and then we conclude that the compact form of the controls in equation (7.16) is

$$\begin{aligned} u_1^* &= \max\left\{0, \min\left\{1, \underbrace{\frac{(\lambda_2-\lambda_1)\beta_h(\mathtt{T})S_h^*I_m^*+(\lambda_6-\lambda_5)\beta_m(\mathtt{T})S_m^*I_h^*}{\mathtt{D}_1}}_{=z_1^*}\right\}\right\}, \\ u_2^* &= \max\left\{0, \min\left\{1, \underbrace{\frac{(\lambda_3-\lambda_4)I_h^*}{\mathtt{D}_2}}_{=z_2^*}\right\}\right\}, \\ u_3^* &= \max\left\{0, \min\left\{1, \underbrace{\frac{(\lambda_5 S_m^*+\lambda_6 \mathtt{E}_m^*+\lambda_7 I_m^*)}{\mathtt{D}_3}}_{=z_3^*}\right\}\right\}. \end{aligned} \tag{7.17}$$

This completes the proof.

7.4 Optimality system

In this section, the optimality system is obtained from the state system, the adjoint system, the optimality condition on control set incorporating with the initial value of state variables and transversal condition of adjoint variables. Then after incorporated, the optimality system

is given by

$$
\begin{cases}
\frac{dS_h}{dt} &= \Psi - (1-u_1^*)\beta_h(\mathtt{T})S_h I_m - \mu_h S_h + \omega_h \mathtt{R}_h, \\
\frac{dE_h}{dt} &= (1-u_1^*)\beta_h(\mathtt{T})S_h I_m - (\mu_h+\alpha_h)\mathtt{E}_h, \\
\frac{dI_h}{dt} &= \alpha_h \mathtt{E}_h - (\mu_h+\delta+\gamma_h+u_2^*)I_h, \\
\frac{dR_h}{dt} &= (\gamma_h+u_2^*)I_h - (\mu_h+\omega_h)\mathtt{R}_h, \\
\frac{dS_m}{dt} &= \Phi(\mathtt{T}) - (1-u_1^*)\beta_m(\mathtt{T})S_m I_h - (\mu_m+u_3^*)S_m, \\
\frac{dE_m}{dt} &= (1-u_1^*)\beta_m(\mathtt{T})S_m I_h - (\mu_m+\alpha_m+u_3^*)\mathtt{E}_m, \\
\frac{dI_m}{dt} &= \alpha_m \mathtt{E}_m - (\mu_m+u_3^*)I_m, \\
\frac{d\mathtt{T}}{dt} &= \mathtt{r}(1-\frac{\mathtt{T}}{\mathtt{T}_{\max}})(\mathtt{T}-\mathtt{T}_0), \\
\frac{d\lambda_1}{dt} &= -((1-u_1^*)\beta_h(\mathtt{T})I_m(\lambda_2-\lambda_1)) + \mu_h\lambda_1, \\
\frac{d\lambda_2}{dt} &= -\mathtt{B}_1 + \lambda_2(\mu_h+\alpha_h) - \alpha_h\lambda_3, \\
\frac{d\lambda_3}{dt} &= -\mathtt{B}_2 - ((1-u_1^*)\beta_m(\mathtt{T})S_m(\lambda_6-\lambda_5)) + \lambda_3(\mu_h+\delta+\gamma_h+u_2^*) - \lambda_4(u_2^*+\gamma_h), \\
\frac{d\lambda_4}{dt} &= -\omega_h\lambda_1 + \lambda_4(\mu_h+\omega_h), \\
\frac{d\lambda_5}{dt} &= -((1-u_1^*)\beta_m(\mathtt{T})I_h(\lambda_6-\lambda_5)) + \lambda_5(u_3^*+\mu_m), \\
\frac{d\lambda_6}{dt} &= \lambda_6(u_3^*+\mu_m+\alpha_m) - \lambda_7\alpha_m, \\
\frac{d\lambda_7}{dt} &= -\mathtt{B}_3 - ((1-u_1^*)\beta_h(\mathtt{T})S_h(\lambda_2-\lambda_1)) + \lambda_7(u_3^*+\mu_m), \\
\frac{d\lambda_8}{dt} &= -r\lambda_8 - r\lambda_8(\frac{\mathtt{T}_0}{\mathtt{T}_{\max}} - \frac{2\mathtt{T}}{\mathtt{T}_{\max}}), \\
u_1^* &= \max\left\{0, \min\left\{1, \frac{(\lambda_2-\lambda_1)\beta_h(\mathtt{T})S_h^* I_m^* + (\lambda_6-\lambda_5)\beta_m(\mathtt{T})S_m^* I_h^*}{\mathtt{D}_1}\right\}\right\}, \\
u_2^* &= \max\left\{0, \min\left\{1, \frac{(\lambda_3-\lambda_4)I_h^*}{\mathtt{D}_2}\right\}\right\}, \\
u_3^* &= \max\left\{0, \min\left\{1, \frac{(\lambda_5 S_m^* + \lambda_6 \mathtt{E}_m^* + \lambda_7 I_m^*)}{\mathtt{D}_3}\right\}\right\},
\end{cases}
\tag{7.18}
$$

$\lambda_i(t_f) = 0,\ \ \mathrm{i} = 1,...8,\ \ \ \mathtt{S}_h(0) = \mathtt{S}_{h0}, \mathtt{E}_h(0) = \mathtt{E}_{h0}, \mathtt{I}_h(0) = \mathtt{I}_{h0}, \mathtt{R}_h(0) = \mathtt{R}_{h0}, \mathtt{S}_m(0) = \mathtt{S}_{m0},$
$\mathtt{E}_m(0) = \mathtt{E}_{m0}, \mathtt{I}_m(0) = \mathtt{I}_{m0}, \mathtt{T}(0) = \mathtt{T}_{\mathrm{m0}}.$

7.5 Numerical simulations

The optimality system (7.18) consists of two systems, the state system (7.1) and co-state system (7.8) having their respective initial conditions and final-time conditions with the controls value state in equation (7.10). The method called fourth forward-backward Runge-Kutta sweep is used to solve this optimality system. Using fourth-order forward Runge-Kutta method, the state equation (7.1) is solved with the initial value of state variables. After obtaining the solution of state functions and the value of optimal controls, the adjoint equations (7.8) were solved using the backward fourth order Runge Kutta due to the transversality conditions. Then we update the controls by using a convex combination of the previous controls and the value from the optimality conditions (7.10). This process is repeated and iterations

are finished when the values at before iterations are near to the ones at the present iterations (Lenhart and Workman, 2007). The optimal control problem is simulated using the parameter values given in Table 4.4 and with the initial conditions used for the state variables are $\mathtt{S}_h(0) = 100, \mathtt{E}_h(0) = 20, \mathtt{I}_h(0) = 10, \mathtt{R}_h(0) = 0, \mathtt{S}_m(0) = 300, \mathtt{E}_m(0) = 60, \mathtt{I}_m(0) = 30$ and $\mathtt{T}(0) = 16.1^oC$. The values of the weight constants of the state and controls that we used are given as $\mathtt{B}_1 = 80, \mathtt{B}_2 = 60, \mathtt{B}_3 = 100, \mathtt{D}_1 = 60, \mathtt{D}_2 = 100$ and $\mathtt{D}_3 = 80$.

In this section, to determine the role of each control on the minimizing of malaria, we used the following strategies with different combination of more than one control at a time and three controls at a time.

Strategy A: Implementing the treated bed net (u_1) and treatment of infected (u_2)
Strategy B: Implementing the treated bed net (u_1) and indoor residual spraying (u_3)
Strategy C: Implementing the treatment of infected (u_2) and indoor spraying (u_3)
Strategy D: Using the treated bed net (u_1), treatment (u_2) and indoor spraying (u_3)

7.1 Strategy A: Implementing the treated bed net (u_1) and treatment with drugs (u_2)

In this strategy, we apply the combinations of two controls by treated bed net u_1 and treatment for the infected human using anti-malaria drugs u_2 to minimize the objective function (7.2) whereas the control indoor spray of insecticides u_3 is set to zero. From the Figures 7.1**a** and 7.1**b** the total population of exposed human and infected human are decreased in the use of controls than the case there is no controls and are tends to their lowest value at the end of the intervention while in Figure 7.1**c** infected mosquito in the presence of controls is decreased. In contrast, in cases without controls, the infected mosquito is increasing. In order to minimize the number of exposed human, infected human, infected mosquito populations and the cost corresponding with the controls u_1 and u_2, the control profiles shown in Figure 7.1**d** indicate that use of the treated bed nets u_1 maintained its maximum level bound 100% throughout the entire time of strategy and treatment the infected human with anti-malaria drugs u_2 is intended upper bound 100% for 6 days before gradually declines to its lower value at the final time.

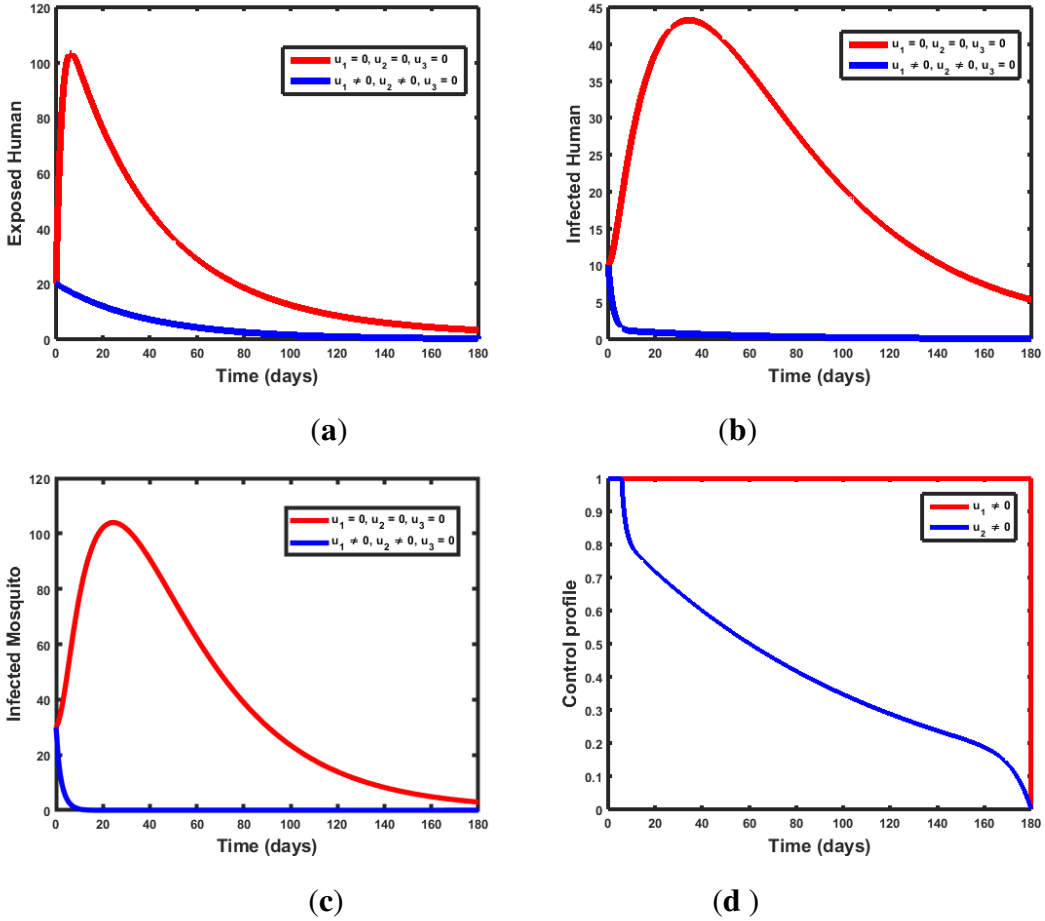

(**a**) (**b**)

(**c**) (**d**)

Figure 7.1: Simulations result with strategy of treated bed net (u_1) and treatment (u_2)

7.2 Strategy B: Implementing the bed net (u_1) and indoor spraying (u_3)

In this strategy to minimize the objective function (7.2) the combinations of two controls protective using treated bed net u_1 and an indoor spraying of insecticides u_3 while the control treatment for the infected human with anti-malarial drugs u_2 is set to zero are implemented. In Figures 7.2**a**, 7.2**a**, and 7.2**c** the total population of exposed human, infected human and infected mosquito are reducing rapidly if there is the use of controls than the case absence of the controls. Using the controls, the total number of exposed human $\mathtt{E}_h$, infected human $\mathtt{I}_h$ and infected mosquito I_m are tends to their lowest value at the end of the intervention. In Figure 7.2**d** the profile of the control implies that the use of the treated bed nets u_1 maintained its the upper bound 100% for 178 days in the entire time of strategy and an indoor spray of insecticides u_3 is retained its high level 100% till 18 days and gradually reduces to their lower bound in the final time.

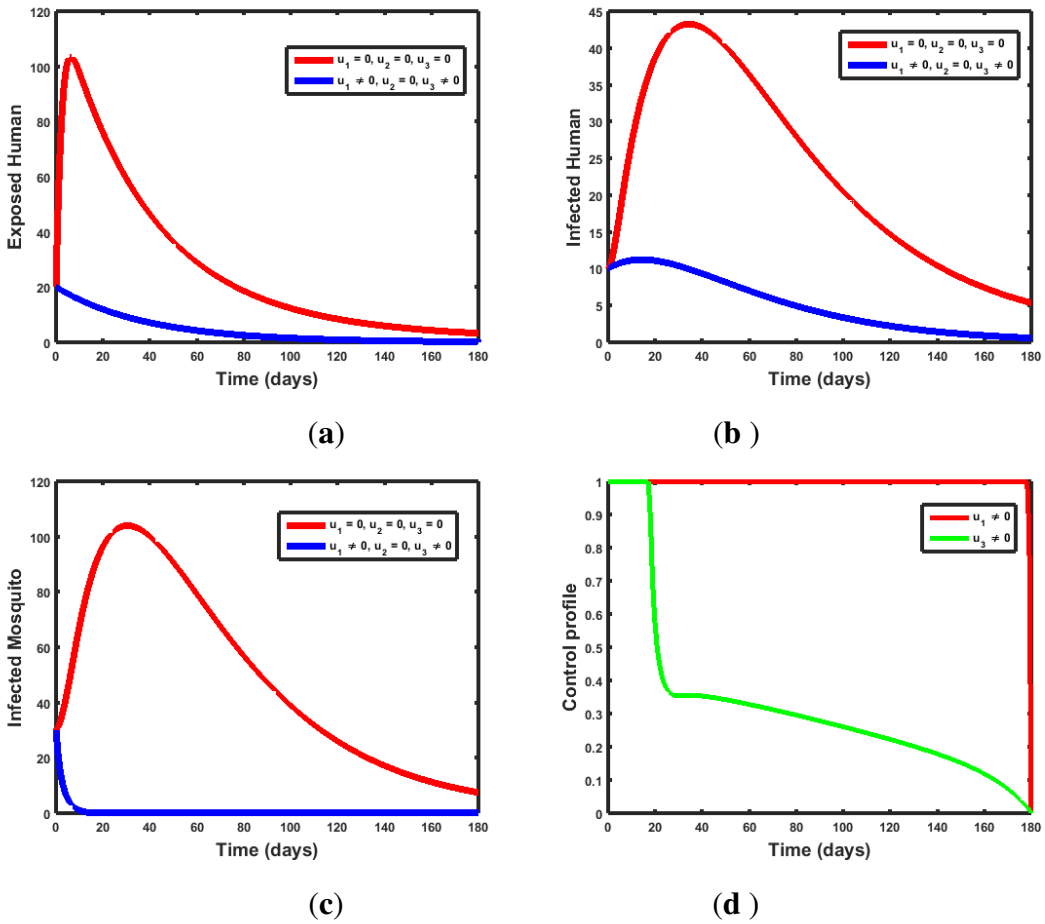

Figure 7.2: Simulations result with treated bed net (u_1) and indoor spraying (u_3)

7.3 Strategy C: Implementing the treatment (u_2) and indoor spraying (u_3)

In this approach, the objective function (7.2) is optimized using the combinations of two controls, treatment of infected human with anti-malarial drugs u_2 and an indoor spraying of insecticides u_3 with the use of treated bed nets u_1 is set to zero. The results in Figures 7.3**a** and 7.3**b** shows that the significant number of human exposed and human infected are higher in the absence of controls than in the case use of controls. The total population number of exposed human E_h and infected humans I_h declines to their lowest value at the end of the day. In Figure 7.3**c**, infected mosquito in the presence of controls is smaller than in case of without controls and downfall to the minimum value at the end of the intervention. Similarly, in Figure 7.3**d**, the control profiles indicate that both treatments of infected human with anti-malaria drugs u_2 and an indoor spraying of insecticides u_3 maintained their upper bound 99% for 30 days and 60 days respectively before gradually reduces to their minimum at the end of the intervention.

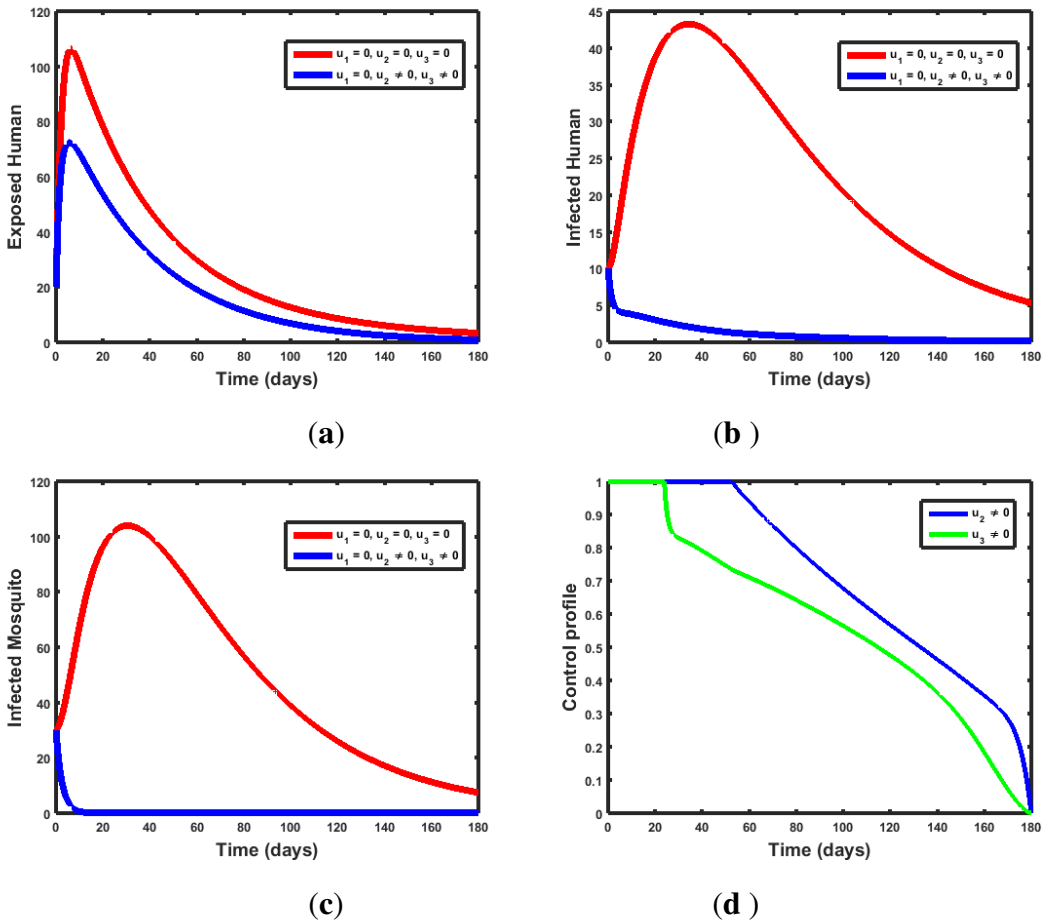

(**a**) (**b**)

(**c**) (**d**)

Figure 7.3: Simulations result with treatment (u_2) and indoor spraying (u_3)

7.4 Strategy D: Using treated (u_1), treatment (u_2) and indoor spraying (u_3)

To minimize the objective function, we used all controls using treated bed net u_1, treatment for the infected human with anti-malaria drugs u_2, and indoor spraying of insecticides u_3. It can be observed that in Figures 7.4**a**, 7.4**b**, and 7.4**c** the total population of exposed human, infected human and infected mosquito populations are increased in the absence of controls while they are decreased in the presence of controls. The total number of exposed human E_h, infected human I_h and infected mosquito I_m are declined to their lowest value at the end of 180 days. From Figure 7.4**d** the control profiles with this strategy, the use of the treated bed nets u_1 almost maintained its maximum level 100% for 176 days in the entire time of the strategy and treatment the infected human with anti-malaria drugs u_2 is retained maximum coverage 100% for 6 days while the control indoor insecticides spraying u_3 keep its maximum average for 16 days before gradually tends to their minimum value at the end of the final time.

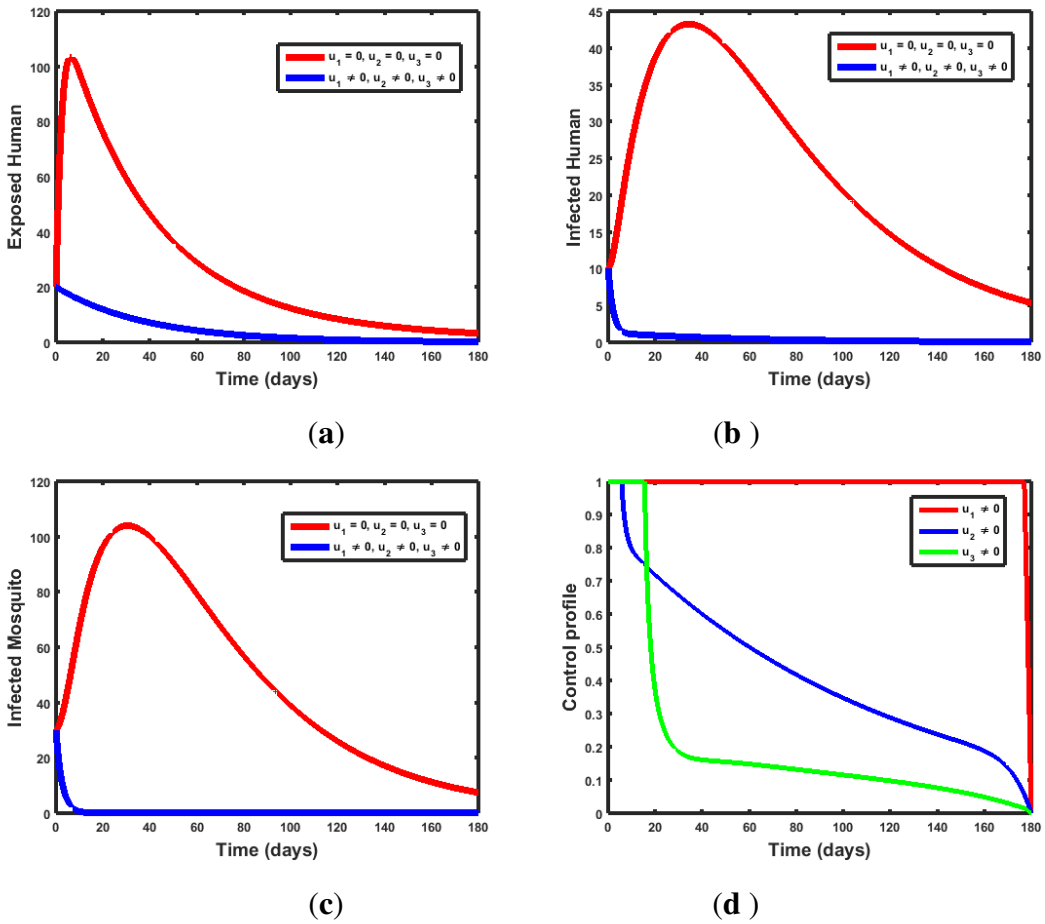

Figure 7.4: Simulations with treated (u_1), treatment (u_2) and indoor spraying (u_3)

7.6 Cost effectiveness analysis

Note that we cannot determine the least cost strategy with limited resources from the above Figures (7.1 - 7.4). In this section, we need to illustrate the most effective and less costly strategy with analysis of cost-effectiveness to find the intervention that used to eradicate the malaria. To obtain this strategy, the method called incremental cost-effectiveness ratio (ICER) is used. Mathematically for two strategies **i** and **j**, the incremental cost-effectiveness ratio is computed by (Akanni et al., 2019)

$$\frac{\text{Difference in averted costs between two strategies } \mathbf{i} \text{ and } \mathbf{j}}{\text{Difference in infections averted bewteen two strategies } \mathbf{i} \text{ and } \mathbf{j}}.$$

Using the numerical simulation result of the malaria model (7.1), the total number of people averted is obtained by subtracting the total number of new cases with control from the total number of new cases without control. The total cost of each strategy can be obtain using their respective cost functions $\frac{1}{2}\mathtt{D}_1 u_1^2$, $\frac{1}{2}\mathtt{D}_2 u_2^2$ and $\frac{1}{2}\mathtt{D}_3 u_3^2$ to calculate over the time of intervention (Handari et al., 2019). From the result of simulation of the system (7.1) using the values of

parameters in Table 4.4, the estimated total number of people averted in increasing order and total cost are listed in Table 7.1.

Table 7.1: Total amount of infection averted and total cost for all strategies

Strategies	**Total infections averted**	**Total cost ($)**
Strategy **B**	3751.40	7011.747
Strategy **C**	4531.14	9099.090
Strategy **A**	4673.15	8304.796
Strategy **D**	4673.16	9152.528

Based on the total amount of people averted and total cost of each strategy as obtained in Table 7.1 to compare two intervention strategies, the incremental cost effectiveness ratio (ICER) for the each competing strategies is estimated as given as

$$\begin{aligned}
\text{ICER}(\mathbf{B}) &= \frac{7011.747}{3751.40} = 1.869 \\
\text{ICER}(\mathbf{C}) &= \frac{9099.090 - 7011.747}{4531.14 - 3751.40} = 779.739 \\
\text{ICER}(\mathbf{A}) &= \frac{8304.796 - 9099.090}{4673.15 - 4531.14} = -5.593 \\
\text{ICER}(\mathbf{D}) &= \frac{9152.528 - 8304.796}{4673.16 - 4673.15} = 84,773.17
\end{aligned}$$

The amount of people averted in Strategy **B**, **C**, **A** and **D** in an increasing rank and the total cost is given in Table 7.2.

Table 7.2: Increasing order of infections averted.

Strategies	**Total infections averted**	**Total cost ($)**	**ICER**
Strategy **B**	3751.40	7011.747	1.869
Strategy **C**	4531.14	9099.090	779.739
Strategy **A**	4673.15	8304.796	-5.593
Strategy **D**	4673.16	9152.528	84,773.17

From the strategies **B** and **C** with their competition in Table 7.2, we obtained that ICER(**B**) is less than ICER(**C**). This implies that strategy **C** is dominated by Strategy **B**. It mean that strategy **C** more expensive than strategy **B**. Thus, we have deleted **C** from the competition strategies. Then again re-calculate the ICER for the remaining competing strategies **B**, **A** and **D** as given in Table 7.3.

Table 7.3: Comparison between interventions **B** and **A**

Strategies	**Total infections averted**	**Total cost ($)**	**ICER**
Strategy **B**	3751.40	7011.747	1.869
Strategy **A**	4673.15	8304.796	1.402
Strategy **D**	4673.16	9152.528	84,773.17

The competition between interventions **B** and **A** was shown in Table 7.3. From this the ICER(**A**) is less than ICER(**B**). This indicates that strategy **B** dominated by strategy **A**. Hence, strategy **A** is more efficient and less cheaper than strategy **B**. So that we excluded strategy **B** from the list of competing and re-calculate the ICER as given in Table 7.4.

Table 7.4: Comparison between interventions **A** and **D**

Strategies	**Total infections averted**	**Total cost ($)**	**ICER**
Strategy **A**	4673.15	8304.796	1.777
Strategy **D**	4673.16	9152.528	84,773.17

In Table 7.4 there is a comparison between strategies **A** and **D**. From this the ICER(**A**) is less than ICER(**D**). This shows that strategy **D** strongly dominated by strategy **A**. So that strategy **A** provided the less cost and the more effective. Obviously, based upon the result, we suggest that strategy **A** which is a combination of treated bed net and treatment is the most effective and least-cost strategy to prevent the disease.

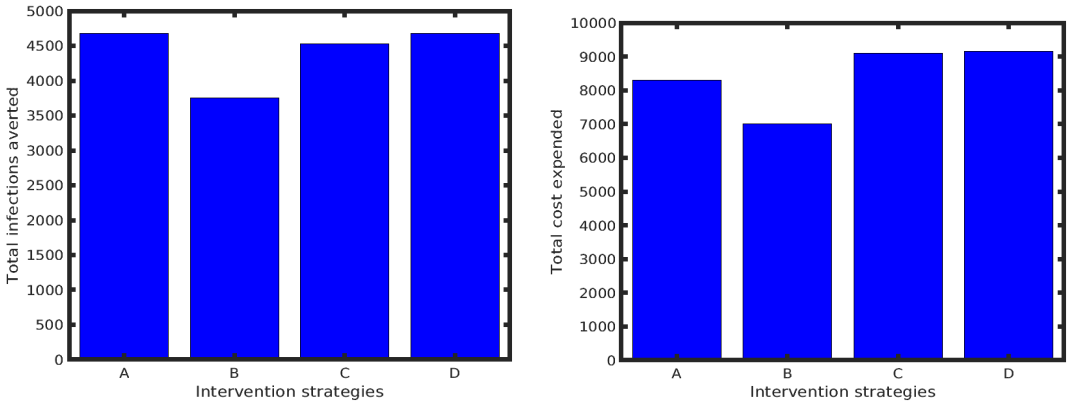

(**a**) (**b**)

Figure 7.5: The total infections averted with their respect total cost expended of strategies

CONCLUSIONS AND RECOMMENDATIONS

Malaria is a parasitic vector-borne disease that is dominant in many parts of the world mostly with large proportion in sub-Saharan Africa (WHO, 2020). In this study, we considered the impact of temperature variation on the transmission dynamics of malaria epidemics and predict an optimal control strategies with least cost effectiveness analysis. In this chapter, we present the conclusions, future research and recommendations.

Conclusions

In this dissertation, deterministic mathematical models have been proposed to illustrate the impact of temperature variability on malaria epidemics. Qualitatively these models have been analyzed. An application of optimal control theory is applied to determine the best optimal strategy. Then the cost effectiveness analysis is implemented to describe the least cost strategy to minimize the malaria burden with limited resources.

In Chapter 4, a non-linear deterministic model is presented that describes the impact of temperature variability on epidemics of malaria. The model analysis showed that all solutions of the systems are positive and bounded with initial conditions in a certain set. The basic reproduction number with respect to the disease free equilibrium was computed using the next generation matrix technique. If the basic reproduction number is less than one, then the disease free equilibrium is both locally and globally asymptotically stable conditionally. On the other hand, the positive endemic equilibrium is locally and globally asymptotically stable if the basic reproduction number is greater than unity. The sensitivity analysis of the model has described and the model exhibits forward and backward bifurcation. Our study confirm that temperature variation plays a significant role on the transmission of malaria. Furthermore, the study reveals that bringing the basic reproduction number less than one is not sufficient condition for the elimination of malaria from the community. Hence, it is important to reduce the mosquito breeding rate and malaria infection. Moreover, we performed the numerical simulation using matlab software. The simulations results agreed with the an-

alytical result of our model.

In Chapter 5, we have extended the model introduced in chapter 5.1 by introducing the exposed class, to the SEIRS (susceptible - exposed - infected - recovered - susceptible) - SEI (susceptible - exposed - infected) malaria transmission model. Firstly, we have shown the invariant region and positivity of the solution which illustrate the biological meaningful and mathematically well-posed of the model. By applying the next-generation matrix method, the basic reproduction number with respect to the malaria disease free equilibrium was computed. The local stability of the equilibrium points is obtained using the Routh-Hurwitz criterion whereas global stability is performed by the Lyapunov function. We proved that if the basic reproduction number is less than unity, then the disease free equilibrium is locally and globally asymptotically stable whereas the unique endemic equilibrium exists if the basic reproduction number is greater than one. Moreover, the sensitivity analysis of the basic reproduction number with respect to all basic parameters was obtained and contact rate is highly sensitive over the basic reproduction number such that increase the contact rate could be increase the basic reproduction number. Using the Centre Manifold theorem we identified that the model has a forward and backward bifurcation. The qualitative analysis reveals that decrease the contact rate, increasing the death rate of mosquito and increase the treated rate of infected human can reduce the malaria burden in the community. The numerical simulation results demonstrate good agreement with our analytical results.

In Chapter 6, we have extended the malaria transmission model (4.1) into the optimal control model considering the crucial time-dependent control variables such as prevention using treated bed net, treatment of infected human with drug and using indoor residual spraying for mosquito reducing strategy. The existence of optimal controls is depicted. The Pontraygin's maximum principle was applied to obtain the necessary condition for the optimal control. A numerical simulation of optimality system is carried out to determine the optimality of different combinations of the controls. The cost-effectiveness analysis is investigated with all the various combinations of the controls considered through the study to obtain the least-cost strategy. To obtain this strategy, we used the method called incremental cost-effectiveness ratio (ICER). Applying this technique we compared more than one competing strategy incrementally, one intervention should be compared with the next less effective alternative. Based on the result of numerical simulations of the optimal control and analysis of cost effectiveness, we suggest that the combination of treatment and indoor insecticide spray is the optimal strategy and less costly to effectively minimize the malaria spread.

In Chapter 7, an optimal control problem was formulated by extending the malaria transmission model (5.1) by incorporating three continuous controls, namely personal protection using treated bed net, treatment of infected human with anti-malarial drug and indoor residual spraying for vector killing strategy. We described the objective function that used to reduce the total amount of exposed human, infected human, infected mosquito and costs of controls. The necessary condition for the optimal control problem is obtained using the Pontraygin's maximum principle. Numerical simulation is performed by considering a combining two controls at a moment then finally implementing all three control variables. Then also the analysis of cost-effectiveness is investigated with all the different combination of the controls. It is revealed that from the cost-effectiveness analysis of the employed strategies, the integrated strategy of treated bed nets and treatment is the most effective and least cost to reduce the transmission of malaria.

Future Research

In this dissertation the deterministic models that we have formulated can be extended into a lot of respects for future research as follows;

- This study focused solely on variation of temperature. However, rainfall variability could be strongly determines the malaria transmission dynamics. Thus, the impact of rainfall variability on the transmission of the malaria is a basic area of research to be investigated.

- An extension of the models in this dissertation to take care of the period between contacting disease and showing clinical symptoms will be interesting. It takes time for mosquito bites the human and then human becomes infectious. Thus, we can develop a delay differential equation models.

- A basic area of research to be investigated is a life cycle of mosquito in a compartmental formulation, starting with aquatic mosquitoes stages, eggs, larvae and pupae grouped into a single compartment and further subdivide adult mosquito into more compartments.

Recommendations

Malaria eradication remains a big challenge to health organizations in most developing countries. Public health policy makers can use the optimal strategies with the appropriate implementation to reduce the malaria. Thus, in the long run this research could help as a baseline to create a link between mathematics and public health organizations. Based on our study it is recommended that

- Our main focus is clearly stated with respect to temperature variation which plays a significant role on the transmission dynamics of malaria. This event does lead to increase mosquitoes breeding rate and malaria infection. Hence, adequate preparation should be made by all concern bodies in order to minimize the transmission dynamics of malaria.
- To reduce the contact between mosquitoes and humans, it is recommended that the stockholders should be using treated bed net and destroying the adult mosquitoes using indoor residual spraying.
- The findings of the study also reveal that the combination of treated bed net, treatment of infected individuals and indoor residual spraying has significant impact on the spread of the disease. Hence, it is recommended to employ these control strategies to minimize the health burden of malaria.

Research Fund Acknowledgment

This research project is funded by Adama Science and Technology University under the grant number ASTU/SP-R/028/17, Adama, Ethiopia.

REFERENCES

Abdullahi, M. B., Hasan, Y. A., and Abdullah, F. A. (2015). Optimal strategy for controlling the spread of plasmodium knowlesi malaria: Treatment and culling. In *AIP Conference Proceedings*, volume 1660, page 050005. AIP Publishing LLC.

Abiodun, G. J. (2017). A mathematical model for studying the impact of climate variability on malaria epidemics in south africa.

Abiodun, G. J., Maharaj, R., Witbooi, P., and Okosun, K. O. (2016). Modelling the influence of temperature and rainfall on the population dynamics of anopheles arabiensis. *Malaria journal*, 15(1):1–15.

Abiodun, G. J., Witbooi, P., and Okosun, K. O. (2018). Modelling the impact of climatic variables on malaria transmission. *Hacettepe Journal of Mathematics and Statistics*, 47(2):219–235.

Abioye, A. I., Ibrahim, M. O., Peter, O. J., and Ogunseye, H. A. (2020). Optimal control on a mathematical model of malaria. *UPB Sci. Bull., Ser. A. Appl. Math. Phys*, 82(3):178–190.

Agusto, F., Gumel, A., and Parham, P. (2015). Qualitative assessment of the role of temperature variations on malaria transmission dynamics. *Journal of Biological Systems*, 23(04):1550030.

Agusto, F. B. (2020). Optimal control and temperature variations of malaria transmission dynamics. *Complexity*, 2020.

Agusto, F. B., Del Valle, S. Y., Blayneh, K. W., Ngonghala, C. N., Goncalves, M. J., Li, N., Zhao, R., and Gong, H. (2013). The impact of bed-net use on malaria prevalence. *Journal of theoretical biology*, 320:58–65.

Agusto, F. B., Marcus, N., and Okosun, K. O. (2012). Application of optimal control to the epidemiology of malaria.

Akanni, J., Akinpelu, F., Olaniyi, S., Oladipo, A., and Ogunsola, A. (2019). Modelling financial crime population dynamics: optimal control and cost-effectiveness analysis. *International Journal of Dynamics and Control*, pages 1–14.

Aldila, D. and Angelina, M. (2021). Optimal control problem and backward bifurcation on malaria transmission with vector bias. *Heliyon*, 7(4):e06824.

Allen, L. J. (2007). *Introduction to mathematical biology*. Pearson/Prentice Hall.

Alonso, D., Bouma, M. J., and Pascual, M. (2011). Epidemic malaria and warmer temperatures in recent decades in an east african highland. *Proceedings of the Royal Society B: Biological Sciences*, 278(1712):1661–1669.

Anderson, R. M. and May, R. M. (1992). *Infectious diseases of humans: dynamics and control*. Oxford university press.

Aron, J. L. and May, R. M. (1982). The population dynamics of malaria. In *The population dynamics of infectious diseases: theory and applications*, pages 139–179. Springer.

Bacaër, N. (2011). *A short history of mathematical population dynamics*. Springer Science & Business Media.

Bakare, E. and Hoskova-Mayerova, S. (2021). Numerical treatment of optimal control theory applied to malaria transmission dynamic model. *Quality & Quantity*, pages 1–23.

Beck, A. (2014). *Introduction to nonlinear optimization: Theory, algorithms, and applications with MATLAB*. SIAM.

Berhe, H. W. (2020). Optimal control strategies and cost-effectiveness analysis applied to real data of cholera outbreak in ethiopia's oromia region. *Chaos, Solitons & Fractals*, 138:109933.

Berhe, H. W., Makinde, O. D., and Theuri, D. M. (2019). Co-dynamics of measles and dysentery diarrhea diseases with optimal control and cost-effectiveness analysis. *Applied Mathematics and Computation*, 347:903–921.

Bhuju, G., Phaijoo, G., and Gurung, D. (2018). Mathematical study on impact of temperature in malaria disease transmission dynamics. *Advances in Computer Sciences*, 1(2):1–8.

Blayneh, K., Cao, Y., and Kwon, H.-D. (2009). Optimal control of vector-borne diseases: treatment and prevention. *Discrete & Continuous Dynamical Systems-B*, 11(3):587.

Boltyanskiy, V., Gamkrelidze, R. V., and Pontryagin, L. S. (1961). Theory of optimal processes. Technical report, JOINT PUBLICATIONS RESEARCH SERVICE ARLINGTON VA.

Boyce, W. E., DiPrima, R. C., and Meade, D. B. (2017). *Elementary differential equations*. John Wiley & Sons.

Castillo-Chavez, C. and Song, B. (2004a). Dynamical models of tuberculosis and their applications. *Mathematical Biosciences & Engineering*, 1(2):361.

Castillo-Chavez, C. and Song, B. (2004b). Dynamical models of tuberculosis and their applications. *Mathematical Biosciences & Engineering*, 1(2):361.

Chitnis, N., Cushing, J. M., and Hyman, J. (2006). Bifurcation analysis of a mathematical model for malaria transmission. *SIAM Journal on Applied Mathematics*, 67(1):24–45.

Chitnis, N., Hyman, J. M., and Cushing, J. M. (2008). Determining important parameters in the spread of malaria through the sensitivity analysis of a mathematical model. *Bulletin of mathematical biology*, 70(5):1272.

Chong, E. K. and Zak, S. H. (2004). *An introduction to optimization*. John Wiley & Sons.

Chu, C. S. and White, N. J. (2021). The prevention and treatment of plasmodium vivax malaria. *PLoS medicine*, 18(4):e1003561.

Chukwu, A., Akinyemi, J., Adeniyi, M., and Salawu, S. (2020). On the reproduction number and the optimal control of infectious diseases in a heterogenous population. *Advances in Difference Equations*, 2020(1):1–14.

Coetzee, M. (2004). Distribution of the african malaria vectors of the anopheles gambiae complex. *The American journal of tropical medicine and hygiene*, 70(2):103–104.

EPHI (2018). Ethiopia national malaria indicator survey. *Ethiopian Public Health Institute, Addis Ababa*.

Fleming, W. and Rishel, R. (1975). Optimal deterministic and stochastic control. *Applications of Mathematics, Springer, Berlin, Germany*.

Garba, S. M. and Danbaba, U. A. (2020). Modeling the effect of temperature variability on malaria control strategies. *Mathematical Modelling of Natural Phenomena*, 15:65.

Gashaw, K. W., Kassa, S. M., and Ouifki, R. (2018). Climate-dependent malaria disease transmission model and its analysis. *PhD dissertation, Department of mathematics, Addis Ababa University, Ethiopia*.

Gashaw, K. W., Kassa, S. M., and Ouifki, R. (2019). Climate-dependent malaria disease transmission model and its analysis. *International Journal of Biomathematics*, 12(08):1950087.

Ghosh, M., Olaniyi, S., and Obabiyi, O. S. (2020). Mathematical analysis of reinfection and relapse in malaria dynamics. *Applied Mathematics and Computation*, 373:125044.

Handari, B. D., Vitra, F., Ahya, R., Aldila, D., et al. (2019). Optimal control in a malaria model: intervention of fumigation and bed nets. *Advances in Difference Equations*, 2019(1):1–25.

Herdicho, F. F., Chukwu, W., Tasman, H., et al. (2021). An optimal control of malaria transmission model with mosquito seasonal factor. *Results in Physics*, 25:104238.

Hirsch, M. W., Smale, S., and Devaney, R. L. (2012). *Differential equations, dynamical systems, and an introduction to chaos*. Academic press.

Huo, H.-F. and Qiu, G.-M. (2014). Stability of a mathematical model of malaria transmission with relapse. In *Abstract and Applied Analysis*, volume 2014. Hindawi.

Ibrahim, M. M., Kamran, M. A., Naeem Mannan, M. M., Kim, S., and Jung, I. H. (2020). Impact of awareness to control malaria disease: A mathematical modeling approach. *Complexity*, 2020.

Jepson, W., Moutia, A., and Courtois, C. (1947). The malaria problem in mauritius: the bionomics of mauritian anophelines. *Bulletin of entomological research*, 38(1):177–208.

John, S. Z., Yusuf, H. U., Usman, S. A., and Adamu, S. (2020). Mathematical model for the dynamics of malaria transmission incorporating vaccine, protection and treatment. In *Science Forum (Journal of Pure and Applied Sciences)*, volume 20, pages 124–130. Faculty of Science, Abubakar Tafawa Balewa University Bauchi.

Khalil, H. K. and Grizzle, J. W. (2002). *Nonlinear systems*, volume 3. Prentice hall Upper Saddle River, NJ.

Koutou, O., Traoré, B., and Sangaré, B. (2018). Mathematical model of malaria transmission dynamics with distributed delay and a wide class of nonlinear incidence rates. *Cogent Mathematics & Statistics*, 5(1):1564531.

Kyere, S., Boateng, F., Hoggar, G., and Jonathan, P. (2018). Stochastic optimal control model of malaria disease. *Adv Comput Sci*, 1:106.

La Salle, J. P. (1976). *The stability of dynamical systems*. SIAM.

Laarabi, H., Labriji, E. H., Rachik, M., and Kaddar, A. (2012). Optimal control of an epidemic model with a saturated incidence rate. *Nonlinear analysis: modelling and control*, 17(4):448–459.

Lenhart, S. and Workman, J. T. (2007). *Optimal control applied to biological models*. CRC press.

Lukes, D. (1982). Differential equations, ser. *Mathematics in Science and Engineering. London: Academic Press Inc.[Harcourt Brace Jovanovich Publishers]*, 162.

Macdonald, G. et al. (1957). The epidemiology and control of malaria. *The Epidemiology and Control of Malaria.*

Makinde, O. D. and Okosun, K. O. (2011). Impact of chemo-therapy on optimal control of malaria disease with infected immigrants. *BioSystems*, 104(1):32–41.

Mandal, S., Sarkar, R. R., and Sinha, S. (2011). Mathematical models of malaria-a review. *Malaria journal*, 10(1):1–19.

Mohammed-Awel, J., Agusto, F., Mickens, R. E., and Gumel, A. B. (2018). Mathematical assessment of the role of vector insecticide resistance and feeding/resting behavior on malaria transmission dynamics: Optimal control analysis. *Infectious Disease Modelling*, 3:301–321.

Mojeeb, A. and Adu, I. K. (2017). Simple mathematical model for malaria transmission. *Journal of Advances in Mathematics and Computer Science*, pages 1–24.

Mordecai, E. A., Paaijmans, K. P., Johnson, L. R., Balzer, C., Ben-Horin, T., de Moor, E., McNally, A., Pawar, S., Ryan, S. J., Smith, T. C., et al. (2013). Optimal temperature for malaria transmission is dramatically lower than previously predicted. *Ecology letters*, 16(1):22–30.

Mwamtobe, P. M., Abelman, S., Tchuenche, J. M., and Kasambara, A. (2015). Optimal (control of) intervention strategies for malaria epidemic in karonga district, malawi. In *Abstract and Applied Analysis*, volume 2014. Hindawi.

Ngarakana-Gwasira, E., Bhunu, C., and Mashonjowa, E. (2014). Assessing the impact of temperature on malaria transmission dynamics. *Afrika Matematika*, 25(4):1095–1112.

Ngarakana-Gwasira, E., Bhunu, C., Masocha, M., and Mashonjowa, E. (2016). Assessing the role of climate change in malaria transmission in africa. *Malaria research and treatment*, 2016.

Ngwa, G. A. and Shu, W. S. (2000). A mathematical model for endemic malaria with variable human and mosquito populations. *Mathematical and computer modelling*, 32(7-8):747–763.

Oke, S. I., Ojo, M. M., Adeniyi, M. O., and Matadi, M. B. (2020). Mathematical modeling of malaria disease with control strategy. *Commun. Math. Biol. Neurosci.*, 2020:Article–ID.

Okosun, K. and Makinde, O. (2013). Optimal control analysis of malaria in the presence of non-linear incidence rate. *Appl. Comput. Math*, 12(1):20–32.

Okosun, K. and Makinde, O. D. (2014). A co-infection model of malaria and cholera diseases with optimal control. *Mathematical biosciences*, 258:19–32.

Okosun, K. O., Ouifki, R., and Marcus, N. (2011). Optimal control analysis of a malaria disease transmission model that includes treatment and vaccination with waning immunity. *Biosystems*, 106(2-3):136–145.

Okosun, K. O., Rachid, O., and Marcus, N. (2013). Optimal control strategies and cost-effectiveness analysis of a malaria model. *BioSystems*, 111(2):83–101.

Okuneye, K., Eikenberry, S. E., and Gumel, A. B. (2019). Weather-driven malaria transmission model with gonotrophic and sporogonic cycles. *Journal of biological dynamics*, 13(sup1):288–324.

Olaniyi, S., Okosun, K., Adesanya, S., and Lebelo, R. (2020). Modelling malaria dynamics with partial immunity and protected travellers: optimal control and cost-effectiveness analysis. *Journal of biological dynamics*, 14(1):90–115.

Olaniyi, S., Okosun, K. O., Adesanya, S. O., and Areo, E. A. (2018). Global stability and optimal control analysis of malaria dynamics in the presence of human travelers. *The Open Infectious Diseases Journal*, 10(1).

Otieno, G., Koske, J. K., and Mutiso, J. M. (2016). Transmission dynamics and optimal control of malaria in kenya. *Discrete Dynamics in Nature and Society*, 2016.

Paaijmans, K. P., Wandago, M. O., Githeko, A. K., and Takken, W. (2007). Unexpected high losses of anopheles gambiae larvae due to rainfall. *PloS one*, 2(11):e1146.

Pontryagin, L. S. (2018). *Mathematical theory of optimal processes*. Routledge.

Romero-Leiton, J. P., Castellanos, J. E., and Ibargüen-Mondragón, E. (2019). An optimal control problem and cost-effectiveness analysis of malaria disease with vertical transmission applied to san andrés de tumaco (colombia). *Computational and Applied Mathematics*, 38(3):1–24.

Romero-Leiton, J. P., Montoya-Aguilar, J., and Ibargüen-Mondragón, E. (2018). An optimal control problem applied to malaria disease in colombia. *Applied Mathematical Sciences*, 12(6):279–292.

Ross, R. (1911). *The prevention of malaria*. John Murray.

Srivastav, A. K. and Ghosh, M. (2021). Modeling the transmission dynamics of malaria with saturated treatment: a case study of india. *Journal of Applied Mathematics and Computing*, pages 1–22.

Tchoumi, S., Diagne, M., Rwezaura, H., and Tchuenche, J. (2021). Malaria and covid-19 co-dynamics: A mathematical model and optimal control. *Applied Mathematical Modelling*.

Thomson, M., Connor, S., Milligan, P., and Flasse, S. (1997). Mapping malaria risk in africa: What can satellite data contribute? *Parasitology Today*, 13(8):313–318.

Tilahun, G. T., Makinde, O. D., and Malonza, D. (2018). Co-dynamics of pneumonia and typhoid fever diseases with cost effective optimal control analysis. *Applied Mathematics and Computation*, 316:438–459.

Traoré, B., Koutou, O., and Sangaré, B. (2020). A global mathematical model of malaria transmission dynamics with structured mosquito population and temperature variations. *Nonlinear Analysis: Real World Applications*, 53:103081.

United Nation, D. o. E. and affairs population dynamics report, S. (2019).

Van den Driessche, P. and Watmough, J. (2002). Reproduction numbers and sub-threshold endemic equilibria for compartmental models of disease transmission. *Mathematical biosciences*, 180(1-2):29–48.

Wang, S.-F., Hu, L., and Nie, L.-F. (2021). Global dynamics and optimal control of an age-structure malaria transmission model with vaccination and relapse. *Chaos, Solitons & Fractals*, 150:111216.

WHO (2020). World health organization. world malaria report 2020, available from: https://www.who.int/publications/i/item/9789240015791.

Wiggins, S. (2003). *Introduction to applied nonlinear dynamical systems and chaos*, volume 2. Springer Science & Business Media.

Yang, H., Wei, H., and Li, X. (2010). Global stability of an epidemic model for vector-borne disease. *Journal of Systems Science and Complexity*, 23(2):279–292.

Yang, H. M. (2000). Malaria transmission model for different levels of acquired immunity and temperature-dependent parameters (vector). *Revista de saude publica*, 34:223–231.

Yiga, V., Nampala, H., and Tumwiine, J. (2020). Analysis of the model on the effect of seasonal factors on malaria transmission dynamics. *Journal of Applied Mathematics*, 2020.

Zone, E. S. A. (2019). East shewa administration zone.

APPENDIX A

MATHEMATICAL PRELIMINARIES

In this section, we described the basic concept in mathematical models. Those basic concepts includes the basic differential equations, local and global stability analysis of dynamical systems, bifurcation analysis, optimal control theory involving intervention strategies to combating the spread of the diseases with minimal cost. In the next parts, we present in the sequel some basic mathematical preliminaries that are critical in the use of differential equations to model infectious diseases.

1. Ordinary differential equations

A differential equation is an equation involving a function together with its derivatives with respect to some independent variable(s). A differential equation is said to be an ordinary differential equation if the derivative depends on only one variable. Infectious disease modelling are mostly deterministic models and are ordinary differential equations. This thesis involves deterministic models and therefore emphasis would be on ordinary differential equations.

Definition 1.1 Let x be the state of a dynamical system. Then a generalized deterministic model involving x is given by

$$\frac{dx}{dt} = f(x,t,\vartheta) \tag{19}$$

where $x \in \mathbb{R}^n$, t denotes time and $\vartheta \in \mathbb{R}^m$ denotes the parameters upon which the evolution of the system depends. An equation (19) is called an ordinary differential equation(ODE). An ordinary differential equation in which the time variable explicitly appears are said to be *non-autonomous* whereas those in which the time variable does not explicitly appear are said to be *autonomous*. Almost epidemic models including those considered that the autonomous

systems which can be written in the form

$$\frac{dx}{dt} = f(x) \tag{20}$$

where $x = (x_1, x_2, ..., x_n)$ and $\frac{dx}{dt} = f(x)$ denotes derivatives of the state variable with respect to time. In other words, a given system with n compartments, a general dynamical system that describes the evolution of the system is given as

$$\begin{cases} \frac{dx_1}{dt} = f_1(x_1, x_2, ..., x_n) \\ \frac{dx_2}{dt} = f_2(x_1, x_2, ..., x_n) \\ \qquad\qquad \vdots \\ \frac{dx_{n-1}}{dt} = f_{n-1}(x_1, x_2, ..., x_n) \\ \frac{dx_n}{dt} = f_n(x_1, x_2, ..., x_n). \end{cases} \tag{21}$$

And the dynamical system of eq. (20) is the compact of the dynamical system of the (21).

Definition 1.2 (Khalil and Grizzle, 2002) A function $f(x)$ is said to be *locally Lipschitz* on a domain $\Theta \in \mathbb{R}^n$ if each point of Θ has a neighborhood Θ_0 such that f satisfies

$$|f(x) - f(y)| \leq \mathtt{M}|x - y| \quad \text{for all} \quad x, y \in \Theta_0. \tag{22}$$

f is *globally Lipschitz* if it is *locally Lipschitz* for every neighborhood Θ_0 of $\mathbb{R}^n$.

Theorem 1.1 (Hirsch et al., 2012) Suppose that $f \in C^1(\mathbb{R}^n)$ and that $f(x)$ satisfies the *global Lipschitz* condition

$$|f(x) - f(y)| \leq \mathtt{M}|x - y| \tag{23}$$

for all $x, y \in \mathbb{R}^n$. Then for $x_0 \in \mathbb{R}^n$, the initial value problem (20) has a unique solution $x(t)$ defined for all $t \in \mathbb{R}$.

2. Stability of equilibria of the system

Definition 2.1 (Equilibrium point (Boyce et al., 2017)) A point $x^* \in \mathbb{R}^n$ is said to be an equilibrium point of the equation (20) if $f(x^*) = 0$. And the equilibrium points are also called critical points, fixed point or steady state solution of the model. An ordinary differential equation epidemic models given in the equation (20), their equilibrium points are always computed by equating the left hand-sides of the equations zero and then compute for the state variable.

Definition 2.2 (**Locally stability** (Boyce et al., 2017)) An equilibrium point x^* of the equation (20) is said to be *locally stable* if all solutions sufficiently close to x^* stay nearby for all $t \geq 0$. That is $\forall \varepsilon \geq 0, \exists \delta \geq 0$ such that $|x - x^*| \leq \delta \Rightarrow |x(t) - x^*| \leq \varepsilon$. An equilibrium point which is not locally stable is said to be unstable.

Definition 2.3 (**Asymptotic stability** (Boyce et al., 2017)) An equilibrium point x^* of the equation (20) is said to be *locally asymptotically stable* if it is locally stable and all solutions starting near x^* tend towards x^* as time tends to infinity. That is $\forall \varepsilon \geq 0, \exists \delta \geq 0$ such that $|x - x^*| \leq \delta \Rightarrow \lim_{x \to \infty} x(t) = x^*$.

3. Local stability of equilibrium points

The basic important point is to know the behavior of a dynamical system near an equilibrium point. The Jacobian matrix is the matrix of the partial derivatives of each function with respect to each variable that provides a linear approximation of a system at equilibrium points. In mathematical modelling so that to linearize the system, we should compute the Jacobian matrix of the system.

Definition 3.1 The Jacobian of the dynamical system in equation (21) is given by

$$\mathtt{J} = Df(x) = \begin{pmatrix} \frac{\partial f_1}{\partial x_1} & \frac{\partial f_1}{\partial x_2} & \cdots & \frac{\partial f_1}{\partial x_{n-1}} & \frac{\partial f_1}{\partial x_n} \\ \frac{\partial f_2}{\partial x_1} & \frac{\partial f_2}{\partial x_2} & \cdots & \frac{\partial f_2}{\partial x_{n-1}} & \frac{\partial f_2}{\partial x_n} \\ \vdots & \vdots & \cdots & \vdots & \vdots \\ \frac{\partial f_{n-1}}{\partial x_1} & \frac{\partial f_{n-1}}{\partial x_2} & \cdots & \frac{\partial f_{n-1}}{\partial x_{n-1}} & \frac{\partial f_{n-1}}{\partial x_n} \\ \frac{\partial f_n}{\partial x_1} & \frac{\partial f_n}{\partial x_2} & \cdots & \frac{\partial f_n}{\partial x_{n-1}} & \frac{\partial f_n}{\partial x_n} \end{pmatrix}. \tag{24}$$

Definition 3.2 A critical point x^* of a dynamical system is said to be locally stable if all eigenvalues of the Jacobian evaluated at x^* are negative.

Definition 3.3 (**Routh Hurwitz Criteria** (Allen, 2007)) Consider the characteristic equation given as

$$\mathtt{P}(\lambda) = \lambda^n + a_1\lambda^{n-1} + a_2\lambda^{n-2} + \ldots + a_{n-1}\lambda + a_n = 0, \tag{25}$$

determining the n eigenvalues λ of a real $n\ x\ n$ square matrix A. Then the eigenvalues λ all have negative real parts if $det(\mathtt{H}_j) > 0$ for $j = 1,2,..,n$ and `where`,

$$\mathtt{H}_1 = a_1,\ \mathtt{H}_2 = \begin{pmatrix} a_1 & 1 \\ a_3 & a_2 \end{pmatrix},\ \mathtt{H}_3 = \begin{pmatrix} a_1 & 1 & 0 \\ a_3 & a_2 & a_1 \\ a_5 & a_4 & a_3 \end{pmatrix},\ \mathtt{H}_4 = \begin{pmatrix} a_1 & 1 & 0 & 0 \\ a_3 & a_2 & a_1 & 1 \\ a_5 & a_4 & a_3 & a_2 \\ a_7 & a_6 & a_5 & a_4 \end{pmatrix},...,$$

and

$$\mathtt{H}_n = \begin{pmatrix} a_1 & 1 & 0 & 0 & \cdots & 0 \\ a_3 & a_2 & a_1 & 1 & \cdots & 0 \\ a_5 & a_4 & a_3 & a_2 & \cdots & 0 \\ \vdots & \vdots & \vdots & \vdots & \cdots & \vdots \\ 0 & 0 & 0 & 0 & \cdots & a_n \end{pmatrix}.$$

Note that the steady state is stable (that is, $Re(\lambda) < 0$) for all λ if and only if $det(H_j) \geq 0$ for all $j = 1,2,3,...,n$ and the Routh-Hurwitz criterion is establish the local stability of equilibria points.

4. Global stability of equilibrium points

Definition 4.1 An equilibrium point x^* of (20) is said to be globally asymptotically stable if it is asymptotically stable for all initial condition $x_0 \in \mathbb{R}^n$.

Definition 4.2 (**Positive definite functions** (Wiggins, 2003))
A continuously differentiable function $V : \mathbb{R}^m \to \mathbb{R}$ is said to be positive definite in a region $U \in \mathbb{R}^m$ that contains the origin if $V(0) = 0$ and $V(x) > 0$ for $x \in U$ and $x \neq 0$. Conversely, $V(x)$ is said to be negative definite if $V(x) < 0$.

Definition 4.3 (**Lyapunov functions** (Wiggins, 2003))
A continuous differentiable function $\mathtt{V} : U \to \mathbb{R}$, where $U \subseteq \mathbb{R}^m$, is a Lyapunov function for $\dot{x} = f(x)$ at $x \in U$ if $\mathtt{V}(x)$ is positive definite at x^* and $\dot{\mathtt{V}}(x) \leq 0$ for all $x \in U$. Moreover, $\dot{\mathtt{V}}(x)$ is negative definite at x^*, then $\mathtt{V}$ is a strict Lyapunov function.

Theorem 4.1 (Global stability in terms of Lyapunov (Khalil and Grizzle, 2002))
Suppose that x^* is a equilibrium point of $\dot{x} = f(x)$. Suppose that for some open set $U \in \mathbb{R}^m$ containing x^* there exists $V : U \to \mathbb{R}$ such that V is Lyapunov at x^*. Then x^* is Lyapunov-stable. If V is strictly Lyapunov at x^*. Then x^* is asymptotic Lyapunov-stable.

Moreover, the applications of this theorem is difficult since there are no set rules for constructing the Lyapunov functions. However, some functional forms are often serve as baseline for Lyapunov functions are quadratic functions and logarithmic functions, respectively, with an equilibrium point of $x^* = (x_1^*, x_2^*, ..., x_n^*)$ given as

$$\mathtt{L}(x) = \sum_{i=1}^{n} (x - x_i^*)^2 \text{ and } \mathtt{L}(x) = \sum_{i=1}^{n} \left(x - x_i^* ln(\frac{x_i}{x_i^*}) \right). \tag{26}$$

5. Bifurcation analysis

Definition 5.1 Bifurcation is defined as a change in the qualitative behavior of a given dynamical system if an associated parameter is varied. Bifurcation point is the point at which the changes of parameters usually occur. An alternative approach used to study the stability of endemic equilibrium point is the center manifold theory (Castillo-Chavez and Song, 2004b). This approach is stated as the following result;

Theorem 5.1 (Castillo-Chavez and Song, 2004b) Considering the general system of ordinary differential equations with a parameter ϕ;

$$\frac{dx}{dt} = f(x, \phi), f : \mathbb{R}^n \times \mathbb{R} \to \mathbb{R} \text{ and } f \in C^2(\mathbb{R}^n \times \mathbb{R}), \tag{27}$$

where 0 is an equilibrium point of the system of differential equations ($f(0, \phi) \equiv 0$) for every ϕ and assume;

- $A = D_x f(0,0) = \left(\frac{\partial f_i}{\partial x_j}(0,0) \right)$ is the linearization matrix of (27) at equilibrium point 0 with ϕ evaluated at 0. Where zero is simply an eigenvalue of A and other eigenvalues of A have negative real parts;

- The matrix A has a right eigenvector w and a left eigenvector v with each corresponding to the zero eigenvalue. Then let f_k be the k^{th} component of f and

$$a = \sum_{i,j,k=1}^{n} v_k w_i v_j \frac{\partial^2 f_k}{\partial x_i \partial x_j}(0,0), \tag{28}$$
$$b = \sum_{k,i=1}^{n} v_k w_i \frac{\partial^2 f_k}{\partial x_i \partial \phi}(0,0).$$

The local dynamics of the system (27) around 0 is totally determined by the signs of a and b;

- If $a > 0, b > 0$ and $\phi < 0$ with $|\phi| \leq 1$, then 0 is locally asymptotically stable and there exists a positive unstable equilibrium; when $0 < \phi \leq 1$, 0 is unstable and there exists a negative and locally asymptotically stable equilibrium;

- If $a < 0, b < 0$ and $\phi < 0$ with $|\phi| \leq 1$, then 0 is unstable; when $0 < \phi \leq 1$, 0 is locally asymptotically stable and there exists a positive unstable equilibrium;

- If $a > 0, b < 0$ and $\phi < 0$ with $|\phi| \leq 1$, then 0 is unstable; when $0 < \phi \leq 1, 0$ is unstable and there exists a locally asymptotically stable negative equilibrium; when $0 < \phi \leq 1, 0$ is stable and there exists a positive unstable equilibrium;

- If $a < 0, b > 0$ and ϕ changes from positive to negative, then 0 changes its stability from stable to unstable; A negative unstable equilibrium turns positive and locally asymptotically stable.
  Particular, when $a > 0$ and $b > 0$, then a backward bifurcation is said to occur at $\phi = 0$.

6. Basic reproduction number $(\Re_0)$

In epidemic models, the basic reproduction number gives or tells the state of disease with time. It is very important in disease modelling because it gives an indication regarding the future state of the infection that tells us whether or not the disease will persist or will be eradicated in due course.

Definition 6.1 (Basic reproduction number (Van den Driessche and Watmough, 2002))
The basic reproductive number is denoted by $\Re_0$ and used to measure the ability of the disease to reproduce. This is described as the expected number of secondary cases reproduced by one infected individual in its entire infectious period. Obviously, when basic reproduction number $(\Re_0)$ is less than unity each infected individual can produce an average of less than one new infected individual during his entire period of infectiousness and the disease will not persist in the population and may be eradicated. However, in a situation where basic reproduction number $(\Re_0)$ is greater than unity implies that each infected individuals during the entire period of infectiousness can produce more than one new infected individual and indicates that the disease can persist and invade the population.

Definition 6.2 (Next generation method (Van den Driessche and Watmough, 2002))
The general method used to compute a basic reproduction number $\Re_0$ in cases where one or more classes of infective are involved is called next generation matrix method. Let us

assume that there are n compartments of which the first m compartments correspond to infected individuals, $f_i(x)$ be the rate of appearance of new infections in compartment i, $\mathrm{v}_i^+(x)$ be the rate of transfer of individuals into compartment i by all other means, $\mathrm{v}_i^-(x)$ be the rate of transfer of individuals out of compartment i and $v_i(x) = \mathrm{v}_i^-(x) - \mathrm{v}_i^+(x)$ is the rate of disease progression, death and recovery decrease the i^{th} compartment. The disease transmission model consists of nonnegative initial conditions together with the following system of equations

$$\frac{dx_i}{dt} = \mathtt{f}_i(x) = f_i(x) - v_i(x), \quad i = 1, ..., n, \tag{29}$$

It is assumed that each functions are continuously differentiable and the computation of the m x m square matrices $\wp$ and ϑ which are defined by

$$\wp = \left[\frac{\partial f_i}{\partial x_j}(x_0)\right] \text{ and } \vartheta = \left[\frac{\partial v_i}{\partial x_j}(x_0)\right] \tag{30}$$

where $1 \leq i,\ j \leq$ m and x_0 is the disease free equilibrium point of (29). And since ϑ is non-singular matrix (its determinant is different from zero), then of ϑ^{-1} is exist. The matrix $\wp\vartheta^{-1}$ is called the next generation matrix. Consequently, the basic reproduction number is computed as $\Re_0 = \rho(\wp\vartheta^{-1})$ where $\rho(\wp\vartheta^{-1})$ denotes the spectral radius of a matrix and is the dominant of the non-negative eigenvalue of the next generation matrix.

7. Optimal control theory

Optimal control theory is a powerful mathematical tool that can be used to make decisions involving complex biological situations (Lenhart and Workman, 2007). The best methods of preventing the spread of malaria disease stated in the part of the thesis employs concepts in mathematical optimal control theory. An optimal control problem is an optimization problem that tends to optimize (minimise or maximize) the objective functional subject to a system of equations (constraints) (20) with some given (initial or boundary conditions).

7.1 Optimal Control with Bounded Controls

Many problems require bounds on the control to achieve a realistic solution. An optimal control problems with bounds on the values of the controls where Ω is a closed subset of $\mathbb{R}^m$ is given by

$$\begin{aligned} &\text{Maximize} \int_0^{t_f} f(t, x(t), u(t))dt, \\ &\text{Subject to } \dot{x}(t) = g(t, x(t), u(t)),\ \forall\ t \in [t_0, t_f], \\ &x(t_0) = x_0, \quad u(t) \in \Omega. \end{aligned} \tag{31}$$

To solve optimal control problems (31) with bounds on the values of the controls, we need the full power of Pontryagin Maximum Principle.

Theorem 7.1 (Pontryagin's Maximum Principle (Boltyanskiy et al., 1961))
Let $(x(t),u(t))$ be a maximizer for optimal control problem (31), then there exist $\lambda(t)$ called the adjoint variable such that the following conditions satisfies for all t;

- the maximality condition

$$\mathscr{H}(t,x(t),u(t),\lambda(t)) = \max \mathscr{H}(t,x(t),w,\lambda(t)); \quad w \in \Omega, \tag{32}$$

- the Hamiltonian system

$$\begin{aligned} \dot{x}(t) &= \frac{\partial \mathscr{H}}{\partial \lambda}(t,x(t),u(t),\lambda(t)), \\ \dot{\lambda}(t) &= -\frac{\partial \mathscr{H}}{\partial x}(t,x(t),u(t),\lambda(t)), \end{aligned} \tag{33}$$

- the transversality condition

$$\lambda(t_f) = 0; \tag{34}$$

`where` the Hamiltonian $\mathscr{H}$ is defined by

$$\mathscr{H}(t,x(t),\lambda(t),u(t)) = f(t,x(t),u(t)) + \lambda(t)g(t,x(t),u(t)). \tag{35}$$

7.2. Numerical solution of optimal control problem

Numerical solution is used to solve optimal control problem given by (31) involves finding piecewise continuous functions $u_i(t)$ that optimize the objective functional. Numerical methods for solving boundary value problems can then be employed to solve the resulting two-point boundary value problem. The optimality system that contained two systems such are ordinary differential system from the state and rest from the adjoint equations. The iterative method so called the forward-backward sweep is used to solve the state system and the adjoint system. In solving state equations (33) due to the initial value of state variables the forward fourth order Runge-Kutta is used. Due to the transversality condition (34) with the solution of state functions and the value of optimal controls, the adjoint equations are solved using backward fourth order Runge Kutta. Using a convex combination of the previous controls and the value from the optimality conditions then the controls are updated (32). And this situation continues until two consecutive iterations are close enough each other. The

rough outline of the procedures that generates an approximation to an optimal solutions is given below (Lenhart and Workman, 2007);

Forward-Backward Runge Kutta sweep method

Input:	Setting the initial parameter values of the model (31).

Step 1. Make an initial guess for u over the interval. Store the initial guess as u.

Step 2. Using the initial condition $x(t_0) = x_0$ and the stored values for u, solve x forward in time according to it differential equation in the optimality system.

Step 3. Using the transversality condition $\lambda(t_f) = 0$ and the stored values for x and u, solve λ backward in time according to its differential equation in the optimality system.

Step 4. Update the control u by entering the new x and λ values into the characterization.

Step 5. If values of the variables in this iteration and the last iteration are negligibly small, output current values as solutions. If values are not small, return to step 2.

Note that to verify the convergence taking delta (δ) as the tolerance the require to be small $||u(i) - u_{old}(i)|| \leq \delta||u(i)||$ `where` $u(i)$ is the values of the control during the current iteration and $u_{old}(i)$ is the vector of estimated values from the previous iteration.

APPENDIX B

FAMOUS MATHEMATICIANS

$\mathscr{A}$. Ronald Ross (1857 - 1932)

Ronald Ross was born in 1857 in the North of India, where his father was an officer in the British army. He studied medicine in London but preferred to write poems and dramas. After working for a year on a ship as surgeon, he managed to enter the Indian Medical Service in 1881. His medical work in India left him plenty of free time, during which he wrote literary works and taught himself some mathematics. From 1895 till 1898, Ross continued his research in India and tested Manson's idea. His superiors having sent him to Calcutta during a season where malaria cases were rare, he decided to study malaria in cage birds. He found the parasite in the salivary glands of anopheles mosquitoes and managed to infect experimentally healthy birds by letting mosquitoes bite them: this proved that malaria is transmitted by mosquito bites and not by ingestion of contaminated water. He was elected to the Royal Society in 1901 and received in 1902 the Nobel Prize in Physiology or Medicine for his work on malaria. Ross published a Report on the Prevention of Malaria in Mauritius in 1908 and The Prevention of Malaria in 1910. He tried to build mathematical models of the transmission of malaria for the first time in 1991 and Ross died in London in 1932 (Bacaër, 2011).

Ronald Ross (1857 - 1932), (Bacaër, 2011)

$\mathscr{B}$. Lev Semyonovich Pontryagin (1908 - 1988)

Lev Semyonovich Pontryagin is a Soviet mathematician. He was born in the Moscow, Russian Empire and lost his eyesight completely due to an unsuccessful eye surgery after a primus stove explosion when he was 14 years old. Despite his blindness he was able to become one of the greatest mathematicians of the 20th century, partially with the help of his mother Tatyana Andreevna who read mathematical books and papers (notably those of Heinz Hopf, J. H. C. Whitehead, and Hassler Whitney) to him. He made major discoveries in a number of fields of mathematics, including algebraic topology and differential topology. Pontryagin worked on duality theory for homology while still a student. He went on to lay foundations for the abstract theory of the Fourier transform, now called Pontryagin duality. In 1942 he introduced the cohomology operations now called Pontryagin squares. Moreover, in operator theory there are specific instances of Krein spaces called Pontryagin spaces. Later in his career he worked in optimal control theory. His maximum principle is fundamental to the modern theory of optimization. He also introduced there the idea of a bang-bang principle, to describe situations where the applied control at each moment is either the maximum steer or none and Pontryagin died in Mosco in 1988.

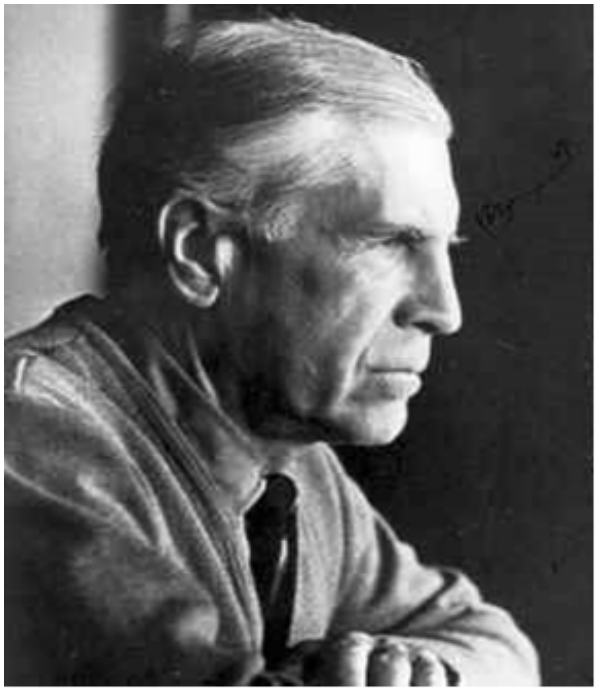

Pontryagin (1908 - 1988), (Wikipedia: May 7, 2021)

APPENDIX C

MATLAB CODE

Malaria model simulation main program

```
function y = system4(t,A1,A2,A3,B1,B2,B3,x1,x2,x3,x4,x5,x6,x7)
test = -1; delta = 0.001;N=1000; A1=80; A2=60; A3=100; B1=60; B2=100; B3=80;
t=linspace(0,180,N+1); t0=0; tf=100; h=(tf-t0)/N; h2=h/2;
```

Model parameters

```
m=0.058;l=0.055; d=0.068; g=0.0035; y=0.041; Q0m=0.071; Q1m=0.09; w=0.09; B0h=0.03;
B1h=0.05; B0m=0.04; B1m=0.07; uh=0.00004; um=0.05; r=0.007; Tmax=28; T0=16; M1=0;M2=1;
```

Model variables

```
u1=zeros(1,N+1); u2=zeros(1,N+1); u3=zeros(1,N+1); x1=zeros(1,N+1); x2=zeros(1,N+1);
x3=zeros(1,N+1);x4=zeros(1,N+1); x5=zeros(1,N+1); x6=zeros(1,N+1); x7=zeros(1,N+1);
x8=zeros(1,N+1); lambda1=zeros(1,N+1); lambda2=zeros(1,N+1); lambda3=zeros(1,N+1);
lambda4=zeros(1,N+1); lambda5=zeros(1,N+1); lambda6=zeros(1,N+1); lambda7=zeros(1,N+1);
lambda8=zeros(1,N+1);
```

Initial conditions of the model

```
x1(1)=100; x2(1)=20; x3(1)=10; x4(1)=0; x5(1)=300; x6(1)=60; x7(1)=30; x8(1)=16.1;
```

Iterations of the method

```
while(test < 0)
oldu1=u1;oldu2=u2; oldu3=u3; oldx1=x1; oldx2=x2; oldx3=x3; oldx4=x4; oldx5=x5; oldx6=x6;
oldx7=x7; oldx8=x8; oldlambda1=lambda1; oldlambda2=lambda2;
oldlambda3=lambda3; oldlambda4=lambda4; oldlambda5=lambda5; oldlambda6=lambda6;
oldlambda7=lambda7; oldlambda8=lambda8;
```

Runge-Kutta parameter in state variables

```
for i = 1:N
k11=y-(1-u1(i))*(B0h+B1h*((x8(i)-T0)./Tmax))*x1(i)*x7(i)-uh*x1(i)+w*x4(i);
k12=(1-u1(i))*(B0h+B1h*((x8(i)-T0)./Tmax))*x1(i)*x7(i)-(uh+m)*x2(i);
k13=m*x2(i)-(u2(i)+uh+d+g)*x3(i);
k14=(u2(i)+g)*x3(i)-(uh+w)*x4(i);
k15=(Q0m+Q1m*((x8(i)-T0)./Tmax))-(1-u1(i))*(B0m+B1m*((x8(i)-T0)./Tmax))*x5(i)*x3(i)-
(u3(i)+um)*x5(i);
k16=(B0m+B1m*((x8(i)-T0)./Tmax))*x5(i)*x3(i)-(u3(i)+um+l)*x6(i);
k17=l*x6(i)-(u3(i)+um)*x7(i);
k18=r*(1-(x8(i)./Tmax))*(x8(i)-T0);
```

Second Runge-Kutta iterations in state variables

```
k21=y-(1-0.5*(u1(i)+u1(i+1)))*(B0h+B1h*(((x8(i)+h2*k18)-T0)./Tmax))*(x1(i)+h2*k11)
*(x7(i)+h2*k17)-uh*(x1(i)+h2*k11)+w*(x4(i)+h2*k14);
k22=(1-0.5*(u1(i)+u1(i+1)))*(B0h+B1h*(((x8(i)+h2*k18)-T0)./Tmax))*(x1(i)+h2*k11)
*(x7(i)+h2*k17)-(uh+m)*(x2(i)+h2*k12);
k23=m*(x2(i)+h2*k12)-(0.5*(u2(i)+u2(i+1))+uh+d+g)*(x3(i)+h2*k13);
k24=(0.5*(u2(i)+u2(i+1))+g)*(x3(i)+h2*k13)-(uh+w)*(x4(i)+h2*k14);
k25=(Q0m+Q1m*(((x8(i)+h2*k18)-T0)./Tmax))-(1-0.5*(u1(i)+u1(i+1)))*(B0m+B1m
*(((x8(i)+h2*k18)-T0)./Tmax))*(x5(i)+h2*k15)*(x3(i)+h2*k13)
-(0.5*(u3(i)+u3(i+1))+um)*(x5(i)+h2*k15);
k26=(B0m+B1m*(((x8(i)+h2*k18)-T0)./Tmax))*(x5(i)+h2*k15)*(x3(i)+h2*k13)
-(0.5*(u3(i)+u3(i+1))+um+l)*(x6(i)+h2*k16);
k27=l*(x6(i)+h2*k16)-(0.5*(u3(i)+u3(i+1))+um)*(x7(i)+h2*k17);
k28=r*(1-(x8(i)+h2*k18)./Tmax)*((x8(i)+h2*k18)-T0);
```

Third Runge-Kutta iterations in state variables

```
k31=y-(1-0.5*(u1(i)+u1(i+1)))*(B0h+B1h*(((x8(i)+h2*k28)-T0)./Tmax))*(x1(i)+h2*k21)
*(x7(i)+h2*k27)-uh*(x1(i)+h2*k21)+w*(x4(i)+h2*k24);
k32=(1-0.5*(u1(i)+u1(i+1)))*(B0h+B1h*(((x8(i)+h2*k28)-T0)./Tmax))*(x1(i)+h2*k21)
```

*(x7(i)+h2*k27)-(uh+m)*(x2(i)+h2*k22);

k33=m*(x2(i)+h2*k22)-(0.5*(u2(i)+u2(i+1))+uh+d+g)*(x3(i)+h2*k23);

k34=(0.5*(u2(i)+u2(i+1))+g)*(x3(i)+h2*k23)-(uh+w)*(x4(i)+h2*k24);

k35=(Q0m+Q1m*(((x8(i)+h2*k28)-T0)./Tmax))-(1-0.5*(u1(i)+u1(i+1)))

(B0m+B1m(((x8(i)+h2*k28)-T0)./Tmax))*(x5(i)+h2*k25)*(x3(i)+h2*k23)

-(0.5*(u3(i)+u3(i+1))+um)*(x5(i)+h2*k25);

k36=(B0m+B1m*(((x8(i)+h2*k28)-T0)./Tmax))*(x5(i)+h2*k25)*(x3(i)+h2*k23)

-(0.5*(u3(i)+u3(i+1))+um+l)*(x6(i)+h2*k26);

k37=l*(x6(i)+h2*k26)-(0.5*(u3(i)+u3(i+1))+um)*(x7(i)+h2*k27);

k38=r*(1-(x8(i)+h2*k28)./Tmax)*((x8(i)+h2*k28)-T0);

Fourth Runge-Kutta iterations in state variables

---

k41=y-(1-u1(i+1))*(B0h+B1h*(((x8(i)+h*k38)-T0)./Tmax))*(x1(i)+h*k31)*(x7(i)+h*k37)

-uh*(x1(i)+h*k31)+w*(x4(i)+h*k24);

k42=(1-u1(i+1))*(B0h+B1h*(((x8(i)+h*k38)-T0)./Tmax))*(x1(i)+h2*k31)*(x7(i)+h*k37)

-(uh+m)*(x2(i)+h*k32);

k43=m*(x2(i)+h*k32)-(u2(i+1)+uh+d+g)*(x3(i)+h*k33);

k44=(u2(i+1)+g)*(x3(i)+h*k33)-(uh+w)*(x4(i)+h*k34);

k45=(Q0m+Q1m*(((x8(i)+h*k38)-T0)./Tmax))-(1-u1(i+1))*(B0m+B1m*(((x8(i)+h*k38)-T0)./Tmax))

*(x5(i)+h*k35)*(x3(i)+h*k33)-(u3(i+1)+um)*(x5(i)+h*k35);

k46=(B0m+B1m*(((x8(i)+h*k38)-T0)./Tmax))*(x5(i)+h*k35)*(x3(i)+h*k33)-(u3(i+1)+um+l)

*(x6(i)+h*k36);

k47=l*(x6(i)+h*k36)-(u3(i+1)+um)*(x7(i)+h*k37);

k48=r*(1-(x8(i)+h*k38)./Tmax)*((x8(i)+h*k38)-T0);

Runge-Kutta new approximation in state

---

x1(i+1) = x1(i) + (h/6)*(k11 + 2*k21 + 2*k31 + k41);

x2(i+1) = x2(i) + (h/6)*(k12 + 2*k22 + 2*k32 + k42);

x3(i+1) = x3(i) + (h/6)*(k13 + 2*k23 + 2*k33 + k43);

x4(i+1) = x4(i) + (h/6)*(k14 + 2*k24 + 2*k34 + k44);

x5(i+1) = x5(i) + (h/6)*(k15 + 2*k25 + 2*k35 + k45);

x6(i+1) = x6(i) + (h/6)*(k16 + 2*k26 + 2*k36 + k46);

x7(i+1) = x7(i) + (h/6)*(k17 + 2*k27 + 2*k37 + k47);

```
x8(i+1) = x8(i) + (h/6)*(k18 + 2*k28 + 2*k38 + k48);
end
```

Backward Runge-Kutta iterations in co-state variables

```
for i=1:N
j=N+2-i;
```

First Runge-Kutta parameter in co-state

```
n11=-((1-u1(j))*(B0h+B1h*((x8(j)-T0)./Tmax))*x7(j)*(lambda2(j)-lambda1(j))-uh*lambda1(j));
n12=lambda2(j)*(uh+m)-lambda3(j)*uh-A1;
n13=-((1-u1(j))*(B0m+B1m*((x8(j)-T0)./Tmax))*x5(j)*(lambda6(j)-lambda5(j))
+lambda4(j)*(u2(j)+g)-lambda3(j)*(u2(j)+uh+d+g))-A2;
n14=-(lambda1(j)*w)+lambda4(j)*(uh+w);
n15=-((1-u1(j))*(B0m+B1m*((x8(j)-T0)./Tmax))*x3(j)*(lambda6(j)-lambda5(j))
-lambda5(j)*(u3(j)+um));
n16=lambda6(j)*(u3(j)*uh+l)-lambda7(j)*l;
n17=-((1-u1(j))*(B0h+B1h*((x8(j)-T0)./Tmax))*x1(j)*(lambda2(j)-lambda1(j))
-lambda7(j)*(u3(j)+um))-A3;
n18= -r*lambda8(j)-r*lambda8(j)*((T0-2*x8(j))./Tmax);
```

Second Runge-Kutta parameter in co-state

```
n21=-((1-0.5*(u1(j)+u1(j-1)))*(B0h+B1h*(((0.5*x8(j)+x8(j-1))-T0)./Tmax))*0.5*(x7(j)+x7(j-
1))*((lambda2(j)-h2*n12)-(lambda1(j)-h2*n11))-uh*(lambda1(j)-h2*n11));
n22=(lambda2(j)-h2*n12)*(uh+m)-(lambda3(j)-h2*n13)*uh-A1;
n23=-((1-0.5*(u1(j)+u1(j-1)))*(B0m+B1m*(((0.5*x8(j)+x8(j-1))-T0)./Tmax))*0.5*(x5(j)+x5(j-
1))*((lambda6(j)-h2*n16)-(lambda5(j)-h2*n15))+(lambda4(j)-h2*n14)*(0.5*(u2(j)+u2(j-1))+uh+g)-
(lambda3(j)-h2*n13)*(0.5*(u2(j)+u2(j-1))+uh+d+g))-A2;
n24=-((lambda1(j)-h2*n11)*w)+(lambda4(j)-h2*n14)*(uh+w);
n25=-((1-0.5*(u1(j)+u1(j-1)))*(B0m+B1m*(((0.5*x8(j)+x8(j-1))-T0)./Tmax))*0.5*(x3(j)+x3(j-
1))*((lambda6(j)-h2*n16)-(lambda5(j)-h2*n15))-(lambda5(j)-h2*n15)*(0.5*(u3(j)+u3(j-1))+um));
n26=(lambda6(j)-h2*n16)*(u3(j)*uh+l)-(lambda7(j)-h2*n17)*l;
n27=-((1-0.5*(u1(j)+u1(j-1)))*(B0h+B1h*(((0.5*x8(j)+x8(j-1))-T0)./Tmax))*0.5*(x1(j)+x1(j-
```

1))*((lambda2(j)-h2*n12)-(lambda1(j)-h2*n11))-(lambda7(j)-h2*n17)*(0.5*(u3(j)+u3(j-1))+um))-A3;

n28= -r*(lambda8(j)-h2*n18)-r*(lambda8(j)-h2*n18)*((T0-2*(0.5*x8(j)+x8(j-1))./Tmax);

Third Runge-Kutta parameter in co-state

---

n31=-((1-0.5*(u1(j)+u1(j-1)))*(B0h+B1h*(((0.5*x8(j)+x8(j-1))-T0)./Tmax))*0.5*(x7(j)+x7(j-1))*((lambda2(j)-h2*n22)-(lambda1(j)-h2*n21))-uh*(lambda1(j)-h2*n21));

n32=(lambda2(j)-h2*n22)*(uh+m)-(lambda3(j)-h2*n23)*uh-A1;

n33=-((1-0.5*(u1(j)+u1(j-1)))*(B0m+B1m*(((0.5*x8(j)+x8(j-1))-T0)./Tmax))*(0.5*(x5(j)+x5(j-1)))*((lambda6(j)-h2*n26)-(lambda5(j)-h2*n25))+(lambda4(j)-h2*n24)*(0.5*(u2(j)+u2(j-1))+uh+g)-(lambda3(j)-h2*n23)*(0.5*(u2(j)+u2(j-1))+uh+d+g))-A2;

n34=-((lambda1(j)-h2*n21)*w)+(lambda4(j)-h2*n24)*(uh+w);

n35=-((1-0.5*(u1(j)+u1(j-1)))*(B0m+B1m*(((0.5*x8(j)+x8(j-1))-T0)./Tmax))*0.5*(x3(j)+x3(j-1))*((lambda6(j)-h2*n26)-(lambda5(j)-h2*n25))-(lambda5(j)-h2*n25)*(0.5*(u3(j)+u3(j-1))+um));

n36=(lambda6(j)-h2*n26)*(u3(j)*uh+l)-(lambda7(j)-h2*n27)*l;

n37=-((1-0.5*(u1(j)+u1(j-1)))*(B0h+B1h*(((0.5*x8(j)+x8(j-1))-T0)./Tmax))*0.5*(x1(j)+x1(j-1))*((lambda2(j)-h2*n22)-(lambda1(j)-h2*n21))-(lambda7(j)-h2*n27)*(0.5*(u3(j)+u3(j-1))+um))-A3;

n38=-r*(lambda8(j)-h2*n28)-r*(lambda8(j)-h2*n28)*((T0-2*(0.5*x8(j)+x8(j-1))./Tmax);

Fourth Runge-Kutta parameter in co-state

---

n41=-((1-u1(j-1))*(B0h+B1h*(((0.5*x8(j)+x8(j-1))-T0)./Tmax))*x7(j-1)*((lambda2(j)-h*n32)-(lambda1(j)-h*n31))-uh*(lambda1(j)-h*n31));

n42=(lambda2(j)-h*n32)*(uh+m)-(lambda3(j)-h*n33)*uh-A1;

n43=-((1-u1(j-1))*(B0m+B1m*(((0.5*x8(j)+x8(j-1))-T0)./Tmax))*x5(j-1)*((lambda6(j)-h*n36)-(lambda5(j)-h*n35))+(lambda4(j)-h*n34)*(u2(j-1)+uh+g)-(lambda3(j)-h2*n23)*(u2(j-1)+uh+d+g))-A2;

n44=-((lambda1(j)-h*n31)*w)+(lambda4(j)-h*n34)*(uh+w);

n45=-((1-u1(j-1))*(B0m+B1m*(((0.5*x8(j)+x8(j-1))-T0)./Tmax))*x3(j-1)*((lambda6(j)-h*n36)-(lambda5(j)-h*n35))-(lambda5(j)-h*n35)*(u3(j-1)+um));

n46=(lambda6(j)-h2*n26)*(u3(j)*uh+l)-(lambda7(j)-h2*n27)*l;

n47=-((1-u1(j-1))*(B0h+B1h*(((0.5*x8(j)+x8(j-1))-T0)./Tmax))*x1(j-1)*((lambda2(j)-h*n32)-(lambda1(j)-h*n31))-(lambda7(j)-h*n37)*(u3(j-1)+um))-A3;

```
n48= -r*(lambda8(j)-h*n38)-r*(lambda8(j)-h*n38)*((T0-2*(0.5*x8(j)+x8(j-1)))./Tmax);
```

Runge-Kutta new approximation in co-state

```
lambda1(j-1)=lambda1(j)-(h/6)*(n11+2*n21+2*n31+n41);
lambda2(j-1)=lambda2(j)-(h/6)*(n12+2*n22+2*n32+n42);
lambda3(j-1)=lambda3(j)-(h/6)*(n13+2*n23+2*n33+n43);
lambda4(j-1)=lambda4(j)-(h/6)*(n14+2*n24+2*n34+n44);
lambda5(j-1)=lambda5(j)-(h/6)*(n15+2*n25+2*n35+n45);
lambda6(j-1)=lambda6(j)-(h/6)*(n16+2*n26+2*n36+n46);
lambda7(j-1)=lambda7(j)-(h/6)*(n17+2*n27+2*n37+n47);
lambda8(j-1)=lambda8(j)-(h/6)*(n18+2*n28+2*n38+n48);
end
u1=max(M1,min(M2,((lambda2.*x1.*x7)-(lambda1.*x1.*x7)*(B0h+B1h*((x8(i+1)-T0)./Tmax))
+(lambda6.*x5.*x3)-(lambda5.*x5.*x3)*(B0m+B1m*((x8(i+1)-T0)./Tmax)))/B1));
u1 = 0.5*(u1+oldu1);
u2 = max(M1,min(M2,((lambda3.*x3) - (lambda4.*x3))/B2));
u2 = 0.5*(u2 + oldu2);
u3 = max(M1, min(M2,((lambda5.*x5)+(lambda6.*x6)+(lambda7.*x7))/B3));
u3 = 0.5*(u3+ oldu3);
```

Absolute error for convergence

```
temp1 = delta*sum(abs(u1)) - sum(abs(oldu1 - u1));
temp2 = delta*sum(abs(u2)) - sum(abs(oldu2 - u2));
temp3 = delta*sum(abs(u3)) - sum(abs(oldu3 - u3));
temp4 = delta*sum(abs(x1)) - sum(abs(oldx1 - x1));
temp5 = delta*sum(abs(x2)) - sum(abs(oldx2 - x2));
temp6 = delta*sum(abs(x3)) - sum(abs(oldx3 - x3));
temp7 = delta*sum(abs(x4)) - sum(abs(oldx4 - x4));
temp8 = delta*sum(abs(x5)) - sum(abs(oldx5 - x5));
temp9 = delta*sum(abs(x6)) - sum(abs(oldx6 - x6));
temp10 = delta*sum(abs(x7))- sum(abs(oldx7 - x7));
temp11 = delta*sum(abs(x8)) - sum(abs(oldx8 - x8));
temp12 = delta*sum(abs(lambda1)) - ... sum(abs(oldlambda1 - lambda1));
```

```
temp13 = delta*sum(abs(lambda2)) - ... sum(abs(oldlambda2 - lambda2));
temp14 = delta*sum(abs(lambda3)) - ... sum(abs(oldlambda3 - lambda3));
temp15 = delta*sum(abs(lambda4)) - ... sum(abs(oldlambda4 - lambda4));
temp16 = delta*sum(abs(lambda5)) - ... sum(abs(oldlambda5 - lambda5));
temp17 = delta*sum(abs(lambda6)) - ... sum(abs(oldlambda6 - lambda6));
temp18 = delta*sum(abs(lambda7)) - ... sum(abs(oldlambda7 - lambda7));
temp19 = delta*sum(abs(lambda8)) - ... sum(abs(oldlambda8 - lambda8));
test= min(temp1, min(temp2,min(temp3,min(temp4,min(temp5, min(temp6,min(temp7,
min(temp8,min(temp9,min(temp10,min(temp11,min(temp12,min(temp13,min(temp14,
min(temp15,min(temp16,min(temp17,min(temp18,temp19))))))))))))))));
end
y1(:,1) = t; y1(:,2) = u1; y1(:,3) = u2; y1(:,4) = u3; y1(:,5) = x1; y1(:,6) = x2;
y1(:,7) = x3; y1(:,8) = x4; y1(:,9) = x5; y1(:,10) = x6; y1(:,11) = x7; y1(:,12) = x8;
y1(:,13) = lambda1; y1(:,14) = lambda2; y1(:,15) = lambda3; y1(:,16) = lambda4;
y1(:,17) = lambda5; y1(:,18) = lambda6; y1(:,19) = lambda7; y1(:,20) = lambda8;
box on
hold on
```

Ploting section

```
plot(y1(:,1),y1(:,11),'b','linewidth',4)
xlabel('Time (days)')
ylabel('Infected Human')
legend('u_1 = 0, u_2 = 0, u_3 = 0','u_1 \neq 0, u_2 \neq 0, u_3 = 0')
set(gca,'linewidth',3)
hold on
```